



UNIVERSITAT  
POLITÈCNICA  
DE VALÈNCIA

Instituto Interuniversitario de Reconocimiento Molecular  
y Desarrollo Tecnológico

**Study of substrate modulation and bioreceptor  
anchoring for the development of high performance  
microarrays**

**PhD. THESIS**

*Pilar Jiménez Meneses*

PhD. Supervisors

*Ángel Maquieira Catalá*

*María José Bañuls Polo*

Valencia, January 2020



## ACKNOWLEDGEMENTS

Agradecer al Ministerio de Economía y Competitividad de España, por su programa de becas doctorales FPI y a la Universitat Politècnica de València por su infraestructura.

Muchas gracias a Ángel Maquieira y María José Bañuls por acogerme en este grupo tan genial, por todo su apoyo, confianza depositada en mí y por su gran esfuerzo para guiarme en mi formación como investigadora.

Gracias a todos los profesores del Departamento de Química, por su buen hacer y simpatía: Sergi Morais, Miguel A. González, Luis Tortajada, M. Asunción Herrero, Pilar Aragón, Patricia Noguera, Julia Atienza,

Por supuesto, gracias a todos los compañeros con los que he compartido numerosos días de trabajo en el laboratorio, por hacer de esta etapa de mi vida única: Victoria González, Sara Martorell, Rafael Alonso, Eric Yamanaka, Noelle do Nascimento, Augusto Juste, Noelia Carbó, Edurne Peña, Miquel Avellá, Daniel González, Sara Santiago, Regina Niñoles, Ahmed Ali, Estrella Fernández, Ana Lázaro, Gabriel Sancho, Zeneida Betancor, María José Juárez, Salvador Mas y todos los TFGs que han pasado.

También me gustaría agradecer a la gente del piso de arriba, Juan Carlos, Andrea y Óscar, por todos los buenos momentos que hemos pasado.

También mencionar, la oportunidad que me ha ofrecido el Departamento de Química para desarrollarme como docente. He disfrutado muchísimo de las prácticas impartidas durante el transcurso de esta tesis doctoral.

Now in English, I am really grateful to all the people who have made possible to enjoy three wonderful placements. Specially thanks to Eva Melnik, Stefan Schrittwieser and Rainer Hainberger (Austrian Institute of Technology, Austria) in my first placement; Odette Gonçalves and Maria Teresa Neves-Petersen in the second one (Aalborg University, Denmark); Elke Bremus-Koebberling and Arnold Gillner, in the last one (Fraunhofer Institute for Laser Technology, Germany); for opening my mind and giving me the chance of joining on their groups. Of course, thank all people I have met during these stays; it was a pleasure.

Agradecer a mis Químicas favoritas, Cris y Alicia, por tantos buenos momentos que vivimos durante la carrera, con todas nuestras tonterías, y porque seguimos estando juntas.

Especial mención a Nuria, por quererme tanto, ser tan genial y aguantar mis días malos, ya que los buenos momentos cualquiera los aguanta.

Finalmente, agradezco enormemente, el esfuerzo que ha hecho toda mi familia, en especial mis padres, Carlos Jiménez y Mercedes Meneses, sin los que no podría haber llegado tan lejos. Siempre me habéis apoyado en perseguir mis sueños y enseñado a trabajar duro. Os quiero mucho. Gracias a mis hermanos, David, Luis, Carlos y Mercedes, mi cuñado favorito Pepe, y mis cuñadas Eva y Toñi, por ayudarme tanto. También a mi sobrina Alicia que es la alegría de la familia, que sólo con ver sus fotos me anima el día.

=)

## **ABSTRACT**

The present thesis, entitled “Study of substrate modulation and bioreceptor anchoring for the development of high performance microarrays”, aims to respond the needs and challenges related to the development of better detection systems.

Thus, this PhD thesis is focused on the study of new approaches able to improve the performance of microarrays. Aspects such as the nature of the surfaces and the probes, functionalization of the substrates, probe printing, immobilization and target detection were considered in the fabrication process. Within all these features, modulation of the surface behavior and probe anchoring were the most challenging aspects, as the interface is key for the immobilization of the receptors and the later detection, which will determine the performance of the final device.

In this work, two microarray types have been developed, one for oligonucleotides and another one for antibodies. Then, a characterization of the reached achievements is done. All the routes have in common the use of light to catalyze the attachment of bioreceptors on the surface substrates, employing click-chemistry reactions.

In the first chapter, the state of the art of microarray technology is overviewed, with special focus in the main aspects of microarray design.

In the second chapter, the goals for this PhD thesis are settled. These general objectives are addressed in the following experimental chapters.

In the third chapter, the effect of hydrophobicity and probe multi-point attachment on the microarray performance are studied. Thus, modulation of glass slide surfaces with alkenyl and alkynyl motifs for the anchoring of mono and multithiolated oligonucleotide probes by thiol-ene and thiol-yne photocoupling reactions, respectively, was accomplished. Surfaces modified with the most hydrophobic silane (alkynyl), or anchoring polythiolated probes, revealed better performances. These microarray systems were applied to the discrimination of SNPs and to detect bacterial genome PCR products.

In the fourth chapter, a rational design for the preparation of microarrays of antibodies, is done. The immobilization approach displays the oriented anchoring of thiol-bearing antibody fragments to alkenylated glass slides by thiol-ene photocoupling reaction. Multiplexed detection of cardiac biomarkers is demonstrated. The designed microarray shows higher recognition capacity in comparison to whole antibody microarrays.

## *Abstract*

In the fifth chapter, improvement of a novel methodology for the anchoring of thiolated oligonucleotides has been developed. Due to the interest on modifying highly hydrophobic surfaces, a new photoinduced reaction is set up. Thanks to the features of the named “fluor-thiol photocoupling reaction”, immobilization of thiolated probes to surfaces containing C-F bonds in a fast, easy and biocompatible with aqueous media way, was achieved. Hydrophobicity of the surfaces was controlled to get successful hybridizations. Because of the high hydrophobicity of the surfaces, a huge confinement of the probes is accomplished, which allows the approximation of the analytes only where the probe is linked, keeping a high repulsion in the remaining surface. The perfluorinated glass slides improved the immobilization densities and detection capacity, regarding to the alkenylated and alkynylated surfaces, and allowed the discrimination of SNPs and detection of bacterial PCR products, as well.

In the sixth chapter, other surfaces different than glass are explored. Thus, polyvinylidene fluoride membranes were employed as substrates for the development of oligonucleotide microarrays. Therefore, a fast, easy and mild functionalization process by UV irradiation and organosilane chemistry, was developed. Then, alkenyl functionalized and non-functionalized membranes were applied to microarray technology by covalent anchoring through thiol-ene and fluor-thiol photocoupling reactions, respectively. Promising results were obtained with both surfaces.

To sum up, modulation of the chemical response of the substrates and anchoring procedures, are here the two keys in the improvement of microarray technology. This work has contributed to the progress of new microarray platforms and the development of a novel photoinduced reaction. Finally, the finding of the fluor-thiol photocoupling reaction, paves the way to build more sensitive devices, which improves the bioassay performances. Moreover, it provides a novel alternative for surface modification.

## RESUMEN

La presente tesis, titulada “Estudio de la modulación de los sustratos y anclaje de bioreceptores para el desarrollo de *microarrays* de alto rendimiento”, tiene como objetivo responder a las necesidades y desafíos relacionados con el desarrollo de mejores sistemas de detección.

Por lo tanto, esta tesis doctoral se centra en el estudio de nuevas aproximaciones capaces de mejorar el rendimiento de los *microarrays*. Aspectos como la naturaleza de las superficies y las sondas, la funcionalización de los sustratos, la impresión, la inmovilización y la detección de las sondas se consideraron en el proceso de fabricación. Dentro de todas estas características, la modulación de la superficie y el anclaje de la sonda fueron los aspectos más desafiantes, ya que la interfaz es clave para la inmovilización de los receptores y la posterior detección, lo que determinará el rendimiento del dispositivo final.

En este trabajo, se han desarrollado dos tipos de *microarrays*, uno para oligonucleótidos y otro para anticuerpos. Luego, se ha realizado una caracterización de los logros alcanzados. Todas las rutas tienen en común el uso de la luz para catalizar la unión de los biorreceptores en los sustratos de la superficie, empleando reacciones de la química clic.

En el primer capítulo, se facilita una visión general del estado del arte de la tecnología de *microarrays* con un enfoque especial en los aspectos principales del diseño de *microarrays*.

En el segundo capítulo, se establecen los objetivos de esta tesis doctoral. Estos objetivos generales se abordan en los siguientes capítulos experimentales.

En el tercer capítulo, se estudia el efecto de la hidrofobia y el uso de sondas con múltiples puntos de unión, en el rendimiento del *microarray*. De este modo, se llevó a cabo la modulación de superficies vidrio con grupos alquenilo y alquinilo para el anclaje de sondas de oligonucleótidos mono y multitioladas mediante las reacciones de foto anclaje del tiol-eno y tiol-ino, respectivamente. Las superficies modificadas con el silano más hidrofóbico (alquinilo) y las sondas politioladas ancladas, revelaron mejores rendimientos. Estos sistemas de *microarrays* se aplicaron a la discriminación de SNPs y a la detección de productos de PCR de bacterias.

## Resumen

En el cuarto capítulo, se realiza un diseño racional para la preparación de *microarrays* de anticuerpos. El enfoque de inmovilización muestra el anclaje orientado de los fragmentos de anticuerpos que contienen tiol sobre superficies de vidrio alqueniladas mediante reacción de foto anclaje del tiol-eno. De esta forma, se demuestra la detección multiplexada de biomarcadores cardíacos. El *microarray* diseñado muestra una mayor capacidad de reconocimiento en comparación con los *microarrays* de anticuerpos completos.

En el quinto capítulo, se ha desarrollado una nueva metodología para mejorar el anclaje de oligonucleótidos tiolados. Dado el interés en modificar superficies altamente hidrófobas, se establece una nueva reacción fotoinducida. Gracias a las características de la llamada "reacción de fotoacoplamiento de fluor-tiol", se logró la inmovilización de sondas tioladas a superficies que contienen enlaces C-F de una manera rápida, fácil y biocompatible con medios acuosos. La hidrofobicidad de las superficies se controló para obtener hibridaciones exitosas. Debido a la alta hidrofobicidad de las superficies, se logra un gran confinamiento de las sondas, lo que permite la aproximación de los analitos solo donde está unida la sonda, manteniendo una alta repulsión en la superficie restante. Las superficies de vidrio perfluoradas mejoraron las densidades de inmovilización y la capacidad de detección, con respecto a las superficies alqueniladas y alquiniladas, y también, permitieron la discriminación de SNPs y la detección de productos de PCR bacterianos.

En el sexto capítulo, se exploran otras superficies diferentes al vidrio. Por lo tanto, membranas de fluoruro de polivinilideno se emplearon como sustratos para el desarrollo de *microarrays* de oligonucleótidos. Para ello, se desarrolló un proceso de funcionalización rápido, fácil y suave, mediante el empleo de irradiación UV y la química de los organosilanos. Luego, se aplicaron dichas membranas funcionalizadas con grupos alquenilo y sin funcionalizar a la tecnología de *microarrays* mediante anclaje covalente a través de las reacciones de foto anclaje de tiol-eno y fluor-tiol, respectivamente. Se obtuvieron resultados prometedores con ambas superficies.

En resumen, la modulación de la respuesta química de los sustratos y los procedimientos de anclaje son las dos claves para mejorar la tecnología de *microarrays*. Este trabajo ha contribuido al progreso de nuevas plataformas de *microarrays* y al desarrollo de una nueva reacción fotoinducida. Finalmente, el hallazgo de la reacción de fotoacoplamiento de fluor-tiol, allana el camino para construir dispositivos más sensibles, lo que mejora el



rendimiento del bioensayo. Además, proporciona una alternativa novedosa para la modificación superficial.

## RESUM

La present tesi, titulada “Estudi de la modulació dels substrats i ancoratge de bioreceptores per al desenvolupament de *microarrays* d'alt rendiment”, té com a objectiu respondre a les necessitats i desafiaments relacionats amb el desenvolupament de millors sistemes de detecció.

Per tant, aquesta tesi doctoral es centra en l'estudi de noves aproximacions capaces de millorar el rendiment dels *microarrays*. Aspectes com ara la naturalesa de les superfícies i les sondes, la funcionalització dels substrats, la impressió, la immobilització i la detecció de les sondes es van considerar en el procés de fabricació. Dins de totes aquestes característiques, la modulació de la superfície i l'ancoratge de la sonda van ser els aspectes més desafiadors, ja que la interfície és clau per a la immobilització dels receptors i la posterior detecció, la qual cosa determinarà el rendiment del dispositiu final.

En aquest treball, s'han desenvolupat dos tipus de *microarrays*, un per a oligonucleòtids i un altre per a anticossos. Després, s'ha realitzat una caracterització dels resultats aconseguits. Totes les rutes tenen en comú l'ús de la llum per a catalitzar la unió dels bioreceptores en els substrats de la superfície, emprant reaccions de la química clic.

En el primer capítol, es facilita una visió general de l'estat de l'art de la tecnologia de *microarrays* amb un enfocament especial en els aspectes principals del disseny de *microarrays*.

En el segon capítol, s'estableixen els objectius d'aquesta tesi doctoral. Aquests objectius generals s'aborden en els següents capítols experimentals.

En el tercer capítol, s'estudia l'efecte de la hidrofòbia i l'ús de sondes amb múltiples punts d'unió, en el rendiment del *microarray*. D'aquesta manera, es va dur a terme la modulació de superfícies de vidre amb grups alquenil i alquinil per a l'ancoratge de sondes de oligonucleòtids mono i multitolades mitjançant les reaccions de foto ancoratge del tiol-doble enllaç i tiol-triple enllaç, respectivament. Les superfícies modificades amb el silà més hidrofòbic (alquinil) i les sondes politiolades ancorades, van revelar els millors rendiments. Aquests sistemes de *microarrays* es van aplicar a la discriminació de SNPs i a la detecció de productes de PCR de bacteris.

En el quart capítol, es realitza un disseny racional per a la preparació de *microarrays* d'anticossos. L'enfocament d'immobilització mostra l'ancoratge orientat dels fragments

d'anticossos que contenen el grup tiol sobre superfícies de vidre alquenilades mitjançant reacció de foto ancoratge del tiol-doble enllaç. D'aquesta forma, es demostra la detecció multiplexada de biomarcadors cardíacs. El *microarray* dissenyat mostra una major capacitat de reconeixement en comparació amb els *microarrays* d'anticossos complets.

En el cinqué capítol, s'ha desenvolupat una nova metodologia per a millorar l'ancoratge de oligonucleòtids tiolats. Donat l'interés de modificar superfícies altament hidròfobes, s'estableix una nova reacció fotoinduïda. Gràcies a les característiques de l'anomenada "reacció de fotoacoplament de fluor-tiol", es va aconseguir la immobilització de sondes tiolades a superfícies que contenen enllaços C-F d'una manera ràpida, fàcil i biocompatible amb medis aquosos. La hidrofobicitat de les superfícies es va controlar per a obtenir bones hibridacions reeixides. A causa de l'alta hidrofobicitat de les superfícies, s'aconsegueix un gran confinament de les sondes, la qual cosa permet l'aproximació dels anàlits únicament on està unida la sonda i manté una alta repulsió en la superfície restant. Les superfícies de vidre perfluorades van millorar les densitats d'immobilització i la capacitat de detecció, respecte a les superfícies alquenilades i alquilades, i també van permetre la discriminació de SNPs i la detecció de productes de PCR bacterians.

En el sisé capítol, s'exploraven altres superfícies diferents al vidre. Per tant, membranes de fluorur de polivinilidè es van emprar com a substrats per al desenvolupament de *microarrays* d'oligonucleòtids. Per a això, es va desenvolupar un procés de funcionalització ràpid, fàcil i suau, mitjançant l'ús d'irradiació UV i la química dels organosilans. Després, es van aplicar aquestes membranes funcionalitzades amb grups alquenil i sense funcionalitzar a la tecnologia de *microarrays* mitjançant ancoratge covalent a través de les reaccions de foto ancoratge de tiol-doble enllaç i fluor-tiol, respectivament. Es van obtenir resultats prometedors amb totes dues superfícies.

En resum, la modulació de la resposta química dels substrats i els procediments d'ancoratge són les dues claus per a millorar la tecnologia de *microarrays*. Aquest treball ha contribuït al progrés de noves plataformes de *microarrays* i al desenvolupament d'una nova reacció fotoinduïda. Finalment, la troballa de la reacció de fotoacoplament de fluor-tiol, aplanava el camí per a construir dispositius més sensibles, la qual cosa millora el rendiment del bioassaig. A més, proporciona una alternativa nova per a la modificació superficial.



## DISSEMINATION OF RESULTS

The results derived from this thesis have led to the follow scientific contributions.

*Published articles in indexed scientific journals:*

1. Jiménez-Meneses, P.; Bañuls, M.-J.; Puchades, R.; Maquieira, Á. Novel and Rapid Activation of Polyvinylidene Fluoride Membranes by UV Light. *React. Funct. Polym.* **2019**, *140*, 56–61.

DOI: 10.1016/j.reactfunctpolym.2019.04.012

Category of the journal: POLYMER SCIENCE

Impact factor (5 years): 2.975

Relative position: 18/87 (Q1)

2. Jiménez-Meneses, P.; Bañuls, M.-J.; Puchades, R.; Maquieira, Á. Fluor-Thiol Photocoupling Reaction for Developing High Performance Nucleic Acid (NA) Microarrays. *Anal. Chem.* **2018**, *90* (19), 11224–11231.

DOI: 10.1021/acs.analchem.8b00265

Category of the journal: CHEMISTRY, ANALYTICAL

Impact factor (5 years): 6.035

Relative position: 4/80 (Q1)

3. Alonso, R.; Jiménez-Meneses, P.; García-Rupérez, J.; Bañuls, M.-J.; Maquieira, Á. Thiol–Ene Click Chemistry towards Easy Microarraying of Half-Antibodies. *Chem. Commun.* **2018**, *54* (48), 6144–6147.

DOI: 10.1039/C8CC01369A

Category of the journal: CHEMISTRY, MULTIDISCIPLINARY

Impact factor (5 years): 6.29

Relative position: 28/ 171 (Q1)

## *Dissemination of results*

4. Bañuls, M.-J.; Jiménez-Meneses, P.; Meyer, A.; Vasseur, J.-J.; Morvan, F.; Escorihuela, J.; Puchades, R.; Maquieira, Á. Improved Performance of DNA Microarray Multiplex Hybridization Using Probes Anchored at Several Points by Thiol–Ene or Thiol–Yne Coupling Chemistry. *Bioconjug. Chem.* **2017**, 28 (2), 496–506.

DOI: 10.1021/acs.bioconjchem.6b00624

Category of the journal: BIOCHEMICAL RESEARCH METHODS

Impact factor (5 years): 4.485

Relative position: 10 / 79 (Q1)

## *Communications in national and international conferences:*

1. Jiménez-Meneses, P.; Bañuls, M.-J.; Puchades, R.; Maquieira, A., “*Thiol-photoclick reactions for polyvinylidene fluoride membranes biofunctionalization*”, XIII International Workshop on Sensors and Molecular Recognition, Valencia (Spain), **2019**.
2. Jiménez-Meneses, P.; Bañuls, M.-J.; Puchades, R.; Maquieira, A., “*Photochemical anchoring of thiolated nucleic acids to C-F bond on surfaces for microarraying*”, XII International Workshop on Sensors and Molecular Recognition, Burjassot (Spain), **2018**.
3. Gonçalves, O.; Bañuls, M.-J.; Alonso, R.; Jiménez-Meneses, P.; Maquieira, A., et al., “*Photonic immobilization techniques used for the detection of cardiovascular disease biomarkers*”, SPIE Photonics Europe 2018, Strasbourg, (France), **2018**.
4. Jiménez-Meneses, P.; Bañuls, M.-J.; Puchades, R.; Maquieira, A., “*Application of a perfluorinated surface to the discrimination of single nucleotide polymorphisms and bacterial DNA detection*”, XXI Reunión de la Sociedad Española de Química Analítica, Valencia (Spain), **2017**.
5. Jiménez-Meneses, P.; Bañuls, M.-J.; Puchades, R.; Maquieira, A., “*A new reaction for the development of nucleic acids microarrays onto glass slides*”, XI International Workshop on Sensors and Molecular Recognition, Valencia (Spain), **2017**.

6. Bañuls, M.-J.; González-Lucas, D.; Jiménez-Meneses, P.; Alonso, R.; Puchades, R.; Maquieira, A., “*La modificación química como herramienta de modulación de propiedades superficiales para la construcción de biosensores ópticos de altas prestaciones*”, XXXVI Reunión Bienal de la Real Sociedad Española de Química, Sitges (Spain), **2017**.
7. Strasser, F.; Melnik, E., Muellner, P.; Jiménez-Meneses, P.; Nechvile, M.; Koppitsch, G.; Lieberzeit, P.; Laemmerhofer, M.; Heer, R.; Hainberger, R., “*Preparation of Mach-Zehnder interferometric photonic biosensors by inkjet printing technology*”, SPIE Optics + Optoelectronics 2017, Prague (Czech Republic), **2017**.
8. Morvan, F.; Bañuls, M.-J.; Jiménez-Meneses, P.; Meyer, A.; Vasseur, J.-J.; Escorihuela, J.; Puchades, R.; Maquieira, A., “*Improved DNA Microarray Hybridization Using Polythiol Probes and their Immobilization by Thiol-Ene Chemistry*”, XXII International Roundtable on Nucleosides, Nucleotides and Nucleic Acids, Paris (France), **2016**.
9. Jiménez-Meneses, P.; Bañuls, M.-J.; Puchades, R.; Maquieira, A., “*Controlled hydrophobicity of surfaces for developing microarrays by covalent anchoring*”, X International Workshop on Sensors and Molecular Recognition, Burjassot (Spain), **2016**.
10. Jiménez-Meneses, P.; Bañuls, M.-J.; Puchades, R.; Maquieira, A., “*Superficies mejoradas para el desarrollo de microarrays por anclaje covalente*”, IX International Workshop on Sensors and Molecular Recognition. Valencia (Spain), **2015**.
11. Bañuls, M.-J.; Jiménez-Meneses, P.; Puchades, R.; Maquieira, A., “*Anclaje de sondas tioladas sobre una superficie perfluorada mediante reacción de “química click”. Obtención de microarrays con mejores prestaciones*”, XX Reunión de la Sociedad Española de Química Analítica, Santiago de Compostela (Spain), **2015**.





**ACRONYMS AND ABBREVIATIONS**

Ab	Antibody
AFM	Atomic Force Microscopy
APTES	3-Aminopropyltriethoxysilane
AR	Anomalous Reflection of Gold
BSA	Bovine Serum Albumin
DNA	Deoxyribonucleic Acid
cDNA	Complementary Deoxyribonucleic Acid
CuACC	Copper(I)-Catalyzed Alkyne-Azide Cycloaddition
Cy3	Cyanine 3
Cy5	Cyanine 5
dsDNA	Double Strand Deoxyribonucleic Acid
DPI	Dual Polarization Interferometry
Fab	Antigen-Binding Fragment
Fc	Crystallizable Fragment
Fs-laser	Femtosecond Laser
Fv	Variable Fragment
GOPTS	(3-Glycidyloxypropyl)trimethoxysilane
hIgG	Half Immunoglobulin G
HRP	Horseradish Peroxidase
IgG	Immunoglobulin G
kDa	Kilodaltons
$\lambda_{exc}$	Excitation Wavelength
$\lambda_{em}$	Emission Wavelength
LSPR	Localized Surface Plasmon Resonance
mRNA	Messenger Ribonucleic Acid
MS	Mass Spectrometry
NA	Nucleic Acid
NHS	N-hydroxysuccinimide

*Acronyms and abbreviations*

OPD	o-Phenylenediamine Dihydrochloride
PBS	Phosphate Buffer Saline
PCR	Polymerase Chain Reaction
PDMS	Polydimethylsiloxane
PEGS	2-[Methoxy(polyethyleneoxy) <sub>6-9</sub> propyl]trimethoxysilane)
PFTS	1H,1H,2H,2H-Perfluorodecyltriethoxysilane
PTFE	Polytetrafluoroethylene
PVDF	Polyvinylidene Fluoride
QCM	Quartz Crystal Microbalance
RSD	Relative Standard Deviation
SERS	Surface-Enhanced Raman Scattering
SFR	Surface Fluorescence Reader
SNPs	Single Nucleotide Polymorphisms
SPR	Surface Plasmon Resonance
SSC	Saline Sodium Citrate
TCA	Trichloroacetic acid
TCEP	Tris(2-carboxyethyl)phosphine hydrochloride
TE	Transverse Electrical
TEC	Thiol-ene Coupling
TF	Transcription factor
THF	Tetrahydrofuran
TM	Transverse Magnetical
TMB	3,3',5,5'-Tetramethylbenzidine
TYC	Thiol-yne Coupling
UV	Ultraviolet
UVOH	UV-Ozone Surface Cleaner
Vis	Visible
VTES	Vinyltriethoxysilane
WCA	Water Contact Angle
XPS	X-Ray Photoelectron Spectroscopy

## TABLE OF CONTENTS

<b>1. Introduction .....</b>	<b>1</b>
1.1 Microarray technology .....	4
1.2 Considerations in microarray fabrication .....	7
1.2.1 Nature of recognition probes and targets .....	7
1.2.2 Nature of the solid substrates .....	12
1.2.2.1 Surface functionalization .....	14
1.2.3 Probe patterning techniques .....	18
1.2.4 Detection mode .....	21
1.3 Anchoring strategies.....	24
1.3.1 Photoinduced reactions and click chemistry .....	30
1.3.1.1 Thiol-ene and thiol-yne reactions .....	32
1.3.1.2 Fluor-thiol photoclick reaction .....	35
1.4 References .....	38
<b>2. Objectives .....</b>	<b>49</b>
<b>3. Probe multiattachment by thiol-ene and thiol-yne coupling reactions for oligonucleotide microarrays .....</b>	<b>53</b>
3.1 Improved performance of DNA microarray multiplex hybridization using probes anchored at several points by thiol-ene or thiol-yne coupling chemistry .....	57
<b>4. Application of thiol-ene coupling reaction for the preparation of half antibodies' microarrays .....</b>	<b>99</b>
4.1 Thiol-ene click chemistry towards easy microarraying of half-antibodies .....	103
<b>5. A novel photocoupling reaction between C-F bonds and thiol groups and its application to microarray technology .....</b>	<b>121</b>
5.1 Fluor-thiol photocoupling reaction for developing high performance nucleic acid (NA) microarrays.....	125
5.2 Study of other irradiation sources for improving the performance of the fluor-thiol reaction .....	155
5.3 Study of microstructuration for the improved performance of oligonucleotide microarray performance .....	173

*Table of contents*

<b>6. Thiol-click reactions for oligonucleotide microarrays onto polyvinylidenfluoride membranes .....</b>	<b>183</b>
6.1 Thiol-click reactions for oligonucleotide microarrays onto polyvinylidenfluoride membranes .....	187
<b>7. Conclusions and perspectives .....</b>	<b>213</b>
<b>8. Annexes.....</b>	<b>219</b>

# **1. Introduction**



## 1. Introduction

*“Many techniques are available to provide information about the matter but no one analytical technique provides all the answers” Adapted from Susan Garrett's presentation.*

During centuries, the curiosity of human being to well understand the nature of the matter has led to the development of numerous analytical techniques. Despite the many advances made since antiquity to elucidate its composition, structure, physical properties, and reactivity, many authors agree with the great shift that all the chemistry and especially the analytical chemistry gave in the 1960s. This fact was mainly occurred due to the transition from the classical to the instrumental analysis. Unlike the classical analytical methods, in which a chemical reaction produces an appreciable physical change in the sample, the instrumental methods are based on the signal related to the analyte nature and quantity. This produced huge progress in the way to analyze the matter and allowed faster detections and much better sensitivity. In this period, a great improvement in the development of numerous separative, spectral and electroanalytical techniques, and the coupling between them was produced.<sup>1</sup> As a consequence, the separation, identification, and quantification of an analyte could be often performed with the same instrument. Nonetheless, it must be considered that this breakthrough has been largely achieved thanks to the revolution of computers in the early '80s. Following that time, another key tool was incorporated into knowledge by fusing biological and chemical techniques, which led to the creation of biochemical and biosensing methodologies.

It must be pointed out that all these advances have been carried out to respond to the needs and challenges that occur in society. Therefore, this growth is a permanent task to encompass the new necessities. Nowadays, there is a need to develop new analytical tools to detect the desired analytes within a complex sample. Properties as fastness, sensitivity, selectivity, robustness, size of the measuring device, reliability, reproducibility, multiplexability, simplicity, portability and cost-effectiveness, are required to reach an affordable methodology for detection and determination of targeted analytes. Besides, minimum sample pretreatment is important. Taking into account all the trailed parameters, there are many approaches to accomplish these features, but there are a lot of avenues to go and discoveries to be made.

## *Introduction*

Regarding these challenges, microarray technology emerges as an opportunity to embrace all these science branches (chemistry, biology, materials) and technology tools, as it enables multiplexed, high throughput analysis using small volumes of sample, miniaturization, and use of different detection modes, among others.

All the features involved in the microarray are of outmost importance to improve the performance of such devices, from the solid substrate to the detection and data analysis. Therefore, the main aspects of microarray technology will be introduced, being the surface properties modulation and the immobilization approaches the most challenging tasks. Regarding the substrate modulation, surface properties are adjusted to the probes to be analyzed, given its importance in the applicability of the system. Also, many of the results demonstrated to microarraying can be applied to other assay formats, materials and detection strategies.

### **1.1 Microarray technology**

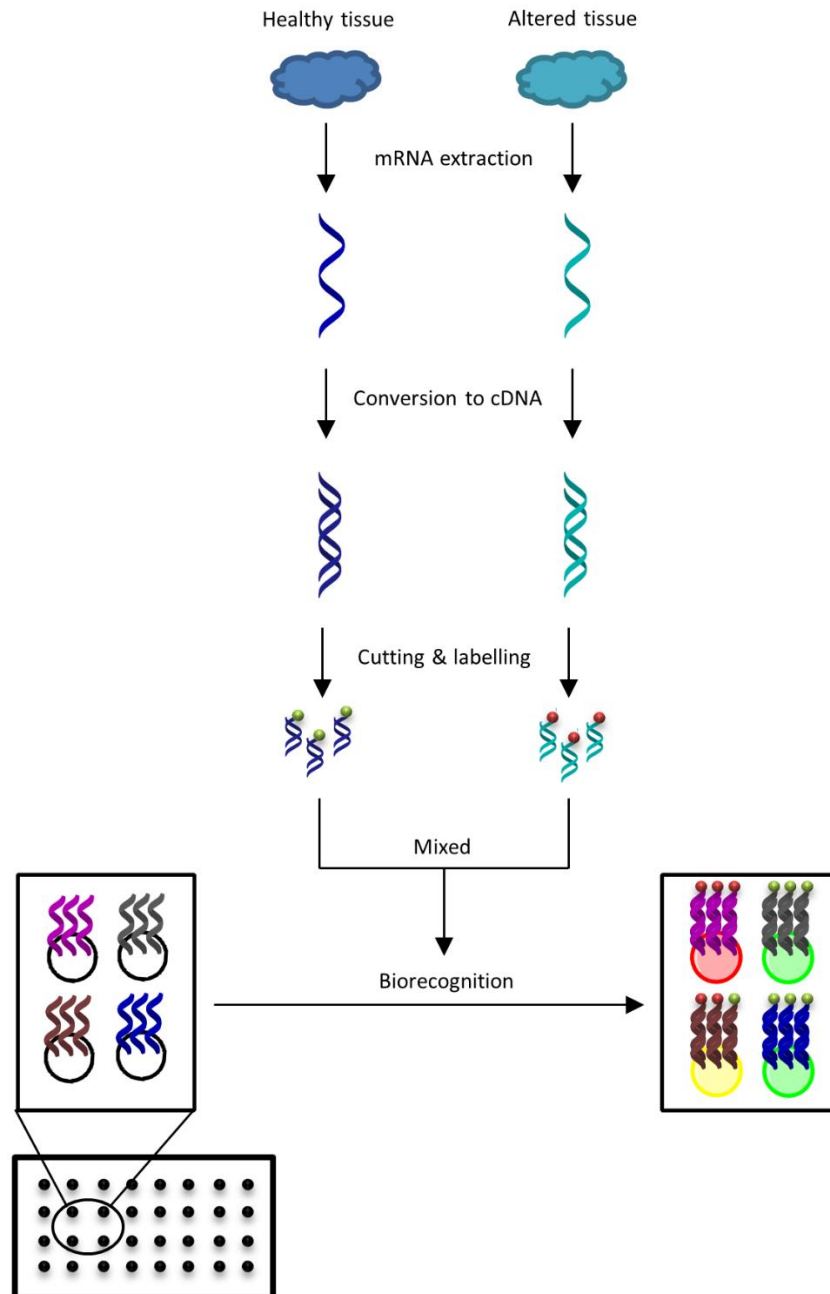
Microarray technology is a term that denotes the miniaturization of thousands of assays in a small space.<sup>2</sup> Thus, a microarray is merely an orderly arrangement of probes attached to a solid surface (Schna 1995).<sup>3</sup> This fundamental principle was developed from an earlier concept called ambient analyte immunoassay, which was first presented by Roger Ekins in 1989.<sup>4</sup> This theory stated that a tiny spot of purified antibody is able to detect analytes with a higher sensitivity than conventional macroscopic immunoassays.<sup>5</sup>

Since the emergence of microarray technology, many advances have been reached. Due to the huge versatility and good properties, numerous researchers have taken its advantages for application to biomedical, agricultural, food and environmental fields, among others.<sup>6-8</sup>

Although there are many approximations in microarray technology development, the working mode of a DNA microarray applied to gene expression analysis is displayed as an example. This methodology is based on the principle that complementary sequences will bind to each other. The use of this approach lets to compare the genetic information of two samples (i.e. infected or altered and healthy samples). Therefore, messenger ribonucleic acid (mRNA) is extracted from the tissues and converted to the more stable complementary deoxyribonucleic acid (cDNA). These long cDNA sequences are cut into smaller fragments and labeled with a marker, most frequently a fluorescent one. Then,



hybridization takes place onto the microarray substrate, which contains up to thousands of specific capture sequences. Complementary sequences bind to each other and the unpaired sequences are washed out. After reading, the fluorescence data are studied (Figure 1).

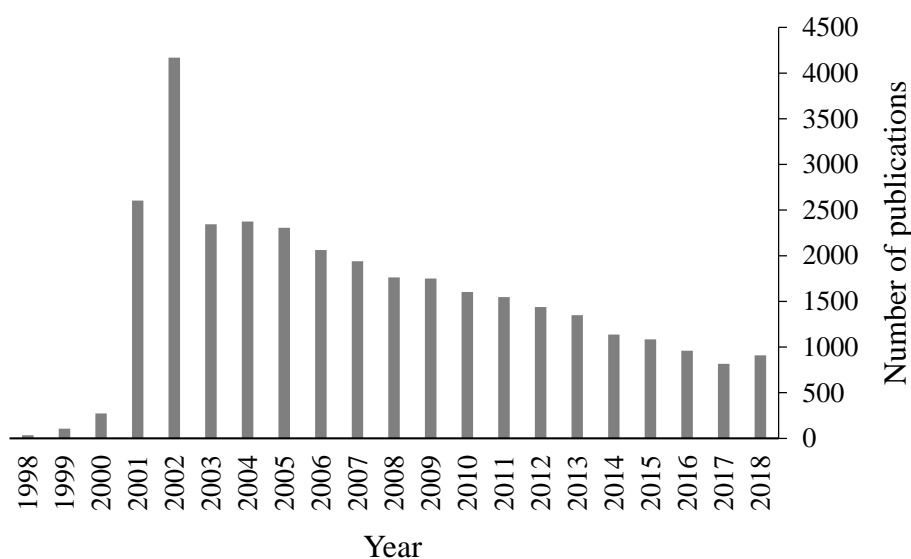


**Figure 1.** Typical working of a DNA microarray using fluorescence as a detection system. Every spot of the microarray contains a specific sequence. Complementary sequences will bind to each other, allowing the DNA identification and quantification.

## Introduction

As presented in the layout, a biorecognition event occurs in a heterogeneous format, which means that more than one phase is involved in the process, unlike the homogeneous assays in which the receptor and target are in the same phase (generally in solution).

Microarray technology has faced numerous challenges since its establishment, but it is still a very useful and powerful technique for many fields. The interest of researchers on the microarray technology and development remains high, attending to the number of publications on this topic. Figure 2 shows that this technology is mature and well consolidated.



**Figure 2.** The number of publications per year in nucleic acid microarray technology since 1998. Data was extracted from SciFinder resources by searching the concept microarray, refining in the nucleic acid field, and categorizing by year.

In addition, this technology shows numerous applications related to nucleic acids analysis, among others. Thus, it can be used in proofs-of-concept, discrimination of SNPs, detection of bacterial PCR products, biomarkers recognition, allergen identification, among many other procedures to be explored.

In the next sections, the main aspects implicated in the preparation and working mode of the microarrays will be discussed.

Annex 1, shows a scheme of microarray methodology, that can be useful during the reading of this thesis for a better understanding of microarray technology.

## 1.2 Considerations in microarray fabrication

Design and fabrication of a microarray assay system is not an easy task, as numerous obstacles and challenges must be overcome. Thus, to follow the most appropriate methodology in the development of a microarray assay, a previous design of the procedure is required. In this section, the main aspects to be considered are discussed: the nature of recognition probes and targets, the nature of substrates, and patterning and detection techniques (Figure 3).



**Figure 3.** Parameters to consider in the fabrication and design of a microarray.

### 1.2.1 Nature of recognition probes and targets

The selection of the proper probe is crucial in the development of microarray assays. The capacity of the receptor to recognize an analyte within a complex sample will strongly determine the performance of the microarray. Parameters as a high affinity towards the target, elevated selectivity to avoid unspecificity, and stability to conserve the activity intact, are required capabilities of the receptors.

Below, microarray classification based on the nature of the probes used is established. Although different receptors are extensively employed for the fabrication of microarrays (such as nucleic acids, proteins, tissues, carbohydrates, peptide, etc.),<sup>9</sup> DNA and protein are the most studied and applied microarrays and will be displayed in this overview of the state of the art.

DNA microarrays are based on the sequence complementarity of two strands of nucleic acids, which allows the detection of specific sequences, and it is the most investigated microarray to date.

Protein microarrays are based on probe interaction with different substances from low molecular chemicals to biomolecules such as proteins, peptides, DNA, and microorganisms (microbes, viruses, etc.). Thus, studying these interactions provides

## Introduction

information to establish the activity and the function of diverse systems. Within protein microarrays, many receptors are used, being immunoassay microarrays those studied in this work.

Then, more detail will be paid in DNA and antibody microarrays.

### I. DNA microarrays

Sustained by the huge advance in genome sequencing projects, DNA microarray technology became the pioneer application of this field. Thanks to the completion of the whole human sequencing, that encodes approximately 18,000 different genes, DNA microarrays have been extensively developed in fields as gene expression profiling, and genotyping, among others.<sup>10</sup> The fundamentals of hybridization (complementary base-pairing) were established by Ed Southern in 1975.<sup>11</sup> DNA technology determines mRNA expression levels of thousands of genes in parallel, however, this technology possesses some limitations because mRNA profiles do not always correlate with protein expression.<sup>2,12-14</sup> In addition, many parts of the genes have unknown or little-known functions that can even be vital for the human being.

DNA microarrays can be classified into two main systems, oligonucleotides and double-stranded DNA (ds-DNA) microarrays:<sup>15</sup>

- Oligonucleotide microarrays employ single oligonucleotide probes that can be directly spotted or *in situ* synthesized (see section 1.2.4). These can be divided into short oligonucleotides (around 25-30 mer) and long oligonucleotides (around 70-80 mer).<sup>16</sup>
- dsDNA microarrays employ dsDNA probes made with double-stranded DNA molecules and are amplified by enzymatic reactions such as polymerase chain reaction (PCR). dsDNA probes are derived from known genomic sequence, shotgun library clones, or cDNA and are  $\geq 500$  bases in length.<sup>3,10</sup> This approach allows the detection of transcription factors (TFs) or DNA sequences. In the last case, the double-strand is denatured in the printing buffer or after immobilization to allow the hybridization with a complementary sequence.<sup>10</sup>

Some controversy is found regarding which system is more appropriate. There are studies comparing results using these two types of probes and investigating optimal probe length and number of oligonucleotide probes needed to achieve reliable expression data.<sup>15,17,18</sup>

It is demonstrated that short oligonucleotides increase the selectivity and decrease the sensitivity, unlike long oligonucleotides or dsDNA. Thus, the detection of polymorphisms is more affordable by using shorter oligonucleotides. To counteract the lower sensitivity of short oligonucleotides, the inclusion of a spacer in the probe to be anchored is a common procedure as it usually improves the hybridization signal.<sup>10</sup> It is important to note that the design of probes is key to get successful results and avoid false positives due to non-specificity.

To avoid misunderstanding, in DNA microarray, nucleic acid anchored to the surface are called probes, while nucleic acids to be detected are named targets.

## II. Antibody microarrays

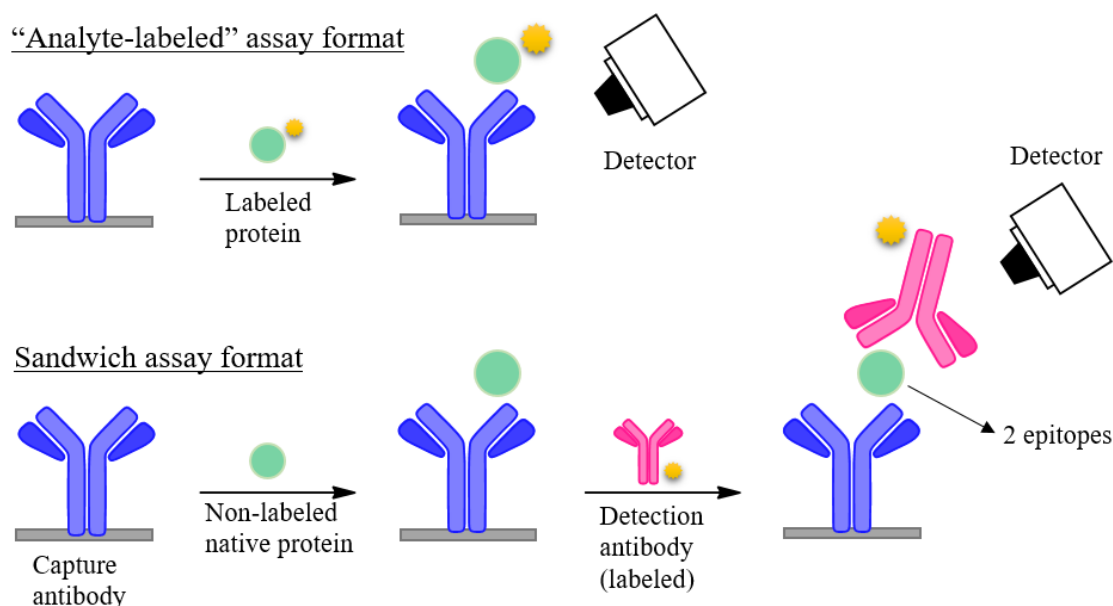
These systems are a specific form of protein microarrays, being the most representative model of analytical protein microarrays. These take advantage of the high selectivity that the antibodies present towards their antigen, the procedure is known as immunoassay.

Antibody microarrays are an alternative to routine ELISA plate procedures since analysis times can be considerably reduced, increasing the working capacity.<sup>19</sup>

The first immunoassay was developed in the 1950s becoming one of the most representative biorecognition assays.<sup>2,20</sup> Immunoassays can be classified into a homogeneous and heterogeneous format. Heterogeneous immunoassays are produced in the interface, between the solid support and the solution. Therefore, the analyte and matrix can be separated. Homogeneous assays do not require physical separation between the analyte and the matrix; thus, interactions take place in the same phase.

The nature of the antibody microarrays involves a heterogeneous format. Although there are direct and indirect competitive assays, non-competitive methods are presented here. In Figure 4, the main formats for antibody microarray recognition, “analyte-labeled” and sandwich assay, are displayed. “Analyte-labeled” assays allow direct detection of the proteins present in the samples. However, it requires the labeling of all the proteins in the sample. While, sandwich setup can improve the selectivity and sensitivity of the microarray, as a labeled secondary antibody recognizes a second epitope of the native protein.<sup>2</sup>

## Introduction



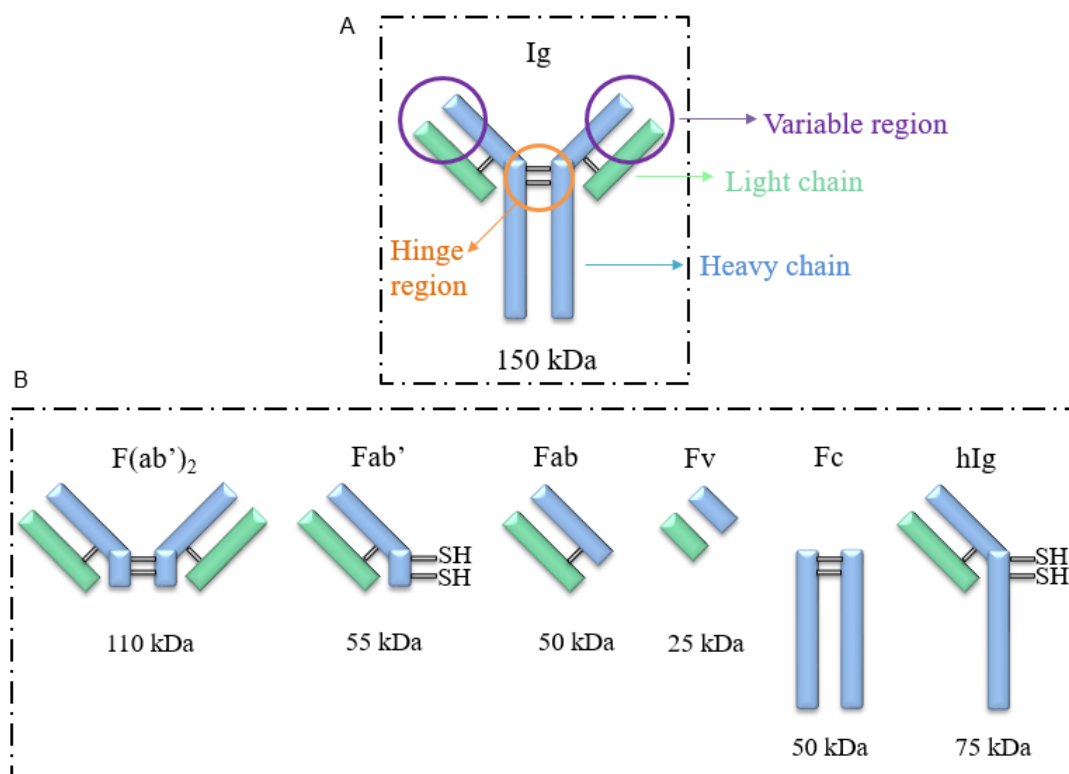
**Figure 4.** Two heterogeneous and non-competitive formats of antibody microarrays are presented: “analyte-labeled” and sandwich assays.

To better understand these methods, a brief introduction of antibody nature and properties is done. An antibody is an immunoglobulin (Ig) protein that comprises two identical pairs of heavy and light chains. It contains a variable region whose paratope recognizes the epitope of its antigen and a constant fraction. To form the basic structure of the antibody, the light chain is bound to a heavy chain and the heavy chain is bound to the other heavy chain (hinge region) through disulfide linkage and non-covalent forces such as hydrogen bonds and hydrophobic interactions (Figure 5).

The structural and molecular composition of the antibody varies depending on the class/isotype (e.g. IgA, IgD, IgG) and even in the subclass (e.g. IgG1, IgG2a, IgG2b, IgG3 and IgG4). Type G, expressed in mammals, is the most typical kind of immunoglobulins used in immunoassays. Its molecular weight is approximately 150 kDa and its molecular dimension is around  $142 \times 85 \times 45 \text{ \AA}^3$ . Even though, these proteins possess different functional groups in its chemical composition (e.g. carboxyl, amine, hydroxyl, sulfhydryl, alkyl, and aryl), molecular engineering modification to improve the anchoring capacity of the antibodies is usually undertaken.

Nevertheless, to accomplish the development of this format assay, attachment of antibodies to a solid substrate is necessary. However, a lack of oriented anchoring, loss of activity, and low immobilization density of the receptors are often observed. Hence, it is important to develop techniques to overcome these limitations.<sup>21,22</sup>

Numerous studies compare random and oriented immobilization of antibodies over the surfaces, demonstrating that oriented anchoring usually provides better recognition capacity.<sup>21,23</sup> For that, an oriented linking of the antibodies is pursued. However, it is hard to anchor such as huge biomolecules with little reactive and accessible groups. Thus, reduction of the antibodies into smaller fragments, using organic reagents or enzymes, and oriented immobilization, are the last tendencies in the fabrication of antibody microarrays.<sup>19,22,24,25</sup> Then, an explanation of the main available antibody fragments is shown in Figure 5.



**Figure 5.** A. Schematic structure of an IgG antibody. B. Classification of the different antibody fragments derived from the selective reduction of whole antibodies molecules. Data from Thermo Scientific resources. (<https://www.thermofisher.com/es/es/home/life-science/antibodies/antibodies-learning-center/antibodies-resource-library/antibody-methods/antibody-fragmentation.html>).

- F(ab')<sub>2</sub> fragments (110 kDa) contain the two antigen-binding regions (paratopes) linked through the disulfide bonds of the hinge region. Thus, it holds a small portion of the Fc region.
- Fab' fragments (55 kDa) comprise an only antigen-binding fragment, and free thiol groups remain in its structure. As it can be obtained by the reduction of F(ab')<sub>2</sub>, it may contain a slight amount of Fc fragment.

## *Introduction*

- Fab fragments (50 kDa) are similar to Fab', excepting the free thiol motifs and the portion of Fc.
- Fv fragments (25 kDa) comprises only the variable region of an antibody. They are the smallest fragment of an antibody and tend to dissociate easily due to the weak interactions (non-covalent bonding) that held both chains together.
- Fc fragments (50 kDa) display different functions as fixation among others and it is easy to crystallize. This region is called a constant fragment, and it does not have antigen-binding activity.
- hIgG fragments (75 kDa) are composed of a heavy and a light chain. When IgGs are exposed to selective reduction, disulfide bonds from the hinge region are fragmented, and two molecules of half IgGs with free sulfhydryl groups are produced. Note that disulfide bonds of hinge region are more accessible and easier to reduce, but especial care must be paid to avoid over reduction.

As seen before, hIgG and Fab' fragments display free thiol groups after reduction, which provide new functionality for its application to microarray technology. Selective reduction at the hinge region, to get hIgG fragments, and later oriented anchoring through free thiol groups, shows an interesting strategy to immobilize active and accessible epitopes and its application to microarray assays.

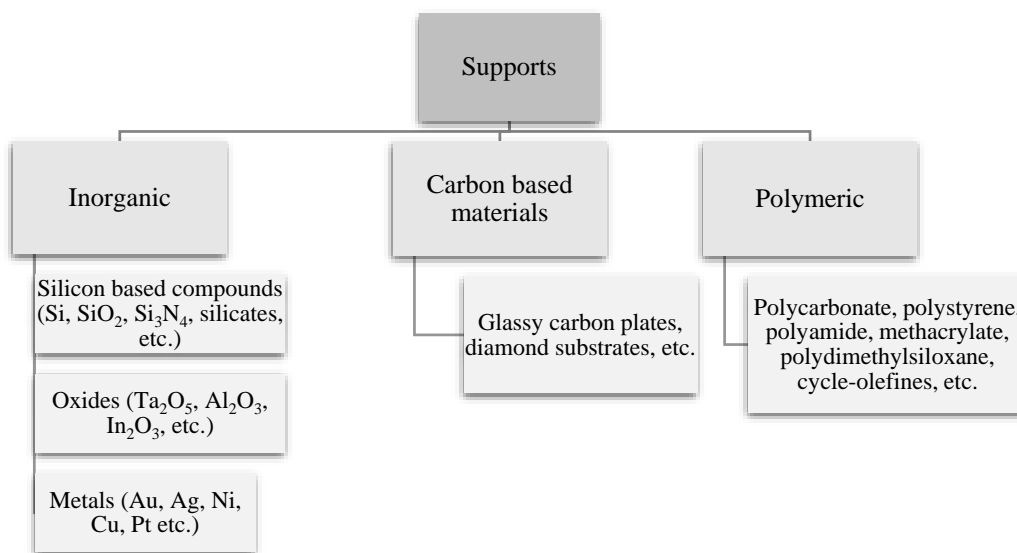
### **1.2.2 Nature of the solid substrates**

Nature of the material, where the interaction probe-target occurs, is of great interest in the development of microarray technology, as chemical and physical properties of the surfaces will determine the performance of the definitive microarray assay.

The solid support is the material area onto which the microarray is formed, and its role is critical to achieving an effective and reliable microarray patterning, and successful biorecognition. At this point, two aspects must be taken into account, the substrate and the functionalization layer. On the one hand, the nature of the substrate will determine the potential modification approximations of its surface. In addition, intrinsic properties such as autofluorescence and resistance will define further developments and applications. On the other hand, modification of the substrate will provide diverse functionalities and properties to the surface support. Properties as wettability and surface free energy will mainly control the quality of the spots.<sup>26</sup>

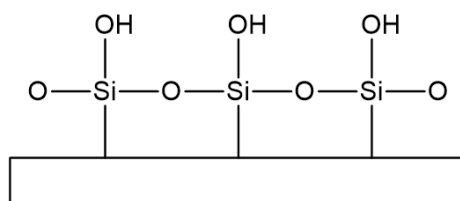


Because of the wide applicability of microarray technology, numerous substrates such as polymers, gold, carbon-based substrates, silicon-based materials on different presentations, have been investigated as supports for microarray production<sup>27</sup> (Figure 6). Between them, glass slides are the most extensively used platforms.



**Figure 6.** Classification of substrates for application to microarray technology.

Its intrinsic properties and the wide availability of glass in research laboratories provided a wide expansion of this material since the early 1990s. Properties as low fluorescence, excellent surface flatness, chemical durability, inertness, and low cost, make it a very appropriate surface for microarray technology.<sup>28,29</sup> Because of fluorescence detection is commonly employed in microarray assays, the low intrinsic autofluorescence of this material is especially important. In addition, the chemical stability of this support provides a good capacity to bear harsh conditions in the fabrication of the microarray. Also, the simple functionalization process of this substrate is another advantage, which will be stated below (Section 1.2.2.1). In figure 7, the typical chemical structure representation of a glass slide is shown.



**Figure 7.** Surface chemical structure of a glass slide.

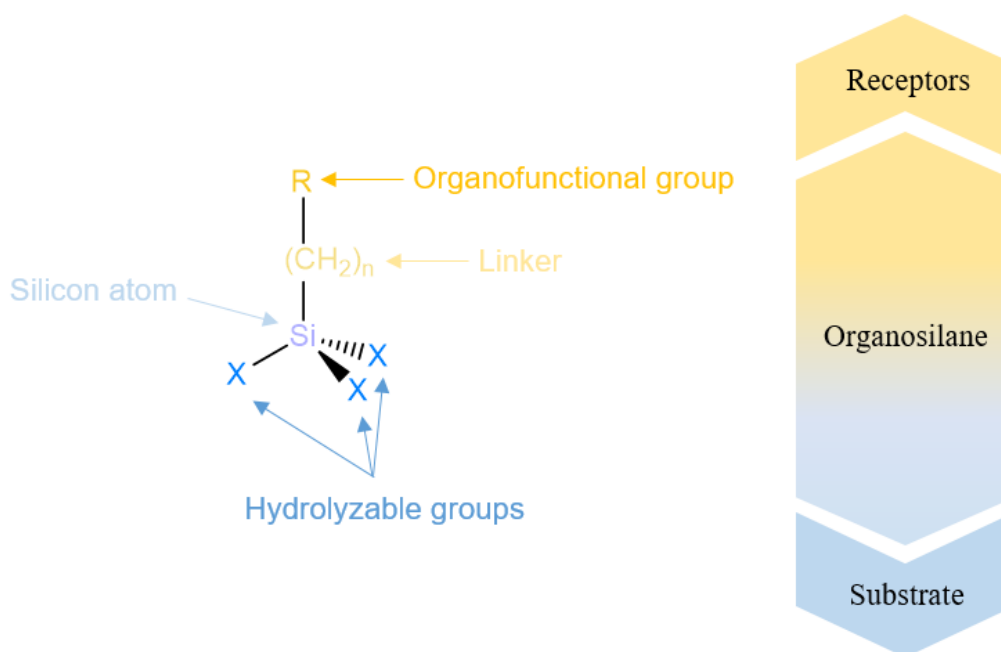
### ***1.2.2.1 Surface functionalization***

As seen previously, the modulation of substrate surface properties is often needed prior to the application of the platforms to microarray technology. Thus, substrates undergo a more or less complex process to acquire the desired features, as a direct immobilization of the probes is not usually attainable. Hence, functionalization using organosilanes (silanization) appears as a widely used approach for biosensor and microarray implementation.<sup>30</sup> This procedure has been extensively performed to modulate the properties of numerous substrates, such as silica-based materials, aluminum, copper, steel iron, and, of course, glass.

In addition, to dispose of the required functional groups over the surface to accomplish the anchoring of the probes, other parameters such as surface wettability and hydrophobicity will determine the proper working of the microarray, in terms of immobilization and biorecognition to provide highly sensitive and specific detection yields. Up to now, the most extended strategies consisted of the blocking of the whole biofunctionalized surface previous the biorecognition step, to avoid the unspecific interactions with the rest of the surface. However, the use of these blocking agents, such as BSA and other reagents, often gives rise to high background signals.<sup>6,31–33</sup>

At this point, two combined strategies appear as a solution to this problematic aspect. On the one hand, modification of surface wettability, using surface chemistry, to provide highly hydrophobic surfaces able to repel the unspecific adsorption, is pursued. On the other hand, effective anchoring of the bioreceptors to these surfaces is required. This way, confinement of the probes in very small and hydrophilic spots is achieved, which increases the immobilization densities of the receptors. This probe immobilization provides highly hydrophilic areas, only where the probes are linked, surrounded by a hydrophobic environment. Therefore, the analyte solution will be confined to these hydrophilic spots, which induces a specific approximation of the analyte to these regions, improving the sensitivity of the microarray.

Going into more detail in the functionalization process, organosilanes features are detailed below (Figure 8). These chemical reagents have three key elements: the organofunctional group, the hydrolyzable groups, and the linker.



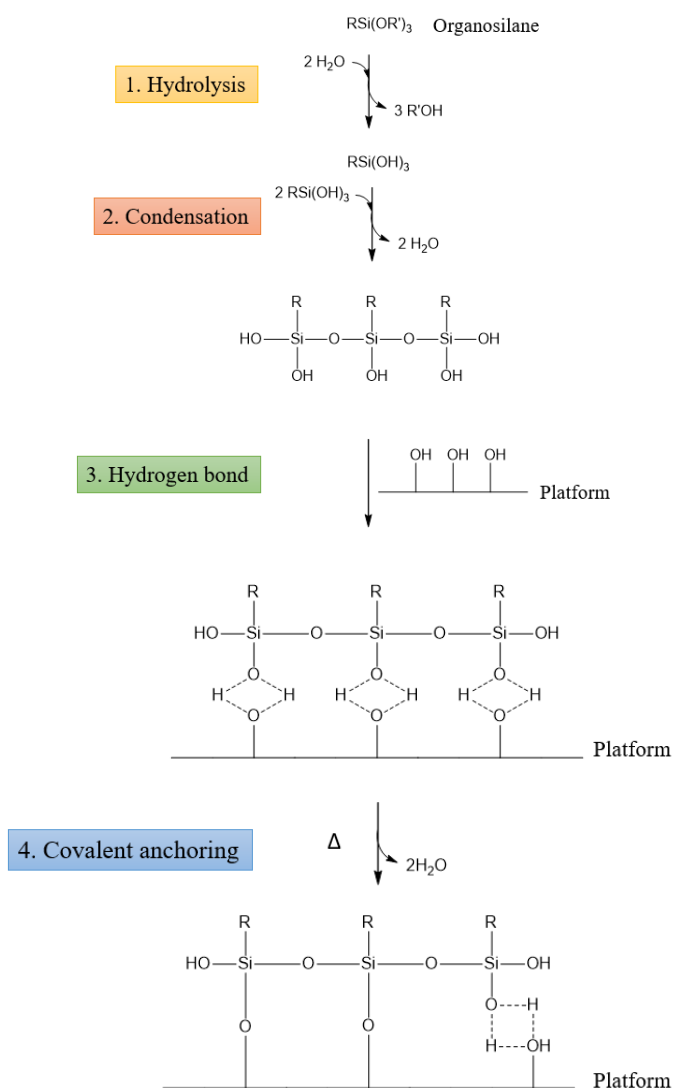
**Figure 8.** The general structure of an organosilane. These coupling agents act as a bridge between the substrate and the receptors to be immobilized.

- An organofunctional group is a non-hydrolyzable group that imparts the functionality desired to the substrate. It can be reactive (e.g. amine, epoxy, sulfur, methacrylate, etc.) or non-reactive (e.g. alkyl, fluoroalkyl).
- Hydrolyzable groups are divided into different categories, regarding their nature (alkoxy, acyloxy, halogen or silazane silanes), displaying distinctive chemical reactivity. Although alkoxy silanes are not the most reactive, methoxy and ethoxy silanes are the mostly used for surface modification, due to their easy handling, and low toxicity of byproducts. The function of these substituents is linking to the organic or inorganic substrate.
- The linker acts as a spacer between the silicon atom and the organofunctional group, being mainly an alkyl or aryl chain. Its length will directly affect the later applications. Although the typical linker length is three carbon atoms, due to the good synthetic accessibility and thermal stability of the propyl group, some works employ different lengths to favor the required features.<sup>34</sup>

Due to their dual reactivity, organosilanes work as a bridge between inorganic or organic substrates and organic/polymeric matrices. Here, we present organosilanes as the link between the platforms and the receptors of the microarray (Figure 8). Then, a detailed silanization procedure of a hydroxylated surface using trialkoxysilanes is shown in Figure

## Introduction

9.<sup>35</sup> This process involves four steps that can occur in a simultaneous way after the initial hydrolysis step, and can be controlled by acidic or basic catalysis.



**Figure 9.** Detailed silanization mechanism for the chemical modulation of surface properties.

1. Hydrolyzable groups undergo hydrolysis to form reactive silanol groups.
2. Silanols condense to form Si-O-Si motifs (oligomers).
3. Formed oligomers interact with the OH groups of the substrate toward hydrogen bonds.
4. Finally, a covalent bond is formed between the oligomers and the substrate during drying or curing, with loss of water. This permanent covalent bonding allows the use of these derivatives modulation of hydroxylated surfaces.

During the silanization process, only a bond from each silicon of the organosilane to the substrate is prone to occur, remaining two silanol groups in the interface (in its condensed

or free form), that can react with its neighbors. This lateral cross-linking between the molecules of organosilane leads to the formation of Self-Assembled Monolayers (SAMs)<sup>30</sup>. Parameters such as temperature, solvent, and water content, are critical in the silanization process, as they will determine the formation of a monolayer or a multilayer and its thickness. Therefore, an exhaustive control of the conditions must be done to get a stable, homogeneous, reproducible and optimal surface density of the silane layer, avoiding an uncontrolled polymerization. The suitable orientation of silane molecules will allow the proper SAM formation. Finally, the R group stays available for further interactions. Generally, that functionalization process is mainly performed by dip coating or chemical vapor deposition techniques.

There are many commercial organosilanes available in the market (i.e. Gelest <https://www.gelest.com/>, Dowsil <https://www.antala.uk/new-brand-name-for-dow-corning-dowsil/>). In addition, because of the importance of this support, glass slides modified with different functionalities are commercially available for microarray development, among others. Not only functionalized substrates with silanes, such as amine, aldehyde, and epoxy motifs are existing. Polymeric coatings with polydimethylsiloxane (PDMS), PVDF, nylon, nitrocellulose polymers are available, as well. Sputtering of the slides with metals such as Au, Ag, Al, Cr, Cu, Ni, Ti elements is also performed. Even chips with coatings of avidin, streptavidin, and protein A/G systems are sold. These are some of the extensively fabricated and commercialized glass slides for microarraying in several companies, (i.e. Arrayit Corporation <http://www.arrayit.com/>), and which are very helpful in research.

Another parameter to bear in mind is that hydroxyl groups are precise to undergo the silanization. Hence, the generation of these groups on the surface substrate prior to the functionalization process is required. Oxygen plasma and piranha solution treatments are mostly used for the activation process.<sup>36</sup> These oxidative procedures allow the cleaning of the surface, as well as, remove the organic pollutants present on the platform. Nevertheless, other activation methods are pursued to improve the process regarding times, toxicity and surface damage.

Besides the numerous works made about functionalization, Gelest guide<sup>37</sup> provides a complete material about the functionalization process, surface properties as hydrophobicity and hydrophilicity, kinds of organosilanes, and solve other additional questions about this modification process.

## *Introduction*

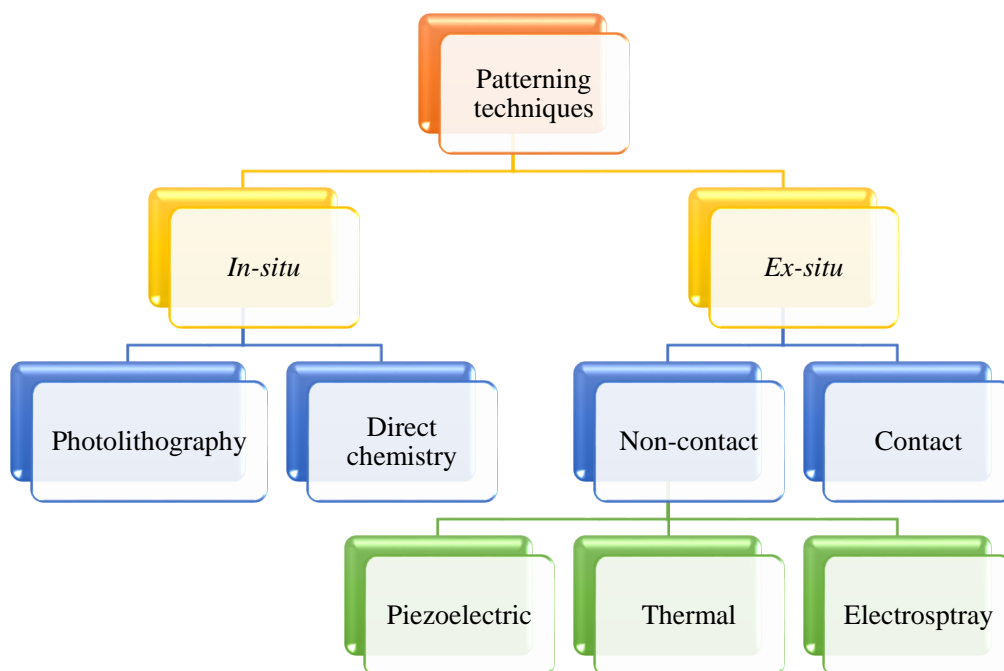
Even though it looks a simple procedure, much attention and care must be paid in the process to achieve homogeneous and good quality substrates in a reproducible way. The right functionalization will determine the later performance of the microarray, affecting hugely to the immobilization and biorecognition stages.

In addition to silanization, other chemicals such as organophosphonates,<sup>38</sup> dextran hydrogels<sup>39</sup>, and dendrimers,<sup>40</sup> which will not be reviewed here, provide interesting alternatives to the functionalization of glass slides with organosilanes.

### **1.2.3 Probe patterning techniques**

Patterning of the substrates is another key step necessary to prepare complex microarrays.<sup>6,9,10,41-44</sup> To achieve high density microarrays in a reproducible, reliable, robust and cost-effective manner is a demanding task. Spot uniformity takes place at this point, as a consistent size and shape of the spots are necessary, avoiding undesired phenomena as the coffee ring effect.<sup>45</sup> This event produces an accumulation of the probes in the border of the drops during the drying procedure, which produces bad quality microarrays. Thus, the microarray performance will be determined by controlling the factors that affect the homogeneity of the spots, such as the sample, the humidity, the substrate surface, the printing system, and its features, etc.

Regarding the probe to be immobilized, diverse strategies come into the fore. Figure 10 shows the available techniques mostly employed for patterning of the surfaces. Probe patterning techniques are divided into two big groups, *in-situ* and *ex-situ* or spotting ones.

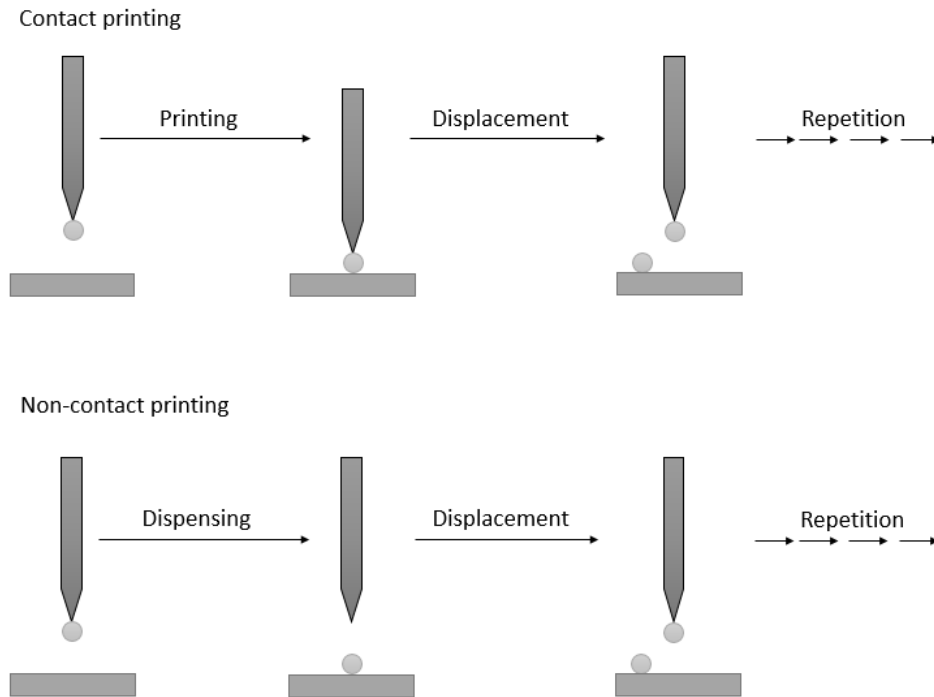


**Figure 10.** Most extensively used patterning techniques for microarray fabrication.

- *In-situ* preparations are performed through the base by base synthesis, and they can be divided into photolithography or direct chemistry. These techniques provide high density microarrays, with a good resolution, which improves the lower density and resolution of spotted microarrays. However, the design and fabrication of these techniques are more expensive and time consuming. In addition, they are less versatile as they are only suitable for short oligonucleotide sequences.

- *Ex-situ* or spotting techniques are based on the patterning of the probes over the surface, using robotic microarrayers. All these techniques are largely automatized and pursue the same goals: uniform deposition of small amounts of probes, reduction of probe consumption, and avoidance of contamination between probes. The volume delivered using these techniques is typically in the picoliter ( $10^{-12}$  L) or nanoliter ( $10^{-9}$  L) range, and allow low to moderate density microarrays. Nevertheless, there is no restriction in the sequence length, and they are cheaper than *in-situ* techniques. Within this procedure, two techniques are available for the deposition of the probes, and they are divided into contact and non-contact mechanisms.<sup>10,42,46,47</sup> Figure 11 shows a scheme of both processes.

## Introduction



**Figure 11.** Schematic representation of contact and non-contact printing procedures.

- A. Contact methods require direct contact between the platform and the deposition device. The most useful deposition devices are the tips, that can be solids or hollows, and the micro-stamps. This methodology is very simple, however, contamination and damage of the deposition device or the platform can be produced.
- B. Non-contact methods reduce the inconvenient of contact methods regarding contamination and damage. In addition, they provide higher throughput. Within this technique, several printing mechanisms as thermal, piezoelectric, and electrospray printing are available.

Then, a comparison between *in-situ* and *ex-situ* techniques is displayed in table 1, as the first ones are the most extensively employed in commercialized devices (e.g. Affymetrix chips).



**Table 1.** Advantages and disadvantages of the main microarray patterning methodologies.

	<b>Advantages</b>	<b>Disadvantages</b>
<b><i>In-situ</i> techniques</b> 3,10,46	Higher probe density Higher resolution	Cost and time-consuming design/fabrication Only for short oligonucleotides sequences
<b><i>Ex-situ</i> or spotting techniques</b> 10,42,46,47	No restriction of sequence length Less expensive	Lower probe density Lower resolution

Given the characteristics of the present techniques, preparation of short nucleic acid microarrays can be done using both, *in-situ* or spotting techniques. However, spotting techniques are the only used for the patterning of protein microarrays because of its intrinsic properties does not allow to synthesize full-length proteins with high performance.<sup>5</sup>

Once patterning of the substrates is performed, different strategies for the immobilization of the probes over the surface can be applied. At this time, surface and probe properties come into play, pursuing strong and oriented immobilization, without activity loss. In section 1.3, these parameters will be studied, and the main immobilization techniques will be settled.

#### 1.2.4 Detection mode

A key step in the design and performance of a microarray is the detection and the assay format. For that, label and label-free techniques can be employed, depending on the features of the microarray and the available instrumentation. Recognition using labels requires a previous tagging of the target, giving place to indirect detection, while label-free techniques provide a direct detection, as an interaction between the probe and the target is measured right away.<sup>48</sup> In this section, some features of both strategies are discussed.

The mostly used label techniques are based on isotopic,<sup>49</sup> fluorescence,<sup>50</sup> chemiluminescence,<sup>51</sup> and colorimetric detection,<sup>52</sup> being radioisotopes one of the first

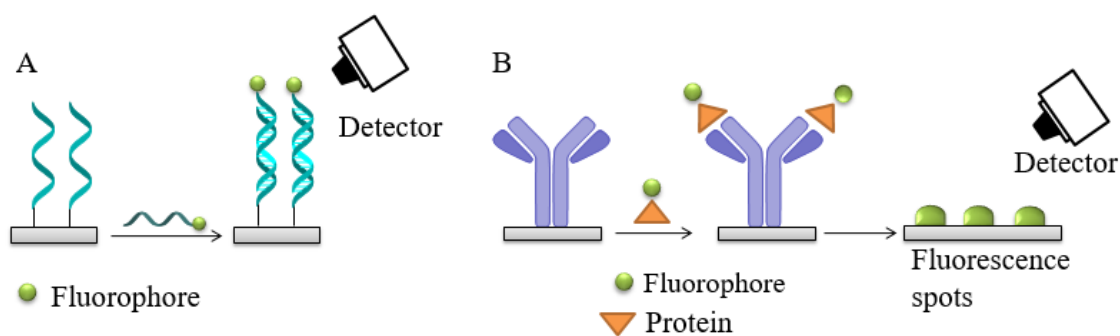
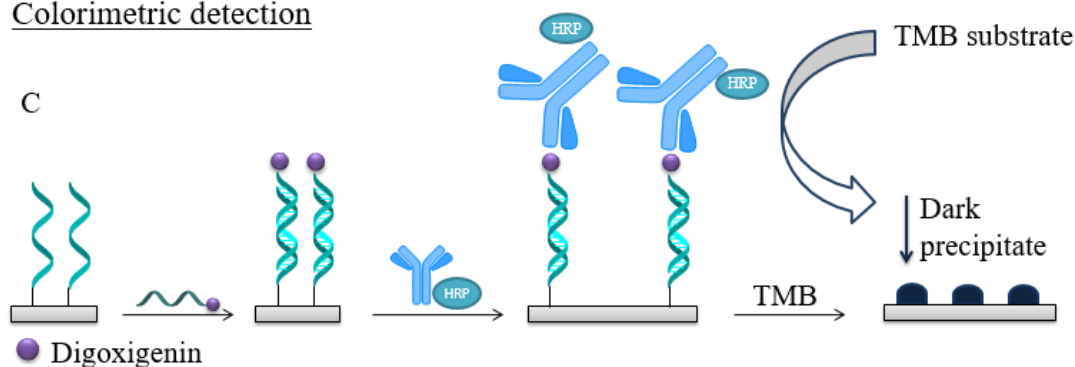
## *Introduction*

labels employed. However, nowadays it is not very extensively used due to its potential risk.<sup>53</sup>

Fluorescent techniques are some extensively used approaches for the detection of biorecognition events. The procedure usually consists of the direct incubation with a labeled biomolecule. Properties as stability, easy handling, good sensitivity and wide dynamic range of measure, make of this technique a very appropriate detection approach in microarray technology. Commonly, it is less expensive and complicated than radioactive and chemiluminescent labeling. In addition, due to the broad amount of available tags, labeling with fluorophores displaying a different color allows multiplexed by cohybridization of different sequences in the same array.<sup>46</sup> Main used fluorophores are cyanines Cy3 ( $\lambda_{exc}= 550 \text{ nm}$ ;  $\lambda_{em}= 570 \text{ nm}$ ), and Cy5 ( $\lambda_{exc}= 650 \text{ nm}$ ;  $\lambda_{em}= 670 \text{ nm}$ ), and AlexaFluor<sup>®</sup> and Atto<sup>®</sup> tags, being the last ones, more photo-stable. Special care must be paid onto the support, as negligible auto-fluorescence is required, and quenching events can occur. In addition, fluorescence attenuation with time happens, so immediate measurement has to be done.

Colorimetric techniques are an alternative to fluorescence detection, providing a direct visual signal, which can be quantified by a standard documental scanner. One of the most extended procedures consists in the employment of an additional detection biomolecule, such as an antibody, which recognizes the analyte already captured on the surface. This biomolecule is usually labeled with HRP (Horseradish Peroxidase Enzyme) or Au. Finally, revealing with the corresponding substrate produces a dark precipitate after the catalytic reaction. When using the HRP enzyme, substrates such as TMB (3,3',5,5'-tetramethylbenzidine) or OPD (o-phenylenediamine dihydrochloride) produce the enzymatic reaction, while silver is the reference substrate to undertake the catalytic reaction with gold. Using these methodologies, additional reagents and steps are necessary, arising with additional inconvenient (Figure 12).

It must be pointed out, that there are fluorescent HRP substrates, commercially available, such as Ample Red and QuantiFlu HRP reagent, as well; thus, an amplification of the signal would be achieved, with a counterpart increase of time. Nevertheless, these substrates have been mainly applied to ELISA plate methods, but not for microarray format.<sup>54</sup>

Fluorimetric detectionColorimetric detection

**Figure 12.** Some examples of fluorimetric (a and b) and colorimetric (c) detection schemes for microarray format are shown.

Although labeled techniques are more widely used in microarray technology, a huge advance in label-free techniques has been done in the last years, due to the progress in nanotechnology among other reasons.

Label-free optical detection methods are based on physicochemical changes that happen during the biorecognition step, being optical, electrochemical or mass alterations some of the most commonly analyzed parameters. This format allows a simplification of the process (fewer steps and reagents are involved) and a more continuous analysis, avoiding possible interferences produced in the recognition process by labels.<sup>6</sup> Nevertheless, these techniques are less available in research laboratories, having more expensive and complex setups. Mass spectrometry (MS),<sup>55</sup> dual polarization interferometry (DPI),<sup>56</sup> quartz crystal microbalance (QCM)<sup>57</sup> and surface plasmon resonance (SPR)<sup>58</sup> are some of the most known label-free techniques, however, application to microarray technology is not always possible. Only some techniques, such as SPR and anomalous reflection of gold (AR), have been adapted to microarray purposes, allowing the imaging of the whole surface. Localized surface plasmon resonance (LSPR), was introduced in 2000,<sup>59</sup> and extensive

## Introduction

advances have been done from then,<sup>60,61</sup> having even commercial devices (Nicoya Lifesciences Inc.). For AR methods, a better spatial resolution is achieved in comparison to the SRP technique, but sensitivity is lower.<sup>48,62</sup> Other less extended techniques are based on photonic crystals,<sup>63</sup> surface-enhanced Raman scattering SERS<sup>64</sup>, and lens-free interferometric microscopy<sup>65,66</sup> techniques, but they are still under development for microarray application.

Although label-free techniques present a huge potential for the detection of biomolecular interactions, further developments are still necessary to reach the commercial viability of current labeling techniques.

In table 2, a comparison between the label and label-free techniques applied to microarray technology is established.

**Table 2.** Advantages and disadvantages of the label and label-free detection systems.<sup>48</sup>

	<b>Advantages</b>	<b>Disadvantages</b>
<b>Label</b>	Cheaper Easier handling Signal amplification The standard detection mode in microarray technology	Indirect detection Requires the previous labeling
<b>Label-free</b>	Direct detection Less steps and reagents	More complex and expensive setups Less available

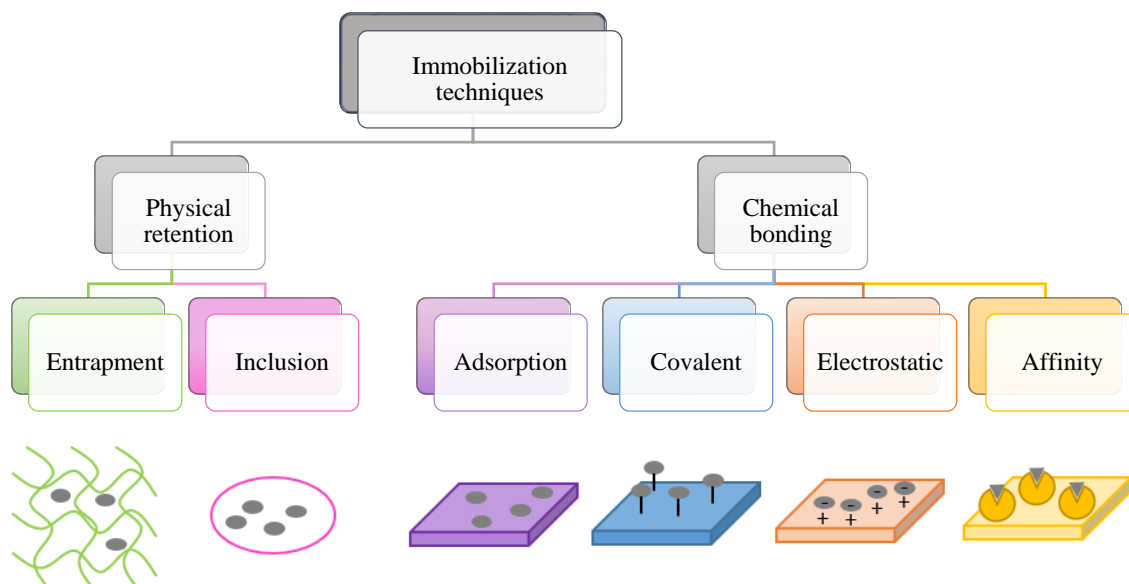
### 1.3 Anchoring strategies

*“God made the bulk; the surface was invented by the devil.” Wolfgang E. Pauli 1900-1958.*

Probe immobilization step is essential to develop a whole range of microarrays with high sensitivity and selectivity. This process will play a key role in the later performance of the microarray. Nevertheless, it is well known that tethering fallouts in activity loss and other negative factors, that will affect the quality of the microarray. For that, the choice of a suitable immobilization approach to achieve a high density of available receptors, in

an oriented, accessible, and stable way, is of utmost importance. In addition, reduction of functional activity damage and minimization of unspecific interactions is required.

Regarding its main features, anchoring techniques can be divided into two categories; physical retention and chemical bonding. Figure 13 displays the main mechanisms of linking that will be discussed individually to select the best method for our purpose.



**Figure 13.** Classification of the main immobilization techniques.

- Entrapment: probes are trapped into a porous support, or a network, or membrane, usually by polymerization together with the monomeric solution. It is generally applied to cells and enzymes.<sup>67</sup>
- Inclusion: probes are encapsulated inside a hydrogel (polymeric matrix) that allows the diffusion of analytes. Configuration and activity is preserved using this technique but mesh size has to be carefully customized.<sup>47</sup>
- Adsorption: probes are fixed over the surface by hydrogen bonds, hydrophobic interactions and/or Van der Waals forces. This is a very simple methodology for tethering the probes to the surface. However, the desorption and random anchoring will reduce noticeably the sensitivity of the final platform.<sup>47,67-70</sup>
- Covalent: probes are chemically anchored to the surface by covalent bonding, allowing very stable and durable detection platforms. Moreover, such immobilization favors a controlled immobilization process of the receptors. The

## *Introduction*

main drawback of this methodology is the need of a linker between the probe and the surface.<sup>47,67–70</sup>

- **Electrostatic:** probes join to surfaces charged with cationic or anionic groups. Probes must provide the opposite charge for linking to the surface.<sup>71</sup> Polylysine surfaces were the first employed for this purpose and, even commercial devices are available. This bio-compatible cationic polymer provides cationic surfaces, due to the protonation of amine groups in physiological media. It is usually applied to cells and DNA adhesion.<sup>72</sup>
- **Affinity:** probes are immobilized by specific affinity interactions through molecules previously anchored to the surface. This methodology improves the orientation of probes, however, it is a more complex, expensive and time consuming approach. The most widely used procedure is based on biotin/avidin or biotin/streptavidin affinity, thanks to its very high affinity constants. In addition, conjugation of biotin through amine or carboxyl groups for biotinylation of proteins or other biomolecules is a simple and well-established method. Nevertheless, exist other based affinity methods such as protein A/G and lectins,<sup>47,68–70</sup> very appropriated to immobilize antibodies and to produce chips with a regular response batch to batch.

Once presented the characteristics of the main immobilization mechanism, interactions between the probes and the substrates, some advantages and disadvantages are summarized in table 3.

**Table 3.** Probe-platform interaction types, and advantages and disadvantages of the main immobilization procedures.

<b>Immobilization method</b>	<b>Interaction types</b>	<b>Advantages</b>	<b>Drawbacks</b>
<b>Entrapment</b>	Retention forces	Simple No previous modification	Low sensitivity Leakage
<b>Inclusion</b>	Retention forces	Simple	Pore size limitation
<b>Adsorption</b>	Hydrogen bonds Hydrophobic interactions Van der Waals forces	Simple Minimal preparation	Random orientation Desorption Efficiency
<b>Covalent bonding</b>	Chemical bonding	Stability Durability (no desorption) Higher control in the immobilization orientation Highly specific	Linker molecules Irreversible
<b>Electrostatic</b>	Ionic interactions	Simple Strong anchoring	Orientation fixed Limited applications
<b>Affinity</b>	Specific interactions	Improved orientation Very good specificity and functionality	Expensive Slow

The selection of a strategy or another one depends on the nature of the probe and the support and the final applicability of the microarray. Within all these methodologies, covalent anchoring was chosen as the best option for the fabrication of the microarrays as it provides a robust link and allows to better control the immobilization process. Then, covalent bonding is presented in more detail.<sup>69</sup>

- Chemisorption

Within the covalent route, chemisorption appears as a methodology for the formation of covalent bonds between thiolated probes and gold surfaces (Au-S bond), due to the strong affinity between them. Thus, anchoring of thiolated molecules to surfaces containing gold is an interesting strategy, widely used in microarray technology, as produces successful immobilization results. In the past, it was employed by our group for the preparation of microarrays on low reflectivity compact discs having a thin layer of gold as a substrate.<sup>73</sup>

## *Introduction*

In addition, it is known the high reactivity of thiol groups to other metals such as silver, and its application to the functionalization of nanoparticles. Nevertheless, silver is too much reactive, which produces high backgrounds, restricting its employment in microarray technology.<sup>74,75</sup>

There is some controversy on this topic, showing a lack of consensus with this classification. Nevertheless, covalent linking looks the most suitable category for this kind of bond.<sup>69</sup>

- Covalent attachment

This methodology allows the anchoring of modified probes to the substrates by a covalent bond. More attention will be paid in the different paths for the covalent immobilization of oligonucleotides and antibody probes.

For oligonucleotide microarrays, covalent anchoring through functional groups at the end of 3' or 5' sequence is usually undertaken. The wide availability of functional groups is present in the market, being amine and thiol motifs the mostly used.<sup>70</sup> Although covalent tethering usually provides very high immobilization densities, space between probes must be controlled. For that, optimization of this parameter to allow the approximation of the target to the anchored probe and avoiding the undesired crowding effect is required.

For antibody microarrays, immobilization through amine groups in the side chain of the antibody (mainly lysine residues) is generally used due to its good reactivity to aldehyde, epoxy and carboxylic acids activated with carbodiimide in presence of N-hydroxysuccinimide (NHS). However, even though a strong covalent bond is generated, the random orientation of the antibodies is achieved due to the high number of lysine residues present in the antibodies. Then, to get a site-specific immobilization of the antibodies, other procedures that require previous carbohydrate oxidation, carbodiimide activation or selective disulfide reduction from the hinge region, have to be employed.<sup>47,68,76</sup> The last approach has displayed two main approximations. On the one hand, the previous selective reduction of the disulfide groups from the hinge region, and its later anchoring to gold surfaces by chemisorption.<sup>77</sup> On the other hand, the direct antibody anchoring by the well-known LAMI (Light-assisted molecular immobilization) technique. This technique is based on the excitation of aromatic amino acid residues next to the disulfide bonds at the hinge region by UV irradiation (~280 nm), which leads to the disruption of these disulfide bridges. Simultaneously, the free thiol groups generated



are tethered by covalent anchoring to surfaces containing thiol motifs. Both strategies are very interesting paths to accomplish a strongly oriented anchoring of half antibodies, under soft conditions.<sup>78</sup>

Having said this, functionalization of glass slide surfaces previously to probes immobilization must be done to provide active functional groups. As seen in section 1.2.3, a vast variety of commercial organosilanes for the formation of silane SAMs is available, being  $-NH_2$ ,  $-COOH$ ,  $-SH$  and epoxy functionalities, some of the most employed.<sup>30,79</sup> The main covalent attachment possibilities are collected in Table 4.

Amine chemistry ( $-NH_2$ ): this functionality is widely employed due to its reactivity to carboxylic acid, aldehyde, and epoxy moieties, as said before.

Carboxylic acid chemistry ( $-COOH$ ): this way allows the anchoring of molecules containing amine groups, which means a good option for protein anchoring, among others.

Thiol chemistry ( $-SH$ ): thiol groups provide anchoring of thiolated molecules thorough disulfide bridge formation. An advantage of disulfide formation is the reusability of the platform, because of the reversibility of disulfide bonds.

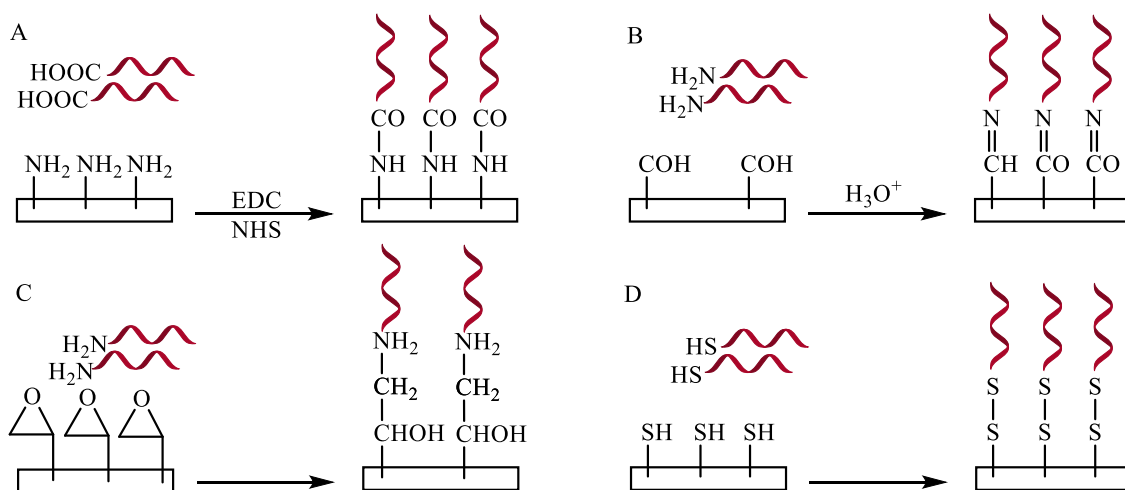
Epoxy chemistry: although it is a slow technique, it allows nucleophilic attack of several moieties such as hydroxyl, amine and sulfhydryl, and even oxidative reactions.

**Table 4.** Combination of some functionalities, and the covalent bond generated between them.

Functionality of the surface	Functionality of the probe	Covalent bond formed
<b>NH<sub>2</sub></b>	CHO, COOH, epoxy	Imine, amide, 1,2-amino-alcohol
<b>SH</b>	SH	Disulfide bond
<b>epoxy</b>	NH <sub>2</sub>	1,2-Amino-alcohol
<b>COOH</b>	NH <sub>2</sub>	Amide
<b>N=C=S</b>	NH <sub>2</sub> , OH	Isourea, urethane
<b>CHO</b>	NH <sub>2</sub>	Imine

In Figure 14, some of the most extensively used immobilization procedures to the formation of a covalent bond, are displayed.

## Introduction



**Figure 14.** Some of the most employed covalent anchoring by classical methodologies, applied to microarray technology. A. Amide formation. B. Imine generation. C. Epoxy ring opening. D. Disulfide bond formation.

Although covalent immobilization is broadly studied and employed for microarray technology, it presents the limitations explained beforehand. Then, the search of a procedure that overcomes all the requirements to achieve a successful site-specific immobilization for the later biorecognition in an easy, fast, oriented, and clean way, is still pursued. Therefore, photoinduced reactions appear as a pathway to prepare microarrays as they allow spatial and temporal control of the immobilization process under mild conditions. Nonetheless, not all the photoinduced reactions are adequate for this goal, so a deepening in the photoinduced reactions has been done.

### 1.3.1 Photoinduced reactions and click chemistry

Photoinduced reactions take advantage of light properties, allowing fast and site-specific immobilization. The huge amount of absorbed energy permits overcome energetic barriers, letting to transformations that would be otherwise inaccessible with thermal counterparts. The main advantages of photochemical reactions are their atom economy, as photons do not leave side products. They also allow milder reaction conditions and are usually greener than thermal processes.

There are many kinds of photoinduced reactions, however, restrictive features for its application to microarray technology, are hunted. Features such as biocompatibility, high yields, simplicity and quickness to get successful immobilization, preserving probe

activity are required. Within all the available photoinduced reactions, those fitting in the characteristics of click chemistry reactions emerge as a worthy choice to accomplish these challenges, thanks to its numerous advantageous properties.

Click chemistry reactions were introduced by Sharpless in 2001 to facilitate the synthesis of organic molecules using heteroatoms as linkers. The goal was to develop an expanding set of powerful, selective, and modular “blocks” that work reliably in both small and large scale applications<sup>80</sup>. Hence, the following characteristics were established as a must for a reaction to be cataloged as a click chemistry reaction:

- Simplicity.
- Orthogonality.
- High efficiency.
- Selectivity.
- Mild conditions.
- No side products.
- No use of solvents or use of benign solvents.
- Quantitative.

Thus, some cycloadditions, nucleophilic ring-opening reactions, non-aldol type carbonyl reactions and additions to carbon-carbon multiple bonds, satisfy these requirements.<sup>81</sup> Every year, more advances are made using click reactions as a mediator in diverse fields (e.g. material science, pharmacological and biomedical areas). Thanks to its interesting properties, improvement, and development of new applications are made (e.g. dendrimers synthesis, surface modification, labeling, tetrazole synthesis, etc.).

Within click chemistry, copper(I)-catalyzed alkyne-azide cycloaddition (CuAAC) “click” reaction, is the most popular to date. This reaction produces a cyclic compound between an azide and an alkyne in the presence of a  $\text{Cu}^{2+}$  ligand as catalyzer and light as the photoinitiator. However, the use of catalyzers presents a drawback, and more concretely copper compounds due to its biotoxicity. For this reason, a copper-free reaction has been developed using more active alkynes as the cyclooctynes.<sup>82</sup>

Nevertheless, other click reactions such as Diels-Alder, Staudinger ligation, and thiol-ene coupling, have been applied not only to organic synthesis and functionalization of different materials but to microarray technology,<sup>83</sup> as well. Due to its advantageous

## *Introduction*

characteristics, that fulfills the main features of click chemistry, they are a good option to incorporate in microarray developing.

Within click chemistry, thiol-photoclick reactions are being studied in our research group for microarray application, being thiol-ene and thiol-yne coupling reactions the most interesting. We established the term “thiol-photoclick” to comprise a series of key photoreactions,<sup>34</sup> which have in common the presence of thiol groups in the probe and the use of UV-light as a reactant. Thanks to the high reactivity of thiols, huge advantages of thiol-ene and thiol-yne coupling reactions over other click reactions are displayed. Their fast kinetics allows accomplishing high conversion in just 1 to 10 seconds.<sup>84</sup> In addition, catalyzers are not necessary, and thiols can be activated by light directly, without the use of other photoactive compounds. This permits the patterning by using photomasks as the light triggers the reaction. Finally, the availability of thiol groups in the biomolecules and the chance of adding thiols chemically or by genetic engineering, make of these reactions appealing candidates when selecting the immobilization procedure.

### ***1.3.1.1 Thiol-ene and thiol-yne coupling reactions***

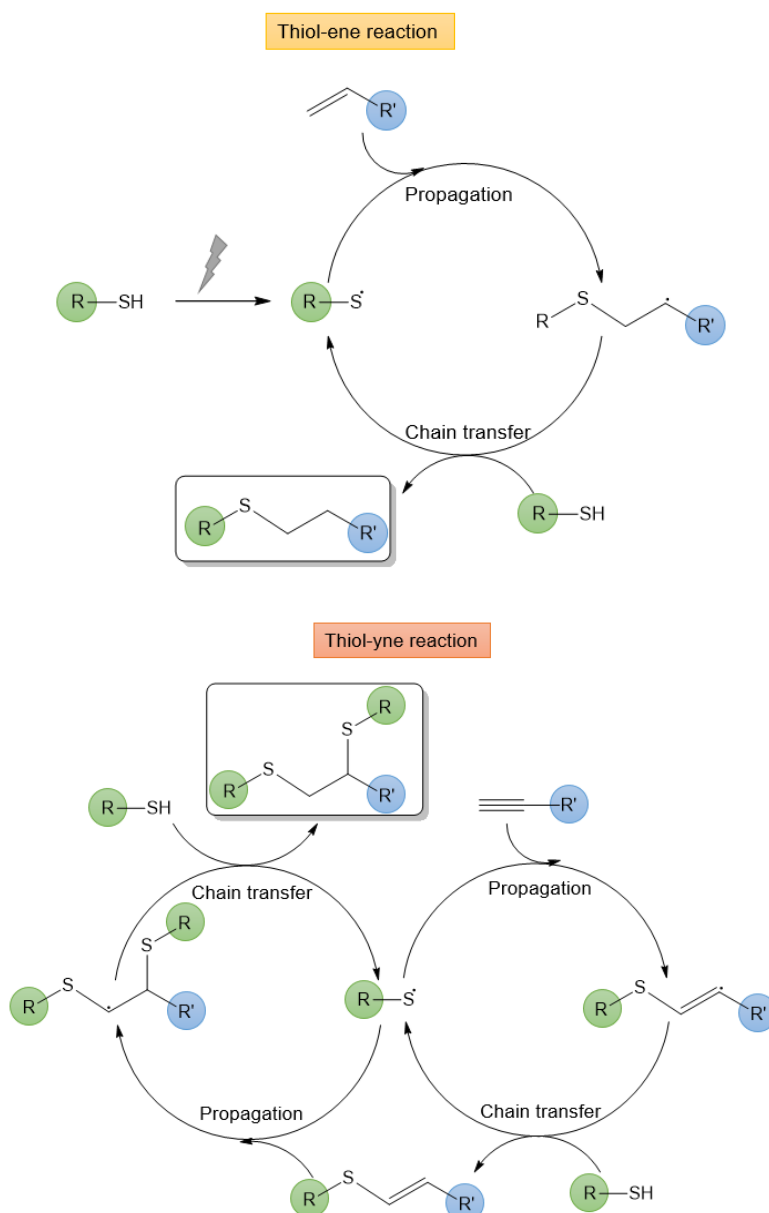
Thiol-ene and thiol-yne reactions are based on the addition reaction of a previously formed radical thiol to a double or a triple bond, respectively. These reactions undergo in aqueous media and can be initiated thermally and photochemically. Hence, both reactions are adequate for probe immobilization by covalent bonds in microarray format in an easy, fast, and guided way, taking the advantages of click chemistry. Besides, using a photoinitiation strategy, the anchoring is only produced where irradiation takes place. Making use of masks,<sup>85-87</sup> a fast patterning can be achieved, which is of utmost importance for industrial fabrication.

Although thiol-ene and thiol-yne reactions were not presented in the review of Sharpless in 2001, nowadays, they are recognized within the click chemistry because of its intrinsic characteristics.<sup>88</sup> Nevertheless, high reactivity between thiols and electron-rich carbon-carbon double bonds was well known since the early 1900s.<sup>89</sup> Figure 15 shows the chemical mechanism of both reactions.

The most remarkable difference between thiol-ene and thiol-yne reactions is that an only molecule of alkyne can react with two thiols groups. This provides higher densities of

immobilized probes for the second one if the steric hindrance of the system allows it. Nevertheless, the thiol-yne reaction is less extensively used.<sup>90-93</sup>

Thiol-ene and thiol-yne reactions have been used in numerous fields such as optics, biomedicine, sensing, and bioorganic modification, being polymer chemistry<sup>94</sup> and organic synthesis<sup>95,96</sup> the main applications. However, advances in biomolecule immobilization through these reactions opened an interesting pathway in microarray technology.<sup>97</sup>



**Figure 15.** Schematic mechanism of thiol-ene and thiol-yne reactions. Alkene motifs provide one anchoring point, while the alkyne group allows up to two thiolated molecules.

## Introduction

Before 2012, only a few studies had demonstrated the employment of thiol-ene or thiol-yne reactions for the successful immobilization of different biomolecules in a microarray format. For example, Weinrich *et al* (2010),<sup>98</sup> developed the anchoring of biotinylated molecules onto glass slides functionalized with thiol or alkene groups using thiol-ene coupling reaction. They also developed oligonucleotide microarrays but employing dendrimers as linkers. For the development of protein microarrays, a new strategy using farnesylated proteins, which provided available alkene groups, was developed by this group as well.<sup>83,99</sup> Gupta *et al.* (2010), also developed protein microarrays but using hydrogels as substrate. Wendeln *et al.* (2010)<sup>100</sup> developed glycoarrays by anchoring thiolated glycosides to functionalized glass slides (alkene and alkyne motifs).

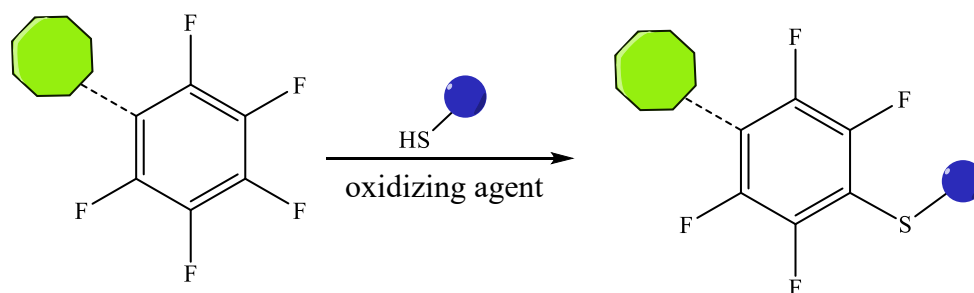
Nevertheless, these approximations show some drawbacks and limitations that must be solved, such as their applicability and fabrication time, among others. For that, further studies that permit a fast, direct, and clean anchoring of the probes were performed by our group. Different strategies were applied for the development of oligonucleotide microarrays onto silicon-based surfaces, using both, thiol-ene and thiol-yne coupling reactions. In the first work, Escorihuela *et al.* (2012),<sup>86</sup> achieved the indirect immobilization of biotinylated oligonucleotides. For that, biotin derivatives with a double bond on their extreme are grafted onto thiolated surfaces by thiol-ene photocoupling reaction. Then, streptavidin molecules are employed to immobilize the biotinylated nucleic acid probes. In the second place, direct immobilization of thiolated and alkenylated oligonucleotides onto functionalized glass slides with alkene and thiol groups, respectively, was reached with successful results.<sup>101</sup> Thirdly, anchoring of monothiolated probes to alkynylated silicon-based surfaces, reaching very sensitive and selective results was accomplished.<sup>87</sup> Finally, both reactions were applied to oligonucleotide microarray fabrication, using other surfaces different from glass, as an acrylated-based polymer further modified with alkene or alkyne moieties, which improved the performance of the microarrays.<sup>102</sup> Although these results are promising, there are numerous drawbacks in the microarray fabrication.

As seen in the previous sections, better anchoring and recognition capacity must be achieved, using fast, clean and green chemistry procedures. In addition, these developed systems were only employed for the development of oligonucleotide microarrays, so application to other types of microarrays (i.e. proteins), is of utmost importance.

During the course of this thesis, scarce works about microarray fabrication using thiol-ene or thiol-yne coupling reactions have been published by other groups, and none new thiol-photoclick reactions have been described. Nonetheless, some interesting works raised in this period are presented here. Buhl *et al.* 2015, settled an enzymatic system by microcontact printing. In this work, glucose oxidase and lactase are immobilized through their free thiols available, (i.e. cysteines) by thiol-ene reaction onto alkenylated glass surfaces. This allowed the detection of enzymatic activity under suitable conditions and their application to develop a lactose sensor.<sup>103</sup> Jönsson *et al.* 2018, biofunctionalized microfluidic devices making use of a very similar approximation of Escorihuela *et al.* 2012 (see above) to demonstrate a fast and simple patterning of different solid substrates, such as porous monoliths.<sup>104</sup> Neumann *et al.* 2017, developed several glycopolymer systems using different carbohydrates. Modified carbohydrates displaying free thiols are immobilized by thiol-ene reaction onto a polymeric surface exhibiting alkenyl groups. This system is a useful tool for high-throughput analysis and quantification of multivalent ligand–protein interactions.<sup>105</sup> But no new publications for antibody thiol-click attachment are approached for the moment. In brief, the application of thiol-photoclick reactions to other systems such as proteins is yet to be studied.

### ***1.3.1.2 Fluor-thiol photoclick reaction***

In the search of better performances of the microarrays, new surfaces and anchoring procedures have been studied. The main interests were the use of highly hydrophobic surfaces that repel unspecific interactions and confine the probes in very hydrophilic and small spots. For that, surfaces containing C-F bonds were foreseen in this thesis. Nevertheless, these platforms are quite inert, so a specific procedure to immobilize the probes must be designed and developed. Regarding the literature, C-F bonds can be cleavage in the presence of radical or strong oxidizing agents.<sup>106</sup> In addition, we found inspiration in the *para*-fluoro-thiol “click” chemistry. In this reaction, the *para* position to perfluorinated aromatic compounds shows high reactivity to nucleophilic attack<sup>107–109</sup> (Figure 16).



**Figure 16.** Scheme of the *para*-fluoro-thiol "click" reaction. In presence of an oxidizing agent, a nucleophilic attack of the thiol group to the *para*-position of the perfluorinated aromatic compound occurs.

Hence, fluor-thiol reaction arises as a novel photoclick reaction with potential in microarray technology in terms of immobilization and hybridization results, and low background. Using this approach, anchoring of thiolated probes to surfaces containing C-F motifs could be achieved. This is of utmost importance as it would allow the modulation of very low reactive surfaces in a simple, clean and fast way. In this thesis, three different material surfaces containing C-F bonds were studied like substrates to demonstrate the versatility of this reaction: perfluorinated glass slides, polyvinylidene fluoride (PVDF) and polytetrafluoroethylene (PTFE) membranes.

To conclude, this thesis is devoted to the study of new strategies for the surface modification and anchoring of different bioreceptors (nucleic acids and proteins) by light, due to the scarce exploitation of its potential in microarray. As a detection system, fluorescence and colorimetric techniques were employed.

Accordingly, in the search of other strategies that improve the milestones already reached, four strategies are mainly addressed in this thesis.

Firstly, multipoint attachment of polythiolated oligonucleotide probes, merged with the use of thiol-ene and thiol-yne (TEC and TYC) photochemical reactions, is an interesting strategy to improve the microarray performance. The multi-point attachment of probes can positively affect their orientation and hybridization performance. For that, the effect of having the probe sequence attached to the surface by one or several points will be comparatively studied.

Secondly, due to the scarce application of thiol-photoclick reactions to other microarray systems out of nucleic acids, such as protein microarrays, attachment of other bioreceptors is pursued. These types of reactions are foreseen of good potential for the



preparation of high-performance antibody-based detection systems. For that, the design and optimization of the anchoring method must be done. Then, making use of the available free thiols of an antibody after selective reduction at the hinge region, an oriented anchoring will be intended.

Thirdly, modulation of the surface hydrophobicity is another parameter of utmost importance in microarray technology. The main goal is that the analyte approaches only to the anchored probe, avoiding the rest of the surface. Hence, the use of modulated surfaces with controlled hydrophobicity is postulated. This pretends the confinement of the probes in hydrophilic and small spots surrounded by a hydrophobic and repellent surface. Minimizing the background and the unspecific binding is then expected. This modulation can be done by physical (structuration) and chemical routes (functionalization) and both approaches will be explored.

Fourthly, the search of new UV initiated reactions, based on the formation of radical thiols, that accomplish the main features of click chemistry, in combination with the surface modulation idea explained before can improve the performance of the system in terms of sensitivity, selectivity, background, unspecific adsorption, and versatility of the substrates. Therefore, the development of novel thiol-photoclick reactions for the anchoring of thiolated probes onto highly hydrophobic substrates was considered.

## 1.4 References

- (1) Martin, M. A.; Olives, A.; del Castillo García, B.; Menendez, J. C. La Química Analítica: Aspectos Conceptuales y Docentes. Evolución, Perspectivas Actuales y Retos del Futuro. *An. Real Acad. Nac. Farm.* **2003**, *69*, 146–164.
- (2) Sutandy, F. X. R.; Qian, J.; Chen, C.-S.; Zhu, H. Overview of Protein Microarrays. *Curr. Protoc. Protein Sci.* **2013**, *72* (1), 27.1.1-27.1.16.
- (3) Schena, M.; Shalon, D.; Davis, R. W.; Brown, P. Quantitative Monitoring of Gene Expression Patterns with a Complementary DNA Microarray. *Science* **1995**, *270*, 467–470.
- (4) Ekins, R. P. Multi-Analyte Immunoassay. *J. Pharm. Biomed. Anal.* **1989**, *7* (2), 155–168.
- (5) Hu, S.; Xie, Z.; Qian, J.; Blackshaw, S.; Zhu, H. Functional Protein Microarray Technology: Functional Protein Microarray Technology. *Wiley Interdiscip. Rev. Syst. Biol. Med.* **2011**, *3* (3), 255–268.
- (6) Ventimiglia, G.; Petralia, S. Recent Advances in DNA Microarray Technology: An Overview on Production Strategies and Detection Methods. *BioNanoScience* **2013**, *3* (4), 428–450.
- (7) Kostrzynska, M.; Bachand, A. Application of DNA Microarray Technology for Detection, Identification, and Characterization of Food-Borne Pathogens. *Can. J. Microbiol.* **2006**, *52* (1), 1–8.
- (8) Heller, M. J. DNA Microarray Technology: Devices, Systems, and Applications. *Annu. Rev. Biomed. Eng.* **2002**, *4* (1), 129–153.
- (9) Li, P. C. H. Overview of Microarray Technology. In *Microarray technology: methods and applications*; Li, P. C. H., Sedighi, A., Wang, L., Eds.; Humana Press: New York, 2016; pp 3–4.
- (10) Miller, M. B.; Tang, Y.-W. Basic Concepts of Microarrays and Potential Applications in Clinical Microbiology. *Clin. Microbiol. Rev.* **2009**, *22* (4), 611–633.
- (11) Southern, E. M. Detection of Specific Sequences among DNA Fragments Separated by Gel Electrophoresis. *J. Mol. Biol.* **1975**, *98* (3), 503–517.

- (12) Gygi, S. P.; Rochon, Y.; Franza, B. R.; Aebersold, R. Correlation between Protein and mRNA Abundance in Yeast. *Mol. Cell. Biol.* **1999**, *19* (3), 1720–1730.
- (13) Zhu, H.; Snyder, M. Protein Arrays and Microarrays. *Curr. Opin. Chem. Biol.* **2001**, *5* (1), 40–45.
- (14) Kopf, E.; Zharhary, D. Antibody Arrays—An Emerging Tool in Cancer Proteomics. *Int. J. Biochem. Cell Biol.* **2007**, *39* (7–8), 1305–1317.
- (15) Chou, C.-C.; Chen, C.-H.; Lee, T.-T.; Peck, K. Optimization of Probe Length and the Number of Probes per Gene for Optimal Microarray Analysis of Gene Expression. *Nucleic Acids Res.* **2004**, *32* (12), e99.
- (16) Lockhart, D. J.; Dong, H.; Byrne, M. C.; Follettie, M. T.; Gallo, M. V.; Chee, M. S.; Mittmann, M.; Wang, C.; Kobayashi, M.; Norton, H.; *et al.* Expression Monitoring by Hybridization to High-Density Oligonucleotide Arrays. *Nat. Biotechnol.* **1996**, *14* (13), 1675–1680.
- (17) Holloway, A. J.; van Laar, R. K.; Tothill, R. W.; Bowtell, D. D. L. Options Available—from Start to Finish—for Obtaining Data from DNA Microarrays II. *Nat. Genet.* **2002**, *32*, 481–489.
- (18) Religio, A.; Schwager, C.; Richter, A.; Ansorge, W.; Valcarcel, J. Optimization of Oligonucleotide-Based DNA Microarrays. *Nucleic Acids Res.* **2002**, *30* (11), e51.
- (19) Shen, M.; Rusling, J. F.; Dixit, C. K. Site-Selective Orientated Immobilization of Antibodies and Conjugates for Immunodiagnostics Development. *Methods* **2017**, *116*, 95–111.
- (20) Darwish, I. A. Immunoassay Methods and Their Applications in Pharmaceutical Analysis: Basic Methodology and Recent Advances. *Int. J. Biomed. Sci. IJBS* **2006**, *2* (3), 217–235.
- (21) Wang, C.; Feng, B. Research Progress on Site-Oriented and Three-Dimensional Immobilization of Protein. *Mol. Biol.* **2015**, *49* (1), 1–20.
- (22) Baniukevic, J.; Kirlyte, J.; Ramanavicius, A.; Ramanaviciene, A. Comparison of Oriented and Random Antibody Immobilization Techniques on the Efficiency of Immunosensor. *Procedia Eng.* **2012**, *47*, 837–840.
- (23) Adak, A. K.; Li, B.-Y.; Huang, L.-D.; Lin, T.-W.; Chang, T.-C.; Hwang, K. C.;

## Introduction

Lin, C.-C. Fabrication of Antibody Microarrays by Light-Induced Covalent and Oriented Immobilization. *ACS Appl. Mater. Interfaces* **2014**, *6* (13), 10452–10460.

(24) Vashist, S. K.; Luong, J. H. T. Antibody Immobilization and Surface Functionalization Chemistries for Immunodiagnosics. In *Handbook of Immunoassay Technologies*; Vashist, S. K., Luong, J. H. T., Eds.; Academic Press, 2018; pp 19–46.

(25) Tsugimura, K.; Ohnuki, H.; Wu, H.; Endo, H.; Tsuya, D.; Izumi, M. Oriented Antibody Immobilization on Self-Assembled Monolayers Applied as Impedance Biosensors. *J. Phys. Conf. Ser.* **2017**, *924*, 012015.

(26) McHale, G. Surface Free Energy and Microarray Deposition Technology. *The Analyst* **2007**, *132*, 192–195.

(27) Bañuls, M.-J.; Morais, S. B.; Tortajada-Genaro, L. A.; Maquieira, Á. Microarray Developed on Plastic Substrates. In *Microarray Technology*; Li, P. C. H., Sedighi, A., Wang, L., Eds.; Springer US: New York, NY, 2016; pp 37–51.

(28) Aboytes, K.; Humphreys, J.; Reis, S.; Ward, B. Slide Coating and DNA Immobilization Chemistries. In *A Beginner's Guide to Microarrays*; Blalock, E. M., Ed.; Springer US: Boston, MA, 2003; pp 1–41.

(29) Conzone, S. D.; Pantano, C. G. Glass Slides to DNA Microarrays. *Mater. Today* **2004**, *7* (3), 20–26.

(30) Dugas, V.; Demesmay, C.; Chevlot, Y.; Souteyrand, E. *Use of Organosilanes in Biosensors*, 1st ed.; Nova Science Publishers, Incorporated, 2010.

(31) Jeyachandran, Y. L.; Mielczarski, J. A.; Mielczarski, E.; Rai, B. Efficiency of Blocking of Non-Specific Interaction of Different Proteins by BSA Adsorbed on Hydrophobic and Hydrophilic Surfaces. *J. Colloid Interface Sci.* **2010**, *341* (1), 136–142.

(32) Sun, Y.-S.; Zhu, X. Characterization of Bovine Serum Albumin Blocking Efficiency on Epoxy-Functionalized Substrates for Microarray Applications. *J. Lab. Autom.* **2016**, *21* (5), 625–631.

(33) Taylor, S. Impact of Surface Chemistry and Blocking Strategies on DNA Microarrays. *Nucleic Acids Res.* **2003**, *31* (16), e87.

(34) Bañuls, M.-J.; González-Martínez, M. Á.; Sabek, J.; García-Rupérez, J.; Maquieira, Á. Thiol-Click Photochemistry for Surface Functionalization Applied to

Optical Biosensing. *Anal. Chim. Acta* **2019**, *1060*, 103–113.

(35) Materne, T.; de Buyl, F.; Witucki, G. L. *Organosilane Technology in Coating Applications: Review and Perspectives*, 1st ed.; Dow Corning Corporation, USA, 2006.

(36) Bañuls, M.-J.; Puchades, R.; Maquieira, Á. Chemical Surface Modifications for the Development of Silicon-Based Label-Free Integrated Optical (IO) Biosensors: A Review. *Anal. Chim. Acta* **2013**, *777*, 1–16.

(37) Arkles, B. *Hydrophobicity, Hydrophilicity and Silane Surface Modification*, 2nd ed.; Gelest Inc., USA, 2011

(38) Shang, J.; Cheng, F.; Dubey, M.; Kaplan, J. M.; Rawal, M.; Jiang, X.; Newburg, D. S.; Sullivan, P. A.; Andrade, R. B.; Ratner, D. M. An Organophosphonate Strategy for Functionalizing Silicon Photonic Biosensors. *Langmuir* **2012**, *28* (6), 3338–3344.

(39) Vollmer, F.; Arnold, S.; Braun, D.; Teraoka, I.; Libchaber, A. Multiplexed DNA Quantification by Spectroscopic Shift of Two Microsphere Cavities. *Biophys. J.* **2003**, *85* (3), 1974–1979.

(40) Satija, J.; Sai, V. V. R.; Mukherji, S. Dendrimers in Biosensors: Concept and Applications. *J. Mater. Chem.* **2011**, *21* (38), 14367–14386.

(41) Martinsky, T. Printing Technologies and Microarray Manufacturing Techniques: Making the Perfect Microarray. In *A Beginner's Guide to Microarrays*; Blalock, E. M., Ed.; Springer US: Boston, MA, 2003; pp 93–122.

(42) Schena, M. Microarrays: Biotechnology's Discovery Platform for Functional Genomics. *Trends Biotechnol.* **1998**, *16* (7), 301–306.

(43) Fodor, S.; Read, J.; Pirrung, M.; Stryer, L.; Lu, A.; Solas, D. Light-Directed, Spatially Addressable Parallel Chemical Synthesis. *Science* **1991**, *251* (4995), 767–773.

(44) Barbulovic-Nad, I.; Lucente, M.; Sun, Y.; Zhang, M.; Wheeler, A. R.; Busmann, M. Bio-Microarray Fabrication Techniques—A Review. *Crit. Rev. Biotechnol.* **2006**, *26* (4), 237–259.

(45) Dufva, M. Fabrication of High Quality Microarrays. *Biomol. Eng.* **2005**, *22* (5–6), 173–184.

(46) Bumgarner, R. Overview of DNA Microarrays: Types, Applications, and Their Future. In *Current Protocols in Molecular Biology*; Ausubel, F. M., Brent, R., Kingston,

## Introduction

R. E., Moore, D. D., Seidman, J. G., Smith, J. A., Struhl, K., Eds.; John Wiley & Sons, Inc.: Hoboken, NJ, USA, 2013.

(47) Desmet, C.; Marquette, C. A. Surface Functionalization for Immobilization of Probes on Microarrays. In *Microarray Technology*; Li, P. C. H., Sedighi, A., Wang, L., Eds.; Springer New York: New York, NY, 2016; pp 7–23.

(48) Syahir, A.; Usui, K.; Tomizaki, K.; Kajikawa, K.; Mihara, H. Label and Label-Free Detection Techniques for Protein Microarrays. *Microarrays* **2015**, *4* (2), 228–244.

(49) MacBeath, G.; Schreiber, S. L. Printing Proteins as Microarrays for High-Throughput Function Determination. **2000**, *289* (5485), 1760–1763.

(50) DeRisi, J. L. Exploring the Metabolic and Genetic Control of Gene Expression on a Genomic Scale. *Science* **1997**, *278* (5338), 680–686.

(51) Zhu, H. Global Analysis of Protein Activities Using Proteome Chips. *Science* **2001**, *293* (5537), 2101–2105.

(52) Liang, R.-Q.; Tan, C.-Y.; Ruan, K.-C. Colorimetric Detection of Protein Microarrays Based on Nanogold Probe Coupled with Silver Enhancement. *J. Immunol. Methods* **2004**, *285* (2), 157–163.

(53) Hall, D. A.; Ptacek, J.; Snyder, M. Protein Microarray Technology. **2007**, *128* (1), 161–167.

(54) Acharya, A. P.; Nafisi, P. M.; Gardner, A.; MacKay, J. L.; Kundu, K.; Kumar, S.; Murthy, N. A Fluorescent Peroxidase Probe Increases the Sensitivity of Commercial ELISAs by Two Orders of Magnitude. *Chem. Commun.* **2013**, *49* (88), 10379.

(55) Gobert, G. N.; McInnes, R.; Moertel, L.; Nelson, C.; Jones, M. K.; Hu, W.; McManus, D. P. Transcriptomics Tool for the Human Schistosoma Blood Flukes Using Microarray Gene Expression Profiling. *Exp. Parasitol.* **2006**, *114* (3), 160–172.

(56) Sassolas, A.; Leca-Bouvier, B. D.; Blum, L. J. DNA Biosensors and Microarrays. *Chem. Rev.* **2008**, *108* (1), 109–139.

(57) Tateno, H.; Uchiyama, N.; Kuno, A.; Togayachi, A.; Sato, T.; Narimatsu, H.; Hirabayashi, J. A Novel Strategy for Mammalian Cell Surface Glycome Profiling Using Lectin Microarray. *Glycobiology* **2007**, *17* (10), 1138–1146.

(58) Jordan, C. E.; Frutos, A. G.; Thiel, A. J.; Corn, R. M. Surface Plasmon Resonance

Imaging Measurements of DNA Hybridization Adsorption and Streptavidin/DNA Multilayer Formation at Chemically Modified Gold Surfaces. *Anal. Chem.* **1997**, *69* (24), 4939–4947.

(59) Jensen, T. R.; Malinsky, M. D.; Haynes, C. L.; Van Duyne, R. P. Nanosphere Lithography: Tunable Localized Surface Plasmon Resonance Spectra of Silver Nanoparticles. *J. Phys. Chem. B* **2000**, *104* (45), 10549–10556.

(60) Endo, T.; Kerman, K.; Nagatani, N.; Hiepa, H. M.; Kim, D.-K.; Yonezawa, Y.; Nakano, K.; Tamiya, E. Multiple Label-Free Detection of Antigen–Antibody Reaction Using Localized Surface Plasmon Resonance-Based Core–Shell Structured Nanoparticle Layer Nanochip. *Anal. Chem.* **2006**, *78* (18), 6465–6475.

(61) Raphael, M. P.; Christodoulides, J. A.; Mulvaney, S. P.; Miller, M. M.; Long, J. P.; Byers, J. M. A New Methodology for Quantitative LSPR Biosensing and Imaging. *Anal. Chem.* **2012**, *84* (3), 1367–1373.

(62) Fukuba, S.; Naraoka, R.; Tsuboi, K.; Kajikawa, K. A New Imaging Method for Gold-Surface Adsorbates Based on Anomalous Reflection. *Opt. Commun.* **2009**, *282* (16), 3386–3391.

(63) Chakravarty, S.; Lai, W.-C.; Zou, Y.; Gemmill, R. M.; Chen, R. T. Silicon Photonic Crystal Microarrays for High Throughput Label-Free Detection of Lung Cancer Cell Line Lysates with Sensitivity and Specificity. In *Progress in Biomedical Optics and Imaging - Proceedings of SPIE*; 2013; Vol. 8570.

(64) Hong, K. Y.; Brolo, A. G. Polarization-Dependent Surface-Enhanced Raman Scattering (SERS) from Microarrays. *Anal. Chim. Acta* **2017**, *972*, 73–80.

(65) Terborg, R. A.; Pello, J.; Mannelli, I.; Torres, J. P.; Pruneri, V. Ultrasensitive Interferometric On-Chip Microscopy of Transparent Objects. *Sci. Adv.* **2016**, *2* (6), e1600077.

(66) Dey, P.; Fabri-Faja, N.; Calvo-Lozano, O.; Terborg, R. A.; Belushkin, A.; Yesilkoy, F.; Fàbrega, A.; Ruiz-Rodríguez, J. C.; Ferrer, R.; González-López, J. J.; *et al.* Label-Free Bacteria Quantification in Blood Plasma by a Bioprinted Microarray Based Interferometric Point-of-Care Device. *ACS Sens.* **2019**, *4* (1), 52–60.

(67) Mohamad, N. R.; Marzuki, N. H. C.; Buang, N. A.; Huyop, F.; Wahab, R. A. An Overview of Technologies for Immobilization of Enzymes and Surface Analysis

## Introduction

Techniques for Immobilized Enzymes. *Biotechnol. Biotechnol. Equip.* **2015**, *29* (2), 205–220.

(68) Jung, Y.; Jeong, J. Y.; Chung, B. H. Recent Advances in Immobilization Methods of Antibodies on Solid Supports. *The Analyst* **2008**, *133* (6), 697–701.

(69) Nimse, S.; Song, K.; Sonawane, M.; Sayyed, D.; Kim, T. Immobilization Techniques for Microarray: Challenges and Applications. *Sensors* **2014**, *14* (12), 22208–22229.

(70) Rashid, J. I. A.; Yusof, N. A. The Strategies of DNA Immobilization and Hybridization Detection Mechanism in the Construction of Electrochemical DNA Sensor: A Review. *Sens. Bio-Sens. Res.* **2017**, *16*, 19–31.

(71) Zhou, X. C.; Huang, L. Q.; Li, S. F. Y. Microgravimetric DNA Sensor Based on Quartz Crystal Microbalance: Comparison of Oligonucleotide Immobilization Methods and the Application in Genetic Diagnosis. *Biosens. Bioelectron.* **2001**, *16* (1–2), 85–95.

(72) Mazia, D. Adhesion of Cells to Surfaces Coated with Polylysine. Applications to Electron Microscopy. *J. Cell Biol.* **1975**, *66* (1), 198–200.

(73) Brun, E.; Puchades, R.; Maquieira, A. Gold, Carbon, and Aluminum Low-Reflectivity Compact Discs as Microassaying Platforms. *Anal. Chem.* **2013**, *85* (8), 4178–4186.

(74) Kamińska, A.; Kudelski, A.; Bukowska, J. Chemisorption of Cysteamine on Silver Studied by Surface-Enhanced Raman Scattering. *Langmuir* **2000**, *16* (26), 10236–10242.

(75) Schmidt, M.; Masson, A.; Cheng, H.; Brechignac, C. Physisorption and Chemisorption on Silver Clusters. *ChemPhysChem* **2015**, *16* (4), 855–865.

(76) Sun, Y.; Du, H.; Feng, C.; Lan, Y. Oriented Immobilization of Antibody through Carbodiimide Reaction and Controlling Electric Field. *J. Solid State Electrochem.* **2015**, *19* (10), 3035–3043.

(77) Karyakin, A. A.; Presnova, G. V.; Rubtsova, M. Yu.; Egorov, A. M. Oriented Immobilization of Antibodies onto the Gold Surfaces via Their Native Thiol Groups. *Anal. Chem.* **2000**, *72* (16), 3805–3811.

(78) Neves-Petersen, M. T. Photonic Activation of Disulfide Bridges Achieves



Oriented Protein Immobilization on Biosensor Surfaces. *Protein Sci.* **2006**, *15* (2), 343–351.

(79) Hermanson, G. T. Silane Coupling Agents. In *Bioconjugate Techniques*; Elsevier, 2013; pp 535–548.

(80) Kolb, H. C.; Finn, M. G.; Sharpless, K. B. Click Chemistry: Diverse Chemical Function from a Few Good Reactions. *Angew Chem Int Ed* **2001**, *40*, 2004–2021.

(81) Hoyle, C. E.; Bowman, C. N. Thiol-Ene Click Chemistry. *Angew Chem Int Ed* **2010**, *49*, 1540–1573.

(82) Agard, N. J.; Prescher, J. A.; Bertozzi, C. R. A Strain-Promoted [3 + 2] Azide–Alkyne Cycloaddition for Covalent Modification of Biomolecules in Living Systems. *J. Am. Chem. Soc.* **2004**, *126* (46), 15046–15047.

(83) Lin, P.-C.; Weinrich, D.; Waldmann, H. Protein Biochips: Oriented Surface Immobilization of Proteins. *Macromol. Chem. Phys.* **2010**, *211* (2), 136–144.

(84) Meghani, N. M.; Amin, H. H.; Lee, B.-J. Mechanistic Applications of Click Chemistry for Pharmaceutical Drug Discovery and Drug Delivery. *Drug Discov. Today* **2017**, *22* (11), 1604–1619.

(85) Escorihuela, J.; Bañuls, M.-J.; Puchades, R.; Maquieira, Á. Development of Oligonucleotide Microarrays onto Si-Based Surfaces via Thioether Linkage Mediated by UV Irradiation. *Bioconjug. Chem.* **2012**, *23* (10), 2121–2128.

(86) Escorihuela, J.; Bañuls, M. J.; Puchades, R.; Maquieira, Á. DNA Microarrays on Silicon Surfaces through Thiol-Ene Chemistry. *Chem. Commun.* **2012**, *48*, 2116–2118.

(87) Escorihuela, J.; Bañuls, M.-J.; Puchades, R.; Maquieira, Á. Site-Specific Immobilization of DNA on Silicon Surfaces by Using the Thiol–Yne Reaction. *J Mater Chem B* **2014**, *2*, 8510–8517.

(88) Gress, A.; Völkel, A.; Schlaad, H. Thio-Click Modification of Poly[2-(3-Butenyl)-2-Oxazoline]. *Macromolecules* **2007**, *40* (22), 7928–7933.

(89) Posner, T. Zur Kenntniss Der  $\beta$ -Aminosäuren. *Berichte Dtsch. Chem. Ges.* **1905**, *38* (2), 2316–2325.

(90) Lowe, A. B.; Hoyle, C. E.; Bowman, C. N. Thiol-Yne Click Chemistry: A Powerful and Versatile Methodology for Materials Synthesis. *J. Mater. Chem.* **2010**, *20*

(23), 4745–4750.

(91) Meziane, D.; Barras, A.; Kromka, A.; Houdkova, J.; Boukherroub, R.; Szunerits, S. Thiol-Yne Reaction on Boron-Doped Diamond Electrodes: Application for the Electrochemical Detection of DNA–DNA Hybridization Events. *Anal. Chem.* **2012**, *84* (1), 194–200.

(92) Fairbanks, B. D.; Sims, E. A.; Anseth, K. S.; Bowman, C. N. Reaction Rates and Mechanisms for Radical, Photoinitiated Addition of Thiols to Alkynes, and Implications for Thiol–Yne Photopolymerizations and Click Reactions. *Macromolecules* **2010**, *43* (9), 4113–4119.

(93) Park, H. Y.; Kloxin, C. J.; Scott, T. F.; Bowman, C. N. Covalent Adaptable Networks as Dental Restorative Resins: Stress Relaxation by Addition–Fragmentation Chain Transfer in Allyl Sulfide-Containing Resins. *Dent. Mater.* **2010**, *26* (10), 1010–1016.

(94) Hoyle, C. E.; Lee, T. Y.; Roper, T. Thiol-Enes: Chemistry of the Past with Promise for the Future. *J. Polym. Sci. Part Polym. Chem.* **2004**, *42* (21), 5301–5338.

(95) Killops, K. L.; Campos, L. M.; Hawker, C. J. Robust, Efficient, and Orthogonal Synthesis of Dendrimers via Thiol-Ene “Click” Chemistry. *J. Am. Chem. Soc.* **2008**, *130* (15), 5062–5064.

(96) Triola, G.; Brunsveld, L.; Waldmann, H. Racemization-Free Synthesis of S-Alkylated Cysteines via Thiol-Ene Reaction. *J. Org. Chem.* **2008**, *73* (9), 3646–3649.

(97) Jonkheijm, P.; Weinrich, D.; Köhn, M.; Engelkamp, H.; Christianen, P. C. M.; Kuhlmann, J.; Maan, J. C.; Nüsse, D.; Schroeder, H.; Wacker, R.; *et al.* Photochemical Surface Patterning by the Thiol-Ene Reaction. *Angew. Chem. Int. Ed.* **2008**, *47* (23), 4421–4424.

(98) Weinrich, D.; Köhn, M.; Jonkheijm, P.; Westerlind, U.; Dehmelt, L.; Engelkamp, H.; Christianen, P. C. M.; Kuhlmann, J.; Maan, J. C.; Nüsse, D.; *et al.* Preparation of Biomolecule Microstructures and Microarrays by Thiol-Ene Photoimmobilization. *ChemBioChem* **2010**, *11* (2), 235–247.

(99) Weinrich, D.; Lin, P.-C.; Jonkheijm, P.; Nguyen, U. T. T.; Schröder, H.; Niemeyer, C. M.; Alexandrov, K.; Goody, R.; Waldmann, H. Oriented Immobilization of Farnesylated Proteins by the Thiol-Ene Reaction. *Angew. Chem. Int. Ed.* **2010**, *49* (7),

1252–1257.

(100) Wendeln, C.; Rinnen, S.; Schulz, C.; Arlinghaus, H. F.; Ravoo, B. J. Photochemical Microcontact Printing by Thiol–Ene and Thiol–Yne Click Chemistry. *Langmuir* **2010**, *26* (20), 15966–15971.

(101) Escorihuela, J.; Bañuls, M. J.; Grijalvo, S.; Eritja, R.; Puchades, R.; Maquieira, Á. Direct Covalent Attachment of DNA Microarrays by Rapid Thiol-Ene “Click” Chemistry. *Bioconjug. Chem.* **2014**, *25*, 618–627.

(102) González-Lucas, D.; Bañuls, M. J.; Puchades, R.; Maquieira, Á. Versatile and Easy Fabrication of Advanced Surfaces for High Performance DNA Microarrays. *Adv. Mater. Interfaces* **2016**, *3*, 1500850.

(103) Buhl, M.; Vonhören, B.; Ravoo, B. J. Immobilization of Enzymes via Microcontact Printing and Thiol–Ene Click Chemistry. *Bioconjug. Chem.* **2015**, *26* (6), 1017–1020.

(104) Neumann, K.; Conde-González, A.; Owens, M.; Venturato, A.; Zhang, Y.; Geng, J.; Bradley, M. An Approach to the High-Throughput Fabrication of Glycopolymer Microarrays through Thiol–Ene Chemistry. *Macromolecules* **2017**, *50* (16), 6026–6031.

(105) Jönsson, A.; Lafleur, J. P. Fabrication of Biomolecule Microarrays Using Rapid Photochemical Surface Patterning in Thiol–Ene-Based Microfluidic Devices. In *Cell-Based Microarrays*; Ertl, P., Rothbauer, M., Eds.; Springer: New York, 2018; pp 171–182.

(106) Al-Gharabli, S.; Kujawa, J.; Mavukkandy, M. O.; Arafat, H. A. Functional Groups Docking on PVDF Membranes: Novel Piranha Approach. *Eur. Polym. J.* **2017**, *96*, 414–428.

(107) Becer, C. R.; Babiuch, K.; Pilz, D.; Hornig, S.; Heinze, T.; Gottschaldt, M.; Schubert, U. S. Clicking Pentafluorostyrene Copolymers: Synthesis, Nanoprecipitation, and Glycosylation. *Macromolecules* **2009**, *42*, 2387–2394.

(108) Slavin, S.; Burns, J.; Haddleton, D. M.; Becer, C. R. Synthesis of Glycopolymers via Click Reactions. *Eur Polym J* **2011**, *47*, 435–446.

(109) Wild, A.; Winter, A.; Hager, M. D.; Görls, H.; Schubert, U. S. Perfluorophenyl-Terpyridine Ruthenium Complex as Monomer for Fast, Efficient, and Mild Metallopolymerizations. *Macromol. Rapid Commun.* **2012**, *33*, 517–521.



## **2. Objectives**



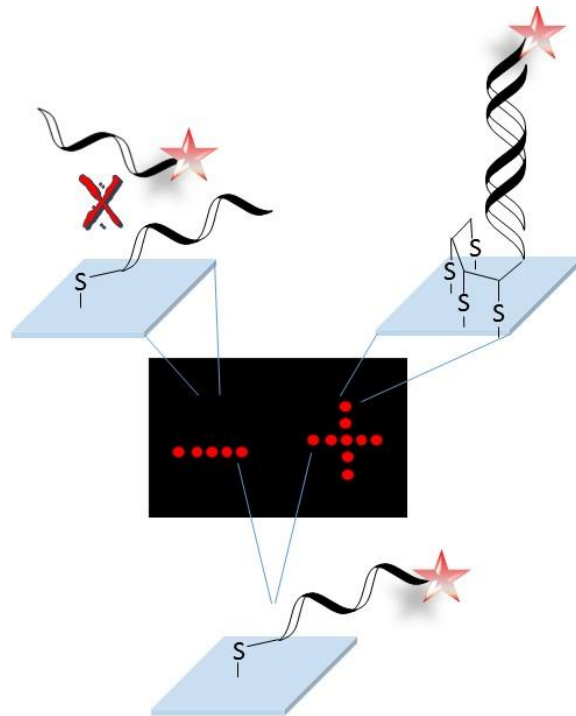
The general goal of the present thesis is to develop a rational design for microarray fabrication, which improves the current performances. This will be approached by two routes. On the one hand, the study of new immobilization routes of nucleic acids (NA) and IgG antibodies, by probe photoattachment. On the other hand, the study of chemical modulation of the surface hydrophobicity to let the analyte approximate only where the probe is immobilized, while repulsion over the rest of the surface is increased. Thus, the unspecific signal is reduced and the sensitivity of the microarray response is improved.

This general objective is pursued through the following specific objectives:

- ✓ To study the effect of multipoint probe attachment and surface hydrophobicity in the performance of NA microarrays generated using thiol-ene and thiol-yne probe coupling reactions.
- ✓ To explore the applicability of the thiol-ene coupling reactions for fabricating antibody microarrays. To this end, a selective reduction of disulfide bridges at the antibody's hinge region will be optimized. The oriented immobilization of antibody fragments through their hinge region will be done by thiol-ene coupling reaction. In such a way, its microarray performance will be compared to whole antibody microarrays.
- ✓ To develop novel UV initiated radical reactions for the anchoring of thiolated biomolecules on highly hydrophobic surfaces. Modulation of the surfaces will be a key point in this task to allow successful immobilization and recognition procedures.
- ✓ To analyze the applicability of the developed probe anchoring strategies to other substrates different than glass, such as organic polymer surfaces.







### **3. Probe multiattachment by thiol-ene and thiol-yne coupling reactions for oligonucleotide microarrays**



As seen in the general introduction, nowadays, there is a continuous progress in the search of new approaches to respond the needs and challenges of the society. The requirement of identifying and quantifying targeted analytes within a complex sample, implies an advance in the development of new detection methodologies. Nevertheless, there is a lack of devices to get fast, sensitive, selective, reliable, and easy detection analysis. Thus, microarray technology appears as an interesting solution to accomplish these challenges, because of their features enables multiplexability, high throughput analysis, miniaturization, and portability, among others.

Many aspects have to be taken in to account at the time of designing and preparing the microarrays, such as the nature of the probes and the targets, the nature of the solid substrates and its functionalization, and the patterning and detection approaches, as microarray performance and applicability will depend directly on these features.

In this chapter, with the goal of improving the microarray performance, surface modulation and anchoring methodology are thoroughly studied, as these are the most critical steps in the preparation of a micorarray.

Then, single and multipoint attachment of thiolated oligonucleotide probes, by the well-known thiol-ene and thiol-yne photoclick reactions, is developed, using glass slides as substrates. To undertake the reaction, substrates are to be functionalized with alkenyl and alkynyl groups.

Making use of probes with several anchoring points, a higher immobilization density is pursued, with an effect in the probe orientation, too. In addition, the use of photoclick reactions allow a site-specific immobilization of the probes in an easy and fast manner. Making use of UV irradiation, energetic barriers are overcome, which lets to transformations that would not be accessible under mild conditions. Finally, the use of more hydrophobic surfaces, induces a higher confinement of the probes and reduces the unspecific adsorption.

As proof of concept, application of the developed systems to the discrimination of SNPs and the detection of bacterial PCR products, has been fully demonstrated.



### **3.1 Improved Performance of DNA Microarray Multiplex Hybridization Using Probes Anchored at Several Points by Thiol-Ene or Thiol-Yne Coupling Chemistry**

"Reprinted with permission from *Bioconjug. Chem.* **2017**, 28, 496–506. Copyright 2017 American Chemical Society."



## ABSTRACT

Nucleic acid microarray-based assay technology has shown lacks in reproducibility, reliability and analytical sensitivity. Here, a new strategy of probe attachment modes for silicon-based materials is built up. Thus, hybridization ability is enhanced combining thiol-ene or thiol-yne click chemistry reactions, with a multi-point attachment of polythiolated probes. The viability and performance of this approach was demonstrated specifically determining *Salmonella* PCR products up to 20 pM sensitivity level.

## 1. Introduction

The development of high-performance methods for the sensitive and selective detection of DNA and RNA targets has become a key point in biomedical and clinical studies,<sup>1</sup> agricultural, food and environmental fields.<sup>2-4</sup> Among the working techniques, microarraying emerges as a tool showing parallel and high throughput assay capabilities.<sup>5</sup> However, both clinical and analytical metrics produced by microarray-based assay technology have recognized lacks in reproducibility, reliability and analytical sensitivity.<sup>6</sup> Most of these drawbacks are attributed to poor probe attachment and solid-liquid interface control.<sup>7</sup>

Indeed, the success of microarray-based techniques depends on the good accessibility and functionality of the surface-bound probes, which closely relates to the chemistry of attachment (support nature, probe orientation, probe density, reproducibility).<sup>8,9</sup> Many work have been developed in this field involving passive immobilization by adsorption forces,<sup>10</sup> electrostatic interactions,<sup>11</sup> affinity reactions<sup>12</sup> and covalent bonding.<sup>13-15</sup> But, nowadays there is still a need for better attachment modes providing high performance in the developed microarray; specially regarding sensitivity and selectivity.

Generally, covalent binding is the preferred approach for the probe attachment, because it provides good stability and high binding strength, controlling also orientation and density of probes. However, it has several drawbacks as the need of linker molecules, slow procedures and crowding effects.<sup>7</sup>

Despite the many methods described for microarray probe covalent anchoring; the most interesting reported approaches to overcome the abovementioned drawbacks, are those based on click chemistry reactions.<sup>16</sup> Thiol-ene<sup>17,18</sup> and thiol-yne<sup>19,20</sup> coupling chemistries belong to this family, which are characterized by orthogonality, high yields, regioselectivity, compatibility with aqueous media, mild reaction conditions, use of

benign catalysts and solvents, and high reaction rates. The good performance of these coupling chemistries made them useful for many applications such as in polymers, dendrimers, bioconjugation and surface photografting.<sup>21-23</sup>

However, few examples can be found employing these click reactions for microarray fabrication.<sup>24-30</sup> Regarding thiol-ene coupling, the most interesting contributions are those by Waldmann and colleagues,<sup>27-30</sup> but they are basically centered in the use of farnesylated proteins to induce surface photopatterning. Recently, we reported the use of thiol-ene<sup>31,32</sup> and thiol-yne<sup>33</sup> click reactions to couple monothiolated oligonucleotides onto alkenylated or alkynylated silicon-based surfaces in a direct, clean and quick way. The obtained DNA microarrays detected bacterial PCR products with high sensitivity and selectivity.

Aiming to improve the performance of the fabricated microarrays even more, several important technical issues still remain challenging. These include reducing surface effects such as steric hindrance and electrostatic interactions and controlled arranging of the capture biomolecules in an oriented manner, providing a solution-phase-like environment for biorecognition.

Recently, Morvan and colleagues<sup>34</sup> reported rapid genotyping of hepatitis C virus using polythiolated probes. These probes developed in this study displayed an increased sensitivity in both in vitro ELOSA on maleimide activated plates and electrochemical assays on gold electrodes.

Here, analogous polythiolated probes are used for the first time on silicon-based materials by thiol-ene and thiol-yne click chemistries to tether the nucleic acids in an optimal manner. The method should provide quick, fast, clean, environmentally friendly and optimally oriented probe immobilization. Thus, a new generation of microarrays is constructed where hybridization ability is enhanced due to the combination of click chemistry orthogonality and multipoint surface attachment of polythiols. In this way, the less hydrophobic surfaces can reach similar performance than the more hydrophobic ones just by multi-point attachment of the probe. Sensitivity and selectivity for real samples are evaluated by detecting *Salmonella* and *Campylobacter* PCR products.

## 2. Experimental section

*Chemicals, Reagents, and Buffers.* Silicon-based wafers were provided by Valencia Nanophotonics Technology Center (NTC) at Universitat Politècnica de València (Spain)



from SIEGERT WAFER GmbH (Aachen, Germany) as a 2 mm thick silicon oxide layer grown on a (1 0 0) silicon wafer. Glass microscope slides were obtained from Labbox (Barcelona, Spain).

Allyltrimethoxysilane, vinyl trimethoxysilane, (3-glycidyloxypropyl)trimethoxysilane (GOPTS), propargylamine, tris(2-carboxyethyl)phosphine hydrochloride (TCEP), and silver developer solutions A and B were purchased from Sigma-Aldrich Química (Madrid, Spain). Toluene, 2-propanol, and formamide were purchased from Scharlau (Madrid, Spain).

Oligonucleotide sequences Target A\* and Target B were acquired from Eurofins Genomics (Ebersberg, Germany). Monothiolated oligonucleotide sequences T1.I\*, T1.H and T1.Cam were acquired from Aldrich (Madrid, Spain).

Polythiolated-modified probes T2.I\*, T4.I\*, T2.H, T4.H, T1.Sal, T2.Sal, T4.Sal, T4.Cam (Table 4) were synthesized on a 1  $\mu$ mol-scale by standard phosphoramidite chemistry using a 394 ABI DNA synthesizer. Cy5 solid support was purchased from Link Technologies (Lanarkshire, Scotland). For the coupling step, benzylmercaptotetrazole (BMT) was used as the activator (0.3 M in anhydrous CH<sub>3</sub>CN) along with commercially available nucleoside phosphoramidites (dT, dABz, dCBz and dGtBuPac) at 0.075 M in anhydrous CH<sub>3</sub>CN introduced with a 20 s coupling time, 1-O-(4,4'-dimethoxytrityl)-2-(6-S-acetylthio hexyl oxymethyl)-2-methyl-3-(diisopropylamino  $\beta$ -cyanoethyl phosphoramidite)-propane-1,3-diol<sup>27</sup> now commercially available from Chemgenes Corporation (0.1 M in anhydrous CH<sub>3</sub>CN) with a 60 s coupling time. The capping step was performed with phenoxyacetic anhydride using commercial solutions (Cap A: Pac<sub>2</sub>O, pyridine, THF 10/10/80 and Cap B: 10% N-methylimidazole in THF) for 60 s. Oxidation was performed with a commercial solution of iodide (0.1 M I<sub>2</sub>, THF/pyridine/water 90/5/5) for 13 s. Detritylation was performed with 3% TCA in CH<sub>2</sub>Cl<sub>2</sub> for 65 s.

**Table 4.** Oligonucleotide sequences list, including functionalities.

Name	Sequence (5' to 3')	5' end	3' end
<b>T1.I*</b>	CCCGATTGACCAGCTAGCATT	1 SH	Cy5
<b>T2.I*</b>	CCCGATTGACCAGCTAGCATT	2 SH	Cy5
<b>T4.I*</b>	CCCGATTGACCAGCTAGCATT	4 SH	Cy5
<b>T1.H</b>	CCCGATTGACCAGCTAGCATT	1 SH	
<b>T2.H</b>	CCCGATTGACCAGCTAGCATT	2 SH	
<b>T4.H</b>	CCCGATTGACCAGCTAGCATT	4 SH	

<b>Target A*</b>	AATGCTAGCTGGTCAATCGGG	Cy5
<b>Target B</b>	AATGCTAGCTGGTCAATCGGG	
<b>T1.Sal</b>	T4GATTACAGCCGGTGTACGACCCT	1 SH
<b>T2.Sal</b>	T4GATTACAGCCGGTGTACGACCCT	2 SH
<b>T4.Sal</b>	T4GATTACAGCCGGTGTACGACCCT	4 SH
<b>T1.Cam</b>	T4AGACGCAATACCGCGAGGTGGAGCA	1 SH
<b>T4.Cam</b>	T4AGACGCAATACCGCGAGGTGGAGCA	4 SH

*Protocol for deprotection.* After elongation, the solid-supported S-acetylthiol-oligonucleotides were treated with a solution of 10% piperidine in dry CH<sub>3</sub>CN in a continuous flow manner (5 mL over 15 min), before being washed with dry CH<sub>3</sub>CN and dried using a flush of nitrogen. Then, solid-supported thiolated oligonucleotides were treated with concentrated ammonia for 2 h at room temperature. The filtrate was withdrawn and evaporated affording the polythiolated probes. The residue was dissolved in 1 mL of water and washed three times with ethyl acetate to remove benzamide and tert-butylphenoxyacetamide. After MALDI-TOF characterization (Table S1), the crude modified oligonucleotides were lyophilized and stored at -20°C. The structure of the thiolated probes can be seen in Figure S1 (Supporting Information)

Milli-Q water 18 mΩ was used to prepare aqueous solutions. The buffers employed, phosphate buffer saline (PBS1x, 0.008M sodium phosphate dibasic, 0.002 M sodium phosphate monobasic, 0.137 M sodium chloride, 0.003 M potassium chloride, pH 7.5), PBS-T (PBS10x containing 0.05% Tween 20), saline sodium citrate (SSC10x, 0.9 M sodium chloride, 0.09 M sodium citrate, pH 7) and washing solutions were filtered through a 0.22 μm pore size nitrocellulose membrane from Whatman GmbH (Dassel, Germany) before use.

Digoxigenin-labeled PCR products from *Salmonella* were obtained in the laboratory, as previously described,<sup>35,36</sup> with a concentration of 546.38 ng/mL (5 nM) determined by fluorescence.

Anti-digoxigenin recombinant monoclonal antibody from rabbit and goat anti-rabbit Alexa Fluor 647 antibody were purchased from Invitrogen Life Technologies (Carlsbad, CA). Gold labeled goat anti-rabbit was ordered from Sigma-Aldrich (Madrid, Spain).

*Instrumental methods.* Surface activation was carried out with a UV-Ozone cleaning system UVOH150 LAB (FHR, Ottendorf-Okrilla, Germany).

Microarrays were printed with a low volume noncontact dispensing system from Biodot (Irvine, CA), model AD1500.

Probe photoattachment was done with a mercury capillary lamp Jelight (6 mW/cm<sup>2</sup>, Jelight Irvine, CA).

Contact angle measurements were carried out with Dino-Lite Microscope and image treated with Dino Capture software (Torrance, CA). The measurements were done in triplicate at room temperature with a volume drop of 5  $\mu$ L employing 18 m $\Omega$  water quality.

The fluorescence signal of the spots in the microarrays was registered with a homemade surface fluorescence reader (SFR),<sup>37</sup> having a high sensitivity charge coupled device camera Retiga EXi from Qimaging, Inc. (Burnaby, Canada), with light emitting diodes Toshiba TLOH157P as light source. Microarray image treatment and quantification was done using GenePix Pro 4.0 software from Molecular Devices, Inc. (Sunnyvale, CA).

Dual Polarization Interferometry studies were carried out with an Analight2000 device (Biolin Scientific, Stockholm, Sweden). Raw silicon oxynitride Anachips (Biolin Scientific) were employed and biofunctionalized as required in each case.

MALDI-ToF mass spectra were registered on a Voyager mass spectrometer (Perspective Biosystems, Framingham, MA) equipped with a nitrogen laser. MALDI conditions were: accelerating voltage 24000 V; guide wire 0.05% of the accelerating voltage; grid voltage 94% of the accelerating voltage; delay extraction time 700 ns. 1  $\mu$ L of sample was mixed with 5  $\mu$ L of a saturated solution of THAP in acetonitrile/water (1:1, v/v) containing 10% of ammonium citrate and few beads of DOWEX 50W-X8 ammonium sulfonic acid resin were added. Then, 1  $\mu$ L of the mixture was placed on a plate and dried at room temperature and pressure.

X-ray photoelectron spectra were recorded with a Sage 150 spectrophotometer from SPECS Surface Nano Analysis GmbH (Berlin, Germany). Non-monochromatic Al K $\alpha$  radiation (1486.6 eV) was used as the X-ray source operating at 30 eV constant pass energy for elemental specific energy binding analysis. Vacuum in the spectrometer chamber was  $9 \times 10^{-9}$  hPa and the sample area analyzed was 1 mm<sup>2</sup>. Atomic Force Microscopy (AFM) measurements were carried out with a Veeco model Dimension 3100 Nanoman from Veeco Metrology, (Santa Barbara, CA) using tapping mode at 300 kHz. Imaging was performed in AC mode in air using OMCL-AC240 silicon cantilevers (Olympus Corporation, Japan). The images were captured using tips from Nano World with a radius of 8 nm. All AFM images were processed with WSxM software.<sup>38</sup>

*Surface chemical modification.* Silicon wafers were cut into pieces of 2 x 1 cm<sup>2</sup>, cleaned with water first, then with 2-propanol and blow dried. Afterwards, they were placed in the UV-ozone cleaner, and irradiated for 7 min. The chips were functionalized immediately after activation.

For alkenylation, activated chips were introduced into a solution of vinyltrimethoxy silane (2% v/v in toluene) for 2 h at room temperature. The chips were cleaned with toluene, then with 2-propanol, and blow dried with compressed air. Then they were baked at 150 °C in an oven for 30 min.

To introduce the alkynyl groups, the chips were immersed under argon atmosphere into a solution of (3-glycidyloxypropyl)trimethoxysilane (GOPTS) 2% in toluene for 2 h at room temperature. After 2 h, the chips were washed with 2-propanol and air-dried. Next, the chips were baked for 30 min at 150 °C and after cooling at room temperature, they were immersed in a solution of propargylamine 2% in toluene for 4 h. Finally, the chips were washed with 2-propanol, air-dried, and baked for 30 min at 150 °C.

*Probe immobilization studies.* To perform this study, solutions of oligonucleotides T1.I\*, T2.I\* and T4.I\* at 2, 1 and 0.5 μM were prepared in PBS1x from a starting concentration of 20 μM (50 μL of oligonucleotide 100 μM, 150 μL MilliQ water and 50 μL of TCEP 0.1M in MilliQ water).

These solutions were spotted (40 nL/spot, humidity set at 95%) onto the functionalized surfaces creating microarrays where each row contained 5 replicas (spots); the number of rows was nine (one row per oligo and concentration).

The microarrays were then exposed to UV-light at 365 nm, with the lamp placed at a fixed distance (5 cm) from the slide, for 60 min to induce the immobilization (mono or multipoint attachment). Finally, slides were thoroughly rinsed with water and air-dried. By the SFR, fluorescence measurements let us to quantify the immobilization yield. Measurements were made by accumulation of emitted light by the samples during 15 seconds with a device gain of 3.

*Hybridization studies.* Solutions of oligonucleotides T1.H, T2.H and T4.H 0.1, 0.2, 0.4, 0.5 1, 2, 3 and 5 μM were prepared in PBS1x from a starting concentration of 20 μM. For each type of oligonucleotide, a microarray was printed on a functionalized surface (5 spots/row, 40 nL/spot, 8 rows, humidity set at 95%) using the robotic arrayer. The slides were then irradiated as before, rinsed with water, and air dried. Afterwards, 50 μL of Target A\* (0.5 μM in SSC1x) were spread over the entire surface with a coverslip. After

incubation in a slim box for 45 min at 37 °C, the coverslip was gently removed and the chip washed with SSC0.1x and air dried. The fluorescence intensity of the spots was registered with the SFR as described above.

*Salmonella PCR products detection.* Glass slides were cut in 2 x 1 cm<sup>2</sup> pieces and activated and functionalized with alkene groups as described above for silicon surfaces. Then microarrays of probes T1.Sal, T2.Sal, T4.Sal at 2 μM in PBS1x, T1.I\* as immobilization control, and T4.Cam as non-specific hybridization control (both at 2 μM), were printed and immobilized as described before.

After irradiation, washing and drying, the chips were ready for hybridization. Firstly, they were pre-hybridized in SSC1x, 15% formamide, at 37 °C for 30 min. Then, 35 μL of PCR product (dilutions ranging from 1/10 to 1/100) in SSC1x, 15% formamide, were dispensed on the chips and spread out over the surface using a coverslip. The target PCR products were denaturalized at 95 °C for 5 min and then cooled down in ice for 2 min immediately before the hybridization. The chips were incubated at 37 °C for 60 min, then washed with SSC0.1x and air dried.

For naked-eye detection, a mixture containing rabbit anti-digoxigenin antibody (1/10000) and gold labeled goat anti-rabbit antibody (1/100) in PBS-T were applied over the chip, and incubated for 30 min at room temperature. After washing with PBS-T, the chips were incubated with 20 μL of silver developer solution, and after 12 min, positive results (silver deposition) appeared on the microarrays.

For fluorescence detection and quantification, 30 μL of anti-digoxigenin antibody produced in rabbit, 1/100 in PBS-T, were spread over the chip and incubated for 30 min at room temperature. After washing with PBS-T, 30 μL of Alexa647-labeled goat anti-rabbit antibody, 1/50 in PBS-T, were incubated over the chip for another 30 min at room temperature. Finally, the chip was washed with PBS-T, water and air dried, and the fluorescence registered with the SFR.

*DPI hybridization experiments.* Unmodified Anachips were functionalized with alkenyl or alkynyl groups as described before. One of the channels was used to immobilize T1.H, while the other channel was employed to attach T2.H in one case, and T4.H in the other case. The spatial selectivity for the probe tethering only on one of the two channels available was achieved by selective irradiation using a homemade photomask. The chip was inserted in the device, and calibrated following fabricant instructions. The carrier buffer was SSC1x. Target B 5 μM in SSC1x was flowed over both channels for 25 min

at a flow rate of 10  $\mu\text{L}/\text{min}$ . Afterwards, water (25 min, 10  $\mu\text{L}/\text{min}$ ) was injected to dehybridize. Then, a non-complementary strand (25  $\mu\text{M}$ , 10  $\mu\text{L}/\text{min}$ , 5 min) was flowed to assess the specificity of the recognition.

### 3. Results and discussion

The process of DNA hybridization at surfaces is a critical part of nucleic acid-based array technology and fundamental understanding of this process under relevant conditions for actual assays is currently very challenging. Thus, controlling probe density on substrates to further optimize probe-target binding kinetics is important.

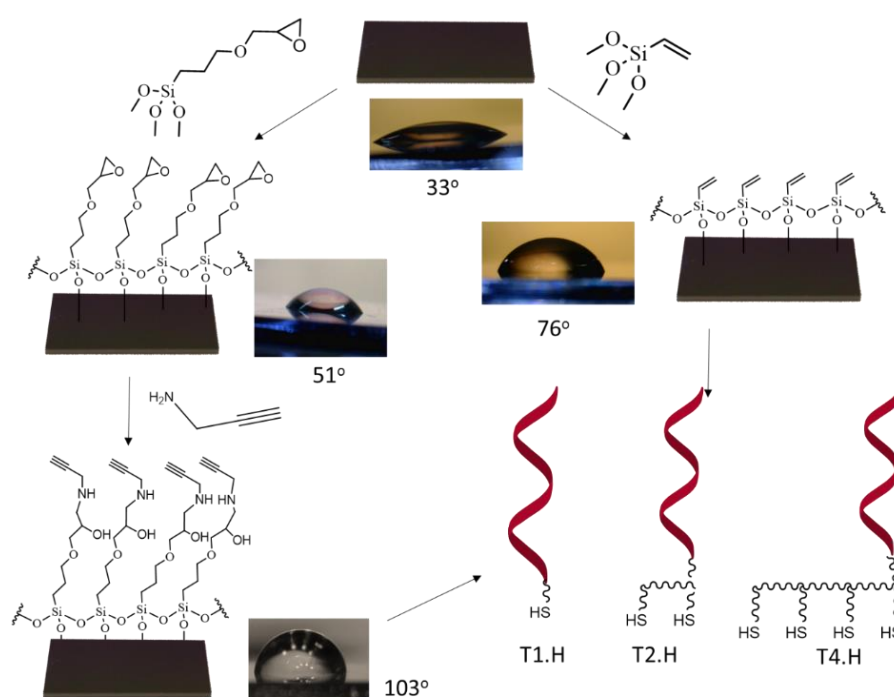
This will allow to develop new microarray surfaces with better performance within complex media. For the first time, a double control on the microarray performance is exerted by combining surface hydrophobicity tuning and multi-point probe attachment. The modulation of the hybridization capability allows detecting the presence of bacterial DNA and, at the same time, in the same chip, quantifying the microorganism level.

Polythiolated oligonucleotides with and without Cy5 dye were obtained on a DNA synthesizer according to standard phosphoramidite chemistry, starting from nucleoside or Cy5 solid supports. After elongation of the sequence, the thiol functions were introduced with the same chemistry allowing a straightforward obtaining of mono and polythiolated oligonucleotides.<sup>34</sup> The crucial point was to remove the cyanoethyl protecting group of the phosphate before deprotection of the thiol functions. Indeed, the acrylonitrile formed during classic ammonia treatment strongly reacts with a thiol leading to further unreactive thiol-cyanoethyl. For that purpose, the solid-supported thiolated oligonucleotides were firstly treated with piperidine allowing the selective removal of the cyanoethyl groups. Secondly, after washes, the ammonia treatment was applied for the release from the solid support and the deprotection of the oligonucleotide. Note that the thiol function rapidly oxidized due to oxygen dissolved in solvent leading to a disulfide bridge that should be reduced before immobilization of the mono and polythiolated oligonucleotides on a surface.

*Studies in microarray format.* Before organosilanization, the silicon oxide chips were activated employing a UV-ozone cleaning system. Different exposition times were tried, and water contact angles measured. Finally, an activation time of 7 min was set (Figure S2, Supporting Information.). Immediately after activation, the chips were immersed into

a solution of 2% organosilane in toluene for 2 h, under mild stirring. In the case of alkenyl surfaces, two organosilanes were tried showing similar results, allyltrimethoxysilane and vinyltrimethoxysilane, we decided to use vinyltrimethoxysilane for further studies. In the case of alkynyl derivatization, after silanization, the chips were treated with 2% propargylamine in toluene for 4 h. The success in the surface functionalization was evaluated by measuring the water contact angle (Figure 1 and Table S2, Supporting Information).

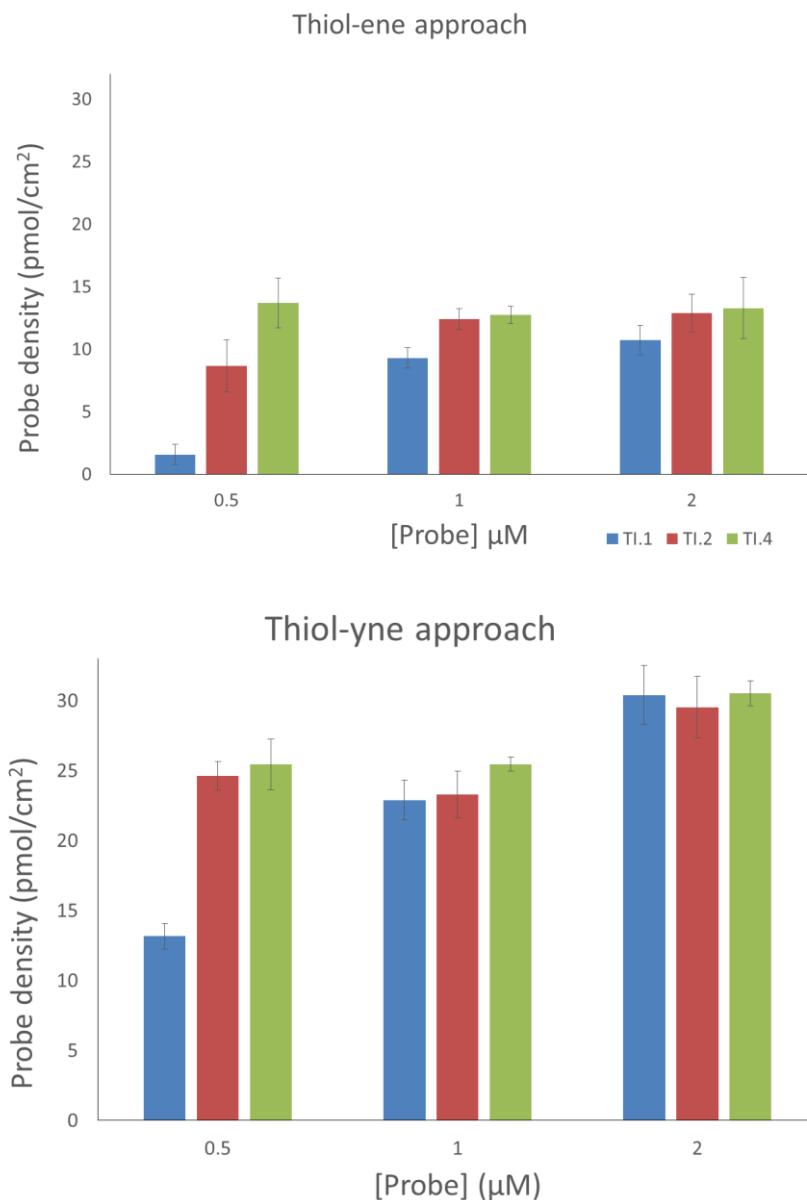
In this way, alkenylated and alkynylated surfaces were ready to immobilize mono, di and tetra-thiolated oligonucleotide probes using thiol-ene and thiol-yne coupling chemistries.



**Figure 1.** Scheme showing the different functionalization approaches providing alkyne and alkene ended surfaces, to attach mono-, di- and tetra-thiolated oligonucleotides. Water contact angles were measured for each surface to assess the progress in the derivatization

Firstly, the mono and polythiolated probes were compared regarding their immobilization capabilities. For this, an array was created onto the functionalized surfaces containing T1.I\*, T2.I\* and T4.I\* at three different concentrations (0.5, 1 and 2  $\mu$ M). T1.I\* stands for the monothiolated probe, while T2.I\* and T4.I\* correspond to the di- and tetra-thiolated probes, respectively. All of them bore a fluorescence tag. Three replicas of each microarray were done and, after irradiating at 365 nm and washing, the fluorescence was registered and compared. The results are summarized in Figure 2, where immobilized

probe density is plotted against the spotted probe concentration for each attachment approach. The amount of immobilized probe was calculated from the decrease in the fluorescence signal after washings, and considering the printed volume (40 nL) and the area of the spots.



**Figure 2.** Immobilized probe density ( $\text{pmol}/\text{cm}^2$ ) for mono (blue), di (red) and tetrathiolated (green) oligonucleotides onto alkenylated (thiol-ene coupling: TEC) and alkynylated (thiol-yne coupling: TYC) surfaces after irradiation at 365 nm for 1h.

The conclusion extracted for alkenyl-terminated surfaces was that polythiolated probes immobilized more effectively on the surface than the monothiolated ones when the probes were spotted at low concentration (0.5 and 1  $\mu\text{M}$ ). For alkynyl-ended surfaces, the three probes showed similar immobilization behavior, with no significant differences between



them for concentration of 1 and 2  $\mu\text{M}$ , while at 0.5  $\mu\text{M}$  concentration, the monothiolated probe exhibited a much lower density of immobilization. In all cases, the amount of immobilized probes was higher for thiol-yne coupling chemistry (30.52 pmol/cm<sup>2</sup>) than for thiol-ene one (13.27 pmol/cm<sup>2</sup>) (Table S3).

Besides, the use of tetrathiolated probes reached the maximal immobilization density regardless the probe concentration used, whereas for the mono- and di-thiolated probes, higher probe concentrations were needed to achieve maximum immobilization densities. Experiments carried out by Raman spectroscopy and using the Ellman's test did not show evidence of free thiol on the surface after the attachment. However, no conclusive results were obtained. The Ellman's test was not sensitive enough to detect amounts of thiols in the order of our amounts. In the Raman spectra, the presence of other bands from the oligonucleotide structure overlapped the band at 2546 cm<sup>-1</sup> specific for free thiols.

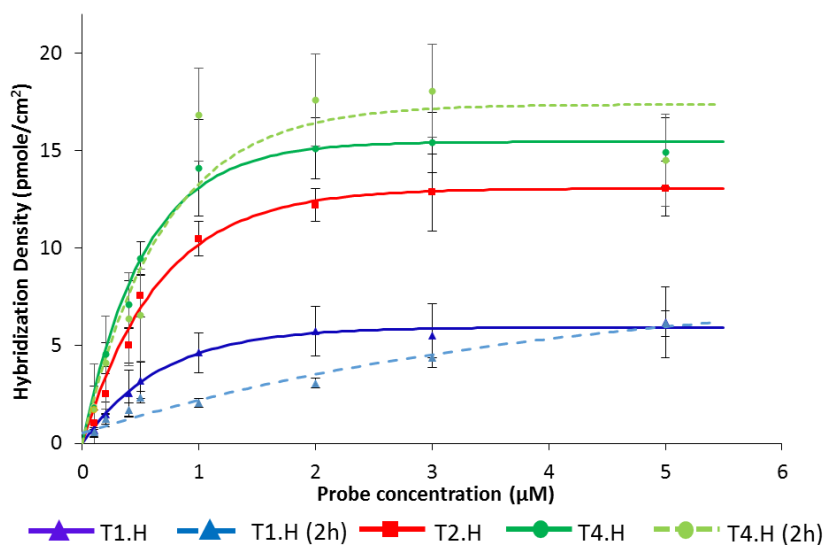
As it is known, a higher immobilization density can render less effective hybridization yield.<sup>7</sup> Thus, a new set of chips were functionalized and arrays of probes printed as before, but now using T1.H, T2.H and T4.H. These probes were similar to T1.I\*, T2.I\* and T4.I\* but without the fluorescent tag. Microarrays with growing concentrations of probe (from 0.5 to 5  $\mu\text{M}$ ) were printed. After irradiation at 365 nm for 60 min, and washing, the chips were hybridized with Target A\* 0.5  $\mu\text{M}$  in SSC1x for 60 min at 37 °C. The amount of hybridized oligonucleotide was determined interpolating the fluorescence intensity in the corresponding calibration curve (Figure S3, Supporting Information). What is explained on the basis of the higher surface hydrophobicity, which reduces the contact area and forces the probes to anchor the surface in a denser way.

The hybridization densities were higher for thiol-yne coupling chemistry than for thiol-ene coupling, indicating that the highest immobilization density still allows for the complementary strand to reach most of the probes, and there is not crowding effects.

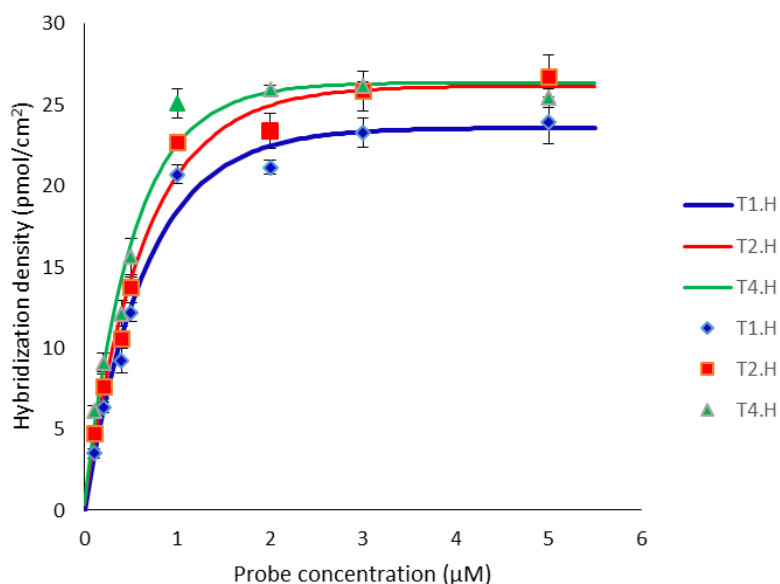
Thus, the immobilized probe density was double in thiol-yne than in thiol-ene coupling, and also the hybridization densities. However, the most important feature for our study was that in thiol-ene approach, the multipoint attachment of probes improved significantly the immobilization density and thus the hybridization with the complementary strand (Figure 3a).

From the obtained data of immobilization densities for probes T1.I\*, T2.I\* and T4.I\* at 1 and 2  $\mu\text{M}$ ; and referring them to the values of hybridization density, it was possible to calculate the hybridization efficiency in each case. In Table 1, the estimated hybridization yields are shown.

a)



b)



**Figure 3.** Hybridization densities obtained for Target A\* 0.5  $\mu\text{M}$  in microarrays with growing concentrations of mono- (T1.H), di- (T2.H) and tetra-thiolated (T4.H) probes attached to the surface by means of a) thiol-ene coupling and b) thiol-yne coupling. In a) the dashed lines are for hybridization curves obtained under similar hybridization conditions, but for TH.1 and TH.4 irradiated for 2 h instead of 1 h.

Regardless of the concentration of spotted probe (1 or 2  $\mu\text{M}$ ), the hybridization efficiency increased when the number of thiols contained in the probe grew. This feature was observed for both thiol-ene and thiol-yne approaches. However, it was enhanced in the case of thiol-ene coupling, where the hybridization yield increased from 54% for T1.H at

1  $\mu\text{M}$  to 85% and 100% for T2.H and T4.H, respectively. In the case of thiol-yne approach, the effect was less pronounced due to the high yields obtained in all the cases. Thus, yields changed from 90% for T1.H (1  $\mu\text{M}$ ) to 98 and 99% for T2.H and T4.H, respectively. Same pattern was observed at the 2  $\mu\text{M}$  concentration.

In the case of thiol-ene coupling, longer reaction times did not lead to higher probe immobilization or better hybridization densities. Thus, irradiation times of 2 h instead of 1 h provided hybridization yields very similar to that obtained for 1 h irradiation, for both TH.1 and TH.4 (Figure 3a, dashed lines)

When analyzing the influence of the multipoint attachment in the molecular crowding effect, higher differences between thiol-ene and thiol-yne coupling were appraised. Thus, when comparing the hybridization percentages under saturation of probe, changing from 1 to 2  $\mu\text{M}$ , for T1.H, meant a decrease in hybridization efficiency, which lowered from 53% to 42%. This fact, although, was not noticed for T2.H and T4.H, which even increased the hybridization yields (from 85 to 96% in T2.H). T4.H kept the maximal hybridization efficiency for both probe concentrations (Table 1).

**Table 1:** Hybridization percentage referred to the immobilized density for a probe concentration of 1 and 2  $\mu\text{M}$ , for thiol-ene and thiol-yne approaches and using mono-, di- and tetra-thiolated probes.

Probe conc. ( $\mu\text{M}$ )	Thiol-ene approach			Thiol-yne approach		
	T1.I*	T2.I*	T4.I*	T1.I*	T2.I*	T4.I*
	Immobilized density (pmol/cm <sup>2</sup> )					
<b>1</b>	8.7	12.4	12.9	22.9	23.3	25.5
<b>2</b>	13.7	12.7	13.3	30.4	29.5	30.5
	Hybridization density (pmol/cm <sup>2</sup> )					
<b>1</b>	4.6	10.5	14.1	20.7	22.7	25.1
<b>2</b>	5.7	12.2	15.1	21.2	23.4	26.0
	Hybridization yield (%)					
<b>1</b>	54	85	100	90	98	99
<b>2</b>	42	96	100	70	79	85

The molecular crowding effect was also noticed using the monothiolated probe in thiol-yne coupling surfaces, lowering the yield from 90 to 70%, when spotted concentrations of T1.H moved from 1 to 2  $\mu\text{M}$ . Di- and tetra-thiolated probes showed also a slight

crowding effect. However, it was much lower than in the case of the monothiolated probe. Thus, the hybridization yield decreased from 98 to 79% in T2.H, and from 99 to 85% in T4.H. To assess reproducibility, the assays were done in triplicate, and repeated on different days. The intrachip RSD oscillated between 5% and 12%, meanwhile interchip RSD was in the range from 12% to 15%.

AFM and XPS studies on alkene biofunctionalized chips were also performed before and after hybridization (Figures S4 and S5, Supporting Information). The results agreed with that observed in the microarrays, the amount of immobilized probe was higher for di and tetrathiolated probes than for monothiolated one.

As conclusion, the use of di- and tetra-thiolated improved the performance of the hybridization, especially in the case of thiol-ene coupling surfaces or when the crowding effect acted. Briefly, there are two ways to improve the performance of a microarray: to focus on the surface functionalization and tune its features, or to link the probe using a multipoint attachment. Both options seem to be closely related to the configuration adopted by the probe once attached, which determines its bioavailability, and which is influenced by the properties of the surface itself (hydrophobicity, etc.) and the anchoring way.

In order to look more deeply in the hybridization process for the different situations, a complete study was done using dual polarization interferometry (DPI). In this technique, the hybridization is monitored label-free in real time and thus, data about the mass surface density, the change in thickness and density are obtained. This can give some light on how the immobilized probes are set in each case, and the changes that they experience after hybridization.

For that purpose, unmodified Anachips (containing two channels available for measurements) were derivatized with alkenyl or alkynyl groups. Taking advantage of our immobilization chemistry, the chips were functionalized with a different thiolated probe on each channel, using selective irradiation through a homemade photomask. Thus, a set of four chips were ready for DPI studies containing the following pairs of probes immobilized in the channels: Probes T1.H vs T2.H as well as T1.H vs T4.H by thiol-ene coupling chemistry and the pairs T1.H vs T2.H and T1.H vs T4.H anchored by thiol-yne coupling chemistry. In all the cases, the concentration of probe was 1  $\mu\text{M}$ . For each chip the experiment was the same, after flowing hybridization buffer (SSC1x), Target B at 5  $\mu\text{M}$  was injected in both chips and flowed over for 25 min (Figure S6, Supporting Information). After flowing buffer for several min, water was injected to dehybridize and

a non-complementary strand was later flowed in order to assess the specificity in the hybridization. From the transverse electric (TE) and transverse magnetic (TM) plots, quantitative data were extracted, as mass density, volume density, refractive index variations, and layer thickness.

Considering the immobilization density obtained from the microarray assays for 1  $\mu\text{M}$  probe concentration, hybridization efficiencies were calculated in each case and compared with those obtained in microarray format. Trends observed in these DPI experiments were in agreement with the observed in microarrays. For thiol-ene coupling approach, the density of hybridized oligonucleotide rose as the number of thiol moieties in the probe increased. However, for thiol-yne immobilization, the hybridization efficiency remained constant regardless the number of thiols present in the probe. Interestingly, the same ratio of improvement in the hybridization efficiency was observed for both microarray assays and DPI experiments in thiol-ene coupling and thiol-yne coupling plots, when the number of thiols in the probes grew.

Using DPI, in thiol-ene coupling to move from one to two points attachment in the probe increased the hybridization density 3.85-fold (in the case of microarray, it was 2.3-fold), and to move from one to four thiols improved it 4.4-fold (3-fold for microarray). In the case of thiol-yne immobilization, to change from one to two thiols raised the hybridization density 1.24-fold (1.07-fold for microarray assays); and 1.4-fold more hybridization was obtained when changing from one to four thiol groups (1.14-fold in the microarray). Thus, using thiol-yne approach, the number of thiol moieties in the probe did not enhance significantly the hybridization efficiency, as it was close to the maximal in all the cases. On the contrary, the use of polythiolated probes is very adequate when working with thiol-ene immobilization approach.

Regarding DPI data interpretation, the results pointed towards a tilted probe immobilization, as was previously described,<sup>32</sup> where the hybridization takes place also in planar orientation. It is supported by the values of thickness increase and density obtained after hybridization. As shown in Table 2, the thickness increase was very low and nearly constant for all the cases, about 0.3 nm, whereas the density increased considerably when mass was loaded on the surface by the effect of hybridization.

**Table 2:** DPI figures obtained for thiol-ene and thiol-yne coupling for T1.H, T2.H and T4.H after hybridization with Target B 0.5  $\mu\text{M}$ .

	Thiol-ene			Thiol-yne		
	T1.H	T2.H	T4.H	T1.H	T2.H	T4.H
<b>Refractive Index</b>	1.36	1.41	1.43	1.49	1.50	1.53
<b>Thickness (nm)</b>	0.33	0.34	0.29	0.28	0.32	0.39
<b>Mass (ng/mm<sup>2</sup>)</b>	0.04	0.14	0.15	0.24	0.30	0.42
<b>Density (g/cm<sup>3</sup>)</b>	0.11	0.42	0.53	0.87	0.94	1.06
<b>Mass* (pmol/cm<sup>2</sup>)</b>	0.50	1.89	2.16	3.37	4.18	5.87

\*Calculated from the mass surface and considering a molecular weight for Target B of 7,127 g/mol

Considering the theoretical density of a double stranded DNA, 1.7 g/cm<sup>3</sup>, the obtained densities would correlate with the following percentages of dsDNA after hybridization having one, two and four thiol groups in the probe, respectively: 6%, 25% and 31% for thiol-ene coupling approach, and 51%, 55%, and 62% for thiol-yne strategy (Table 3).

**Table 3:** Probe immobilized density obtained from microarray assays, and hybridization efficiencies obtained in DPI experiments calculated considering the immobilized probe and the theoretical density of a double stranded DNA.

	Thiol-ene			Thiol-yne		
	T1.I*	T2.I*	T4.I*	T1.I*	T2.I*	T4.I*
<b>Immobilized density (pmol/cm<sup>2</sup>)<sup>a</sup></b>	8.08	12.6	13.11	22.9	23.3	25.5
<b>Hybridization yield<sup>b</sup> (%)</b>	6	15	17	12	15	20
<b>Hybridization yield<sup>c</sup> (%)</b>	6	25	31	51	55	62

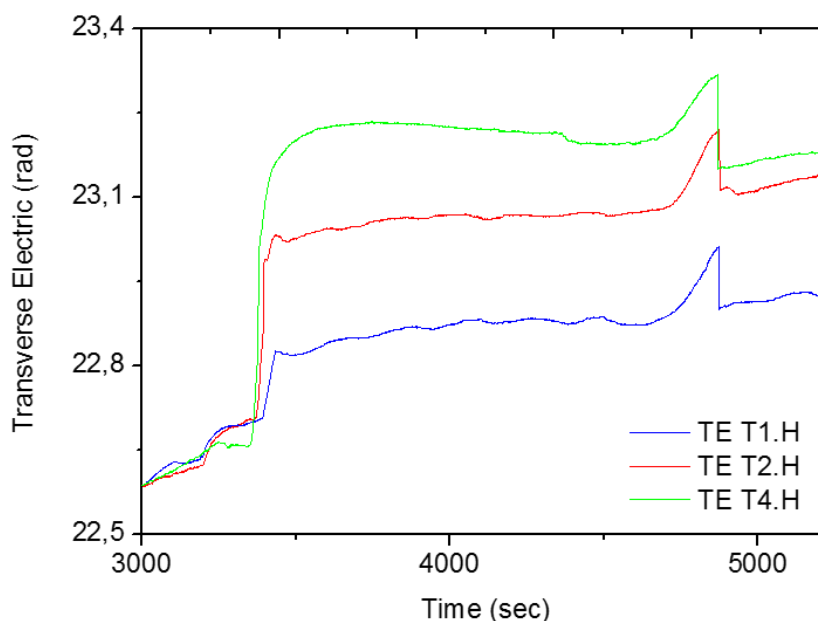
<sup>a</sup>Microarray data for 1  $\mu\text{M}$  of probe, <sup>b</sup>calculated using the mass obtained in DPI, and the immobilized density determined by microarray, <sup>c</sup>calculated using the density obtained in DPI and the theoretical density of a double stranded DNA.

Nevertheless, taking into account that the amount of immobilized probe by thiol-ene coupling was half the immobilized probe reached by thiol-yne approach, we concluded that the four-thiol attachment enhances the performance in hybridization of thiol-ene coupling strategy, reaching the level of efficiency of thiol-yne coupling. This indicates that the control in the solid-probe-fluid interface can be done by using different surface chemistries, or by using probe multi-point attachment as well.

DPI experimental data suggest that the probes stand up in all cases for thiol-yne coupling attachment, while in the case of thiol-ene coupling attachment, the monothiolated probe lays down on the surface, and polythiolated probes stand up on the surface. This is determined by the theoretical thickness increase considering a perfect close packed dsDNA layer on the surface (when the surface coverage is less than 20%, the provided thickness is the averaged thickness, that is  $0.20 \times \text{Thickness dsDNA}$ ). Thus, when dividing the obtained experimental thickness by the hybridization percentage, the theoretical thickness obtained resulted 2 nm for all cases, except for the case of thiol-ene coupled monothiolated probe, whose thickness resulted 5.5 nm. This indicates that the probe, in the last case has been straightened much more than in the other cases, which means that it was much more tilted, laying down on the surface. This would difficult target accessibility, diminishing then the hybridization capability.

It is worth noticing that DPI usually yields worse hybridization than microarray because the incubation time is shorter, 25 min instead of 1 h, and the flow can negatively affect the hybridization process.

In Figure 4, the Transverse Electric (TE) variation is plotted is shown for hybridization of T1.H, T2.H and T4.H attached by thiol-ene coupling. The evolution of TE follows the same trend in the three cases but the change in TE is bigger as the number of thiols in the probe increases.



**Figure 4:** Transverse Electric evolution during hybridization of  $0.5 \mu\text{M}$  of Target B in DPI for immobilized probes T1.H, T2.H and T4.H ( $1 \mu\text{M}$ ). Black arrows indicate the start and the end of the Target B injection in the channels.

*PCR products detection*

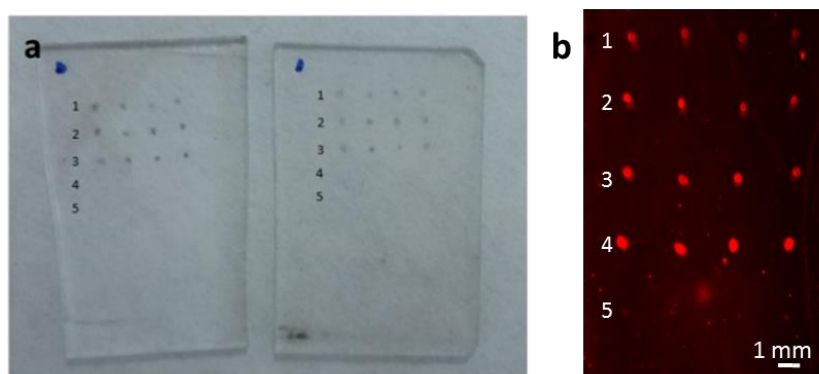
Finally, in order to demonstrate the applicability of the developments for real samples, further experiments were done to detect PCR products of an innocuous specie of *Salmonella*. In this case, glass was used as solid support instead of silica. The reason was to assay colorimetric detection, which would allow naked eye identification without any instrumental detection.

The functionalization proceeded in the same way as silica, as glass surfaces respond also very well to organosilane functionalization. Three glass chips were functionalized with vinyl triethoxysilane as before. Then each array was printed with the probes specific for *Salmonella* T1.Sal, T2.Sal, and T4.Sal, containing one, two and four thiol groups, respectively. Two sequences were also printed: the T1.I\* as immobilization control and the T4.Cam targeting *Campylobacter* as a probe specificity control. Hybridization was carried out for 1 h at 37 °C with a 1/10 dilution of the PCR products corresponding to a 500 pM concentration.

After hybridization with *Salmonella* digoxigenin-labeled PCR products, two chips were incubated with a mixture containing anti-digoxigenin rabbit antibody (1/10000) and gold-labeled goat anti-rabbit antibody (1/100). The microarrays were then developed with silver enhancer solution, showing a black precipitate only in the rows corresponding to T1.Sal, T2.Sal and T4.Sal (Figure 5a).

The third chip was treated, after PCR products hybridization, with anti-digoxigenin rabbit antibody (1/100) in PBS-T for 30 min, washed with water and incubated again with Alexa647-labeled goat anti-rabbit antibody 1/50 in PBS-T for another 30 min. After washing, the fluorescence was measured (Figure 5b). Fluorescence signal could be observed for the rows T1.Sal, T2.Sal and T4.Sal, and for control T1.I\* as well.





**Figure 5.** Microarrays on glass after hybridization with *Salmonella* PCR products. a) Colorimetric detection using silver development format and b) Fluorescence detection. First row corresponds to T1.Sal, row 2 corresponds to T2.Sal, row 3 corresponds to T4.Sal, row 4 is T1.I\*, and row 5 corresponds to T4.Cam, both controls.

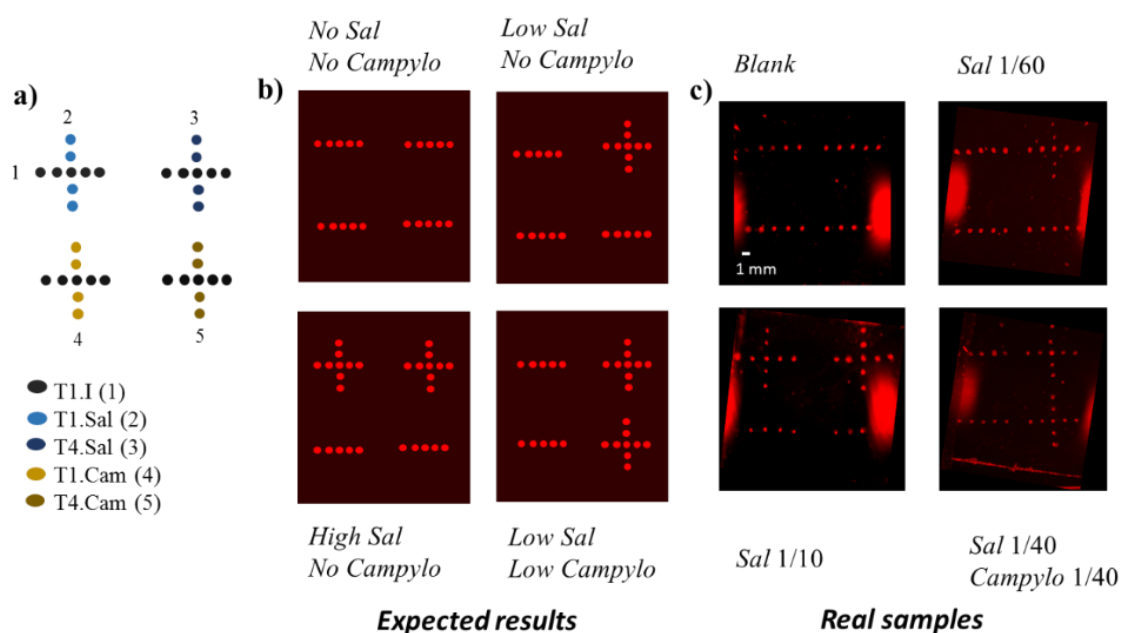
Fluorescence labelling allowed detection and quantification of the signal reached for each probe. We observed that the dithiolated probe enhanced the signal 10% related to the monothiolated T1.Sal, while tetrathiolated probe raised the signal up to 26% (Table S4, Supporting Information). Although good sensitivity was obtained for all probes, it was demonstrated again that multipoint probe attachment improved the hybridization efficiency, even for large DNA fragments such the current PCR products (150 bp). In addition, no hybridization was observed with the T4.Cam probe, demonstrating the selectivity of the hybridization and the absence of non-specific immobilization on the chip.

Using colorimetric detection, further experiments with more diluted PCR products (from 1/10 to 1/100) were done. Hybridization was detected up to dilution 1/40, which corresponds to a concentration of 125 pM.

For dilutions below 1/40, only T4.Sal showed positive results. Thus, serial dilutions were done and assayed for the tetrathiolated probe, in order to determine the lowest concentration to be detected using the most sensitive probe (Figure S7, Supporting Information). Under these conditions, the probe hybridized with dilutions up to 1/240, which means a concentration of 20 pM. The selectivity of the probe of this concentration level was assessed including a control row with a tetrathiolated probe specific for *Campylobacter* bacteria. This probe didn't develop positive assay for *Salmonella* PCR products but did for *Campylobacter* PCR products at 1/100.

As final demonstration of the applicability of the method proposed herein, a fluorescence-based microarray assay was designed. In it T1.Sal, T4.Sal, T1.Cam, T4.Cam and T1.I\* were immobilized as depicted in Figure 6a).

This design would allow easy differentiation of samples containing higher and lower concentrations of *Salmonella*, and the same for *Campylobacter* (Figure 6b). These arrays were prepared and assayed (by duplicate) with samples containing PCR products of *Salmonella* and/or *Campylobacter* at different concentrations. The results obtained are shown in Figure 6c, where two plus marks were obtained for *Salmonella* 1/10, while only one plus mark was observed for dilution 1/60. The number and location of plus marks indicated the bacteria specie present in the sample (*Salmonella*, *Campylobacter* or both) and the concentration level (two plus marks for dilution up to 1/40, and only one mark for higher dilutions).



**Figure 6.** a) Scheme of the designed microarray where rows are printed with immobilization control probe T1.I\*, whereas columns are printed with monothiolated (2) and tetrathiolated (3) probes for *Salmonella* and monothiolated (4) and tetrathiolated (5) probes for *Campylobacter* (1  $\mu$ M) b) expected results for different situations with low or high concentrations of bacterial DNA in samples c) obtained results for samples without bacterial DNA (top-left), with low (top-right) and high (bottom-left) concentration of *Salmonella*'s DNA and with a mixture of *Salmonella* and *Campylobacter* PCR products (bottom-right).

#### 4. Conclusions

In this work, thiol-ene and thiol-yne coupling chemistries have been evaluated to attach mono and polythiolated probes onto alkenylated and alkynylated surfaces, respectively. Studies tackled by dual polarization interferometry and on chip microarray fluorescence format indicated that alkynyl terminated surfaces rendered higher immobilization yields than thiol-ene linking. Polythiolated probes were more effectively immobilized on the surface than the monothiolated ones. Closely related to the immobilized probe, the hybridization density was also double in thiol-yne approach. However, it was observed with the thiol-ene coupling chemistry that multipoint probe attachment improved significantly the immobilization density and thus, the hybridization yield with the complementary strand. This trend was also observed for thiol-yne coupling although less pronounced. Also, for hybridization of large DNA strands, such as real bacterial PCR products, the same behavior was noticed and detection was improved using multi-point attachment in thiol-ene approach.

Consequently, there are two ways to improve the performance of a microarray; the first one is to focus on the surface functionalization, tuning surface properties such as hydrophobicity, and the second one is to control the surface-probe-fluid interface by multi-point probe attachment. Both approaches seem to be closely related to the configuration adopted by the attached probe, leading to its good availability for hybridization with

PCR product. Considering these issues together when designing new microarrays could help to reach advanced performance in the hybridization assays.

As demonstrated in the experiments, the created microarrays can be used with both colorimetric and fluorescence detection techniques. The first provides higher sensitivity; however, the second presents the advantages of lower number of steps and rapid readout. The flexibility in the detection approach would allow the development of an assay where the presence and concentration of bacterial DNA would be read by the naked eye.

## ACKNOWLEDGMENTS

The authors thank Dr. Elena Pinilla for her helpful discussion about AFM results. This work was funded by EU's program Horizon 2020 ICT-26-2014-644242, Spanish Ministry MINECO CTQ/2013/45875-R FEDER and local administration GVA PROMETEO II 2014/40. The authors acknowledge Tortajada-Genaro, Luis and Niñoles Rodenes, Regina for kindly providing the *Salmonella* and *Campylobacter* PCR products. F.M. is member of Inserm.

## REFERENCES

- (1) Huys, I., Matthijs, G., and Van Overwalle, G. (2012) The fate and future of patents on human genes and genetic diagnostic methods. *Nat. Rev. Genet.* *13*, 441–8.
- (2) Sett, A., Das, S., and Bora, U. (2014) Functional nucleic-acid-based sensors for environmental monitoring. *Appl. Biochem. Biotechnol.* *174*, 1073–91.
- (3) Sett, A. (2012) Aptasensors in Health, Environment and Food Safety Monitoring. *Open J. Appl. Biosens.* *1*, 9–19.
- (4) Scheler, O., Glynn, B., and Kurg, A. (2014) Nucleic acid detection technologies and marker molecules in bacterial diagnostics. *Expert Rev. Mol. Diagn.* *14*, 489–500.
- (5) Sassolas, A., Leca-Bouvier, B. D., and Blum, L. J. (2008) DNA biosensors and microarrays. *Chem. Rev.* *108*, 109–139.
- (6) Ji, H., and Davis, R. W. (2006) Data quality in genomics and microarrays. *Nat. Biotechnol.* *24*, 1112–1113.
- (7) Rao, A. N., and Grainger, D. W. (2014) Biophysical properties of nucleic acids at surfaces relevant to microarray performance. *Biomater. Sci.* *2*, 436.
- (8) Heller, M. J. (2002) DNA Microarray Technology: Devices, Systems, and Applications. *Annu. Rev. Biomed. Eng.* *4*, 129–153.
- (9) Barbulovic-Nad, I., Lucente, M., Sun, Y., Zhang, M., Wheeler, A. R., and Busmann, M. (2006) Bio-Microarray Fabrication Techniques—A Review. *Crit. Rev. Biotechnol.* *26*, 237–259.
- (10) Wu, P., Castner, D. G., and Grainger, D. W. (2008) Diagnostic devices as

biomaterials: a review of nucleic acid and protein microarray surface performance issues. *J. Biomater. Sci. Polym. Ed.* 19, 725–53.

(11) Zhou, X. C., Huang, L. Q., and Li, S. F. Y. (2001) Microgravimetric DNA sensor based on quartz crystal microbalance: comparison of oligonucleotide immobilization methods and the application in genetic diagnosis. *Biosens. Bioelectron.* 16, 85–95.

(12) Pan, S., and Rothberg, L. (2005) Chemical Control of Electrode Functionalization for Detection of DNA Hybridization by Electrochemical Impedance Spectroscopy. *Langmuir* 21, 1022–1027.

(13) Manning, B., and Eritja, R. (2012) Functionalization of Surfaces with Synthetic Oligonucleotides., Melba Navarro and Josep A. Planell (eds.), *Nanotechnology in Regenerative Medicine: Methods and Protocols, Methods in Molecular Biology*, 811, 89–100.

(14) Singh, V., Zharnikov, M., Gulino, A., and Gupta, T. (2011) DNA immobilization, delivery and cleavage on solid supports. *J. Mater. Chem.* 21, 10602.

(15) Nimse, S., Song, K., Sonawane, M., Sayyed, D., and Kim, T. (2014) Immobilization Techniques for Microarray: Challenges and Applications. *Sensors* 14, 22208–22229.

(16) Kolb, H. C., Finn, M. G., and Sharpless, K. B. (2001) Click chemistry: Diverse chemical function from a few good reactions. *Angew. Chemie - Int. Ed.* 40, 2004–2021.

(17) Hoyle, C. E., and Bowman, C. N. (2010) Thiol-ene click chemistry. *Angew. Chemie - Int. Ed.* 49, 1540–1573.

(18) Dondoni, A. (2008) The emergence of thiol-ene coupling as a click process for materials and bioorganic chemistry. *Angew. Chemie - Int. Ed.* 47, 8995–8997.

(19) Massi, A., and Nanni, D. (2012) Thiol–yne coupling: revisiting old concepts as a breakthrough for up-to-date applications. *Org. Biomol. Chem.* 10, 3791.

(20) Hoogenboom, R. (2010) Thiol-yne chemistry: A powerful tool for creating highly functional materials. *Angew. Chemie - Int. Ed.* 49, 3415–3417.

(21) Wendeln, C., Rinnen, S., Schulz, C., Arlinghaus, H. F., and Ravoo, B. J. (2010) Photochemical microcontact printing by thiol-ene and thiol-yne click chemistry. *Langmuir* 26, 15966–15971.

- (22) Campos, M. a C., Paulusse, J. M. J., and Zuilhof, H. (2010) Functional monolayers on oxide-free silicon surfaces via thiol-ene click chemistry. *Chem. Commun.* 46, 5512–5514.
- (23) Mehlich, J., and Ravoo, B. J. (2011) Click chemistry by microcontact printing on self-assembled monolayers: a structure-reactivity study by fluorescence microscopy. *Org. Biomol. Chem.* 9, 4108–4115.
- (24) Bertin, A., and Schlaad, H. (2009) Mild and Versatile (Bio-)Functionalization of Glass Surfaces via Thiol–Ene Photochemistry. *Chem. Mater.* 21, 5698–5700.
- (25) Iwasaki, Y., and Ota, T. (2011) Efficient biotinylation of methacryloyl-functionalized nonadherent cells for formation of cell microarrays. *Chem. Commun. (Camb)*. 47, 10329–10331.
- (26) Wendeln, C., Rinnen, S., Schulz, C., Kaufmann, T., Arlinghaus, H. F., and Ravoo, B. J. (2012) Rapid preparation of multifunctional surfaces for orthogonal ligation by microcontact chemistry. *Chem. - A Eur. J.* 18, 5880–5888.
- (27) Jonkheijm, P., Weinrich, D., Köhn, M., Engelkamp, H., Christianen, P. C. M., Kuhlmann, J., Maan, J. C., Nüsse, D., Schroeder, H., Wacker, R., et al. (2008) Photochemical surface patterning by the thiol-ene reaction. *Angew. Chemie - Int. Ed.* 47, 4421–4424.
- (28) Weinrich, D., Köhn, M., Jonkheijm, P., Westerlind, U., Dehmelt, L., Engelkamp, H., Christianen, P. C. M., Kuhlmann, J., Maan, J. C., Nüsse, D., et al. (2010) Preparation of biomolecule microstructures and microarrays by thiol-ene photoimmobilization. *ChemBioChem* 11, 235–247.
- (29) Weinrich, D., Lin, P. C., Jonkheijm, P., Nguyen, U. T. T., Schröder, H., Niemeyer, C. M., Alexandrov, K., Goody, R., and Waldmann, H. (2010) Oriented immobilization of farnesylated proteins by the thiol-ene reaction. *Angew. Chemie - Int. Ed.* 49, 1252–1257.
- (30) Lin, P. C., Weinrich, D., and Waldmann, H. (2010) Protein biochips: Oriented surface immobilization of proteins. *Macromol. Chem. Phys.* 211, 136–144.
- (31) Escorihuela, J., Bañuls, M. J., Puchades, R., and Maquieira, Á. (2012) DNA microarrays on silicon surfaces through thiol-ene chemistry. *Chem. Commun.* 48, 2116.

- (32) Escorihuela, J., Bañuls, M. J., Grijalvo, S., Eritja, R., Puchades, R., and Maquieira, Á. (2014) Direct covalent attachment of DNA microarrays by rapid thiol-ene “click” chemistry. *Bioconjug. Chem.* 25, 618–627.
- (33) Escorihuela, J., Bañuls, M.-J., Puchades, R., and Maquieira, Á. (2014) Site-specific immobilization of DNA on silicon surfaces by using the thiol–yne reaction. *J. Mater. Chem. B* 2, 8510–8517.
- (34) Lereau, M., Fournier-Wirth, C., Mayen, J., Farre, C., Meyer, A., Dugas, V., Cantaloube, J. F., Chaix, C., Vasseur, J. J., and Morvan, F. (2013) Development of innovative and versatile polythiol probes for use on elosa or electrochemical biosensors: Application in hepatitis c virus genotyping. *Anal. Chem.* 85, 9204–9212.
- (35) Arnandis-Chover, T., Morais, S., Tortajada-Genaro, L. a., Puchades, R., Maquieira, a., Berganza, J., and Olabarria, G. (2012) Detection of food-borne pathogens with DNA arrays on disk. *Talanta* 101, 405–412.
- (36) Santiago-Felipe, S., Tortajada-Genaro, L. A., Morais, S., Puchades, R., and Maquieira, Á. (2015) Isothermal DNA amplification strategies for duplex microorganism detection. *Food Chem.* 174, 509–515.
- (37) Mira, D., Llorente, R., Morais, S., Puchades, R., Maquieira, A., and Marti, J. (2004) High-throughput screening of surface-enhanced fluorescence on industrial standard digital recording media, in *European Symposium on Optics and Photonics for Defence and Security* (Carrano, J. C., and Zukauskas, A., Eds.), pp 364–373. International Society for Optics and Photonics.
- (38) Horcas, I., Fernández, R., Gómez-Rodríguez, J. M., Colchero, J., Gómez-Herrero, J., Baro, A. M. (2007) WSXM: A Software for Scanning Probe Microscopy and a Tool for Nanotechnology. *Rev. Sci. Instrum.* 78, 013705–8





## SUPPORTING INFORMATION

### Improved Performance of DNA Microarray Multiplex Hybridization Using Probes Anchored at Several Points by Thiol-Ene or Thiol-Yne Coupling Chemistry

List of contents:

**Table S1:** MALDI-TOF MS of oligonucleotides.

**Table S2.** Contact angle values (°) obtained for each functionalization step.

**Table S3:** Immobilization density for thiol-ene coupling (TEC) and thiol-yne coupling (TYC) approaches using mono, di and tetrathiolated probes.

**Table S4:** Fluorescence intensity after PCR products hybridization.

**Figure S1:** Structure of thiolated probes.

**Figure S2.** Contact angle variation with the irradiation time.

**Figure S3.** Calibration curve for Target A\*.

**Figure S4:** AFM Surface characterization of alkene-ended surfaces.

**Figure S5.** XPS C1s deconvolution of alkene-ended surfaces.

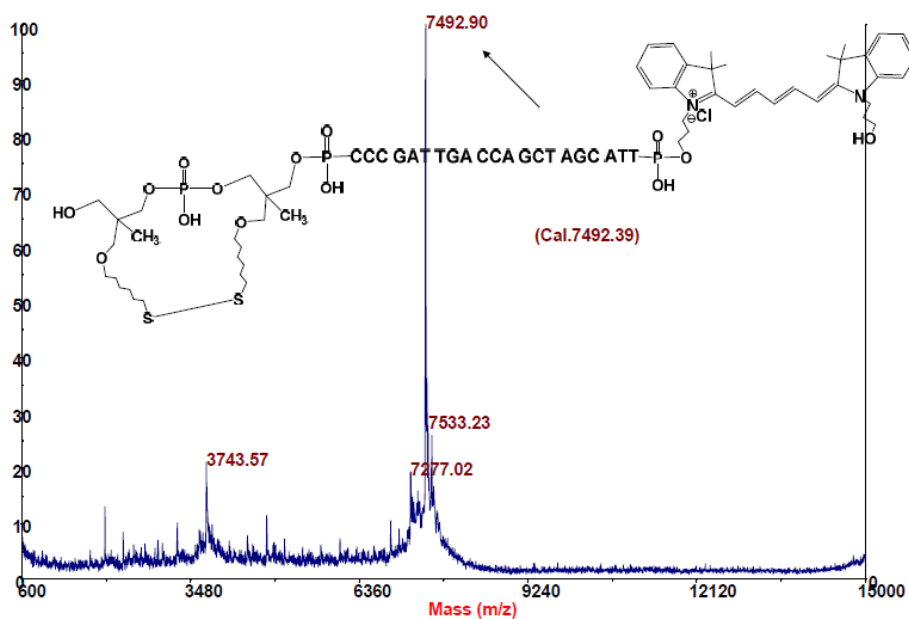
**Figure S6.** Screen print of data obtained with Dual Polarization Interferometry.

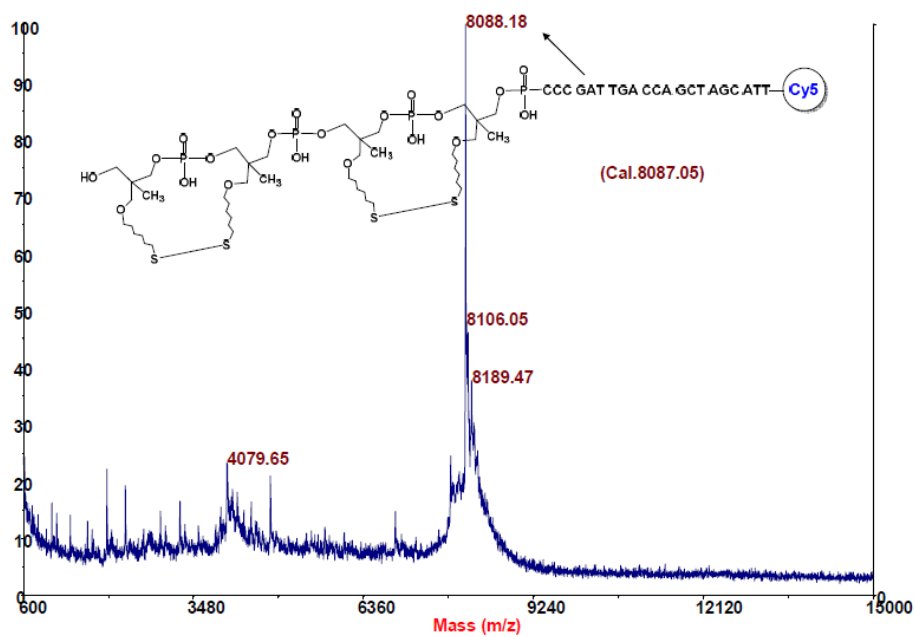
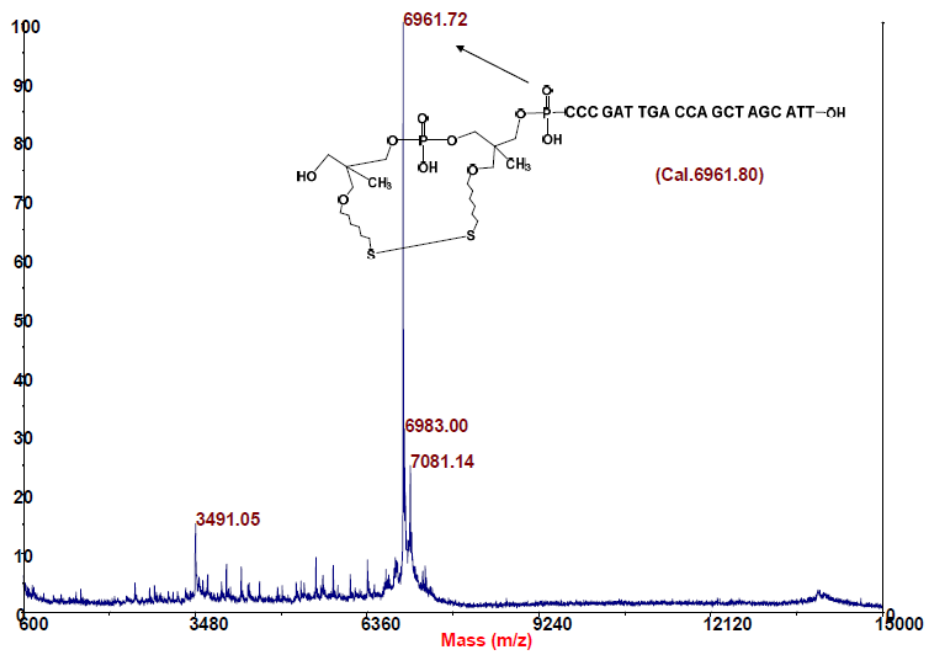
**Figure S7.** Results obtained for a microarray containing T4.Sal and T4.Cam, attached by thiol-ene approach, and hybridized with different dilutions of PCR products from Salmonella.

**Table S1:** MALDI-TOF MS of oligonucleotides.

	Sequence (5' to 3')	5'-end	3'-end	MALDI-TOF MS	
				Found	Calculated
T2.I*	CCC GAT TGA CCA GCT AGC ATT	2 SH	Cy5	7492.39	7492.90
T4.I*	CCC GAT TGA CCA GCT AGC ATT	4 SH	Cy5	8087.05	8088.18
T2.H	CCC GAT TGA CCA GCT AGC ATT	2 SH		6961.80	6961.72
T4.H	CCC GAT TGA CCA GCT AGC ATT	4 SH		7558.47	7558.65
T1.Sal	T <sub>4</sub> GATTACAGCCGGTGTACGACCCT	1 SH		8539.43	8538.65
T2.Sal	T <sub>4</sub> GATTACAGCCGGTGTACGACCCT	2 SH		8836.13	8836.98
T4.Sal	T <sub>4</sub> GATTACAGCCGGTGTACGACCCT	4 SH		9432.95	9433.66
T4.Cam	T <sub>4</sub> AGACGCAATACCGCGAGGTGGAGCA	4 SH		10159.30	10159.13

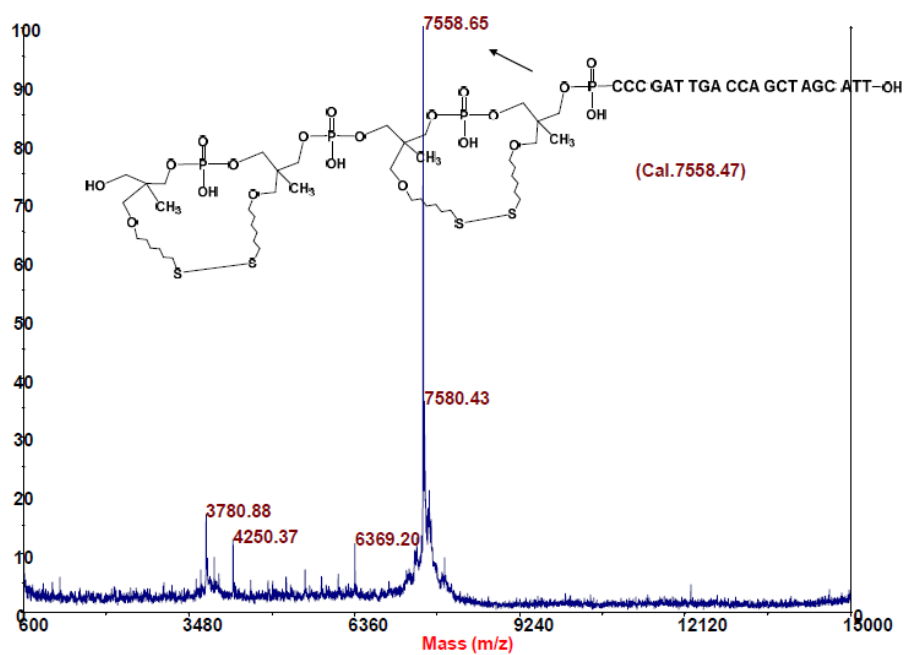
## MALDI-TOF MS spectra

**T2.I\***Maldi of 5'-SS-CCC GAT TGA CCA GCT AGC ATT-Cy5-3' with NH<sub>4</sub>OH and Extraction

**T4.I\***Maldi of 5'-SSSS-CCC GAT TGA CCA GCT AGC ATT-Cy5-3' with NH<sub>4</sub>OH and Extraction**T2.H**Maldi of 5'-SS-CCC GAT TGA CCA GCT AGC ATT-3' with NH<sub>4</sub>OH and Extraction

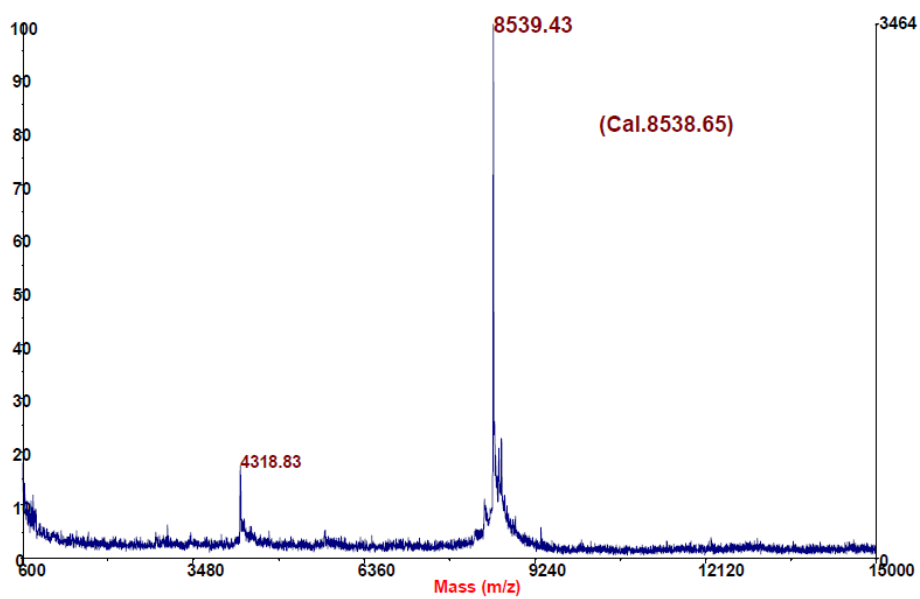
### T4.H

Maldi of 5'-SSSS-CCC GAT TGA CCA GCT AGC ATT-3' with NH<sub>4</sub>OH and Extraction



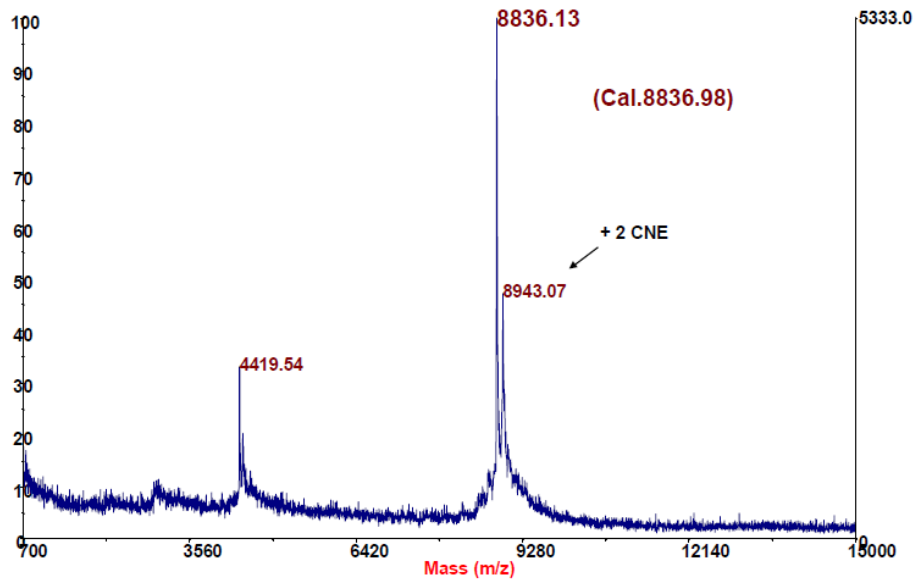
### T1.Sal

Maldi of 5'-S-TTTT-GAT TAC AGC CGG TGT ACG ACC CT-3' PUR

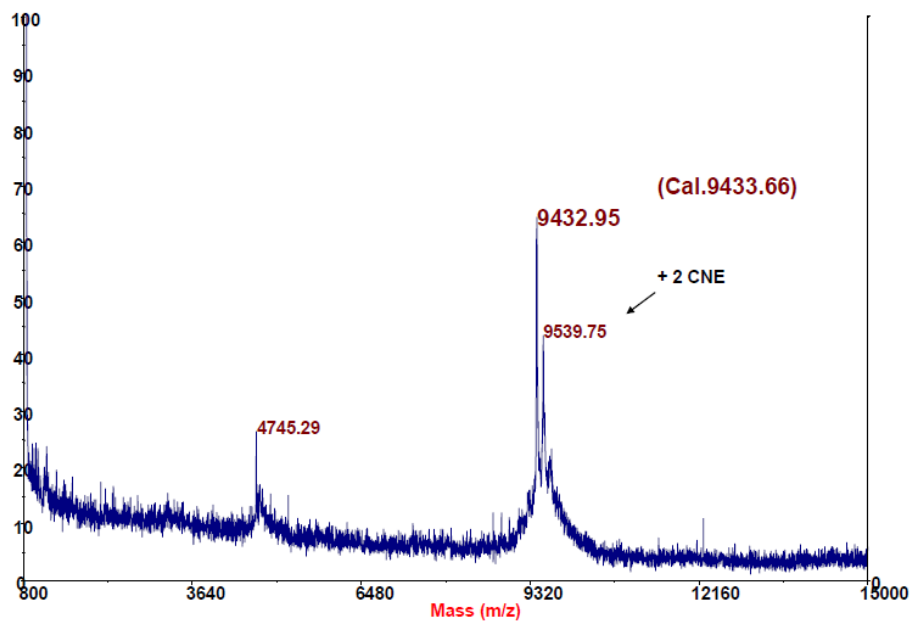


**T2.Sal**

Maldi of 5'-SS-TTTT-GAT TAC AGC CGG TGT ACG ACC CT-3'

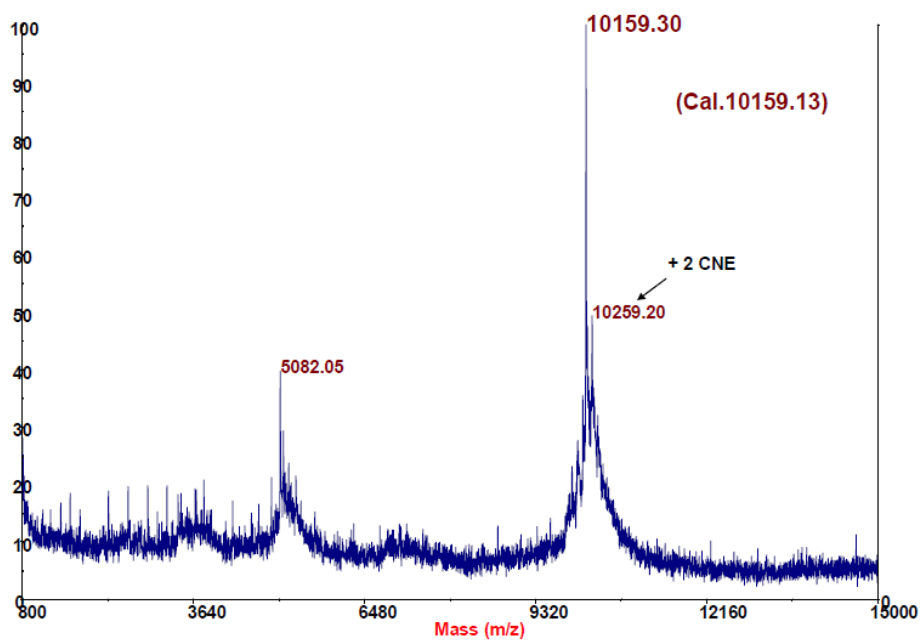
**T4.Sal**

Maldi of 5'-SSSS-TTTT-GAT TAC AGC CGG TGT ACG ACC CT-3'



## T4.Cam'

Maldi of 5'-SSSS-TTTT-AGA CGC AAT ACC GCG AGG TGG AGC A-3'

**Table S2.** Contact angle values ( $^{\circ}$ ) obtained for each functionalization step.

Raw	$33 \pm 2$
Ozone Activated	$\approx 0$
Vinyl functionalized	$68 \pm 3$
Vinyl functionalized after baking	$76 \pm 2$
Glycidyoxy functionalized	$51 \pm 2$
Glycidyoxy functionalized after baking	$56 \pm 2$
Alkynyl functionalized	$103 \pm 2$
Oligonucleotide functionalized	$50 \pm 2$

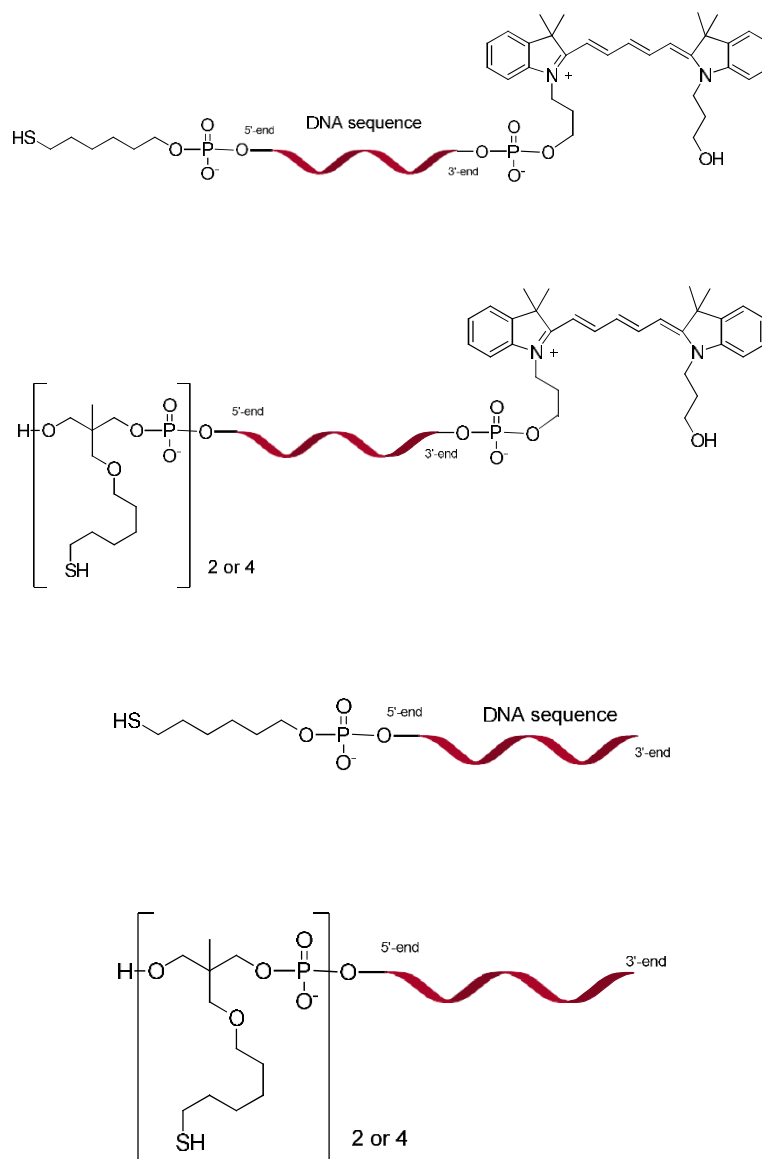
**Table S3:** Immobilization density for thiol-ene coupling (TEC) and thiol-yne coupling (TYC) approaches using mono, di and tetrathiolated probes, calculated by interpolation in the corresponding calibration curve. Immobilization yields calculated by the quotient of the actual density obtained and the theoretical density to be reached, assuming that all the probes in the spot are anchored to the surface.

[Probe] $\mu\text{M}$	Theoretical Immobilization Dens. ( $\text{pmol}/\text{cm}^2$ )	Immobilized Density ( $\text{pmol}/\text{cm}^2$ )					
		TEC			TYC		
		T1.I*	T2.I*	T4.I*	T1.I*	T2.I*	T4.I*
0.5	15.915	1.57	9.29	10.74	7.74	14.9	15.9
1	31.83	8.66	12.38	12.87	22.9	23.3	25.45
2	63.66	13.69	12.74	13.27	30.4	29.54	30.52
		Immobilization Yield (%)					
		TEC			TYC		
[Probe] $\mu\text{M}$		T1.I*	T2.I*	T4.I*	T1.I*	T2.I*	T4.I*
0.5		10	58	67	49	94	100
1		27	39	40	72	73	80
2		22	20	21	48	46	48

**Table S4:** Fluorescence intensity and signal increase (referred to T1.Sal) for T1.Sal, T2.Sal and T4.Sal, after PCR products hybridization and development with anti-digoxigenin rabbit antibody and Alexa647-labeled goat anti-rabbit antibody.

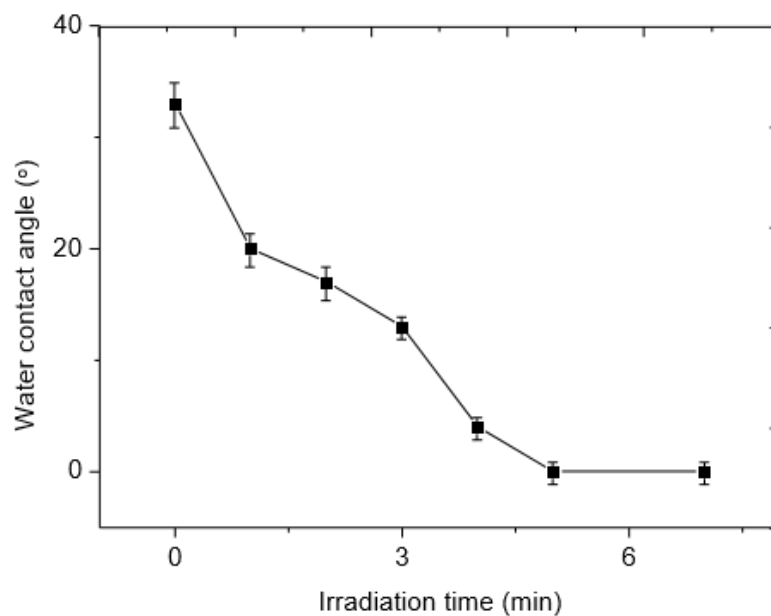
Probe	Neat intensity (a.u.)	Signal increase (%)
T1.Sal	4903.3	-
T2.Sal	5394.0	10
T4.Sal	6192.3	26

**Figure S1:** Structure of thiolated probes with and without cyanine 5 (Cy5) dye.

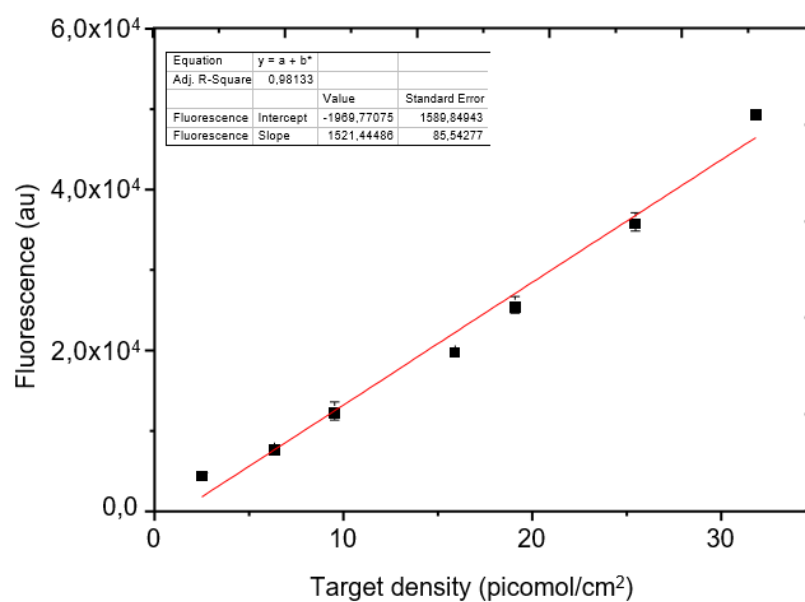




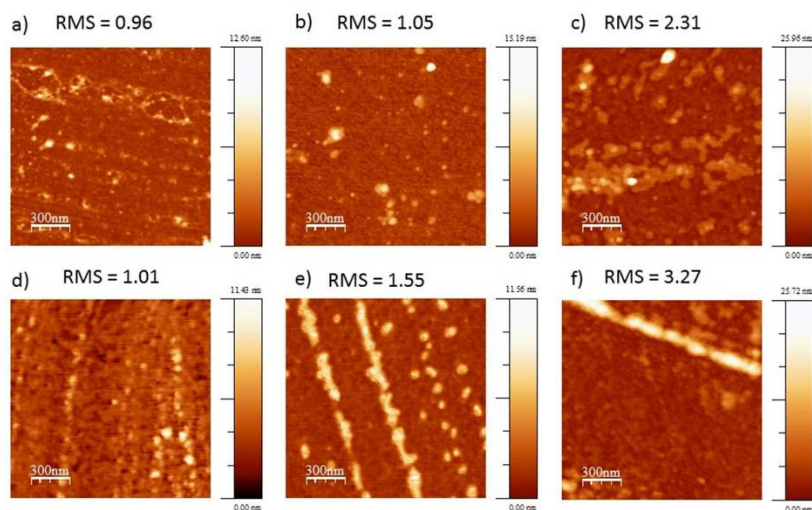
**Figure S2.** Contact angle variation with the irradiation time for surface activation at 264 nm wavelength.



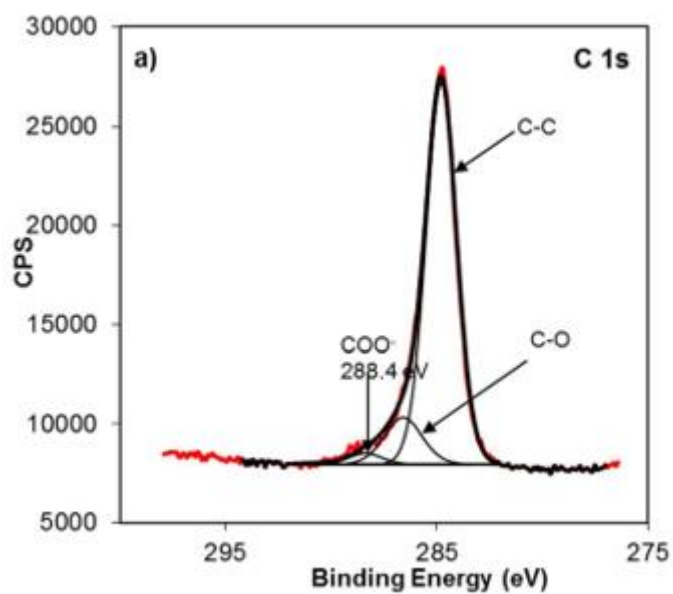
**Figure S3.** Calibration curve for Target A\* used in hybridization assays.

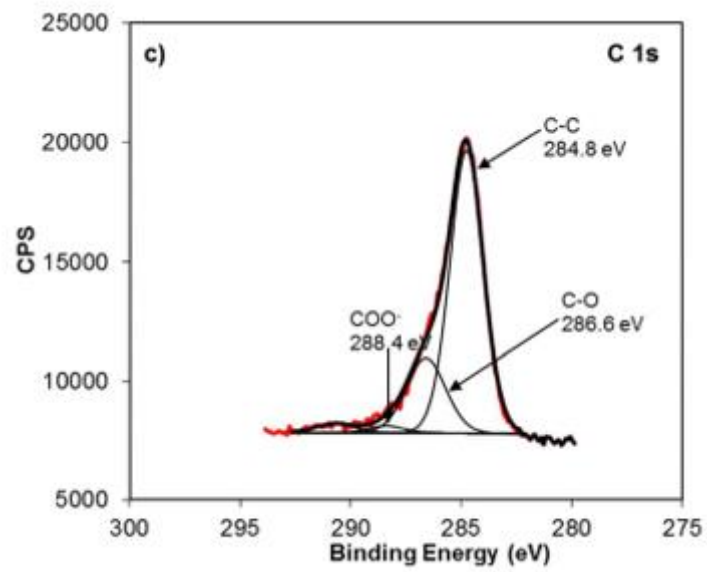
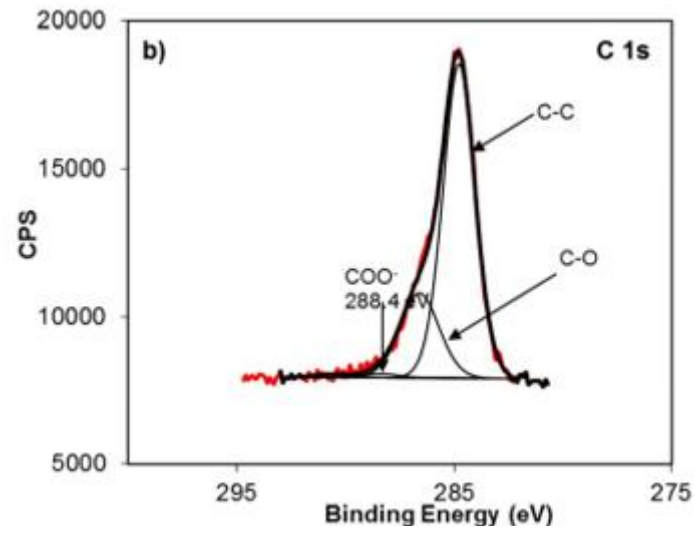


**Figure S4:** AFM Surface characterization of alkene-ended surfaces (topography 1.5x1.5  $\mu\text{m}$ ), with a) mono-thiolated, b) dithiolated, and c) tetrathiolated probes attached, resulting rms values are also shown. d) –f) Characterization of those surfaces after hybridization with the complementary strand.



**Figure S5.** XPS C1s deconvolution of alkene-ended surfaces, with a) mono-, b) di- and tetrathiolated probes (1  $\mu\text{M}$ ) attached. The increase in C-O peak contribution in b) and c) agrees with the higher probe immobilization detected by microarray.



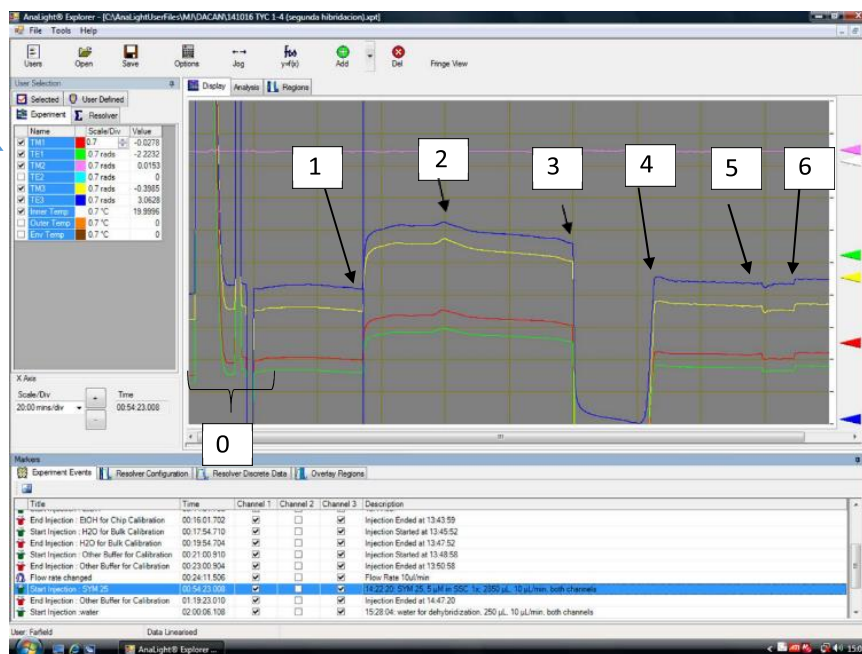


### Chapter 3

**Figure S6.** Screen print of data obtained with Dual Polarization Interferometry for thiol-ene coupling immobilization. The DPI has three channels in each chip, T1.H was immobilized in Channel 1, and T4.H in Channel 3. Channel 2 is the reference channel and no liquid pass through it.

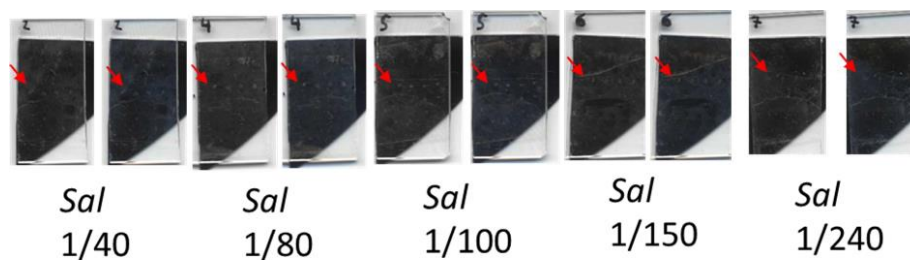
TM and TE  
of Channel 1

TM and TE  
of Channel 3



1. Chip calibration
2. Start injection of complementary strand (both channels)
3. Ends injection
4. Water injection for dehybridization
5. Water injection ends
6. Start injection of non-complementary strand (both channels)
7. Ends injection of non-complementary strand

**Figure S7.** Results obtained for a microarray containing T4.Sal (1x4 spots) and T4.Cam (1x4 spots) at 10  $\mu$ M, attached by thiol-ene approach, and hybridized with different dilutions (from 1/40 to 1/240) of PCR products from *Salmonella*. The microarray was developed using digoxin labelled PCR products, incubating with anti-digoxigenin primary antibody from rabbit, and gold-labelled goat antirabbit secondary antibody, and finally developing with silver enhancer solution. The images were taken with a conventional document scanner placing a piece of silicon on the back of the glass slide. Red arrows indicate the row that develop positive assay, and which corresponds to T4.Sal probe, T4.Cam did not developed black precipitate, as expected.











This chapter focuses on the development of protein microarrays as an alternative to DNA microarrays. Due to the limitations of DNA microarrays and the advances made in proteomics, protein microarrays appears as an alternative to overcome the current challenges.

Within the protein microarray category, antibodies were chosen due to the wide applicability of these systems. Nonetheless, as it is mentioned in the general introduction, an oriented anchoring, without loss of activity is hard to achieve. Thus, the following strategy is studied. Because of the successful results reached with the thiol-ene photocoupling reaction in the previous chapter, glass slides functionalized with alkenyl groups were employed. In addition, it is the first time that thiol-ene photocoupling reaction is applied to the development of antibody microarrays.

At this point, free thiol groups are necessary to accomplish our goals. Therefore, a selective reduction of the hinge region is performed, providing the required motifs in the biorecognition probe. This way, half antibodies are anchored to the surfaces with the paratope accessible to the analytes.

This work allowed the detection and quantification of interesting biomarkers with a higher performance than the whole antibody system. In addition, it opens the way to numerous biorecognition events, due to the great affinity and selectivity of the antibodies for its antigen.



## **4.1 Thiol-ene click chemistry towards easy microarraying of half-antibodies**

"Reproduced from Chem. Commun. **2018**, 54 (48), 6144–6147 with permission from the Royal Society of Chemistry."



## ABSTRACT

A UV light-induced thiol-ene coupling reaction (TEC) between half-antibodies (hIgG) and vinyl functionalized glass surfaces was run for biosensing in the microarray format. The accomplished performance improved that obtained with whole antibodies.

### 1. Introduction

The thiol-ene coupling reaction (TEC) fulfills all the desirable requirements of a click reaction [1]. It is highly effective, proceeds in high yields under mild reaction conditions and does not generate side products. TEC is normally initiated by UV light, which induces the formation of a thiol radical that reacts with a carbon-carbon double bond and leads to a thioether. This reaction is extremely tolerant to a variety of functional groups and is orthogonal [2]. Moreover, it can be performed in aqueous media, which allows this methodology to be used for biomolecules [3,4]. All these features make the TEC reaction a very interesting methodology for the covalent immobilization of biomolecules in microarray format and for its use in biosensing.

Liu et al. recently reported the use of thiol-ene click chemistry for an efficient and cysteine-selective thiol-ene click reaction-based bioconjugation strategy using colloidal nanoparticles [5]. They demonstrated its applicability with thiolated organic compounds, aptamers and enzymes (HRP), but not for antibodies, which is surely due to the difficulty of making free thiol moieties available in them.

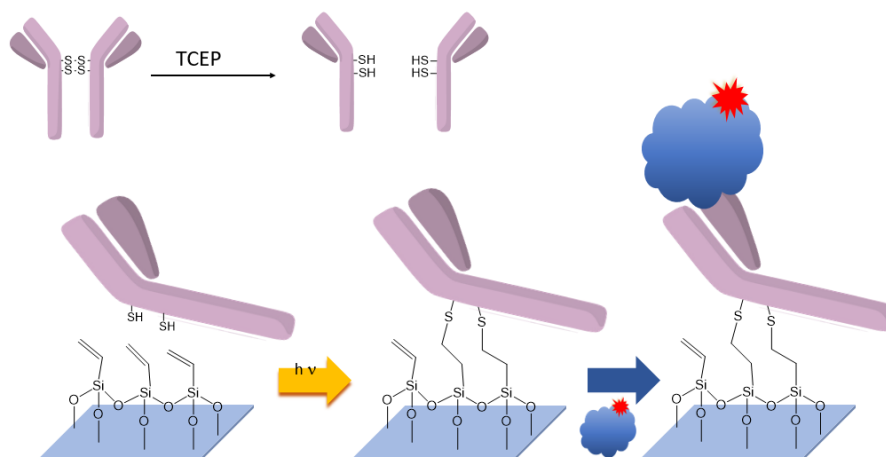
In line with our previous studies on the microarraying of thiolated oligonucleotides onto silicon-based surfaces by means of TEC [6–10], we envisioned the use of UV light-induced thiol-ene coupling to pattern antibodies microarrays rapidly and cleanly.

Immunoglobulin G antibodies (IgG) are the most prominent class of immunoglobulins employed in biosensing. They consist of four subunits, two heavy protein chains (H) and two light protein chains (L). The two halves are connected through the hinge region by a number of disulphide bonds, which depends on both the species [11] and the antibody subclass [12]. IgG immobilization is key in the development of sensing devices to detect analytes, such as proteins or drugs. IgGs can be immobilized either randomly or in an oriented fashion [13,14]. The latter is especially relevant for immunosensing applications since the antibody's paratopes must be available for antigens to be captured. Several approaches are reported for the oriented immobilization of IgGs, of which the most

relevant are those that employ protein A or G [15,16]. Due to unique capabilities of the antibody microarray and its applicability in a range of biomedical projects, a series of different antibody microarrays have been developed, of which some have become commercially available [17]. However, regardless the rapid technological advances in the last years, there are still technical issues that need to be overcome to ensure high-specificity and reproducibility of antibody arrays, to ensure high impact data and meaningful conclusions. The surface chemistry and the mode of antibody immobilization are within the experimental factors that may help to solve these problems.

Besides the whole antibody, antibody fragments like Fab' and scFv fragments can also be successfully employed as probes for immunosensing [18]. For the purpose of using the TEC approach to create antibody microarrays, we selected half antibodies (hIgG) as capture probes. Then the disulphide bonds bridging the two halves of an IgG must be properly reduced, which results in two half-antibodies that bear as many free-thiol groups as the disulphide bonds that exist in the hinge region [19]. hIgG have been reported to covalently link to maleimide-functionalized surfaces [20] and to chemisorb onto gold [21,22] and zinc [23] surfaces. However, a direct, rapid and efficient attachment of hIgGs on glass or other Si-based surfaces has not yet been reported.

More importantly, none of the reported approaches allows the site-directed immobilization of probes. Thus we hypothesized the use of UV light-induced thiol-ene coupling for the reaction between the exposed sulfhydryl groups in hIgG and alkene functionalized glass surfaces. The new free thiol moieties generated by the reduction of antibodies would be available for reaction via TEC with alkenes attached to surfaces, which would allow them to be immobilized in an oriented fashion, and be ready to be employed in biosensing. Figure 1.



**Figure 1.** Reduction of Immunoglobulin G antibodies (IgG) to half-antibodies (hIgG) and their use to generate planar microarrays on alkene-functionalized surfaces.

## 2. Experimental section

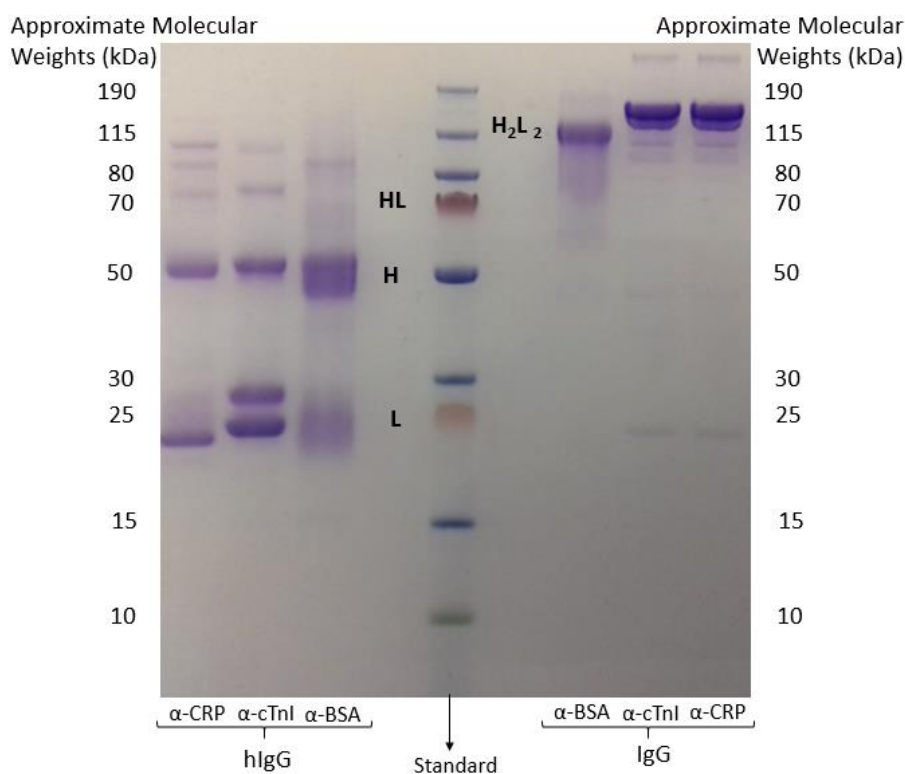
*Chemical, Reagents and Buffers.* Glass microscope slides were obtained from Labbox (Barcelona, Spain). Triethoxyvinylsilane, tris(2-carboxyethyl)phosphine (TCEP), bovine serum albumin (BSA), human C-reactive protein (CRP) and bovine serum albumin polyclonal antibody (IgG  $\alpha$ BSA) were purchased from Sigma Aldrich. The human C-reactive protein monoclonal antibody (IgG  $\alpha$ CRP) and Alexa Fluor 647 NHS ester, and NuPAGE™ Bis-Tris Welcome Pack, 4-12%, for SDS electrophoresis were purchased from ThermoFisher Scientific. Human cardiac troponin I (cTnI) and the human cardiac troponin I monoclonal capture antibody (IgG  $\alpha$ cTnI) were ordered from Abcam. The human cardiac troponin I monoclonal detection antibody (IgG  $\alpha$ cTnI) was obtained from Hytest and then labelled by the methodology described below. Toluene and 2-propanol were purchased from Scharlau. Ellman's reagent 5,5'-dithiobis(2-nitrobenzoic acid) (DTNB) was acquired from Acros Organics. Milli-Q water with a resistivity above 18 m $\Omega$  was used to prepare the aqueous solutions. The employed buffers were phosphate buffer saline (PBS 1x, 0.008 M sodium phosphate dibasic, 0.002 M sodium phosphate monobasic, 0.137 M sodium chloride, 0.003 M potassium chloride, pH 7.5), PBS-T (PBS 1x containing 0.05 % Tween 20), acetate buffer (0.15 M sodium acetate, 0.01 M EDTA, 0.1 M sodium chloride, pH 4.5) and bicarbonate buffer (0.1 M sodium bicarbonate, pH 8.3). All the buffer solutions were filtered through a 0.22  $\mu$ m pore size nitrocellulose membrane from Whatman GmbH (Dassel, Germany) before use.

*Instrumental methods.* Surface activation was carried out with a UV–ozone cleaning system UVOH150 LAB (FHR, Ottendorf-Okrilla, Germany). Microarrays were printed with a low-volume non-contact dispensing system from Biodot (Irvine, CA, USA), model AD1500. Probe photoattachment was done with the same UV-ozone cleaning system described above. Contact angle measurements were taken with Attension Theta Lite (by Biolin Scientific) and images were processed with OneAttension (version 3.1; Biolin Scientific). Measurements were taken in triplicate at room temperature with a volume drop of 5  $\mu$ L employing 18 m $\Omega$  water quality. The fluorescence signal of the spots in the microarrays was recorded with a homemade surface fluorescence reader (SFR) [27], with a high-sensitivity charge-coupled device camera Retiga EXi from Qimaging, Inc. (Burnaby, Canada), equipped with light-emitting diodes Toshiba TLOH157P as the light source or with a GenePix 4000B Microarray Scanner (Axon instruments). Microarray image treatment and quantification were done using the GenePix Pro 4.0 software from Molecular Devices, Inc. (Sunnyvale, CA, USA). The concentrations of proteins and antibodies were determined by measuring the optical density at 280 nm in a NanoDrop ND 1000 Spectrophotometer (ThermoFisher Scientific, Wilmington, Delaware, USA).

*Reduction of IgG to hIgG.* IgG in acetate buffer (0.15 M sodium acetate, 0.01 M EDTA, 0.1 M sodium chloride, pH 4.5) at the 4 mg/mL concentration, in the presence of 25 mmol/L TCEP, were incubated for 90 minutes at 37°C. The corresponding hIgG were purified by employing a 50 kDa centrifugal filter unit. The concentrations of the solutions were determined by a NanoDrop spectrophotometer. hIgG were characterized by Ellman's assay and SDS-PAGE electrophoresis.

*SDS-PAGE electrophoresis.* SDS-PAGE assays were performed using NuPAGE 4-12% Bis-Tris minigels under non-reducing conditions. Figure 2. Firstly, 5  $\mu$ g of whole antibodies and antibody fragments were solved in 2.5  $\mu$ L NuPAGE LDS sample buffer and water up to a volume of 20  $\mu$ L. Then each sample was loaded to a well and gels were run at a constant voltage of 200 V for 35 minutes. After electrophoresis, gels were developed with Coomassie Brilliant Blue R solution for 1 h, washed with water milli-Q and destained 3 times with acetic acid/methanol (40%/10%) for 15 minutes until any excess staining was removed. Finally, gels were rehydrated in milli-Q water.



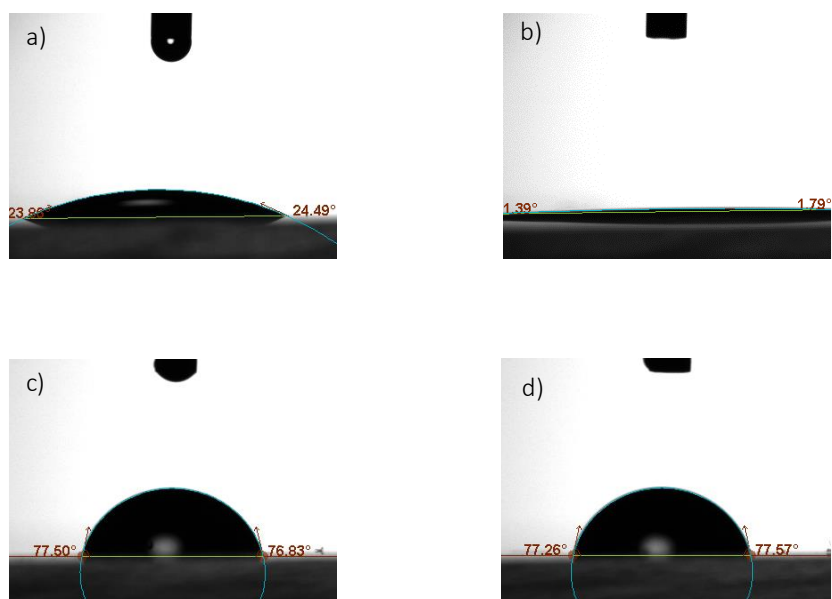


**Figure 2.** SDS-PAGE analysis of  $\alpha$ -BSA,  $\alpha$ -CRP and  $\alpha$ -cTnI in the reduced and non-reduced forms. IgG antibodies show mainly the expected H<sub>2</sub>L<sub>2</sub> bands, while hIgG antibodies display the corresponding HL, H and L fragments.

*Ellman's assay.* Ellman's reagent (10-fold molar excess) was added to a solution of 3.5 mg/mL in phosphate buffer and the resulting solution was stirred at room temperature for 15 minutes. The formation of 2-nitro-5-thiobenzoic acid was quantitatively determined at 412 nm with an extinction coefficient of  $14,150 \text{ M}^{-1}\text{cm}^{-1}$ .

*Surface chemical modification.* Glass microscope slides were cut into pieces of  $\approx 2 \times 1 \text{ cm}^2$ , cleaned with water and 2-propanol, and then air-dried. Afterwards they were placed in the UV-ozone cleaner and irradiated for 10 min at 254 nm. Subsequently, chips were immersed in a solution of triethoxyvinylsilane 2% in toluene for 2 h at room temperature. Finally, chips were washed with 2-propanol and air-dried before being baked for 20 min at  $100^\circ\text{C}$ .

The surface was characterized by the WCA (water contact angle), with evidence for the presence of alkene groups on the surface shown in all cases. Figure 3.



**Figure 3.** The water contact angle for the surface a) before and b) after activation using UV light, c) for the surface functionalized with triethoxyvinylsilane and d) for the vinylated surface after the baking step.

*Labelling probes with Alexa Fluor 647 (BSA,  $\alpha$ BSA, CRP, acTnI).* Firstly, 1 mg of protein was dissolved in 0.1 mL of bicarbonate buffer. Amine-reactive Alexa Fluor 647 (0.1 mg) was dissolved in 0.01 mL of DMSO and the resulting solution was immediately added to the solution of protein while stirring. The resulting mixture was protected from ambient light and stirred at room temperature for 1 h. The reaction mixture was purified by employing 30 kDa centrifugal filter units. The concentration and the label to probe ratio were determined by spectrophotometry.

*Photoimmobilization procedure.* hIgG microarrays were printed over the previously functionalized glass chips with the low-volume non-contact dispensing system from Biodot. The buffer employed was acetate buffer (0.15 M sodium acetate, 0.01 M EDTA, 0.1 M sodium chloride, pH 4.5), and 25 nL/spot were employed for the microarrays read with the microarray scanner, while 50 nL/spot were dispensed for the microarrays read with the SFR. The microarray had 4 spots per row and in both cases only one drop was printed on a single spot.

Five minutes after printing, chips were irradiated for 5 seconds with UV light ( $\lambda = 254$  nm) with the UV-ozone

cleaner. Afterwards, chips were stored in the dark for 10 minutes and then washed with PBS-T, rinsed with water and dried. They were subsequently incubated in the dark with

the labelled probe dissolved in 10% human serum for 30 min at ambient temperature. After washing with PBS-T and water, the fluorescence of the dried chips was measured by either the SFR or the microarray scanner. With the sandwich immunoassays, an additional 30-minute incubation step was run with the corresponding labelled detection antibody solution.

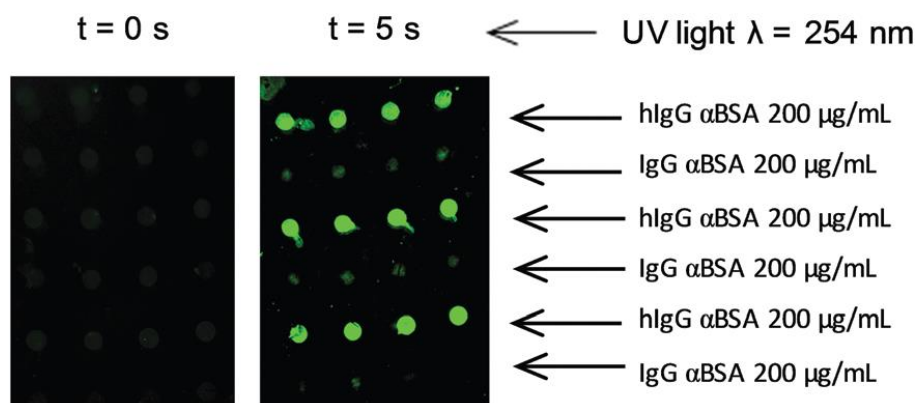
### 3. Results and discussion

Anti-bovine serum albumin polyclonal antibodies (IgG  $\alpha$ BSA), anti-human C-reactive protein monoclonal antibodies (IgG  $\alpha$ CRP) and anti-cardiac troponin I monoclonal antibodies (IgG  $\alpha$ TnI) were chosen as capture probes for microarraying. hIgG were obtained by treating the commercially available whole antibodies with tris(2-carboxyethyl)phosphine (TCEP) [19,24]. When employing other reductants, such as mercaptoethylamine (MEA), over reduction occurred, and additional disulphide bonds between light and heavy chains were cleaved, which led to loss of recognition capability. For the case of TCEP several temperatures, times, and concentrations were assayed. The chosen conditions were those providing the best biorecognition capability of the immobilized hIgG. The hIgG generated by TCEP reduction were characterized by SDS-PAGE electrophoresis (Figure 2). Additionally, in order to determine the available number of free thiol groups after reduction, hIgG were subjected to Ellman's assay [25]. This experimental procedure showed that the polyclonal hIgG  $\alpha$ BSA prepared by TCEP reduction bore 3.7 free sulfhydryl groups while monoclonal hIgG  $\alpha$ TnI had 2.6 thiol groups. These values agree with the average number of disulphide bridges in the hinge region for the rabbit polyclonal and mouse monoclonal IgG2a subtype, respectively [26]. Besides, the maintenance of the recognition ability indicated that the link between H and L was not disrupted.

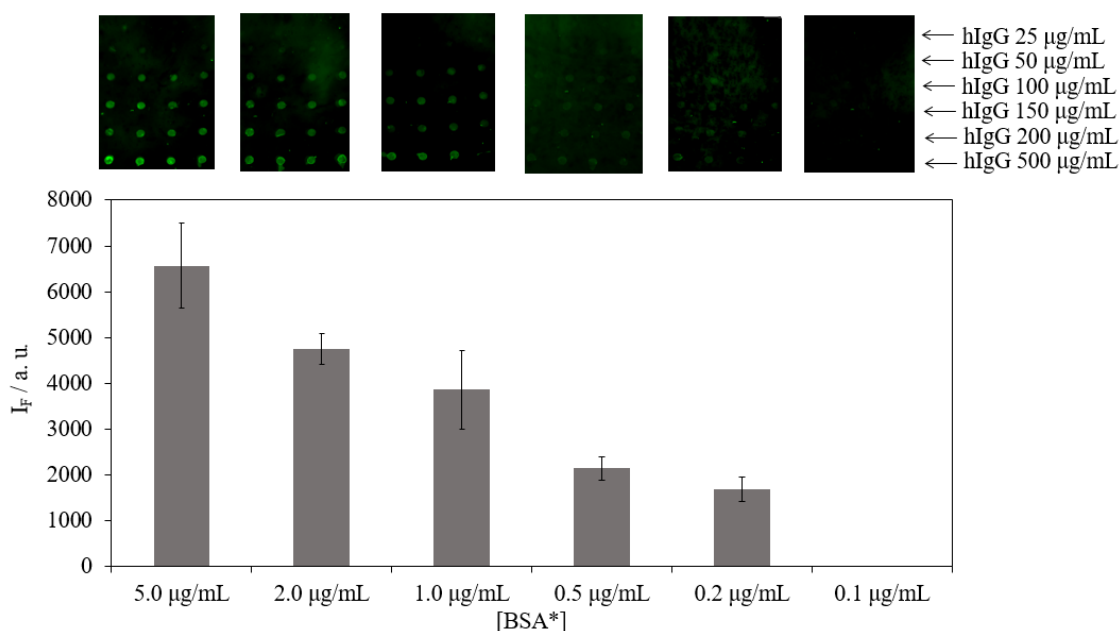
Due to the presence of free thiols after the cleavage of disulphide bonds, the new generated hIgG were used for UV light-induced thiol-ene coupling (TEC) on vinyl-functionalized glass surfaces. Glass slides were activated by UV light irradiation and were subsequently functionalized by immersion in a solution of triethoxyvinylsilane in toluene (2%; 2 h), which led to an alkene coated surface. The water contact angle (WCA) increased from 24° for the non-functionalized surface to 77° for the organosilane coated chip (Figure 3).

The bovine serum albumin (BSA)/rabbit polyclonal hIgG  $\alpha$ BSA system was selected as the model system to optimize the methodology. Thus freshly protein A purified polyclonal IgG  $\alpha$ BSA was reduced with TCEP to the corresponding hIgG. Alexa Fluor 647-labelled hIgG  $\alpha$ BSA was dispensed over the vinyl-functionalized glass chips at different concentrations (0–20  $\mu\text{g mL}^{-1}$ ). Then chips were irradiated for 5 s at 254 nm and were subsequently washed. By measuring the fluorescence emission with a homemade surface fluorescence reader (SFR) [27], the immobilized probe density was determined as  $2.36 \pm 0.18 \text{ pmol cm}^{-2}$  which corresponds to the maximum theoretical immobilization density for a half-antibody by assuming that the dimensions of an antibody are *ca.*  $15 \times 5 \times 5 \text{ nm}^3$ .

Several hIgG  $\alpha$ BSA solutions at different concentrations (between 25 and 500  $\mu\text{g mL}^{-1}$ ) were microarrayed over the vinyl-functionalized glass chips, and irradiated with UV-light to induce TEC. Whole IgG  $\alpha$ BSA antibodies were also immobilized for comparison purposes. After washing, chips were subsequently incubated for 30 min in the dark with different solutions of freshly prepared Alexa Fluor 647-labelled BSA (BSA\*). The fluorescence of the cleaned and dried chips was measured with the SFR. hIgG performed significantly better than the corresponding whole antibodies in all cases. The fluorescence intensity of the signal obtained for hIgG was 7-fold stronger than the signal obtained for the immobilized IgG. When comparing to the performance of a standard microarray created by immobilizing the IgG onto an epoxytated surface, the fluorescence obtained for our microarray was up to 4-fold higher than for the case of the reference microarray. The control experiments done in the absence of UV-light showed that irradiation was needed for the TEC reaction to take place and to immobilize the hIgG. Figure 4. Under these experimental conditions, the sensitivity assay showed that the system can detect up to  $0.2 \mu\text{g mL}^{-1}$  of labelled BSA when the hIgG is immobilized at concentrations that equal or were higher than  $50 \mu\text{g mL}^{-1}$ . Figure 5. The reached sensitivity fell within the limit of detection (LOD) that was intrinsic to the detection system employed and the obtained BSA labelling ratio. The density of labelled protein retained on the surface by the immobilized hIgG resulted  $1.54 \text{ picomol cm}^{-2}$ , which provides a 65% of biorecognition yield from the attached probes.



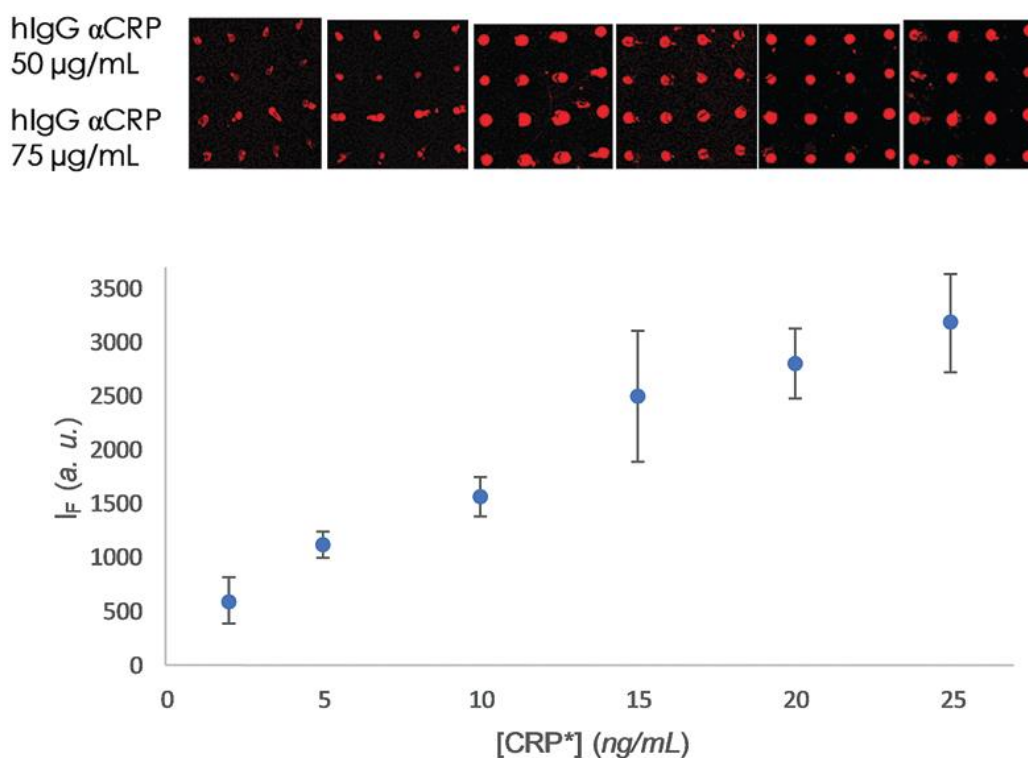
**Figure 4.** Fluorescence intensities recorded for the microarrays obtained by spotting hIgG  $\alpha$ BSA and IgG  $\alpha$ BSA at the 200  $\mu\text{g mL}^{-1}$  concentration for the chips irradiated at 254 nm for either 0 or 5 seconds, and the subsequent incubation with 5  $\mu\text{g mL}^{-1}$  Alexa Fluor 647-labelled BSA.



**Figure 5.** Fluorescence intensities recorded for the microarray of hIgG  $\alpha$ BSA at different concentrations, incubated with decreasing concentrations of Alexa Fluor 647-labelled BSA. The bar graph represents the data for the arrays of hIgG  $\alpha$ BSA immobilized at 150  $\mu\text{g mL}^{-1}$ .

Once the BSA/polyclonal hIgG  $\alpha$ BSA model system was fully optimized, the methodology was applied to detect analytes of clinical interest, C-reactive protein (CRP) and cardiac troponin I (cTnI). CRP is an annular pentameric protein found in blood plasma, whose levels rise in response to inflammation. The sensitivity of the CRP assay using the corresponding monoclonal hIgG was determined by preparing microarrays and incubating them with different concentrations of Alexa Fluor 647 labelled CRP (CRP\*,

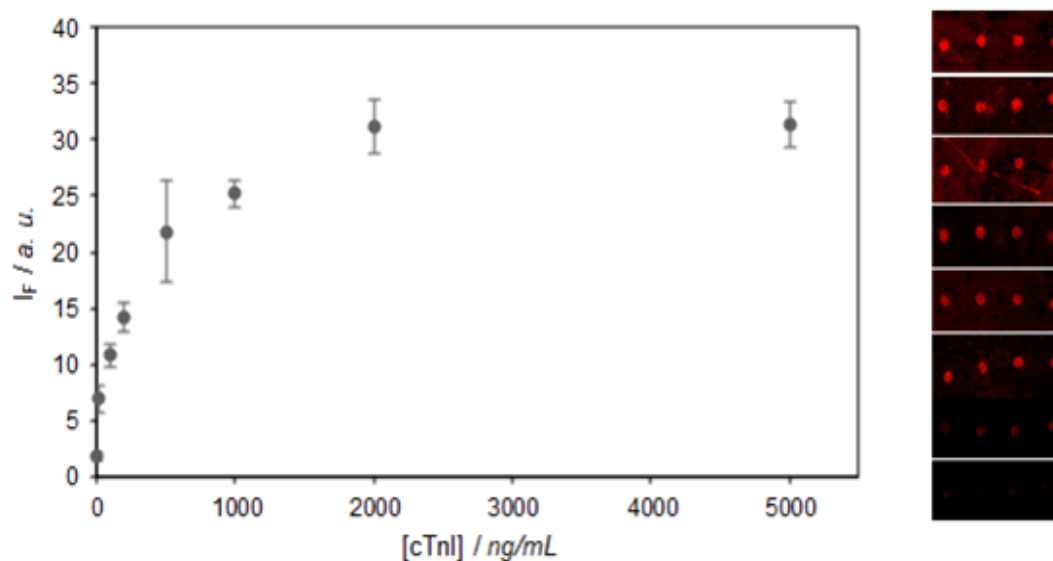
in 10% diluted human serum, following the procedure described for the BSA system). In this case, system performance was assessed by employing a commercially available microarray scanner to avoid the LOD constraints associated with the SFR (when employing the microarray scanner for the BSA/hIgG  $\alpha$ BSA model system the sensitivity reached was  $2.3 \text{ ng mL}^{-1}$ ). The minimum concentration detected under these experimental conditions was  $2 \text{ ng mL}^{-1}$  for a hIgG  $\alpha$ CRP microarray generated by TEC when employing a  $50 \text{ mg mL}^{-1}$  concentration of half-antibody. Figure 6.



**Figure 6.** Sensing curve for recognizing the Alexa Fluor 647 labelled C-reactive protein (CRP\*) by the hIgG  $\alpha$ CRP microarray generated by UV-light-induced thiol-ene coupling for a  $50 \text{ } \mu\text{g mL}^{-1}$  solution of half-antibodies.

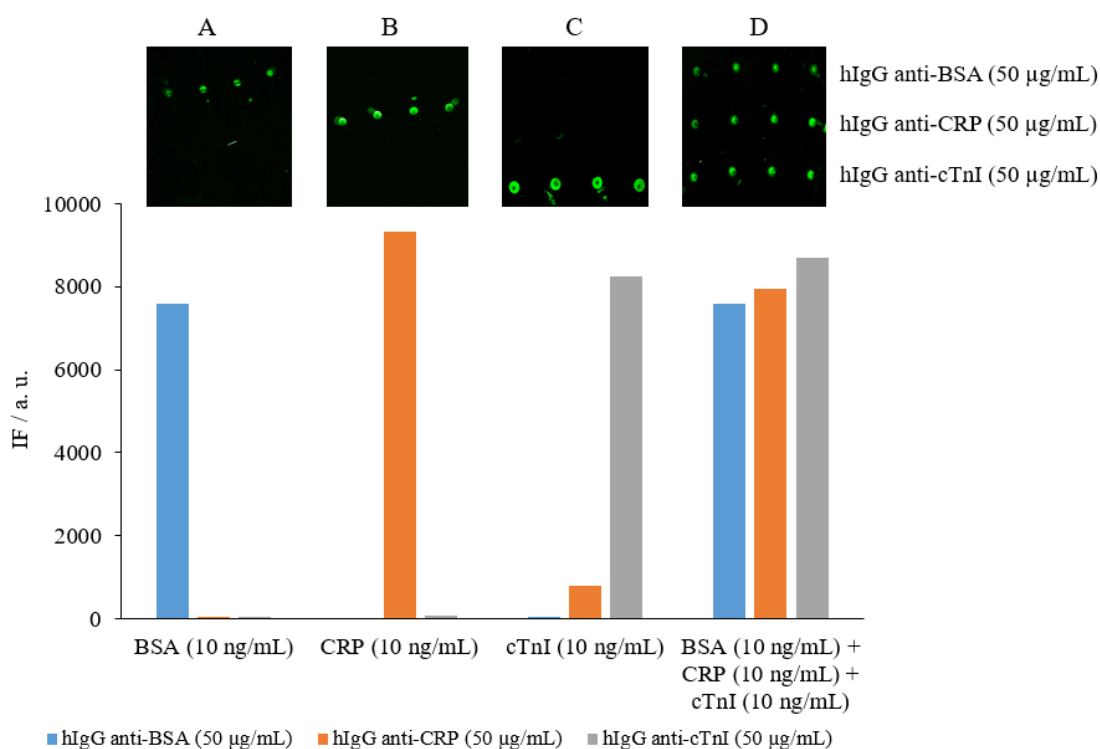
The immunodetection of cTnI was also carried out. cTnI is a cardiac and skeletal muscle protein considered to be the most sensitive and, significantly, the most specific marker in myocardial infarction diagnosis [28]. Due to the fact that cTnI is most unstable to buffer changes, and it could not, therefore, be labelled with the Alexa Fluor fluorophore, a sandwich-type immunoassay had to be performed. Thus the detection of cTnI was done by creating microarrays of the hIgG of monoclonal  $\alpha$ cTnI by the TEC methodology as described above, and by incubating with different cTnI concentrations in 10% diluted

human serum, and by finally developing with a labelled detection antibody. This optimized methodology obtained a sensitivity of  $10 \text{ ng mL}^{-1}$  of cTnI. Figure 7.



**Figure 7.** Sensitivity assay for cTnI using a sandwich immunoassay with hIgG  $\alpha$ cTnI ( $50 \text{ mg mL}^{-1}$ ) immobilized by TEC as the capture agent.

Finally, in order to test the selectivity of the optimized systems, microarrays were created following the same biofunctionalization protocol with a row of each hIgG  $\alpha$ BSA, hIgG  $\alpha$ CRP and hIgG  $\alpha$ cTnI. Some chips were incubated only with labelled BSA, others with labelled CRP, others with cTnI, and others with a mixture of the three targets, in 10% diluted human serum. Fluorescence was recorded after the development step with the labelled detection antibody for cTnI. All the results demonstrated the specificity of capture. Figure 8.



**Figure 8.** Multiplexing assay in the microarray format for protein/antibody systems: BSA/hIgG  $\alpha$ BSA, CRP/hIgG  $\alpha$ CRP and cTnI/hIgG  $\alpha$ cTnI. Incubating with (A) BSA\* ( $10 \text{ ng mL}^{-1}$ ); (B) CRP\* ( $10 \text{ ng mL}^{-1}$ ); (C) cTnI ( $10 \text{ ng mL}^{-1}$ ); (D) mixture of BSA\* ( $10 \text{ ng mL}^{-1}$ ), CRP\* ( $10 \text{ ng mL}^{-1}$ ) and cTnI ( $10 \text{ ng mL}^{-1}$ ).

#### 4. Conclusions

To the best of our knowledge, we herein report the first example of a UV light-induced thiol-ene coupling reaction between the free thiol groups present in half-antibodies and vinyl-functionalized surfaces to construct microarrays. The performance of these half-antibody microarrays generated by TEC dramatically improved the response compared to whole antibody microarrays, which is likely due to the fixed orientation of hIgG under these conditions. The methodology described herein allowed us to successfully determine interesting analytes (CRP and cTnI in this case), perform multiplexing experiments, and represent a non-reported approach for the effective immobilization of antibodies under very mild, rapid and biocompatible conditions. The approach is applicable to a wide range of materials that can be functionalized with organosilane chemistry, and can selectively pattern antibodies on the surface by using selective irradiation through a photomask.



## ACKNOWLEDGMENTS

The authors acknowledge the funding from the European Commission through the project H2020-634013-PHOCNOSIS. This work was also partly supported by MINECO CTQ/2013/45875-R, CTQ/2016/75749-R, FEDER, and GVA PROMETEO II 2014/40.

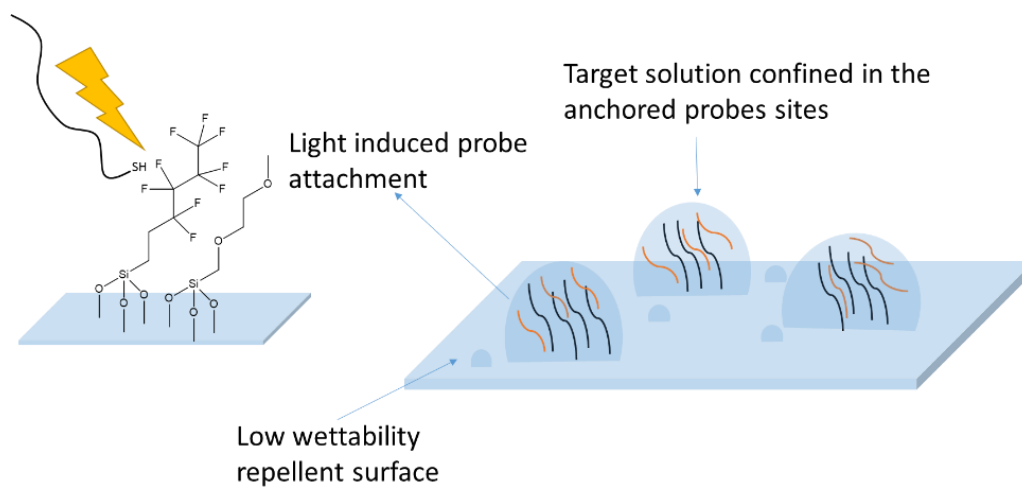
## REFERENCES

- [1] H.C. Kolb, M.G. Finn, K.B. Sharpless, Click Chemistry: Diverse Chemical Function from a Few Good Reactions, *Angew Chem Int Ed.* 40 (2001) 2004–2021.
- [2] C.E. Hoyle, C.N. Bowman, Thiol-Ene Click Chemistry, *Angew. Chem. Int. Ed.* 49 (2010) 1540–1573. doi:10.1002/anie.200903924.
- [3] A. Dondoni, The emergence of thiol-ene coupling as a click process for materials and bioorganic chemistry, *Angew Chem Int Ed.* 47 (2008) 8995–8997.
- [4] D. Weinrich, M. Köhn, P. Jonkheijm, U. Westerlind, L. Dehmelt, H. Engelkamp, P.C.M. Christianen, J. Kuhlmann, J.C. Maan, D. Nüsse, H. Schröder, R. Wacker, E. Voges, R. Breinbauer, H. Kunz, C.M. Niemeyer, H. Waldmann, Preparation of Biomolecule Microstructures and Microarrays by Thiol-ene Photoimmobilization, *ChemBioChem.* 11 (2010) 235–247. doi:10.1002/cbic.200900559.
- [5] Y. Liu, W. Hou, H. Sun, C. Cui, L. Zhang, Y. Jiang, Y. Wu, Y. Wang, J. Li, B.S. Sumerlin, Q. Liu, W. Tan, Thiol-ene click chemistry: a biocompatible way for orthogonal bioconjugation of colloidal nanoparticles, *Chem. Sci.* 8 (2017) 6182–6187. doi:10.1039/C7SC01447C.
- [6] J. Escorihuela, M.J. Bañuls, R. Puchades, Á. Maquieira, DNA microarrays on silicon surfaces through thiol-ene chemistry., *Chem. Commun.* 48 (2012) 2116–2118. doi:10.1039/c2cc17321b.
- [7] J. Escorihuela, M.-J. Bañuls, R. Puchades, Á. Maquieira, Development of Oligonucleotide Microarrays onto Si-Based Surfaces via Thioether Linkage Mediated by UV Irradiation, *Bioconjug. Chem.* 23 (2012) 2121–2128. doi:10.1021/bc300333a.
- [8] J. Escorihuela, M.J. Bañuls, S. Grijalvo, R. Eritja, R. Puchades, Á. Maquieira, Direct covalent attachment of DNA microarrays by rapid thiol-ene “click” chemistry, *Bioconjug. Chem.* 25 (2014) 618–627. doi:10.1021/bc500033d.
- [9] D. González-Lucas, M.J. Bañuls, R. Puchades, Á. Maquieira, Versatile and Easy Fabrication of Advanced Surfaces for High Performance DNA Microarrays, *Adv. Mater. Interfaces.* 3 (2016) 1500850.
- [10] P. Jiménez-Meneses, M.-J. Bañuls, R. Puchades, Á. Maquieira, Fluor-thiol Photocoupling Reaction for Developing High Performance Nucleic Acid (NA) Microarrays, *Anal. Chem.* 90 (2018) 11224–11231. doi:10.1021/acs.analchem.8b00265.

- [11] V. Crivianu-Gaita, A. Romaschin, M. Thompson, High efficiency reduction capability for the formation of Fab' antibody fragments from F(ab)<sub>2</sub> units, *Biochem. Biophys. Rep.* 2 (2015) 23–28. doi:10.1016/j.bbrep.2015.04.004.
- [12] G. Vidarsson, G. Dekkers, T. Rispens, IgG Subclasses and Allotypes: From Structure to Effector Functions, *Front. Immunol.* 5 (2014). doi:10.3389/fimmu.2014.00520.
- [13] P. Jonkheijm, D. Weinrich, H. Schröder, C.M. Niemeyer, H. Waldmann, Chemical Strategies for Generating Protein Biochips, *Angew. Chem. Int. Ed.* 47 (2008) 9618–9647. doi:10.1002/anie.200801711.
- [14] F. Rusmini, Z. Zhong, J. Feijen, Protein Immobilization Strategies for Protein Biochips, *Biomacromolecules.* 8 (2007) 1775–1789. doi:10.1021/bm061197b.
- [15] Y. Jung, J.Y. Jeong, B.H. Chung, Recent advances in immobilization methods of antibodies on solid supports, *The Analyst.* 133 (2008) 697. doi:10.1039/b800014j.
- [16] N. Tajima, M. Takai, K. Ishihara, Significance of Antibody Orientation Unraveled: Well-Oriented Antibodies Recorded High Binding Affinity, *Anal. Chem.* 83 (2011) 1969–1976. doi:10.1021/ac1026786.
- [17] Z. Chen, T. Dodig-Crnković, J.M. Schwenk, S. Tao, Current applications of antibody microarrays, *Clin. Proteomics.* 15 (2018). doi:10.1186/s12014-018-9184-2.
- [18] V. Crivianu-Gaita, M. Thompson, Aptamers, antibody scFv, and antibody Fab' fragments: An overview and comparison of three of the most versatile biosensor biorecognition elements, *Biosens. Bioelectron.* 85 (2016) 32–45. doi:10.1016/j.bios.2016.04.091.
- [19] A. Makaraviciute, C.D. Jackson, P.A. Millner, A. Ramanaviciene, Considerations in producing preferentially reduced half-antibody fragments, *J. Immunol. Methods.* 429 (2016) 50–56. doi:10.1016/j.jim.2016.01.001.
- [20] H.Y. Song, J. Hobley, X. Su, X. Zhou, End-on Covalent Antibody Immobilization on Dual Polarization Interferometry Sensor Chip for Enhanced Immuno-sensing, *Plasmonics.* 9 (2014) 851–858. doi:10.1007/s11468-014-9680-9.
- [21] H. Sharma, R. Mutharasan, Half Antibody Fragments Improve Biosensor Sensitivity without Loss of Selectivity, *Anal. Chem.* 85 (2013) 2472–2477. doi:10.1021/ac3035426.
- [22] S. Wu, H. Liu, X.M. Liang, X. Wu, B. Wang, Q. Zhang, Highly Sensitive Nanomechanical Immunosensor Using Half Antibody Fragments, *Anal. Chem.* 86 (2014) 4271–4277. doi:10.1021/ac404065m.
- [23] M. Pal, S. Lee, D. Kwon, J. Hwang, H. Lee, S. Hwang, S. Jeon, Direct immobilization of antibodies on Zn-doped Fe<sub>3</sub>O<sub>4</sub> nanoclusters for detection of pathogenic bacteria, *Anal. Chim. Acta.* 952 (2017) 81–87. doi:10.1016/j.aca.2016.11.041.
- [24] D.J. Cline, S.E. Redding, S.G. Brohawn, J.N. Psathas, J.P. Schneider, C. Thorpe, New Water-Soluble Phosphines as Reductants of Peptide and Protein Disulfide Bonds: Reactivity and Membrane Permeability †, *Biochemistry.* 43 (2004) 15195–15203. doi:10.1021/bi048329a.

- [25] G.L. Ellman, Tissue sulfhydryl groups, *Arch. Biochem. Biophys.* 82 (1959) 70–77. doi:[https://doi.org/10.1016/0003-9861\(59\)90090-6](https://doi.org/10.1016/0003-9861(59)90090-6).
- [26] L.J. Harris, S.B. Larson, K.W. Hasel, A. McPherson, Refined Structure of an Intact IgG2a Monoclonal Antibody, (n.d.) 17.
- [27] D. Mira, R. Llorente, S. Morais, R. Puchades, A. Maquieira, J. Marti, High throughput screening of surface-enhanced fluorescence on industrial standard digital recording media, *Proc SPIE.* 5617 (2004) 364–373. doi:10.1117/12.578301.
- [28] A.B. Storrow, R.M. Nowak, D.B. Diercks, A.J. Singer, A.H.B. Wu, E. Kulstad, F. LoVecchio, C. Fromm, G. Headden, T. Potis, C.J. Hogan, J.W. Schrock, D.P. Zelinski, M.R. Greenberg, R.H. Christenson, J.C. Ritchie, J.S. Chamberlin, K.R. Bray, D.W. Rhodes, D. Trainor, P.C. Southwick, Absolute and relative changes ( $\Delta$ ) in troponin I for early diagnosis of myocardial infarction: Results of a prospective multicenter trial, *Clin. Biochem.* 48 (2015) 260–267. doi:10.1016/j.clinbiochem.2014.09.012.





## **5. A novel photocoupling reaction between C-F bonds and thiol groups and its application to microarray technology**



With the goal of going a step forward in microarray features and taking into account the results achieved in the chapter 3, development of a novel photocoupling reaction, merged with the use of highly hydrophobic surfaces, is pursued. More concretely, able to provide a quick, clean and biocompatible probe attachment to the support surface.

Regarding to the substrate, highly hydrophobic surfaces containing C-F motifs were chosen to undertake the covalent anchoring, being glass slides functionalized with a perfluorinated organosilane, the main platform employed. These hydrophobic surfaces allow the confinement of the probes in very hydrophilic and small spots, with hydrophobic protein repellent surrounding. This reduces the unspecific interactions, and favors the approximation of the analyte only where the probe is immobilized.

Finally, wettability modulation of these hydrophobic surfaces was performed physical and chemically, and different irradiation sources were studied.

Thus, the development of photoinduced reactions to produce the immobilization of thiolated probes onto these low reactive surfaces, is a very interesting methodology to favor and increase the immobilization densities and detection capacity of the measuring device.

This chapter is arranged in three sections.

The first section (chapter 5.1), displays a scientific publication, reporting all the work carried out to clear up the main aspects of the developed fluor-thiol photoinduced reaction. In this section, three different surfaces containing C-F bonds are employed to corroborate the reaction: perfluorinated glass slides, polyvinylidene fluoride and polytetrafluoroethylene membranes. The role of a thiol group in the molecule to be anchored, and light in the coupling process, is demonstrated in this work. In addition, chemical modulation of surface wettability employing a hydrophilic and repellent organosilane, to increase the immobilization anchoring and recognition capability, is performed. The applicability of this system to the discrimination of SNPs and the detection of bacterial PCR products is proven as well.

The second section (chapter 5.2), shows the results reached through a 2-month placement at the Aalborg University (Denmark). Aiming the improvement of microarray resolution and density immobilization, employment of a more sophisticated laser-based irradiation

system, is pursued. This setup allows a controlled irradiation of the surface through femto-second pulses, which permits the miniaturization and patterning of the microarrays. Combining this irradiation mode and the fluor-thiol photoclick reaction, a high resolution is reached, having immobilization only where the laser beam illuminate. Application to several bioreceptors such as oligonucleotides, antibodies and half antibodies, is demonstrated.

The third section, (chapter 5.3), focuses on the introduction to microstructured surfaces. During a 3-month placement at the Fraunhofer Institute for Laser Technology (Aachen, Germany), physical modulation of glass surface properties (roughness), is studied. With the goal of getting higher microarray performances, surfaces with different topographies are prepared and characterized. We hypothesize that configuration of the surface affects to the emission of light, so controlling the surface roughness, an enhancement of fluorescence intensity would be observed. Then, assays are performed onto these structured surfaces, and compared to non-structured surfaces, to analyze the effect of the different microstructures in the fluorescence signal.



## **5.1 Fluor-thiol photocoupling reaction for developing high performance nucleic acid (NA) microarrays**

"Reprinted with permission from *Anal. Chem.* **2018**, 90 (19), 11224–11231. Copyright 2018 American Chemical Society."



## ABSTRACT

Spatially controlled anchoring of NA probes onto microscope glass slides by a novel fluor-thiol coupling reaction is performed. By this UV-initiated reaction, covalent immobilization in very short times (30 s at 254 nm) is achieved with probe densities of up to 39.6 pmol/cm<sup>2</sup>. Modulating the surface hydrophobicity by combining a hydrophobic silane and a hydrophilic silane allows the fabrication of tuned surfaces where the analyte approaches only the anchored probe, which notably reduces nonspecific adsorption and the background. The generated substrates have proven clear advantages for discriminating single-basepair mismatches, and for detecting bacterial PCR products. The hybridization sensitivity achieved by these high-performance surfaces is about 1.7 pM. Finally, this anchoring reaction is demonstrated using two additional surfaces: polytetrafluoroethylene (PTFE) and polyvinylidene fluoride (PVDF) membranes. This provides a very interesting pathway for anchoring thiolated biomolecules onto surfaces with C–F motifs via a quick clean UV reaction.

## 1. Introduction

Nowadays, the development of new biosensors to diagnose and prevent different illnesses in specifically, selectively and quickly using inexpensive devices is still required. NA microarrays have revolutionized basic research in molecular and cellular biology, biochemistry and genetics.<sup>1-3</sup> Although the technology in NA is most advanced, protein microarrays also emerge as a potential and useful tool.<sup>4,5</sup>

During the fabrication of NA microarrays, glass microscope slides are widely used as a support because of their good optical properties, high resistance and rigidity, low cost, and surface chemical derivatization by organosilane chemistry.<sup>2</sup> Effective surface activation and functionalization protocols are key for microarray production. A good control of these processes improves the performance and quality of assays. For instance, the properties of functionalized surfaces will define efficient immobilization of probes and their biorecognition capacity.

Regarding the immobilization process, covalent anchoring of NA probes is preferred to adsorption because of its robustness and reliability.<sup>6,7</sup> Besides, photoactivated reactions like fluor-thiol photocoupling chemistry that is herein reported, offer several advantages,

such as that associated with click chemistry reactions. These reactions are fast, clean and enviro-friendly, and allow oriented immobilization<sup>8,9</sup> in aqueous media, which is crucial for their bioutilily.<sup>10,11</sup> When light activates the reaction, additional advantages, such as site-specific immobilization, come into play. One example of these photo-click-chemistry reactions that has been recently applied to microarray technology is thiol-ene coupling,<sup>12-15</sup> which allows biomolecules to be anchored to silicon-based surfaces selectively under mild conditions, with quantitative or near-quantitative yields.

Another important parameter to take into account in either the immobilization or the hybridization process is the surface. Superhydrophobic surfaces are based on nonreactive and low-surface energy functional groups which prevent most chemical and biological substances from adhering.<sup>16</sup> Thanks to this good property, hydrophobic surfaces can be applied to develop NA microarrays with a water-repellent background that confines the sample only to the point where the probe is anchored by reducing nonspecificity and improving sensitivity. Nevertheless, poor surface wettability can hamper proper contact between the groups on the surface and the probes in the solution by lowering immobilization yields and hindering effective hybridization.<sup>17,18</sup>

Although the use of perfluorinated surfaces is challenging, it can be very useful for applications in microarray technology, among others.<sup>19-22</sup> In fact in this study we report the fluor-thiol photocoupling reaction to covalently bond thiolated probes directly to a perfluoroalkyl surface for the first time. This methodology allows the probes bearing a thiol group to be anchored to the C-F bond of highly hydrophobic surfaces quickly and cleanly. To support the nature of the formed bond, two additional surfaces (PVDF and PTFE membranes) containing C-F motifs are used apart from silanized glass slides.

Given the extreme hydrophobicity of this surface, which hinders effective hybridization, modulating surface hydrophobicity by an optimal combination of paramount water-repellent silane as 1H,1H,2H,2H-perfluorodecyltriethoxysilane (PFTS) and a hydrophilic repellent silane, such as 2-[methoxy(polyethyleneoxy)<sub>6-9</sub>propyl]trimethoxysilane (PEGS), is necessary in the functionalization process.

The new developed surface favors the selective approach of the target solution only at the point to which the probe is anchored as it is the most hydrophilic area of the entire surface. This fact minimizes the background and nonspecific binding without having to resort to a blocking step before the hybridization assay. Following this strategy, DNA microarrays

can be applied to discriminate single nucleotide polymorphisms (SNPs) and to detect bacterial DNA (e.g. *Salmonella*). SNPs are the most abundant form of genetic variation in the human genome<sup>23</sup> and allow disease predispositions and drug responses to be predicted,<sup>24</sup> whereas *Salmonella* bacteria have been the main cause of foodborne bacterial illnesses in humans in many countries for at least more than 100 years.<sup>25</sup>

## 2. Experimental section

*Chemicals, reagents and buffers.* The glass microscope slides used as substrates for the microarrays were obtained from Labbox Labware, S.L. (Spain). The Immobilon-P PVDF membranes were acquired from Merck (Spain). The PTFE membranes came from Wolfpack (Spain). 2-[Methoxy(polyethyleneoxy)<sub>6-9</sub>propyl]trimethoxysilane was purchased from Gelest (Germany). 1H,1H,2H,2H-Perfluorodecyltriethoxysilane and vinyltrimethoxysilane were supplied by Sigma-Aldrich (Spain). Toluene was purchased from Scharlau (Spain). 3,3',5,5'-Tetramethylbenzidine liquid substrate was acquired from SDT (Germany). Note: all the chemicals were handled following the corresponding material safety data sheets. All the chemicals were used without further purification.

Milli-Q water, with a resistivity above 18 mΩ, was used to prepare the aqueous solutions. The employed buffers, phosphate buffer saline (PBS1x, 0.008 M sodium phosphate dibasic, 0.002 M sodium phosphate monobasic, 0.137 M sodium chloride, 0.003 M potassium chloride, pH 7.5), PBS-T (PBS1x containing 0.05% Tween 20) and saline sodium citrate (SSC1x, 0.15 M sodium chloride, 0.02 M sodium citrate, pH 7) were filtered through a 0.45 μm pore size nitrocellulose membrane of the Fisher brand (Germany) before being used.

The oligonucleotides in Table 1 were acquired from Eurofins Genomic (Ebersberg, Germany). DNA concentration and quality were determined by measuring optical density at 260/280 nm in a NanoDrop ND 1000 Spectrophotometer (Thermo Fisher Scientific, Wilmington, Delaware, USA). The PCR-amplified *Salmonella* products were obtained as previously described.<sup>26, 27</sup>

**Table 1.** Used oligonucleotides sequences

Name	Sequence (5' to 3')	5'-	3'-
Probe 1*	CCCGATTGACCAGCTAGCATT- (T) <sub>15</sub>	Cy5	SH
Probe 1	(T) <sub>15</sub> -CCCGATTGACCAGCTAGCATT	SH	-
Probe 2	(T) <sub>15</sub> -CCCGATTGACC <u>T</u> GCTAGCATT	SH	-
Probe 3	(T) <sub>15</sub> -CCCGATTGAT <u>T</u> AGCTAGCATT	SH	-
Probe 4	(T) <sub>15</sub> -CC <u>A</u> TATTGACCAGCTA <u>T</u> CATT	SH	-
Probe 5	CGCCGATAACTCTGTCTCTGTA	SH	-
Probe 6	TTTTGATTACAGCCGGTGTACGACCCT	SH	-
Probe 7	TTTTAGACGCAATACCGCGAGGTGGAGCA	SH	
Probe 8	TTTTGATTACAGCCGGTGTACGACCCT	SH	Dig <sup>a</sup>
Target 1*	AATGCTAGCTGGTCAATCGGG	Ax <sup>b</sup>	-

<sup>a</sup> Digoxigenin, <sup>b</sup> Alexa Fluor® 647

*Instrumental methods.* Contact angle system OCA20, equipped with the SCA20 software, was provided by Dataphysics Instruments GmbH (Filderstadt, Germany). Measurements were taken in quintuplicate at room temperature with a volume drop of 5  $\mu$ L employing the 18 m $\Omega$  water quality.

Microarray printing was done with a low-volume noncontact dispensing system from Bi-dot (Irvine, CA, USA), model AD1500. Irradiation at 254 nm was carried out in a UV-Ozone Surface Cleaner (UVOH 150 LAB; FHR, Anlagenbau, Germany, GMBH), while irradiation at 365 nm was performed with a mercury capillary lamp (6 mW/cm<sup>2</sup>, Jelight Irvine, CA, USA) placed at a fixed distance (0.5 cm).

The fluorescence signal of the spots was recorded with a homemade surface fluorescence reader (SFR) operating with a high-sensitive charge couple device camera Retiga EXi (Qimaging Inc., Burnaby, Canada) with light-emitting diodes Toshiba TLOH157P as the light source.<sup>28</sup> A microarray scanner Axon4000B (Molecular Devices, CA, USA) was employed for the immobilization density determinations. The GenePix Pro 4.0 software (Molecular Devices, Inc. Sunnyvale, CA, USA) was utilized for the microarray image analysis and subsequent quantification.

X-ray photoelectron spectra were recorded with a Sage 150 spectrophotometer (SPECS Surface Nano Analysis GmbH, Berlin, Germany). Non monochromatic Al K $\alpha$  radiation (1486.6 eV) was used as the X-ray source operating at 30 eV constant pass energy for the elemental specific energy binding analysis. The vacuum in the spectrometer chamber was  $9 \times 10^{-9}$  hPa and the analyzed sample area was 1 mm<sup>2</sup>. Attenuated total reflectance infrared spectra were recorded by a Bruker Tensor 27 FT-IR coupled to a Platinum ATR accessory.

*Silanization of slides.* Commercial glass slides were cut into chips (2 x 1 cm) and were cleaned with a UV-Ozone Surface Cleaner for 7 min at 254 nm to remove organic contaminants. To introduce the reactive functional groups, these chips were immersed in a 2% v/v solution of the corresponding silane in toluene for 45 min at room temperature. Then samples were withdrawn from the silane solution, washed several times with toluene and air-dried. Next chips were baked for 1 h at 110 °C. To generate the hydrophobic surfaces, chips were treated with 1H,1H,2H,2H-perfluorodecyltriethoxysilane (surface A), whereas a combination of 2-[methoxy(polyethyleneoxy)<sub>6-9</sub>propyl] trimethoxysilane and 1H,1H,2H,2H-perfluorodecyltriethoxysilane was used at a ratio of 4:1 v/v (surface B) for the optimized surfaces. The control substrates were functionalized with vinyltrimethoxysilane (surface C), and with 2-[methoxy(polyethyleneoxy)<sub>6-9</sub>propyl] (surface D), as explained before.

*Oligonucleotide immobilization.* The attachment of the thiolated and nonthiolated oligonucleotides onto different surfaces was studied. On the one hand, glass microscope slides were treated following the above-described procedure to obtain the corresponding surface A, B and D. To prove covalent anchoring, Probe 1\* consisting of a 5'-Cy5- and 3'-SH-labeled oligonucleotide, and Target 1\* consisting of a 5'-AlexaFluor®647-labeled oligonucleotide (Table 1), were spotted at 0.5, 1 and 2  $\mu$ M in PBS1x onto surfaces A and D, and were exposed to UV-light at 254 nm for 30 s to induce the immobilization. Afterward slides were thoroughly rinsed with SSC1x and air-dried. On the other hand, the PVDF and PTFE membranes were used as supports with no further modification. Probe 1\* and Target 1\* at 0.5, 1 and 2  $\mu$ M in PBS1x were spotted onto both surfaces and exposed to UV-light at 254 nm for 5 s to encourage immobilization. Afterward substrates were thoroughly rinsed with PBS-T and air-dried. Finally, in order to calculate immobilization density, increasing concentrations of Probe 1\* (from 0.01 to 10  $\mu$ M; 40 nL/spot; 4 spots/row) in PBS1x were spotted onto surface B and exposed to UV-light at 254 nm for 30 s to

produce immobilization. Slides were thoroughly rinsed with SSC1x and air-dried. The immobilization results were obtained from the fluorescence signals using a microarray scanner.

*Hybridization Assays.* To study the hybridization efficiency on the developed surface, glass chips were treated as described above to obtain surface B. Afterward the solutions containing serial dilutions of Probe 1 (from 0.25 to 5  $\mu\text{M}$ ) in PBS1x were spotted (40 nL) onto surface B to create the microarray (four spots per concentration). Then slides were exposed to UV-light at 254 nm for 30 s, washed with SSC1x and air-dried. After washing, 15  $\mu\text{L}$  of Target 1\* (concentrations ranging from 0.0005 to 0.25  $\mu\text{M}$  in SSC1x) were spread over the surface with a coverslip. After incubation in a humid chamber for 1 h at 37 °C, the coverslip was gently removed, and the chip was washed with SSC1x. The fluorescence intensity of the spots was recorded using the SFR as before.

*Mismatches detection.* Four oligonucleotide sequences, Probes 2, 3, 4 and 5 having zero, one, two and three base mismatches for Target 1\*, respectively, and Probe 5 as the negative control (no complementary) were spotted (0.5  $\mu\text{M}$ , 40 nL/spot) with a noncontact dispenser onto surface B to create the microarray. After probe immobilization, the microarray was subjected to hybridization with Target 1\* (50 nM) in SSC under different stringency conditions (salt concentration from 0.1x to 5x and formamide content from 0-25%) for 1 h at 37 °C. After washing and drying, fluorescence was measured with the SFR.

*Detection of the Salmonella PCR products.* Glass slides were perfluoro-functionalized as described above. Then the solutions containing SH-labeled Probe 6 (the Salmonella-specific probe), Probe 7 (the negative hybridization control) and Probe 8 (the positive development control) at 1 and 2  $\mu\text{M}$  were spotted in PBS1x onto surface B to fabricate the microarrays. Afterward slides were exposed to UV-light at 254 nm for 30 s and subsequently washed with SSC1x and air-dried. Then the digoxigenin-labeled PCR product solutions (15  $\mu\text{L}$ ) in hybridization buffer (SSC1x) were distributed over the chip. PCR duplexes were first denatured by a 10-minute incubation at 95 °C followed by fast cooling for 1 min on ice. After incubating 1 h at 37 °C, slides were washed with SSC1x and air-dried. Finally, slides were incubated with an HRP-labeled anti-digoxigenin antibody produced in goat (dilutions ranging from 1/10 to 1/10000 in SSC1x and 15% of formamide) for 30 min at room temperature, washed with SSC1x, air-dried and revealed with TMB solution for around 2 min.



### 3. Results and discussion

*Surface Chemical Derivatization.* Surface functionalization was studied to achieve a reproducible protocol to fabricate homogenous and stable surfaces that allowed the covalent anchoring of NA probes and the hybridization process. First, glass microscope slides were cleaned with a UV-ozone lamp for 7 minutes to provide the high density of the hydroxyl groups on the surface, which are key for effective silanization. Then substrates were functionalized by immersion in organosilane solution (2% in toluene). Given the potential difficulties of the microarray in the later hybridization process due to the high hydrophobicity of perfluorinated surfaces (surface A), different derivatizations to modulate surface wettability were studied. The proper combination of an excellent water repellent as PFTS, with a highly hydrophilic and anti-fouling compound as PEGS, could allow tuned surfaces to be obtained on which the analyte approaches specifically to the appropriate immobilized probe, thus preventing nonspecific adsorption and lowering the background.

In an attempt to achieve a commitment between the surface repellence and bioavailability of the anchored probes, the PEGS-PFTS ratio and functionalization times were optimized. After several experiments to modulate surface hydrophobicity, functionalization times of 45 minutes and a volume ratio of 1:4 (PFTS/PEGS) showed an optimal contact angle (about  $100^\circ$ ) and, thus, promising surfaces for successful hybridization. Longer times or higher PFTS concentrations were not suitable for the hybridization process because of the excessive surface hydrophobicity, which lowered the surface wettability too much by impeding the target solution to properly reach the anchored probes. Thus, every substrate was functionalized for 45 minutes at room temperature to acquire the corresponding surface properties, and hydrophobicity was controlled to ensure reproducible and homogeneous surfaces.

Six different surfaces were used in this study: first, a highly hydrophobic surface only made of PFTS to prove the fluor-thiol reaction (surface A). Second, a wettability-tuned surface with an optimal PFTS-PEGS ratio (1:4) to facilitate the hybridization process (surface B). Third, a control standard surface was functionalized with vinyltrimethoxysilane (surface C)<sup>29</sup> in comparison to surface B. Fourth, an anti-fouling control surface using organosilane PEGS (surface D) was prepared. Finally, two additional surfaces (PVDF and PTFE membranes) were used to support the anchoring mechanism. These surfaces did not require further activation or functionalization, which cut the assay time.

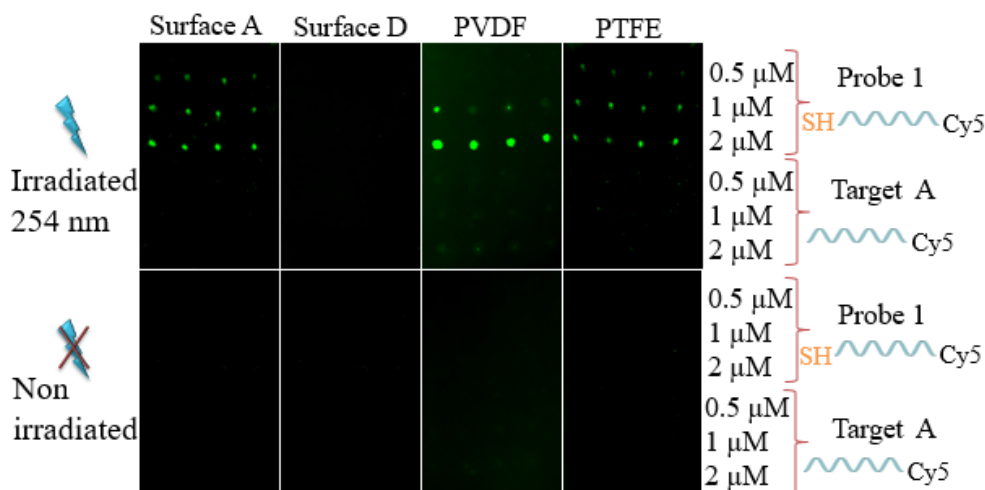
The quality of the surface was monitored by thoroughly measuring the water contact angle (WCA) on the whole surface. As seen in Figure S1, the commercial glass slides displayed a contact angle of  $37^\circ$ , whereas the activated surfaces showed contact angles around  $0^\circ$  by the UV-lamp. This is attributed to an increased number of hydroxyl moieties generated on the surface by the oxidation and cleaning treatment. Upon functionalization with the corresponding organosilanes, hydrophobic surface A, with a WCA of  $110^\circ$ , and modulated surface B, with a WCA of around  $100^\circ$ , were obtained. Surfaces C and D provided a WCA of around  $70^\circ$  and  $27^\circ$ , respectively. The raw PVDF and PTFE membranes displayed a contact angle of  $130^\circ$  and  $148^\circ$ , respectively.

The X-ray photoelectron spectroscopy (XPS) experiments with the raw glass slides, and with surfaces A and B, were performed. The emergence of  $\text{CF}_2$  and  $\text{CF}_3$  peaks at 290 and 292 eV on the functionalized surfaces corroborated the success of the functionalization process (Figure S2). The chemical composition of modulated surface B was established from high-resolution XPS as a part of the surface characterization (Table S1).

*DNA immobilization assays.* Based on the paper of Al-Gharabli et al. who established C-F cleavage in the presence of an oxidizing agent,<sup>30</sup> immobilization of a thiolated probe for its reactivity with perfluorinated surfaces under UV irradiation was investigated. This is an unknown reaction with an excellent potential in microarray technology, among others, inspired in the *para*-fluoro-thiol “click” chemistry. In this reaction, the *para*-F position in the aromatic ring showed high reactivity to nucleophilic substitution.<sup>19–21</sup> Thus in order to demonstrate the use of the fluor-thiol photochemical reaction for tethering thiolated DNA, a 5' thiol-ended probe, labeled with Cy5 at its 3' end (Table 1, Probe 1\*), was spotted at different concentrations in PBS 1x (from 0.01 to 4  $\mu\text{M}$ ; 40 nL/spot; 4 spots/row) onto surface A, and displayed successful fluorescence intensity after thorough washing. Several irradiation times (from a few seconds to 1 h) and two wavelengths (365 and 254 nm) were investigated. The best results in fluorescence intensity terms were obtained for UV exposure times of 30 seconds at 254 nm. This time noticeably reduced those previously reported to create DNA microarrays by thiol-ene and thiol-yne photo click reactions, where times of at least 20 minutes, and 365 nm are used.<sup>11, 13, 29, 31</sup> This difference was due to the low-power irradiation of the 365 nm lamp (6  $\text{mW}/\text{cm}^2$ ) compared to the current 254 nm lamp (50  $\text{mW}/\text{cm}^2$ ), and was also due to the change of wavelength itself from 365 nm to 254 nm, the latter of which is more energetic irradiation.

This novel immobilization has a clear advantage over the published work as regards irradiation times, and is an interesting technique to be applied to many fields, like nanoparticles biofunctionalization.

Several assays were run to corroborate the linking nature and to prove the reliability of the system.

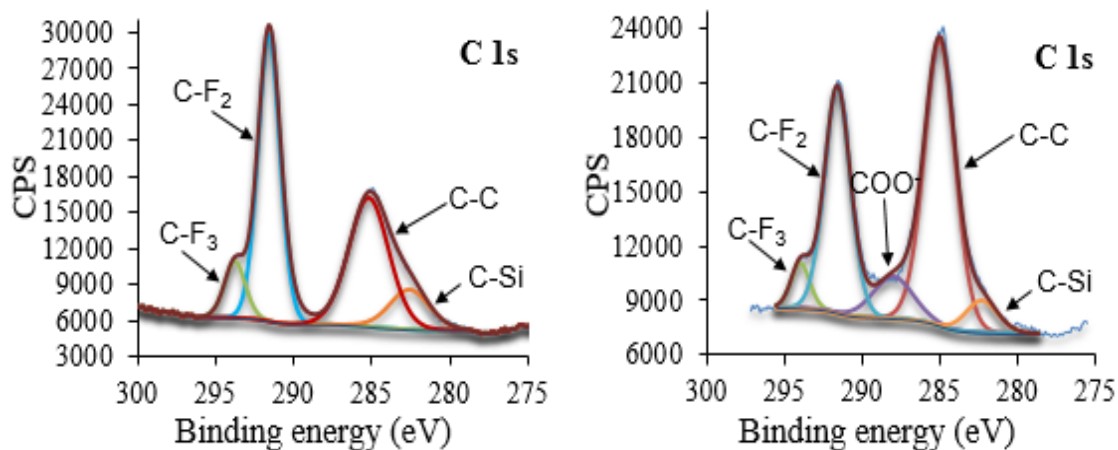


**Figure 1.** The labeled thiolated and nonthiolated probes were spotted at different concentrations onto surfaces A, D, PVDF and PTFE. Afterward, surfaces were irradiated. Fluorescence images were recorded, after washing, by SFR. The control surfaces without irradiation were also measured after the washing steps.

First, immobilization studies on surfaces A and D were performed (Figure 1). Surfaces were spotted with the fluorescence-tagged thiolated and non thiolated probes (Probe 1\* and Target 1\*, respectively) at different concentrations (from 0.5 to 2 μM). Afterward, surfaces were exposed for 30 seconds to UV-light at 254 nm, or were kept in dark, and washed. Then, the fluorescence of the microarray was recorded with the SFR. Successful thiolated probe immobilization onto surface A occurred after irradiation, whereas the nonthiolated probe did not anchor. The thiolated and nonthiolated probes did not adsorb onto surface A when kept in the dark without irradiation. Surface D showed the expected anti-bioadsorption capability, and the thiolated and nonthiolated probes were not immobilized after irradiation. Therefore, we conclude that a thiol motif and UV irradiation are necessary to achieve covalent bonding to surface A, and suggest the formation of a reactive thiol radical.

Second to identify the anchoring moiety on the surface, the above protocol was applied to two additional surfaces: PVDF and PTFE (Figure 1). With surface A, three anchoring points were possible; bonds Si-O, the C-H and C-F. Thus, the PVDF membranes that only had C-H and C-F motifs were used. Different irradiation times, from 1 s to 1 min, were assayed. The assays showed that a 5-second photoexposure were enough to achieve successful probe immobilization. Regarding the results, the attachment of the thiolated probe to this surface continued to occur, whereas the nonthiolated probe did not anchor to the surface. Moreover, without irradiation, no fluorescence signal was detectable. These results ruled out the bonding between the thiol and the silane, and left open the possibility of nucleophilic substitution or dehydrohalogenation taking place. To this end, the same experiments on the PTFE surface  $-(CF_2-CF_2)_n-$  were performed. These surfaces, irradiated with the thiolated probes for only 30 seconds, showed successful probe immobilization with high-fluorescence intensity after thorough washing. Additionally, the nonirradiated surfaces showed no fluorescence, as well as the nonthiolated probes. These results support a covalent attachment between the thiol and the C of the C-F bonds, with F being displaced as it was the only common motif in all the substrates.

Third, X-ray photoelectron spectroscopy (XPS) analyses were done to know the nature of the chemical bonding between a thiolated compound and the perfluorinated surfaces (Figure 2). Surface A was irradiated for 1 minute at 254 nm under the UV lamp in presence of a thiolated probe and washed, and compared with the raw surface A. The contribution of the C-C bond increased dramatically and a new contribution from COO bonds was observed. All this pointed to the attachment of the probe to the surface. It should be noted that the profile of the C1s peak did not vary significantly when the raw surface was irradiated in the absence of the thiolated compound (Figure S2). The  $CF_3/CF_2$  ratio remained unchanged for all the control surfaces and only changed in the case of the surface A irradiated in presence of thiolated probe, demonstrating the role of C-F bonds in the probe attachment.

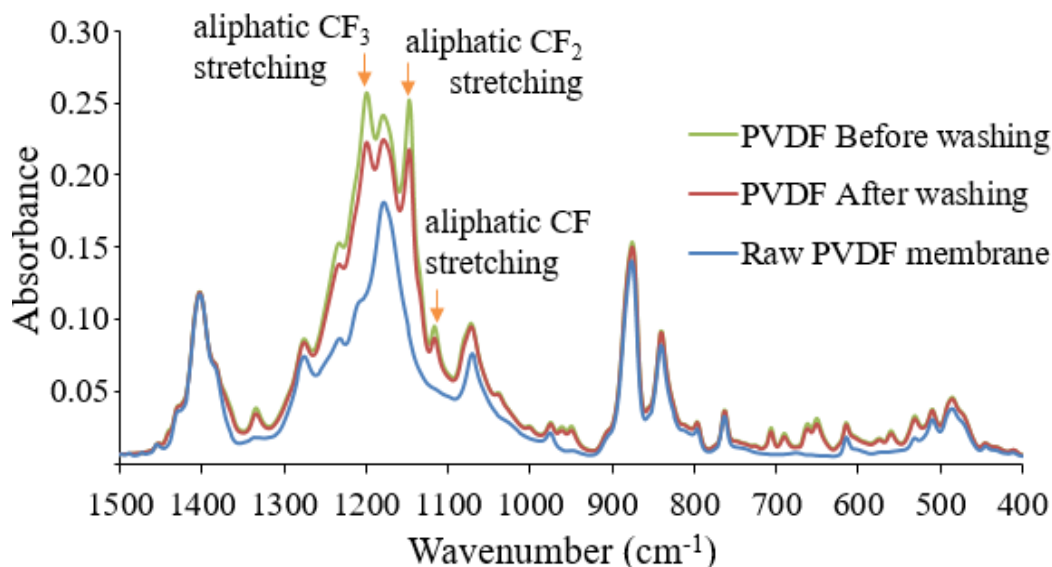


**Figure 2.** XPS high-resolution spectra. Left. C 1s spectrum of surface A. Right C 1s spectrum of surface A + thiolated compound + UV irradiation and washing. C-F<sub>2</sub> bond at 291 eV and C-F<sub>3</sub> bond at 293 eV.

Finally, the ATR-IR experiments on the PVDF membranes were performed. This surface was chosen for its composition to allow very thin layers to be better detected. No changes in the glass slides and Teflon surfaces were detected using these instruments. Microscope glass slides are too wide compared to the thin thiolated compound layer formed. With the Teflon membranes, the C-F signals of the anchored compound matched the C-F peaks of the membrane itself. Thus 40  $\mu$ L of 1H,1H,2H,2H-perfluorodecanethiol 0.90 M in methanol were added to a PVDF membrane (1 x 1 cm). After solvent evaporation, membranes were irradiated for 1 minute at 254 nm under the UV lamp. Afterward, membranes were washed with methanol for 30 minutes to ensure the complete removal of the nonanchored compound. After washing thoroughly, the C-F signals of the thiolated compound remained. However, no significant spectral change was observed after washing when the membrane was not irradiated in the presence of the thiolated compound. This corroborates a covalent attachment between the thiolated compound and the PVDF surface. Figure 3 shows the FTIR-spectra obtained for the raw and treated membranes, where new peaks appear and are attributed to the aliphatic -CF<sub>2</sub> (1000-1150  $\text{cm}^{-1}$ ) and -CF<sub>3</sub> (1350-1100  $\text{cm}^{-1}$ ) stretchings, and, more importantly, to the aliphatic CF stretching (1100-1000  $\text{cm}^{-1}$ ), which supports the bonding of the thiol compound to the CF<sub>2</sub> moieties of the surface.

Therefore, we report that, upon irradiation, the formed radical thiols attack the C of a CF<sub>2</sub> unit by displacing the F of the substrate, and shows the anchoring of a thiolated probe to a C-F bond for the first time (Figure S3).

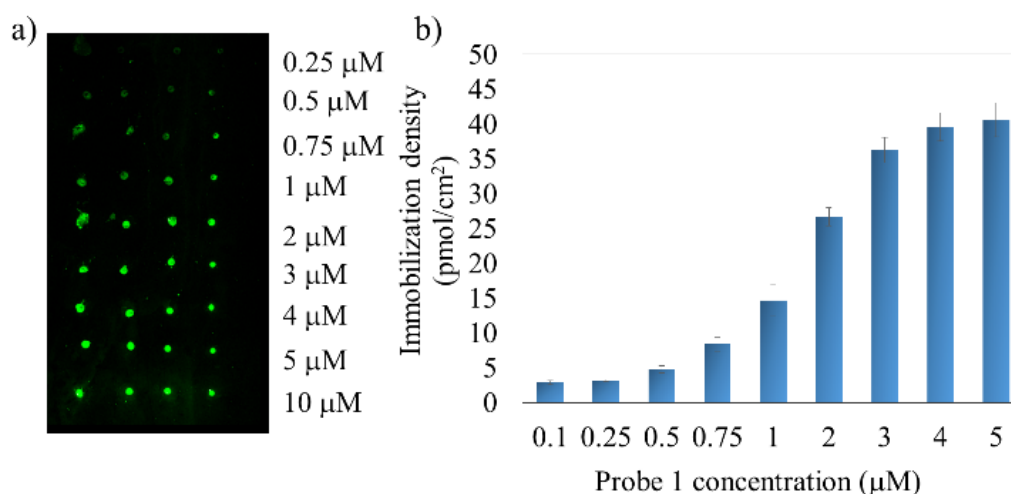
## Immobilization of 1H,1H,2H,2H-perfluorodecanethiol onto PVDF membranes



**Figure 3.** ATR-FTIR spectra. Blue. Raw PVDF membrane. Green. PVDF membrane irradiated in the presence of 1H,1H,2H,2H-perfluorodecanethiol before washing. Red. PVDF membrane irradiated in the presence of 1H,1H,2H,2H-perfluorodecanethiol after washing.

Having demonstrated the fluor-thiol photo-click reactions, and knowing that the low wettability of these surfaces can hinder successful hybridization, immobilization efficiency and further hybridization on surface B were studied. As explained above, the wettability of surface B was tuned by a combination of two different repellent organosilanes to provide an optimal WCA of 100°. Thus a standard calibration curve was constructed by spotting Probe 1\* in PBS1x onto surface B (from 0.01 to 10  $\mu\text{M}$ ), irradiating 30 seconds with the UV-surface cleaner and recording fluorescence with a microarray scanner. After washing, fluorescence was once again recorded and the resulting intensity was interpolated to the calibration curve to determine immobilization density (Figure S4). Under the studied conditions, surface saturation was reached for Probe 1\* at 4  $\mu\text{M}$  with an immobilization density of 39.6  $\text{pmol}/\text{cm}^2$  (Figure 4). Higher concentrations did not lead to any increment in fluorescence intensity. These values were around 8-fold higher than those reported by the thiol-ene coupling reaction on the vinyltrimethoxysilane functionalized surfaces (C).<sup>13</sup> Moreover, surface B led to smaller and reproducible spot sizes, and higher fluorescence intensities than surface C, which implies better performance for the new surfaces. These results support the potential application of a fluorinated surface to construct high-density NA microarrays given that the covalent anchoring of thiolated oligonucleotides to aliphatic fluorinated surfaces by photoactivation is herein demonstrated. Taking into account that the maximum packing density

of double-stranded DNA is around  $3 \times 10^{13}$  molecules/cm<sup>2</sup> (i.e., 50 pmol/cm<sup>2</sup>),<sup>32</sup> our surfaces came close to a maximal feasible surface immobilization.

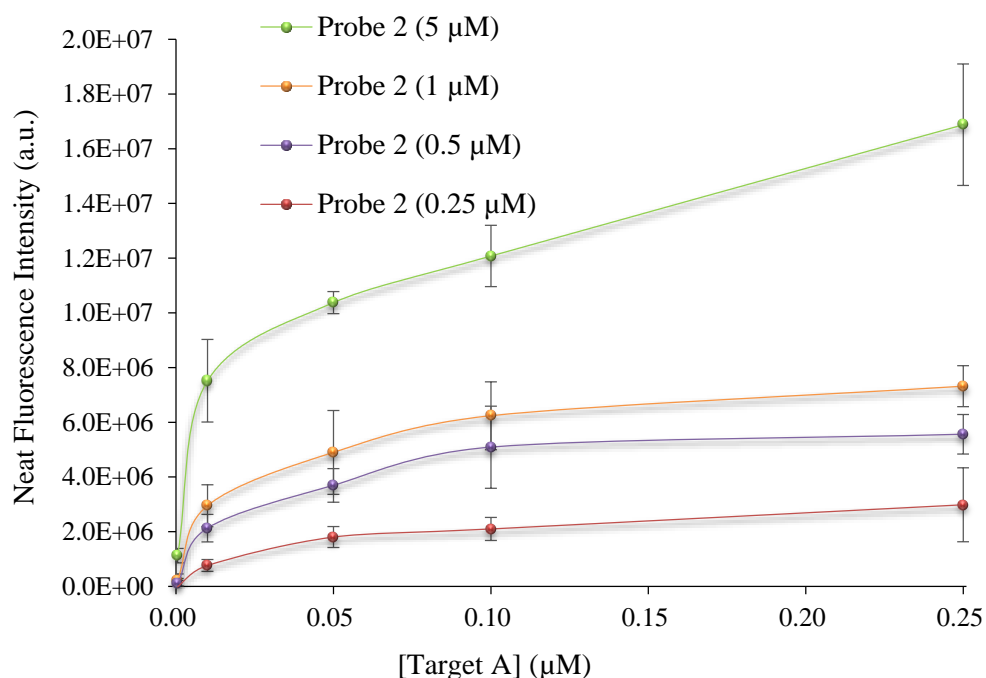


**Figure 4.** (a) Fluorescence image of an array with Probe 1\* immobilized at different concentrations and (b) the oligonucleotide immobilization densities obtained for Probe 1\* vs. the spotted concentration. These values were obtained from the interpolation on the corresponding calibration curve. The error bars were obtained from 3 chips, with 4 spots per concentration for each chip.

*DNA hybridization assays.* To prove the capability of surface B to improve the detection of complementary strands in a sensitive and selective way, hybridization assays were carried out. Serial dilutions of 3' SH nonlabeled Probe 1 (from 0.25 to 5 μM, PBS1x) were immobilized onto surface B as optimized before, and hybridization with AlexaFluor647-labeled fully complementary strand, Target 1\*, at different concentrations (from 0.0005 to 0.25 μM in SSC1x), was performed. After incubation in a humid chamber for 1 h at 37 °C and washing, the fluorescence intensity of the spots was recorded by the SFR. The obtained fluorescence intensity against the Target 1\* concentration is plotted in Figure 5 for each assayed concentration of Probe 1. The hybridization signal increased with target concentration, with up to 0.5 nM detected, which corroborates the suitability of these microarrays to detect hybridized oligonucleotide sequences at very low levels. This excellent sensitivity was attributed to the hydrophobicity modulation, a small spot size and the high immobilization density obtained by the proposed approach. Identical experimental conditions were used on surface C for comparison reasons. The lowest detected Target 1\* concentration improved the value obtained with control surface C 2-fold and, with previous reported work onto alkynyl surfaces,<sup>11</sup> it fell within the order of the estimated limit of detection, for the target, and the detection device used for these experiments (calculated as the concentration providing the blank signal, plus three times its standard deviation). Here, it should be noticed that the ionic

strength used (SSC1x) is low to overcome the electrostatic repulsion due to the high probe coverage achieved. But, the hydrophobic environment surrounding the probe spots concentrates the target solution uniquely on the hydrophilic areas where the probes are attached. Thus, water evaporation leads to a selective concentration of target molecules and salts on the probe spots, improving the efficiency of the hybridization.

Hybridization assays with Target 1\* were replicated to determine the intrachip and interchip relative standard deviations (RSD). Intrachip RSD ranged from 6% to 11%, whereas interchip RSD varied from 9% to 16%. Unlike most of the reported methods in DNA microarrays, a blocking step was not necessary, which simplified the process and reduced times.<sup>33</sup>

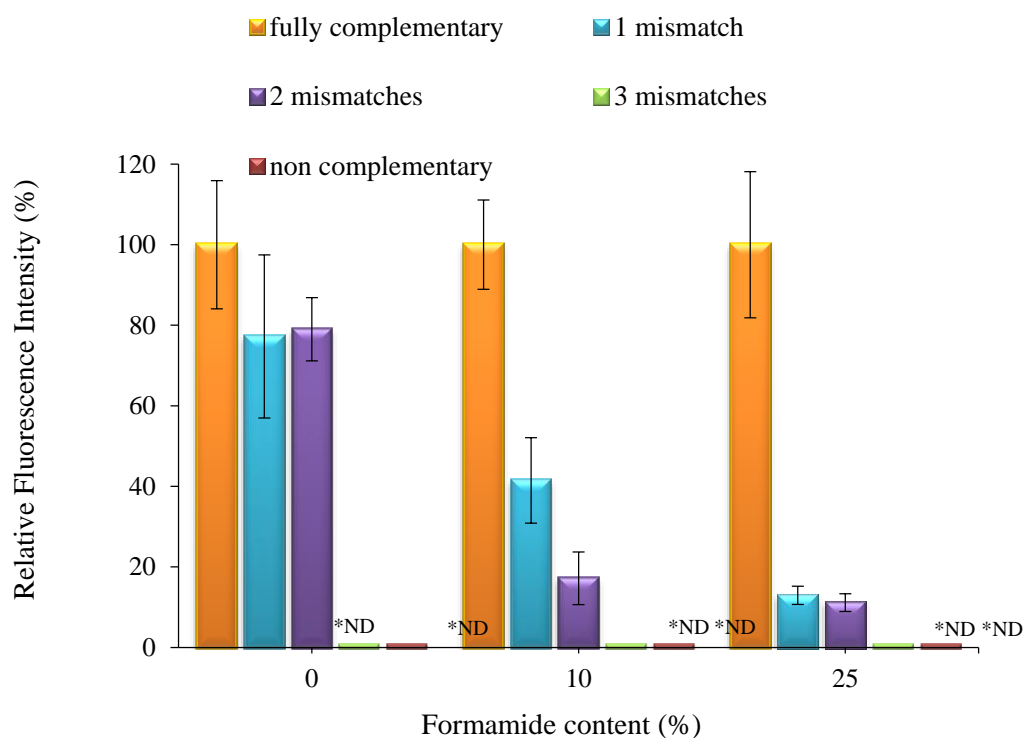


**Figure 5.** Neat fluorescence intensity vs. concentration of Target 1\* for different concentrations of Probe 1. The error bars were obtained from 2 chips, with 4 spots per concentration for each chip.

Having demonstrated the successful hybridization process, which proves the wide applicability of these DNA microarrays, patterned surfaces were used to discriminate single nucleotide polymorphisms (SNPs) and to detect bacterial PCR amplification products with high sensitivity and selectivity.



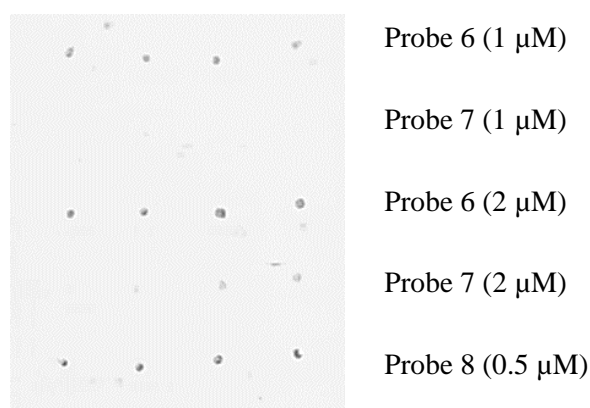
In the medical field, the use of SNPs assays allows the influence of different factors to be studied in disease susceptibility and responses to drugs.<sup>34</sup> The ability to differentiate SNPs in DNA assays is most important in selectivity terms.<sup>23, 35</sup> Therefore, a base mismatch study was performed by immobilizing five 5' SH modified probes at 0.5  $\mu$ M in PBS1x (containing from zero to three mismatches and an additional noncomplementary probe) onto surface B. Afterward, substrates were subjected to hybridization with a labeled target, complementary to the zero mismatches probe, at 50 nM using different salt concentrations (SSC from 0.1x to 5x) and formamide content (from 0% to 25%). Fluorescence was measured by SFR after washing and drying chips. The fully complementary probe displayed the highest fluorescence intensity, while the other probes clearly showed lower fluorescence. A higher formamide concentration and a lower salt concentration made the hybridization process difficult, which rendered it more specific (Figure S5). Using stringency conditions (SSC0.1x, 25% formamide), the results revealed a clear discrimination between the fully complementary probe and all the probes (see Figure 6). The signals obtained for one mismatch and the fully complementary probes were differentiated by 85%, while three mismatches and noncomplementary probes did not exhibit any detectable signal. The results indicate that under the described conditions, the microarray is quite able to distinguish a single base mutant sequence at a very good sensitivity level.



**Figure 6.** The relative fluorescence intensity signals obtained for fully complementary, 1-3 mismatches, and non-complementary probes at 0.5  $\mu\text{M}$  in PBS1x by hybridizing with Target 1\* at 0.05  $\mu\text{M}$  in SSC0.1x to display different formamide contents for the analysis of SNPs on surface B. \*ND not detectable. The error bars were obtained from 3 chips, with 4 spots per concentration for each chip.

The early detection of pathogens, i.e. bacteria strains, in water or food is paramount to maintain good human and animal safety. In our case, as proof of concept, the optimized substrates (surface B) were used to detect PCR products from an innocuous serotype of *Salmonella* bacteria. A specific nucleotide sequence (Probe 6, 1 and 2  $\mu\text{M}$ ), complementary to the central region of a 152 bp amplicon, was immobilized as before. Additional probes, used as a negative hybridization control (Probe 7) and a positive development control (Probe 8), were also included in the microarray. Hybridization with the digoxigenin-labeled PCR product solutions (denatured and cooled with ice previously), incubation with anti-digoxigenin HRP-labeled antibody produced in goat, and development with 3,3',5,5'-tetramethylbenzidine (TMB) substrate, were carried out.

As seen in Figure 7, the spots corresponding to Probe 6 show a dark precipitate, whereas no precipitation happened in the negative controls (Probe 7), which indicates the specificity of the hybridization process. Under the reported conditions, the generated DNA microarray was able to detect up to 1.7 pM of Salmonella amplification products. These figures were 75-fold lower than those reported in the literature for vinyl-functionalized surfaces, where thiolated probes were attached by thiol-ene coupling chemistry.<sup>29</sup> These results corroborate the good performance of our approach to determine genomic DNA at very low levels. Thus combining light-induced probe anchoring with the modulation of surface hydrophobicity properties, an advanced surface material for microarraying was designed.



**Figure 7.** The absorbance signal obtained for the selective recognition of the PCR-amplified DNA samples of Salmonella using specific capture Probe 6 (1 and 2  $\mu\text{M}$ ), Probe 7 (1 and 2  $\mu\text{M}$ ) as the nonspecific hybridization control, and Probe 8 (0.5  $\mu\text{M}$ ) as the development control. Biochip after development read by a document scanner.

#### 4. Conclusions

The fluor-thiol photocoupling reaction has been demonstrated in heterogeneous medium for the first time using non-aromatic fluoride compounds and light as the catalyst. The reaction was successfully applied to prepare DNA microarrays by probe covalent immobilization in a reproducible and oriented manner onto glass microscope slides, PVDF and PTFE membranes as substrates. These surfaces are very useful for the design and development of DNA biosensors as they allow the specific confinement of the analyte solution to the anchored probe sites.

The reported immobilization process is fast, compatible with aqueous media and environmentally friendly. Moreover, like the elevated surface hydrophobicity, platforms showed a high density of probes at the interface, which avoids nonspecific adsorption and significantly reduces the background. Thanks to its simplicity, quickness and use of green chemistry, this route is very promising for the immobilization of thiolated oligos onto any support that involves C-F motifs (e.g. perfluoro-functionalized slides, PVDF and PTFE membranes).

The optimized surfaces showed the maximum immobilization density achievable for a DNA self-assembled monolayer. The wettability modulation of the microscope glass slides through specific functionalization allowed robustness, stability and optimal surface conditions for later DNA probe strand hybridization. This improved by 2-fold the limit of quantification compared to a control surface and to previous works.

As demonstrated, the surface properties modulation and the application of the fluor-thiol coupling reaction enabled to perform interesting applications, like discriminating single nucleotide polymorphisms and the sensitive detection of PCR amplified DNA products, and gave better results compared to conventional methods.

From these results, we offer a very interesting pathway to develop diverse detection devices with a heterogeneous format. Moreover, linking chemistry can be applied to the biofunctionalization of nanoparticles where, for instance, repellent properties would help to avoid aggregation.

## ACKNOWLEDGMENTS

Financial support from INTERBOINTER (project CTQ2013-45875-R) and BIHOLOG (Project CTQ2016-75749-R), FEDER and GVA PROMETEO II 2014/040 is acknowledged. The authors also thank Dr. Tortajada-Genaro and Dr. Niños Rodenes for providing the *Salmonella* and *Campylobacter* PCR-amplified products. P. J.-M. acknowledges the Spanish Ministry of Economy, Industry and Competitiveness for the public FPI grant (Project CTQ2013-45875-R) and the co-financing by the European Social Fund. Dr. Miguel Ángel González-Martínez, Dr. Sergio Navalón and Dr. Patricia Concepción from Universitat Politècnica de València are acknowledged for their help in the XPS analysis.

## REFERENCES

- (1) Schena, M.; Shalon, D.; Davis, R. W.; Brown, P. Quantitative Monitoring of Gene Expression Patterns with a Complementary DNA Microarray. *Science* **1995**, *270*, 467–470. (1)
- (2) Pilarsky, C.; Nanaduri, L. K.; Roy, J. Gene Expression Analysis in the Age of Mass Sequencing. In *Cancer Gene Profiling: Methods and Protocols, Methods in Molecular Biology*; Grutzmann, R., Pilarsky, C., Eds.; Springer Science+Business Media New York 2016, 2016; pp 67–73.
- (3) Gorreta, F.; Carbone, W.; Barzaghi, D. Genomic Profiling: cDNA Arrays and Oligoarrays. In *Molecular Profiling: Methods and Protocols, Methods in Molecular Biology*; Virginia Espina and Lance A. Liotta, Ed.; Springer Science+Business Media, 2012; pp 89–105.
- (4) Gupta, A.; Mishra, A.; Puri, N. Peptide Nucleic Acids: Advanced Tools for Biomedical Applications. *J. Biotech.* **2017**, *259*, 148-159.
- (5) Duarte, J. G.; Blackburn, J. M. Advances in the development of human protein microarrays. *Expert Rev. Proteomics* **2017**, *14*, 627-641.
- (6) Singh, V.; Zharnikov, M.; Gulino, A.; Gupta, T. DNA Immobilization, Delivery and Cleavage on Solid Supports. *J. Mater. Chem.* **2011**, *21*, 10602–10618.
- (7) Lockett, M. R.; Phillips, M. F.; Jarecki, J. L.; Peelen, D.; Smith, L. M. A Tetrafluorophenyl Activated Ester Self-Assembled Monolayer for the Immobilization of Amine-Modified Oligonucleotides. *Langmuir* **2008**, *24*, 69–75.
- (8) Kolb, H. C.; Finn, M. G.; Sharpless, K. B. Click Chemistry: Diverse Chemical Function from a Few Good Reactions. *Angew. Chem. Int. Ed.* **2001**, *40*, 2004–2021.
- (9) Evans, R. A. The Rise of Azide-Alkyne 1,3-Dipolar “click” Cycloaddition and Its Application to Polymer Science and Surface Modification. *Aust. J. Chem.* **2007**, *60*, 384–395.
- (10) Dondoni, A. The Emergence of Thiol-Ene Coupling as a Click Process for Materials and Bioorganic Chemistry. *Angew. Chem. Int. Ed.* **2008**, *47*, 8995–8997.
- (11) Escorihuela, J.; Bañuls, M.-J.; Puchades, R.; Maquieira, Á. Site-Specific Immobilization of DNA on Silicon Surfaces by Using the Thiol–yne Reaction. *J. Mater. Chem. B* **2014**, *2*, 8510–8517.
- (12) Hoyle, C. E.; Bowman, C. N. Thiol-Ene Click Chemistry. *Angew. Chem. Int. Ed.*

**2010**, *49*, 1540–1573.

(13) Escorihuela, J.; Bañuls, M. J.; Grijalvo, S.; Eritja, R.; Puchades, R.; Maquieira, Á. Direct Covalent Attachment of DNA Microarrays by Rapid Thiol-Ene “Click” Chemistry. *Bioconjug. Chem.* **2014**, *25*, 618–627.

(14) Escorihuela, J.; Bañuls, M. J.; Puchades, R.; Maquieira, Á. DNA Microarrays on Silicon Surfaces through Thiol-Ene Chemistry. *Chem. Commun.* **2012**, *48*, 2116–2118.

(15) Gupta, N.; Lin, B. F.; Campos, L. M.; Dimitriou, M. D.; Hikita, S. T.; Treat, N. D.; Tirrell, M. V; Clegg, D. O.; Kramer, E. J.; Hawker, C. J. A Versatile Approach to High-Throughput Microarrays Using Thiol-Ene Chemistry. *Nat. Chem.* **2010**, *2*, 138–145.

(16) Vargo, T. G.; Calvert, J. M.; Chen, M.-S.; Gardella, J. A.; Jeffrey Calvert, J. M. Jeffrey Calvert, J. M. Adhesive Electroless Metallization of Fluoropolymeric Substrates. *Science* **1993**, *262*, 1711–1712.

(17) Li, J.; Li, L.; Du, X.; Feng, W.; Welle, A.; Trapp, O.; Grunze, M.; Hirtz, M.; Levkin, P. A. Reactive Superhydrophobic Surface and Its Photoinduced Disulfide-Ene and Thiol-Ene (Bio)Functionalization. *Nano Lett.* **2015**, *15*, 675–681.

(18) Zhou, H.; Wang, H.; Niu, H.; Gestos, A.; Wang, X.; Lin, T. Fluoroalkyl Silane Modified Silicone Rubber/Nanoparticle Compo-site: A Super Durable, Robust Superhydrophobic Fabric Coating. *Adv. Mater.* **2012**, *24*, 2409–2412.

(19) Becer, C. R.; Babiuch, K.; Pilz, D.; Hornig, S.; Heinze, T.; Gottschaldt, M.; Schubert, U. S. Clicking Pentafluorostyrene Copolymers: Synthesis, Nanoprecipitation, and Glycosylation. *Macromolecules* **2009**, *42*, 2387–2394.

(20) Slavin, S.; Burns, J.; Haddleton, D. M.; Becer, C. R. Synthesis of Glycopolymers via Click Reactions. *Eur. Polym. J* **2011**, *47*, 435–446.

(21) Wild, A.; Winter, A.; Hager, M. D.; Görls, H.; Schubert, U. S. Perfluorophenyl-Terpyridine Ruthenium Complex as Monomer for Fast, Efficient, and Mild Metallopolymerizations. *Macromol. Rapid Commun.* **2012**, *33*, 517–521.

(22) Boyer, C.; Davis, T. P. One-Pot Synthesis and Biofunctionalization of Glycopolymers via RAFT Polymerization and Polymerization and Thiol – Ene Reactions. *Chem. Commun.* **2009**, *40*, 6029–6031.

(23) Banoub, J. H.; Newton, R. P.; Esmans, E.; Ewing, D. F.; Mackenzie, G. Recent Developments in Mass Spectrometry for the Characterization of Nucleosides, Nucleotides, Oligonucleotides, and Nucleic Acids. *Chem. Rev.* **2005**, *105*, 1869–1915.

- (24) Mccarthy, J. J.; Hilfiker, R. The Use of Single-Nucleotide Polymorphism Maps in Pharmacogenomics. *Nat. Biotechnol.* **2000**, *18*, 505–508.
- (25) Crump, J. A.; Gordon, M. A.; Parry, C. M. Epidemiology, Clinical Presentation, Laboratory Diagnosis, Antimicrobial Resistance, and Antimicrobial Management of Invasive Salmonella Infections. *Clin. Microbiol. Rev.* **2015**, *28*, 901–937.
- (26) Arnandis-Chover, T.; Morais, S.; Tortajada-Genaro, L. A.; Puchades, R.; Maquieira, Á.; Berganza, J.; Olabarria, G. Detection of food-borne pathogens with DNA arrays on disk. *Talanta* **2012**, *101*, 405–412.
- (27) Santiago-Felipe, S.; Tortajada-Genaro, L. A.; Morais, S.; Puchades, R.; Maquieira, Á. Isothermal DNA amplification strategies for duplex microorganism detection. *Food Chem.* **2015**, *174*, 509–515.
- (28) Mira, D.; Llorente, R.; Morais, S.; Puchades, R.; Maquieira, A.; Marti, J. High Throughput Screening of Surface-Enhanced Fluorescence on Industrial Standard Digital Recording Media. *Proc. SPIE* **2004**, *5617*, 364–373.
- (29) Bañuls, M.-J.; Jiménez-Meneses, P.; Meyer, A.; Vasseur, J.-J.; Morvan, F.; Escorihuela, J.; Puchades, R.; Maquieira, A. Improved Performance of DNA Microarray Multiplex Hybridization Using Probes Anchored at Several Points by Thiol-Ene or Thiol-Yne Click Chemistry. *Bioconjug. Chem.* **2017**, *28*, 496–506.
- (30) Al-Gharabli, S.; Kujawa, J.; Mavukkandy, M. O.; Arafat, H. A. Functional Groups Docking on PVDF Membranes: Novel Piranha Approach. *Eur. Polym. J.* **2017**, *96*, 414–428.
- (31) González-Lucas, D.; Bañuls, M. J.; Puchades, R.; Maquieira, Á. Versatile and Easy Fabrication of Advanced Surfaces for High Performance DNA Microarrays. *Adv. Mater. Interfaces* **2016**, *3*, 1500850.
- (32) Georgiadis, R., Peterlinz K. P., and Peterson, A. W. Quantitative Measurements and Modeling of Kinetics in Nucleic Acid Monolayer Films Using SPR Spectroscopy. *J. Am. Chem. Soc.* **2000**, *122*, 3166–3173.
- (33) Bammler T, Beyer RP, Bhattacharya S, Boorman GA, Boyles A, Bradford BU, Bumgarner RE, Bushel PR, Chaturvedi K, Choi D, Cunningham ML, Deng S, Dressman HK, Fannin RD, Farin FM, Freedman JH, Fry RC, Harper A, Humble MC, Hurban P, Kavanagh TJ, Kaufmann WK, K, Z. H. M. of the T. R. C. Standardizing Global Gene Expression Analysis between Laboratories and across Platforms. *Nat. Methods* **2005**, *2*, 351–356.

(34) Ostrem, J. M.; Peters, U.; Sos, M. L.; Wells, J. a; Shokat, K. M. K-Ras(G12C) Inhibitors Allosterically Control GTP Affinity and Effector Interactions. *Nature* **2013**, *503*, 548–551.

(35) Wang, K., Tang, Z., Yang, C. J., Kim, Y., Fang, X., Li, W., Wu, Y.; Medley, C. D., Cao, Z., Li, J., Colon, P., Lin, H., and Tan, W. Molecular Engineering of DNA: Molecular Beacons. *Angew. Chem. Int. Ed.* **2009**, *48*, 856–870.



## SUPPORTING INFORMATION

### **Fluor-thiol photocoupling reaction for developing high performance nucleic acid (NA) microarrays**

List of contents:

**Figure S1:** Water contact angles.

**Figure S2:** XPS analysis, C 1s peak deconvolution for functionalized surfaces A and B.


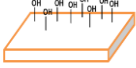
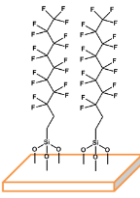
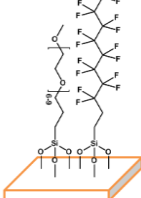
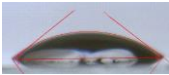

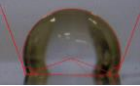
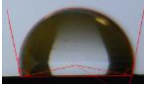
**Table S1:** XPS high-resolution chemical composition onto the surface B for every bound.

**Figure S3:** Possible mechanism of fluor-thiol click reaction.

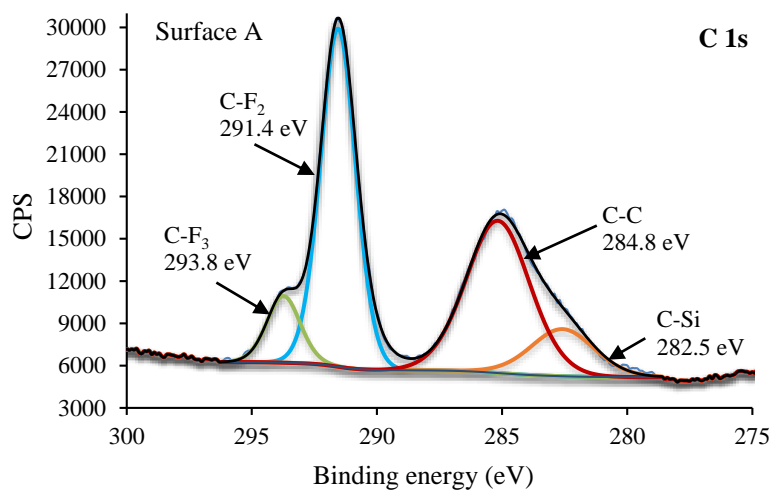
**Figure S4:** Calibration curve for Target 1\* used in the hybridization assays.

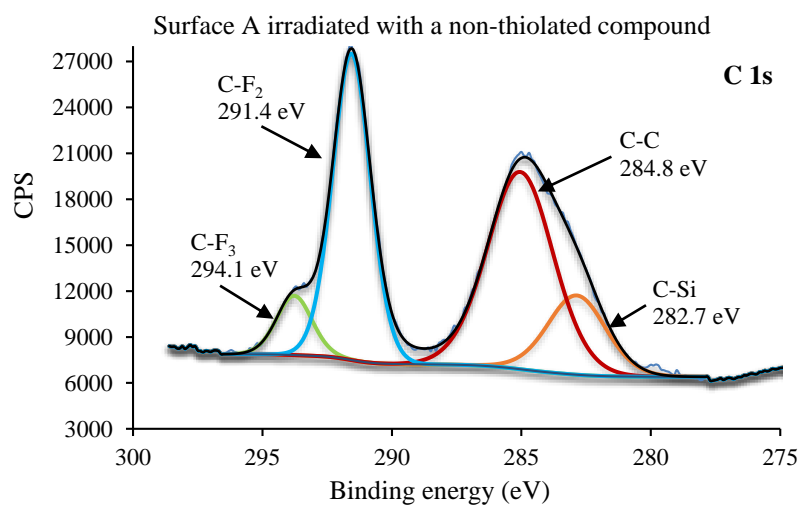
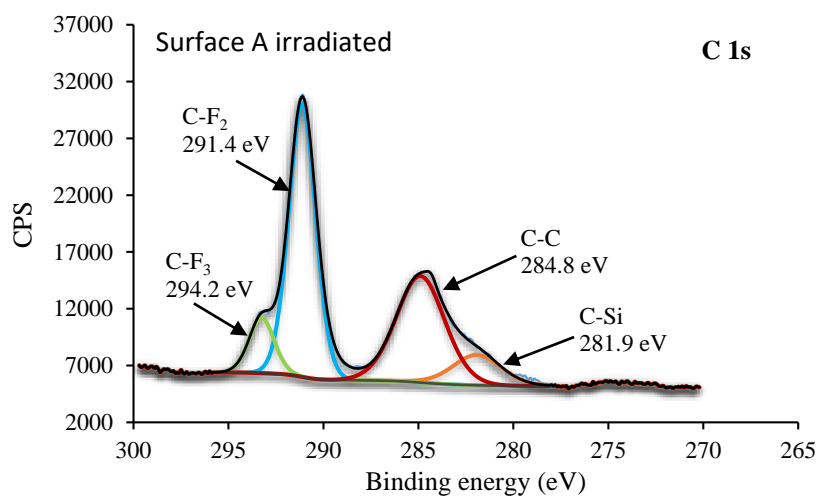
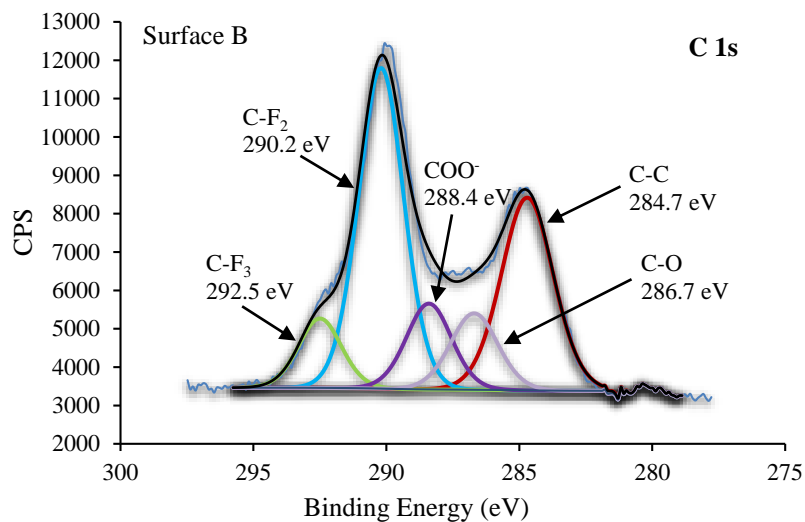
**Figure S5:** Hybridization assay at different conditions to discriminate single nucleotide polymorphisms (SNPs).

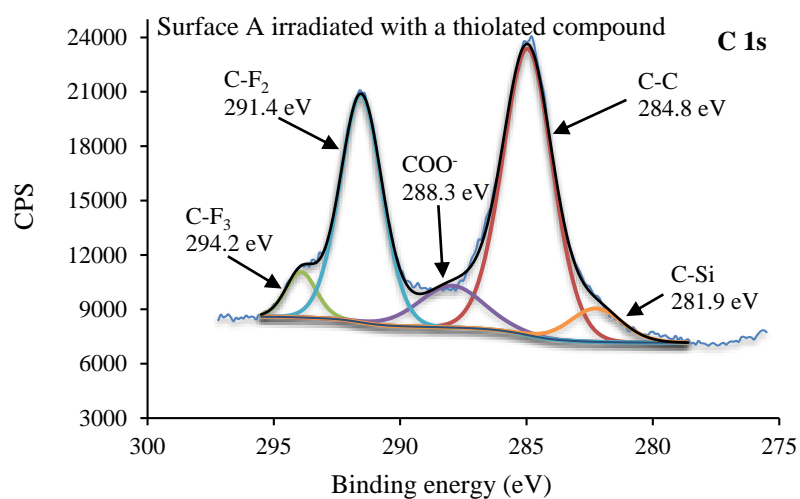
**Figure S1:** Water contact angle obtained for each surface.

Treatment	Non activated	Light activation (254 nm)	Surface A	Surface B
Structure				
WCA	$37 \pm 2^\circ$ 	$\approx 0^\circ$ 	$110 \pm 2^\circ$ 	$100 \pm 3^\circ$ 

**Figure S2:** XPS analysis, C 1s peak deconvolution for functionalized surfaces A, B, surface A irradiated without any compound, Surface A irradiated in presence of a non-thiolated compound and Surface A irradiated in presence of a thiolated compound. The increase in C-C peak in the case of Surface A irradiated with a non-thiolated probe was attributed to organic contamination, as no fluorescence was detected after the immobilization process.



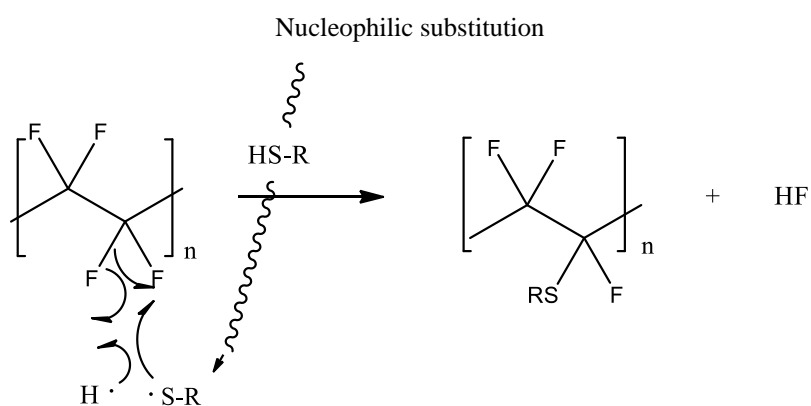


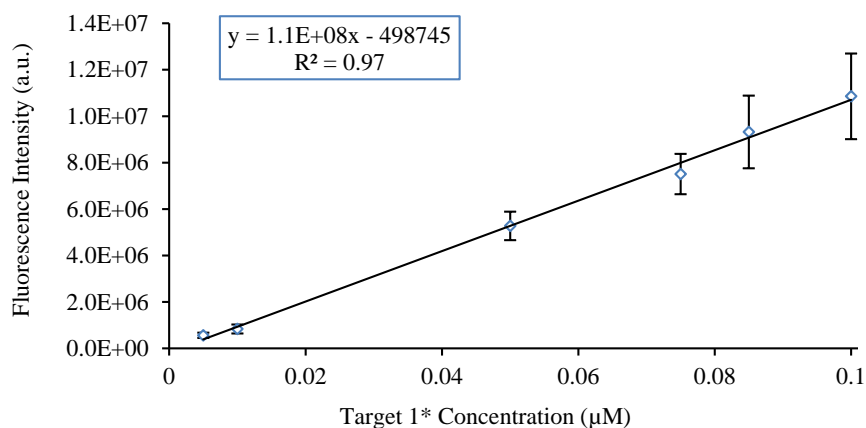


**Table S1:** XPS high-resolution chemical composition onto the surface B for every bound.

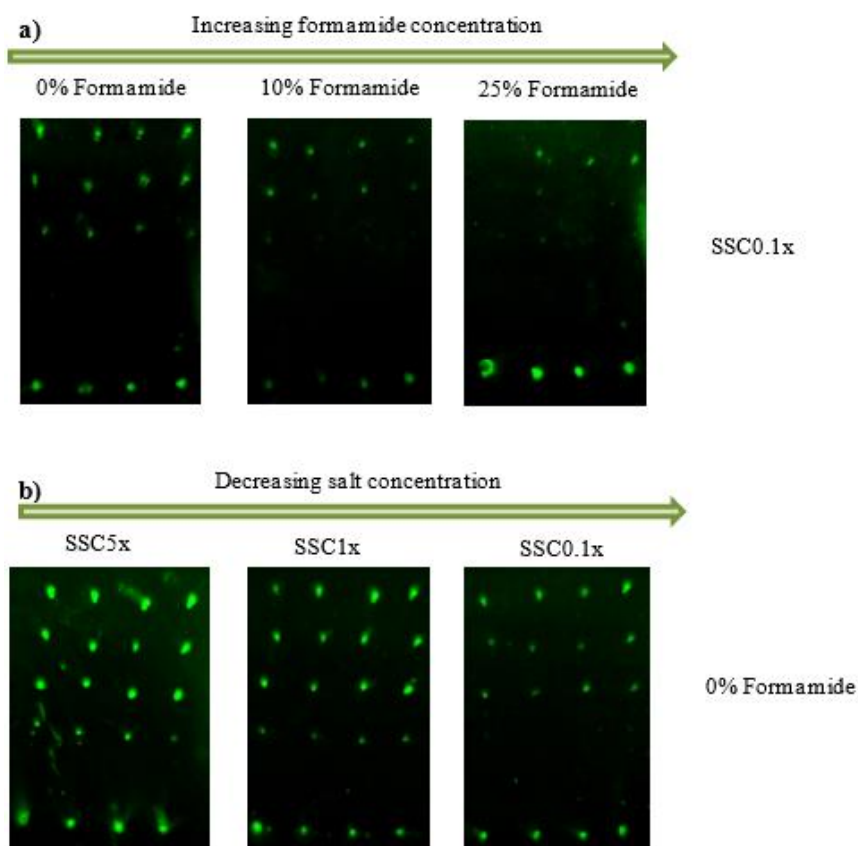
Sample	Surface B				
Name	C-C	C-O	COO <sup>-</sup>	CF <sub>2</sub>	CF <sub>3</sub>
BE (eV)	284.7	286.7	288.4	290.2	292.5
% At	28.6	10.4	11.1	41.4	8.5

**Figure S3:** Possible mechanism of fluor-thiol click reaction.



**Figure S4:** Calibration curve for Target 1\* used in the hybridization assays.

**Figure S5.** SFR images obtained for the microarrays to discriminate SNPs after hybridization under different conditions a) Hybridization assay increasing the formamide concentration using SSC0.1x as buffer. b) Hybridization assay decreasing the salt concentration using 0% of formamide. Row 1 fully complementary sequence, row 2 1-mismatch sequence, row 3 2-mismatches, row 4 3-mismatches sequence, row 4 fully non-complementary sequence, and row 5 labeled probe acting as a positive immobilization control.





## **5.2 Study of other irradiation sources for improving the performance of the fluor-thiol reaction**

This chapter is derived from the work developed through a 2-month placement in the Biophotonics Group headed by Professor Steffen Petersen at Aalborg University (Denmark) in 2017.

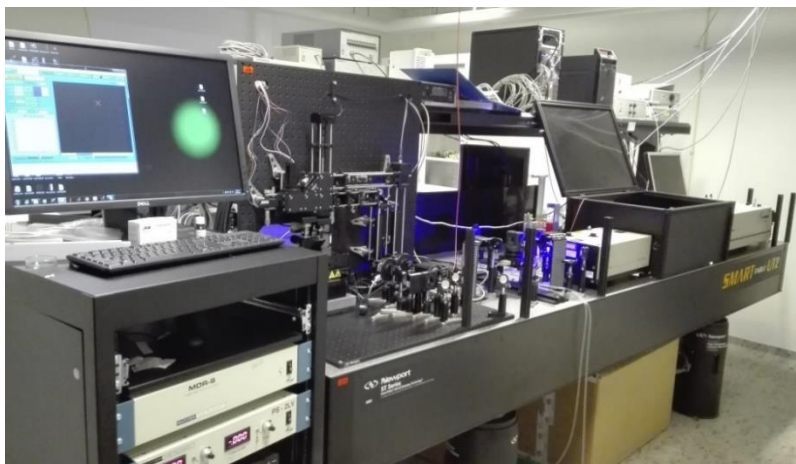




A selective procedure for the anchoring of thiolated oligonucleotides to surfaces containing C-F bonds by simple UV irradiation has been just demonstrated in section 5.1. Nonetheless, the exploration of other irradiation sources aiming for better resolution was pursued. This is of outmost importance for the fabrication of higher density microarrays which improve the performance of the system. Hence, a different UV irradiation system was studied through a placement supervised by Dr. Maria Teresa Neves Petersen, in the Biophotonics Group at the Department of Clinical Medicine of Aalborg University (AUU).

Up to now, printing low density microarrays and irradiation of the whole surface was performed. Using our available irradiation sources, the fluor-thiol photocoupling reaction was proven and optimized as much as possible. Therefore, a controlled illumination using laser pulses was studied. This could lead to the miniaturization of the microarrays, which reduces their fingerprint and increases their high throughput capabilities, and also the sensitivity.

The optical set up available in the host group (Figure 1), was employed to perform photoimmobilization studies of different bioreceptor probes, containing available thiols, on silicon-based surfaces (mainly quartz) using the coupling reactions optimized within this thesis.



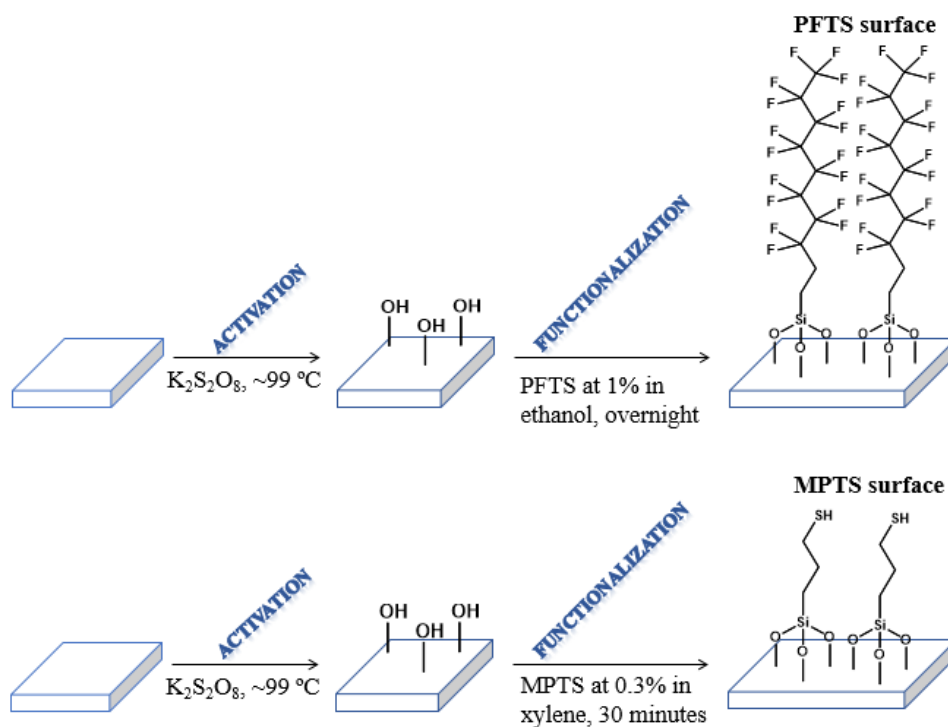
**Figure 1.** The irradiation optical set up available in the host group.

This system consists of a microfabrication stage coupled to a femtosecond laser (fs-laser), through one-photon excitation. The fundamental 840 nm output is tripled to 280 nm and focused onto the sample, leading to one-photon excitation. The sample is placed onto an xyz-stage with a micrometer step resolution. The pattern to be irradiated is uploaded to

the software to control the stage and the shutter. Molecules are attached according to such a pattern. Spatial masks can be inserted in the light path to get sub-micrometer spatial resolution by light diffraction patterns. Patterns are recorded by an inverted confocal fluorescence microscope.

The hosting group optimized the optical set up to be used for the immobilization of proteins by LAMI (Light-assisted molecular immobilization) technique.<sup>1</sup> This technique is based on the excitation of aromatic amino acid residues by UV-light (275-295 nm), which leads to the disruption of the proximal disulfide bridges. Then, the obtained free thiol groups can be attached covalently to thiol reactive surfaces, in an oriented and localized way. Tryptophan (Trp) and tyrosine (Tyr) amino acids are the best absorbers due to their characteristic aromatic structure. Taking advantage of this technology, patterns can be irradiated at ~280 nm with femtosecond pulses to anchor the bioreceptors, which improves the resolution and accuracy of the microarrays.

Hence, during the stay, support surfaces were functionalized through organosilane chemistry. To apply the developed fluor-thiol photocoupling reaction (first section from chapter 3), functionalization of optically flat quartz slides with 1H,1H,2H,2H-perfluorodecyltriethoxysilane was performed to provide C-F bonds over the surface (PFTS surface). For comparison, a thiol ended surface was also employed. This surface, functionalized with (3-mercaptopropyl)trimethoxysilane (MPTS), is used by the host group for the fabrication of their protein microarrays on the basis of LAMI immobilization.<sup>2,3</sup> Quartz slides were chosen instead of glass slides for optical reasons, to avoid the distortion of the pattern due to the capacity of glass slides to absorb light at the working wavelength (280 nm). The functionalization procedure was adjusted to the available resources in the laboratory. Activation by immersion in a hydroxylation solution of  $K_2S_2O_8$  for 1 hour at 99 °C, was carried out. Immersion in respective solutions of organosilanes to incorporate the reactive groups over the quartz slides was done as well. In the case of PFTS surfaces, overnight functionalization at 2% PFTS in ethanol was done. For MPTS surfaces, the same protocol described by the host group was followed, so immersion in MPTS at 0.3% in a xylene solution for 30 minutes was performed (Figure 2).



**Figure 2.** Scheme of the functionalization procedure of both PFTS and MPTS surfaces.

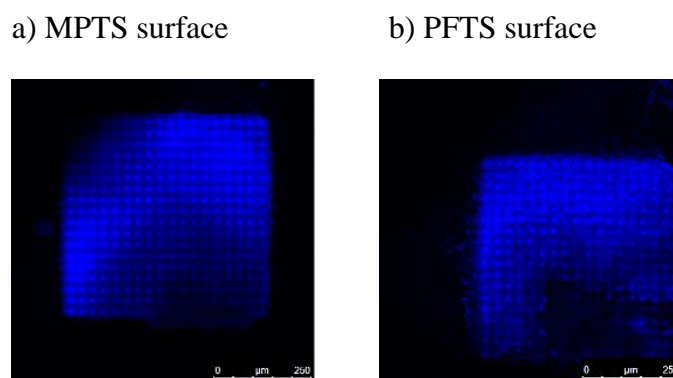
During this placement, the fabrication of different microarrays was studied. As free thiol groups are a requirement for application of the fluor-thiol photocoupling reaction, thiolated oligonucleotides and hIgG fragments were employed. In addition, taking advantage of the LAMI technique which disrupts disulfide groups by activation of proximal aromatic residues, whole antibodies were employed as well. Bioreceptor attachment and further biorecognition capacity were assessed by fluorescence confocal microscopy. As the probes employed were labeled with Cy5 or Alexa-Fluor 647 fluorophores, it was possible to measure the presence of the probe on the surface. Exciting at 633 nm and reading from 670 to 780 nm in a fluorescence confocal microscope, signal intensity was recorded. This way, the extent of the photoimmobilization and recognition could be assessed.

Regarding the photoimmobilization assays, different parameters were studied. Illumination parameters such as pattern, irradiation speed and power are of utmost importance to accomplish successful immobilization results. Regarding the probe to be immobilized, concentration and buffer conditions are also key for the proper working of the assay. Hence, some studies were carried out to provide the best conditions for every system. The results obtained for oligonucleotide microarrays are presented first, followed by the results observed for antibody microarrays.

I. *Oligonucleotide microarrays*

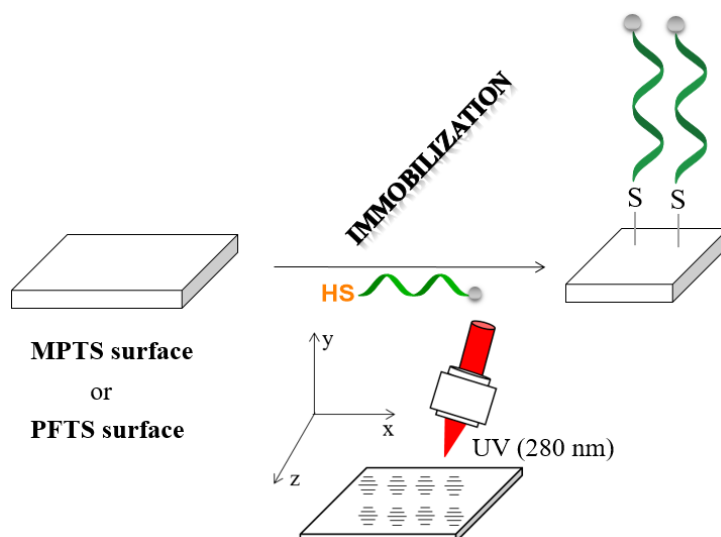
First, the optimization of the fabrication process was performed. For that, 2  $\mu\text{L}$  drops of a labeled thiolated probe (Probe 1\*) at 10  $\mu\text{M}$ , were placed onto both surfaces (MPTS and PFTS platforms). Different buffers such as water, PBS1x and PBS0.5x were studied. After drying, surfaces were placed in the irradiation stage, and the drop to be irradiated was focused. Two patterns (array and lines) were employed for the irradiation process as well. Irradiation speed of 100  $\mu\text{m/s}$  and irradiation power of 40  $\mu\text{W}$  were settled as a first approximation. After irradiation, surfaces were exhaustively washed with PBS1x for 1 hour, and patterns recorded using the fluorescence confocal microscope. Regarding the amount of salts, different effects were observed. For the immobilization of labeled oligonucleotide probes onto the MPTS surfaces, the use of water as a solvent showed good immobilization (Figure 3a), while PFTS surfaces displayed better results with PBS0.5x as a buffer (Figure 3b).

For further information about oligonucleotide sequences, see table 3 in the experimental section.



**Figure 3.** a) Immobilization of Probe 1\* in water onto the MPTS surface. b) Immobilization of Probe 1\* in PBS0.5x onto the PFTS surface. Image recording was performed with a confocal fluorescence microscope.

Regarding the patterning, the array pattern displayed better results than the line pattern. Therefore, a pattern of 500 x 500  $\mu\text{m}$ , having 18 spots for each line was employed for this work. Each spot was made of five lines of different length, very close to each other, so a spherical spot was achieved. Good spatial resolution was accomplished using this methodology, with spot sizes around 10  $\mu\text{m}$ , and a pitch distance (distance between the center of neighboring spots) of 30  $\mu\text{m}$ . Figure 4.



**Figure 4.** The layout of the immobilization of thiolated probes using the fs-laser.

Then, lower concentrations (1 and 5  $\mu\text{M}$ ) were studied, using PBS0.5x and water as buffers, as they displayed better results. Nonetheless, results were not improved, so the probe concentration of 10  $\mu\text{M}$  was established. Finally, irradiation speeds and irradiation powers were studied using three different conditions (Table 1). Nonetheless, spatial resolution was not improved.

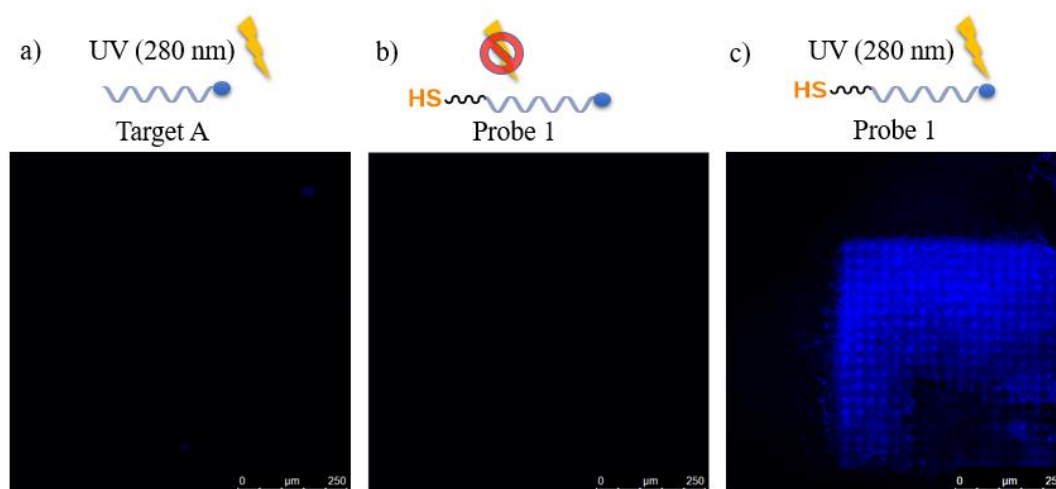
**Table 1.** Studied irradiation parameters.

Irradiation speed ( $\mu\text{m/s}$ )	Irradiation power ( $\mu\text{W}$ )
100	40
100	20
50	40

It is important to note that the fluor-thiol photocoupling reaction displays a wide range of irradiation wavelengths to work. Using this optical set up, successful anchoring of thiolated probes onto surfaces containing C-F moieties irradiating at 280 nm was reached, while in the case of the low density microarrays discussed in section 3.1, the working wavelength was 254 nm. Outside of the irradiated pattern, no immobilization was observed, which corroborates the essential role of light for the anchoring.

The homogeneity of the spots is quite good; however, some dark areas appear in the recorded images due to undesired optic effects. Also, the concentration of salts during drying can lead to poor immobilization.

To corroborate even more the role of the light and the thiol moiety in the fluor-thiol coupling reaction, two controls were completed. On the one hand, a non-thiolated probe (Target 1\*) was deposited onto the PFTS surface (Figure 5a). Irradiation under the same conditions than above and thorough washing was performed. On the other hand, non-irradiation of the thiolated probe (Probe 1\*) and exhaustive washing were made (Figure 5b). A comparison of the previous results was carried out (Figure 5c). As demonstrated in Figure 5, both UV irradiation (280 nm) and thiol group were required to accomplish a successful attachment.

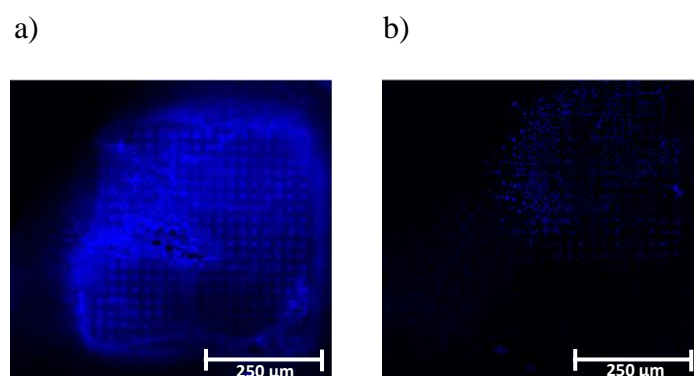


**Figure 5.** a) and b) Negative controls supported the needed of a thiol moiety and irradiation to undertake the fluor-thiol photocoupling reaction c) Anchoring of a thiolated probe was corroborated.

Once optimized the immobilization process, recognition assays were carried out. For that, immobilization of a non-labeled probe (Probe 1), in the optimized conditions of irradiation power (40  $\mu\text{W}$ ), and irradiation speed (100  $\mu\text{m/s}$ ), was done. Later, the hybridization step with the labeled complementary strand (Target 1\*), was performed. Target concentrations from 0.5 to 5  $\mu\text{M}$  in SSC1x, and hybridization times from 1 to 2 hours, at 37  $^{\circ}\text{C}$ , were studied. A concentration of 0.5  $\mu\text{M}$  was enough to get worthy recognition signals. Hybridization times were increased in comparison to chapter 3 experiments (from 1 to 2 hours) to ensure successful hybridizations, while incubation temperatures were kept at 37  $^{\circ}\text{C}$ .

Although probe immobilization in water showed the best results using MPTS functionalized substrates, later hybridization process provided low fluorescence signal. This can be attributed to the poor bioavailability of the anchored probe. For that, other

buffers were studied for probe linking. PBS1x buffer solution gave the best hybridization efficiencies (Figure 6a). In the case of the PFTS modified surface, probe immobilization in PBS0.5x displayed the best hybridization capacity (Figure 6b).



**Figure 6.** a) Immobilization of a non-labeled DNA probe (Probe 1) in PBS0.5x and hybridization with the complementary labeled strand (0.5  $\mu$ M Target 1\* in SSC1x) onto MPTS surface. b) Immobilization of Probe 1 in PBS0.5x and hybridization with 0.5  $\mu$ M Target 1\* in SSC1x onto the PFTS surface.

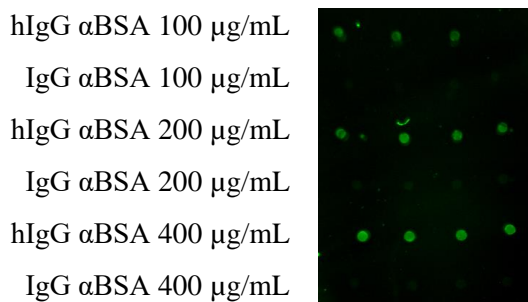
As can be observed in Figure 6, the anchored thiolated probe, through fluor-thiol photocoupling reaction, displayed a successful recognition however the signals obtained with MPTS derivatized surface were higher. It is important to note that irradiation is taking place at a different wavelength (280 nm) that the optimized at the beginning of this chapter to accomplish the fluor-thiol photocoupling reaction (254 nm). Furthermore, optimized surfaces were not able for these experiments. The modified substrates contained PEGS which improved the hydrophilicity of the surfaces. Nonetheless, fully perfluorinated surfaces were employed during this work, which worsens the immobilization and hybridization capacity. Thus, optimization of the surface wettability and irradiation wavelength could lead to improve these promising results.

## II. Antibodies (IgG) and half antibody fragments (hIgG) microarrays.

Before starting with the immobilization of antibodies with the optical setup of the host group, previous optimization work was done at our laboratory regarding the photoinmobilization of hIgG and IgGs using C-F functionalized surfaces. Immobilization of both hIgG and IgG  $\alpha$ BSA at several concentrations (from 100 to 400  $\mu$ g/mL) in PBS1x onto PFTS surfaces by UV irradiation at 254 nm, was studied. These bioreceptors were previously employed in chapter 2, and the same purification and reductive process were followed. After washing with PBS-T and water, incubation with

AlexaFluor 647-labeled BSA (5  $\mu\text{g/mL}$ ) was carried out for 30 minutes at room temperature. Microarrays were recorded using our homemade surface fluorescence reader (SFR).

As preliminary results, a higher recognition capacity of the hIgG  $\alpha\text{BSA}$  versus the IgG  $\alpha\text{BSA}$  was achieved (Figure 7). This is attributed to the orientation of the hIgG fragments which allows more bioavailable receptors. This encouraged us to its implementation with the laser system of the host group.



**Figure 7.** Fluorescence intensities recorded for the microarrays obtained by spotting hIgG  $\alpha\text{BSA}$  and IgG  $\alpha\text{BSA}$  at 100, 200 and 400  $\mu\text{g/mL}$  concentrations. The chip was irradiated at 254 nm for 5 seconds, washed, incubated with AlexaFluor 647-labeled BSA, and washed again.

Having these preliminary results, the immobilization of hIgG and IgG labeled with AlexaFluor647 on PFTS and MPTS modified surfaces was studied using the same fs-laser system explained above for the fabrication of oligonucleotide microarrays.

Based on the expertise of the hosting group for the immobilization of antibodies, irradiation power of 60  $\mu\text{W}$  and speed of 100  $\mu\text{m/s}$  were employed.<sup>1,4</sup> Afterwards, surfaces were washed with PBS-T buffer overnight. Regarding the bioreceptor concentration, IgG  $\alpha\text{BSA}$  was employed at 1000 and 200  $\mu\text{g/mL}$  in PBS1x, while hIgG  $\alpha\text{BSA}$  was used at 100  $\mu\text{g/mL}$  in acetate buffer, as this was the maximum available concentration for this fragment.

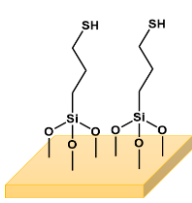
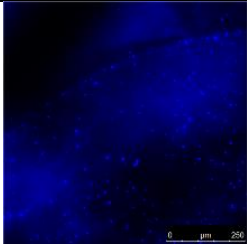
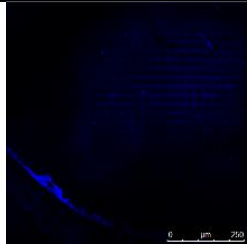
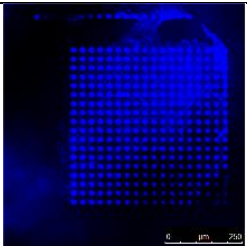
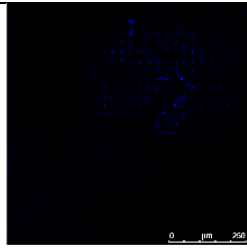
The whole antibody (IgG  $\alpha\text{BSA}$ ) showed good immobilization onto both MPTS and PFTS surfaces, which corroborates the LAMI technique as an adequate method for the photo-assisted immobilization of antibodies. Although both concentrations gave good resolution patterns, the higher concentration (1000  $\mu\text{g/mL}$ ) displayed better results. In the case of the PFTS surface, this technique has been adapted for the anchoring of such antibodies to surfaces containing C-F bonds, taking the advantage of generated free thiol groups during illumination.

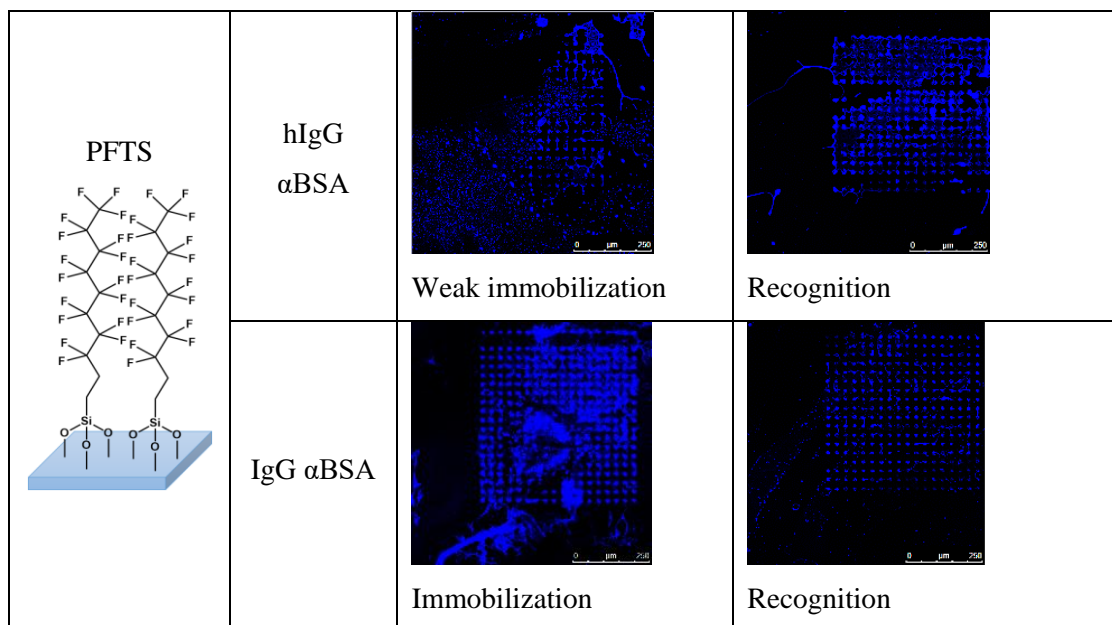


Regarding the hIgG  $\alpha$ BSA fragments, immobilization onto the PFTS modified surface was achieved, while non-successful immobilization was observed onto MPTS surfaces. This could be due to the higher hydrophobicity of PFTS surfaces, which confines the probe solution, and thus concentrates the amount of bioreceptor. A comparison between hIgG and IgG could not be undertaken, as different concentrations were employed.

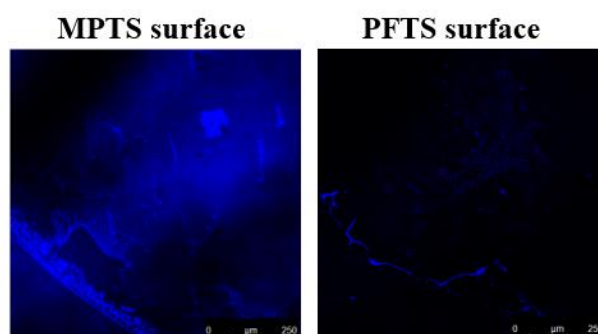
Finally, recognition assays were performed. For that, immobilization of non-labeled bioreceptors (hIgG  $\alpha$ BSA and IgG  $\alpha$ BSA) at 1000  $\mu$ g/mL and incubation with labeled BSA in PBS-T (100  $\mu$ g/mL), for 30 minutes at room temperature, were carried out. MPTS surface showed weak recognition in the case of the IgG  $\alpha$ BSA and an inverted pattern in the case of the hIgG  $\alpha$ BSA. For PFTS surfaces, IgG and hIgG showed good biorecognition capacity, improving the results obtained with the control surfaces. This improvement, using PFTS surfaces, corroborated the advantages of these hydrophobic surfaces for the fabrication of microarrays. Employing these PFTS surfaces, reduction of the undesired non-specific adsorption and minimization of the background was reached. This confirmed our initial hypothesis about perfluorinated surfaces. Confinement effect is favored, allowing the approximation of the analyte only where the bioreceptor is linked, and reducing the background. Table 2 shows the results achieved.

**Table 2.** Immobilization and recognition assays of hIgG  $\alpha$ BSA and IgG  $\alpha$ BSA bioreceptors onto MPTS and PFTS surfaces.

Surface	Bioreceptor	Immobilization	Recognition
<p>MPTS</p> 	hIgG $\alpha$ BSA	 None immobilization	 Weak recognition (inverted pattern)
	IgG $\alpha$ BSA	 Immobilization	 Weak recognition



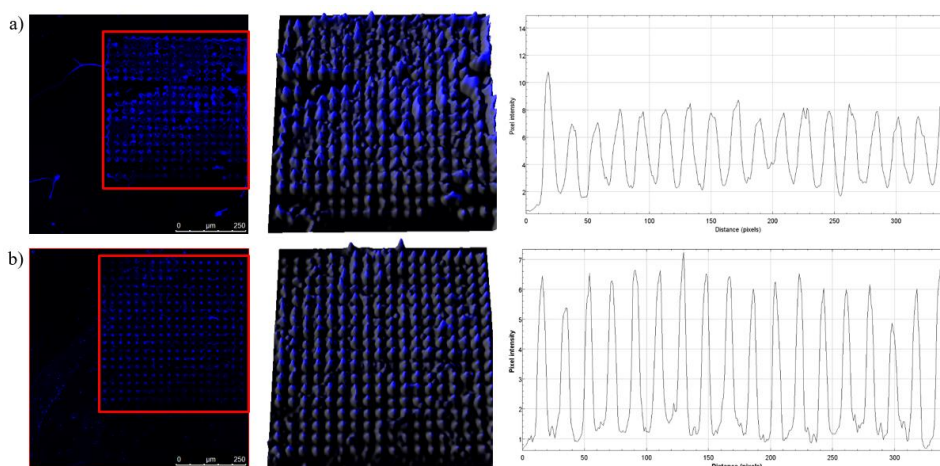
In addition, adsorption experiments were performed onto both surfaces, by placing a 2  $\mu\text{L}$  drop of labeled antibody at 1000  $\mu\text{g}/\text{mL}$  in PBS 1x, resting for 20 minutes, and washing exhaustively with PBS-T. As can be seen in Figure 8, PFTS modified surfaces reduced significantly the non-specific adsorption then lowering the background.



**Figure 8.** Confocal fluorescence images of an adsorbed labeled antibody onto PFTS and MPTS surfaces, after washing.

Lastly, comparing IgG and hIgG results onto the PFTS surface (Figure 9), the whole antibody gave better results, which is opposite to our preliminary results. Nevertheless, the LAMI technique is recognized to break disulfide groups by exciting proximal aromatic residues with UV light (275-295 nm). Therefore, if the LAMI technique is adapted to our perfluorinated surfaces, without previous fragmentation of the antibodies. The program ImageJ was employed to get a profile analysis of the arrays. Figure 9 shows the original image, a 3D plot and the intensity average of the spots. The homogeneity of

the spots is quite good for preliminary results, and high intensities were obtained.



**Figure 9.** a) Left. Detection of labeled BSA by an immobilized hIgG BSA array onto the PFTS surface. Medium. 3D surface plot of the selected area. Right. Analysis of the average fluorescence emission intensity profiles (red line). b) Left. Detection of labeled BSA by an immobilized IgG BSA array onto the PFTS surface. Medium. 3D surface plot of the selected area. Right. Analysis of the average fluorescence emission intensity profiles (red line).

In conclusion, results have demonstrated the anchoring of thiolated bioreceptors (oligonucleotide probes and antibodies), to PFTS quartz slides surfaces, being both UV irradiation (280 nm) and thiol groups required to accomplish a successful attachment. Furthermore, anchoring of whole antibodies in an oriented way, without previous reduction, was achieved by adapting the developed technique in the host group to our system. All this demonstrates the high versatility of the fluor-thiol photocoupling reaction (chapter 3).

## Experimental section

*Chemicals, reagents, and buffers.* Optically flat quartz slides were purchased from ArrayIt (EEUU). 1H,1H,2H,2H-Perfluorodecyltriethoxysilane, (3-mercaptopropyl)trimethoxysilane, potassium persulfate ( $K_2S_2O_8$ )  $\geq 99\%$ , and m-xylene were supplied by Sigma-Aldrich (Denmark). Ethanol 99% and 76% were purchased from Scharlau (Denmark). It is to be noted that all the chemicals were handled following the corresponding material safety data sheets. All chemicals were used without further purification.

Milli-Q water, with a resistivity above 18 m $\Omega$ , was used to prepare the aqueous solutions. The employed buffers, phosphate buffer saline (PBS1x, 0.008 M sodium phosphate

dibasic, 0.002 M sodium phosphate monobasic, 0.137 M sodium chloride, 0.003 M potassium chloride, pH 7.5), PBS-T (PBS1x containing 0.05% Tween 20) and saline sodium citrate (SSC1x, 0.15 M sodium chloride, 0.02 M sodium citrate, pH 7), were filtered through a 0.45  $\mu\text{m}$  pore size nitrocellulose membrane of the Fisher brand (Germany) before being used.

Employed oligonucleotides were acquired from Eurofins Genomic (Germany). Table 3. The DNA concentration and quality were controlled by measuring optical density at 260/280 nm in a NanoDrop ND 1000 Spectrophotometer from Thermo Fisher Scientific (USA).

**Table 3.** Employed oligonucleotide sequences.

Name	Sequence (5' to 3')	5'-	3'-
Probe 1*	CCCGATTGACCAGCTAGCATT- (T) <sub>15</sub>	Cy5	SH
Probe 1	(T) <sub>15</sub> -CCCGATTGACCAGCTAGCATT	SH	-
Target 1*	AATGCTAGCTGGTCAATCGGG	Ax <sup>a</sup>	-

<sup>a</sup> Alexa Fluor 647

Bovine serum albumin (BSA) and bovine serum albumin polyclonal antibody (IgG  $\alpha$ BSA) were purchased from Sigma Aldrich (Spain). hIgG  $\alpha$ BSA was obtained by selective reduction as described in Chapter 2.

*Silanization of slides.* Optically flat quartz slides were hydroxylated by immersion in a solution of K<sub>2</sub>S<sub>2</sub>O<sub>8</sub> (30 g in 600 mL of water milli-Q) for 1 hour at ~99 °C. Washing with deionized water immediately after activation, to avoid the formation of crystals over the surface was performed. To introduce the reactive functional groups, these chips were immersed in the corresponding solution. For the control surfaces, immersion into a solution of 0.3% v/v (3-mercaptopropyl)trimethoxysilane in m-xylene for 30 min was carried out. Subsequently, the surfaces were washed with pure xylene, 76% ethanol and deionized water, dried with compressed dry air and placed in an oven for 1 hour at 100 °C. For the perfluorinated surfaces, immersion into a 1% v/v solution of 1H,1H,2H,2H-perfluorodecyltriethoxysilane in ethanol 99% overnight at room temperature, was done. Then, samples were withdrawn from the silane solution, washed with ethanol (76%), air-dried, and baking into an oven for 1 hour at 100 °C.

*UV irradiation optical setup.* The one-photon UV optical setup employed for the immobilization of the patterned microarrays onto the functionalized quartz slides and the software used to control the experimental setup have been described previously<sup>1,4</sup>. In brief, the laser light resource is a Tsunami XP (Spectra-Physics, USA), pumped by a Millennia eV (Spectra-Physics, USA). This femtosecond laser source (100 fs pulse width and 80 MHz repetition rate) is manually tunable in a range between 700-1080 nm. For LAMI illumination, typical operation wavelength is around 840 nm with a maximum average power of 3 W. The output of the Tsunami is frequency tripled in a UGH module (Spectra-Physics, USA) to produce ~280 nm UV femtosecond pulses, with an efficiency of ~10%. The third harmonic is then directed into the illumination setup through a different path of the fundamental 840 nm beam. The third harmonic beam at 280 nm passes through a computer controlled attenuator (PR50CC-Newport, USA) and a polarized beam cube. Power is monitored by a photodiode placed after each attenuator. In order to control sample exposure to light, the beam is also directed through safety shutters (LS6S2ZM1, Vincent Associates, USA). A CCD camera (MCE-B013-UW, Mightex, Canada) is placed above the objective through which the 280 nm light is finally directed onto the sample to allow sample visualization.

*XYZ Moving stage.* To simplify positioning of the sample a custom holder was settled to allow transmitted LED illumination (LCS-0420-03-22, LCS-0850-03-22, Mightex, Canada). The sample holder is fixed to an XYZ stage stack contained two XMS100 stages (XY) and one VP-5ZA (Z). All stages, including the rotation stages for power control, the piezo Z stage for fine positioning, and the XYZ stack, are controlled with the Newport XPS-Q8 (USA) motion controller with appropriate driver cards. This system allows the patterning with micrometer spatial resolution.

*DNA immobilization assays.* Anchoring of labeled oligonucleotide probes (Probe 1\*) onto MPTS and PFTS functionalized quartz slides was extensively studied. Thus, 2  $\mu$ L drops of Probe 1\* (10  $\mu$ M) were placed onto the surface and let them dry. Then, irradiation with the laser at 280 nm was performed. Array pattern of 500 x 500  $\mu$ m, with an irradiation speed of 100  $\mu$ m/s, an irradiation power of 40  $\mu$ W and a concentration of 10  $\mu$ M, was performed. Different immobilization buffers were used (PBS1x, PBS0.5x, and water). After irradiation, washing of the surfaces by immersion in PBS1x for 1 hour to remove the non-anchored probes, was carried out.

*DNA hybridization assays.* To carry out the recognition assays, the immobilization of probes was performed as described above. For that, immobilization of a non-labeled probe (Probe 1) in the same conditions of irradiation power, irradiation speed, and concentration were performed. Substrates were washed with PBS1x for 1 hour. Later hybridization step with the labeled complementary strand (Target 1\*; 0.5  $\mu\text{M}$  in SSC1x) for 1 hour at 37 °C, was done. Finally, washing in SSC1x for 1 hour was done.

*Antibody immobilization assays.* Whole antibodies (IgG  $\alpha\text{BSA}$  at 1000  $\mu\text{g}/\text{mL}$ ) and half antibody fragments (hIgG  $\alpha\text{BSA}$  at 100  $\mu\text{g}/\text{mL}$ ) labeled with AlexaFluor647 were immobilized onto both surfaces, as well. As before, immobilization parameters were optimized, and final conditions resulted; an irradiation power of 60  $\mu\text{W}$ , an irradiation speed of 100  $\mu\text{m}/\text{s}$ , an array pattern of 500 x 500  $\mu\text{m}$ , and PBS1x as dilution buffer. After irradiation, surfaces were washed with PBS-T buffer overnight.

*Antibody recognition assays.* Recognition assays were performed as follows. Immobilization of non-labeled bioreceptors (hIgG  $\alpha\text{BSA}$  and IgG BSA) at 1000  $\mu\text{g}/\text{mL}$ , exhaustive washing, and incubation with labeled BSA in PBS-T (100  $\mu\text{g}/\text{mL}$ ) for 30 minutes at room temperature were carried out. Final washing with PBS-T for 15 minutes was performed.

*Probe detection.* After immobilization and recognition assays, the patterns were visualized in an inverted confocal fluorescence microscope (Leica TCS SP5), through UV 10x and 20x objectives. For imaging of the immobilized labeled biomolecules (AlexaFluor647 and Cy5 fluorophores), the patterns were excited using the 633 nm laser line from the HeNe laser and emission was visualized from  $\approx 670\text{-}780$  nm. Visualization of fluorescence patterns could only be observed when successful immobilization and recognition are achieved.

*Data analysis.* Fluorescence intensity profiles and fluorescence intensity 3D plots of the patterns were obtained using the program ImageJ 1.50i.

## REFERENCES

- (1) Neves-Petersen, M. T.; Gonçalves, O. S.; Bañuls, M.-J.; Alonso, R.; Jiménez-Meneses, P.; Maquieira, Á.; Vorum, H.; Petersen, S. B. Photonic Immobilization Techniques Used for the Detection of Cardiovascular Disease Biomarkers. In *Biophotonics: Photonic Solutions for Better Health Care VI*; Popp, J., Tuchin, V. V., Pavone, F. S., Eds.; SPIE: Strasbourg, France, 2018; p 106.
- (2) Neves-Petersen, M. T. Photonic Activation of Disulfide Bridges Achieves Oriented Protein Immobilization on Biosensor Surfaces. *Protein Sci.* **2006**, *15* (2), 343–351.
- (3) Parracino, A.; Neves-Petersen, M. T.; di Gennaro, A. K.; Pettersson, K. Arraying Prostate Specific Antigen PSA and Fab AntiPSA Using Lightassisted Molecular Immobilization Technology. **2010**, *19*, 1751—17599.
- (4) Gonçalves, O.; Snider, S.; Zadoyan, R.; Nguyen, Q.-T.; Vorum, H.; Petersen, S. B.; Neves-Petersen, M. T. Novel Microfabrication Stage Allowing for One-Photon and Multi-Photon Light Assisted Molecular Immobilization and for Multi-Photon Microscope; Achilefu, S., Raghavachari, R., Eds.; San Francisco, California, United States, 2017; p 100790F.





### **5.3 Study of microstructuration for the improved performance of oligonucleotide microarray performance**

This chapter is derived from the work developed through a 2-month placement in the Ablation and Joining Department headed by Dr. -Ing Arnold Gillner at the Fraunhofer Institute for Laser Technology (Germany) in 2018.



The development of oligonucleotide microarrays onto glass and quartz slides by the novel fluor-thiol photocoupling reaction has been just demonstrated by using 2 different irradiation resources. Nonetheless, the exploration of structured slides, aiming better immobilization and sensitivity results was pursued. This is key for the fabrication of higher density microarrays which enhances the performance of the microarray. Hence, the effect of the different microstructures in the fluorescence intensity was studied through a placement in the Biofabrication and Laser Therapy Group, in close relationship with the Microstructuring Group, at the Fraunhofer Institute for Laser Technology (Germany).



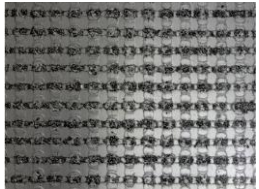
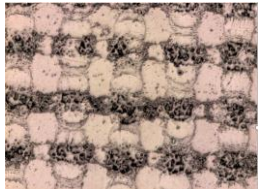
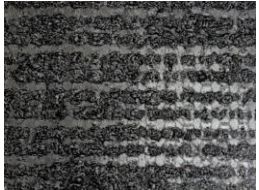

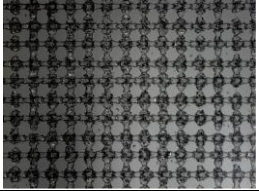
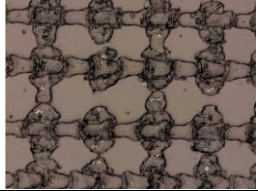
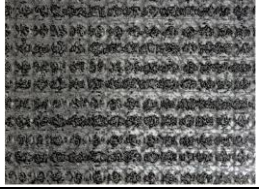

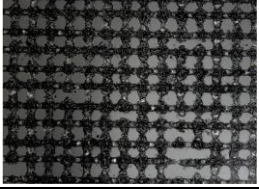
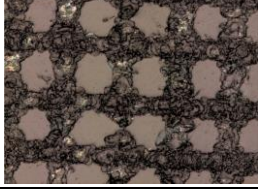
Fabrication of superhydrophobic and superhydrophilic surfaces mimicking natural elements is an interesting idea for the development of DNA microarray technology. The capability of micro/nanostructuring of surfaces to become water-repellant allows a phenomenon known as *lotus* effect. This nanotechnology advances provide the development of new superhydrophobic materials to improve the characteristics of antiadherence, anti-fog, self-cleaning, etc.<sup>1</sup>

In addition, it is known that the surface roughness increases the capacity of the surface to harbor a higher amount of bioreceptors, as the surface available is larger.<sup>2,3</sup> Therefore, controlling the roughness of the surface, immobilization capacity can be improved, so a higher fluorescence signal is obtained. Nonetheless, some studies have demonstrated that there are other factors implicated in this enhancement of fluorescence.<sup>4,5</sup>

To clear up this event, in our laboratory, deposition of the same amount of labeled biomolecule onto surfaces with different roughness and recording of the fluorescence emission was performed. Oligonucleotide and protein systems were studied, employing the surfaces available in the laboratory (glass slides and polymeric substrates), whose roughness varied from 0.02 to 2  $\mu\text{m}$ . Effectively, the results revealed that rough surfaces displayed higher fluorescence intensities, in comparison to smooth surfaces, no matter the analyte, the fluorophore or the composition of the material employed. Based on these preliminary results, a controlled microstructuration of glass slides by the laser technology available in the host group was tackled. Those microstructured surfaces were combined in Section 5.1 to explore whether assay sensitivity and probe immobilization could perform further.

For that, the microstructuration of glass slides was undertaken by using a Hyperrapid 100 laser source with a maximum average power of 100 W and an emission radiation at  $\lambda = 1064$  nm. This ultra-short pulsed laser allowed the microstructuration of the microscope glass slides, achieving different roughness depending on the power employed during radiation. This material is ideal to compare to previous results (section 3.1).

A complete characterization of the different structures is key for a better understanding of the substrate behavior onto the later bioassay processes, exhaustive roughness measurements by 3D Laser Scanning Microscopy (LSM), were performed. The different substrates displayed arithmetic mean roughness ( $R_a$ ) from 20 nm to 1.8  $\mu\text{m}$ . (Figure 1).

Platform	$R_a$ ( $\mu\text{m}$ )	Amplification 50X	Amplification 150X
Glass slides	0.02		
A	0.30		
B	0.35		
C	0.40		
D	0.60		
E	0.85		



**Figure 1.** LSM images of the structured and non-structured platforms at 50x and 150x objective. Roughness measurements were analyzed on the 150x amplification images.

These seven structures were chosen to undertake the assay experiments based on the roughness and topography obtained. Then, preliminary assays were performed to ensure the suitability of the structured platforms for microarray technology. For that, the functionalization of the substrates, by using an adapted methodology to the employed in our laboratory, was carried out (see section 3.1). Water contact measurements of the functionalized substrates with 1H,1H,2H,2H-perfluorodecyltriethoxysilane (PFTS) were checked to control the hydrophobicity of the surfaces (Table 1). Additional LSM measurements demonstrated that functionalization does not affect the surface roughness structure.

**Table 1.** The relation between roughness measured before functionalization and water contact angle obtained after functionalization with PFTS. Water contact angles around 110 ° were achieved.

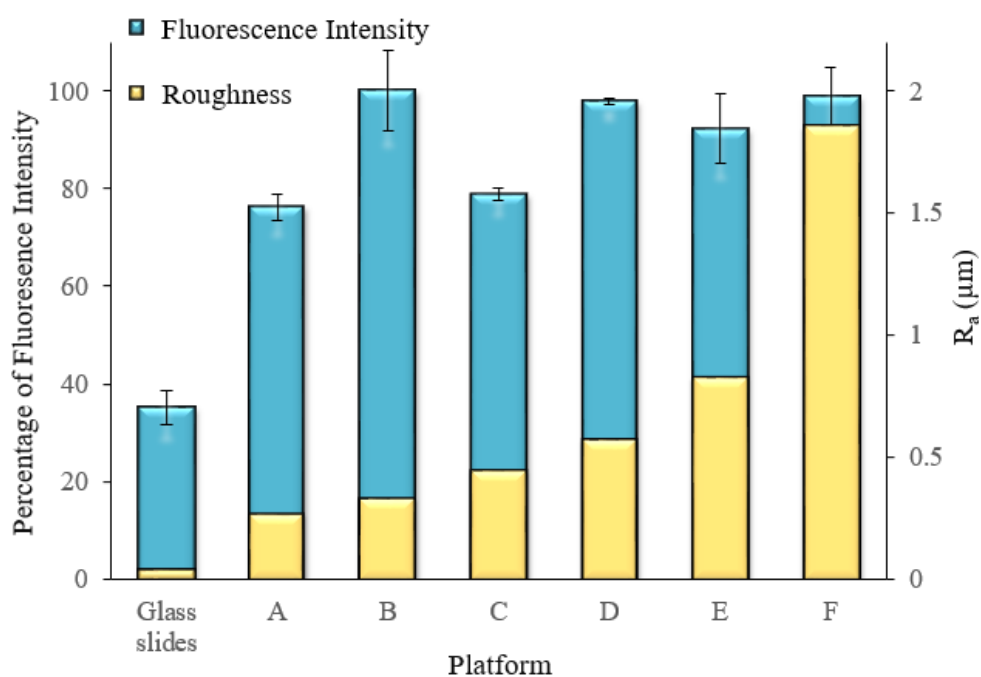
Platform	Glass slides	A	B	C	D	E	F
R <sub>a</sub> (μm)	0.02	0.3	0.35	0.4	0.6	0.85	1.8
WCA (°)	110	107	107	107	108	107	108

Once the substrates were functionalized with a hydrophobic silane, immobilization and hybridization assays of oligonucleotide probes, were performed.

For immobilization, 0.7 μL drops of a thiolated and labeled probe (Probe 1\* at 1 and 2 μM in PBS1x) were placed onto the different microstructures with a standard micropipette. After drying, substrates were irradiated with a portable UV lamp at 254 nm for 5 minutes and washed with PBS1x for 15 minutes. Fluorescence was recorded using a confocal laser scanning microscope (CLSM), by exciting at 633 nm and reading from 640-700 nm. Regarding hybridization, 0.7 μL drops of a thiolated and non-labeled probe (Probe 1 at 1 and 2 μM in PBS1x) were placed onto the different microstructures. After drying, platforms were irradiated as above and washed. Then, platforms were incubated with the complementary strand (Target 1\* at 0.1 μM) for 1 hour at 37 °C. After washing,

imaging of the samples was performed as above. The microstructured surfaces displayed successful immobilization and hybridization results, which corroborates their suitability for the fabrication of oligonucleotide microarrays. Thanks to these successful results, these structured platforms were introduced in our usual fabrication procedure for comparison to all the previous work. Thus, further structures were fabricated keeping the same parameters, and brought to the Department of Chemistry at the Polytechnic University of Valencia, to perform the biofunctionalization and biorecognition assays, using our optimized methodologies.

Henceforth, experiments were performed onto the structured slides accomplished during the placement, but using our optimized fabrication methodology. To carry out the first objective and checking the fluorescence signal enhancement with the roughness, a comparison between  $R_a$  and fluorescence signal intensity was done. For that, the printing of Probe 1\* (40 nL/spot; 4 spots/row; 1 and 2  $\mu\text{M}$  in PBS1x) onto perfluorinated substrates with different roughness by a noncontact dispensing system was done. Registration of fluorescence signal was performed in the surface fluorescence reader (SFR). As can be observed in Figure 2, all the structured platforms (platforms A, B, C, D, and E) displayed a fluorescence signal (blue bars) of at least twice the obtained with the same glass material without structuration on it.



**Figure 2.** Fluorescence intensity after probe spotting of the different platforms (blue bars) in relation to their roughness (yellow bars). Structured platforms revealed higher fluorescence intensity.

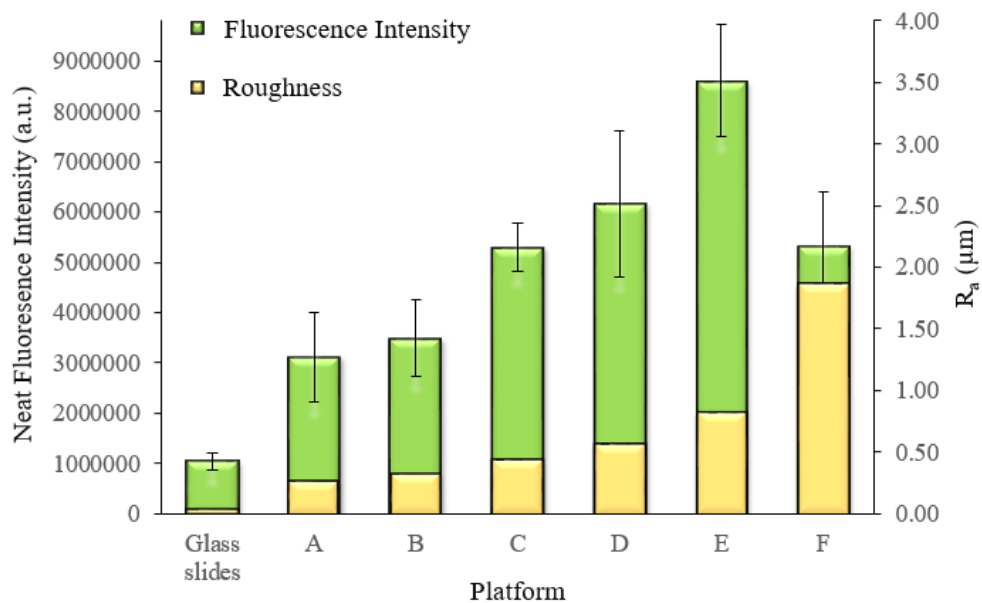
As the amount of labeled probe was exactly the same for all the surfaces, an identical fluorescence intensity would be expected. However, an unknown effect is occurring as different intensities were obtained. Our hypothesis is that due to the increase of the surface roughness, the non-radiative process could be reduced as emitting molecules are partially isolated, which would reduce the spatial vibrations and intermolecular collisions.

Taking advantage of these interesting results, further experiments were undertaken. Therefore, the study of immobilization was performed by spotting the thiolated probe (40 nL of Probe 1\* at 1 and 2  $\mu\text{M}$ ) and irradiating at 254 nm for 5 minutes. As obtained above, successful immobilization was achieved after washing. However, a deeper study of this process was completed this time. For that, the fluorescence intensity of the immobilized biomolecules was compared before and after washing. As may be seen in Table 2, a constant percentage loss of fluorescence was observed for every surface. This means that all the surfaces are displaying a very similar anchoring capacity. This corroborates our previous hypothesis as the higher surface roughness does not provide a higher immobilization density, and the increase in fluorescence intensity is due to other reasons like scattering.

**Table 2.** Percentage of immobilization for Probe 1\* at 2  $\mu\text{M}$ . Fluorescence intensity was measured before and after washing to calculate the immobilization extend.

Platform	Glass slides	A	B	C	D	E	F
Immobilization yield (%)	88	87	86	88	88	87	78
$R_a$ ( $\mu\text{m}$ )	0.02	0.27	0.33	0.45	0.58	0.83	1.86

Finally, sensitivity reached by the different platforms was studied through hybridization assays. For that, the spotting of the non-labeled thiolated probe (Probe 1 at 1 and 2  $\mu\text{M}$  in PBS1x) and irradiation of the surface at 254 nm for 5 minutes was performed. After washing, platforms were incubated with the labeled complementary strand (Target 1\* at 0.1  $\mu\text{M}$  in SSC1x) for 1 hour at 37 °C. Fluorescence intensities were registered in the SFR after washing. All the structured platforms increased significantly the fluorescence intensity (green bars), being the platform E which displayed a higher sensitivity (Figure 3).



**Figure 3.** Neat fluorescence intensity obtained after hybridization assay over each platform (green bars) in relation to their roughness (yellow bars). Sensitivity is significantly enhanced on the structured ones, in comparison to the non-structured surface.

Taking into account all these preliminary results (Figure 2, Table 2 and Figure 3), a different supposition is attained. These results are opposite to the previous hypothesis that attributed the increased of fluorescence to the higher immobilization density that allows the microstructured surfaces. Then, further studies have to be made to understand the process is happening over the surfaces.

With these results in mind, the design of new structured surfaces that improve the performance of the microarrays would be the next challenge, as microstructured surfaces show advantages versus non-structured ones.

Although structuration of glass is not an easy task due to the inertness of glass at high irradiation wavelengths, further studies to create specific patterns onto the surface can help to the performance of the microarray as demonstrated with these preliminary results.

Structuration of other materials, such as metals and polymers, provides a higher versatility than glass, however, the functionalization process should be optimized onto the new surface to apply it to microarray technology.



## Experimental section

*Chemicals, reagents, and buffers.* See section 3.1.

*Instrumental methods.* For controlling the structuration of the surfaces during the stay, the next instruments were employed.

Water contact angle (WCA) measurements were taken using a Mobile Surface Analyzer provided by KRÜSS GmbH (Germany). The analysis was performed making use of the ADVANCE software.

For visualization and roughness measurements, a Color 3D Laser Scanning Microscope (LSM, Keyence, VK-9700, Germany) with a resolution of 1 nm, was employed. Afterward, pictures were analyzed with a special LSM-Software (VK-Analyzer, Keyence)

For fluorescence measurements, a Leica TCS SP2 confocal laser scanning microscope (CLSM, Leica Microsystems Heidelberg GmbH, Germany) was employed. For imaging, the surfaces were illuminated using the HeNe laser at 633 nm at a voltage of 750 V, and reading was made in the emission range from 640-700 nm with a 5x objective.

*Silanization of slides.* See the Experimental section from chapter 3.1 for the fabrication of PFTS surfaces.

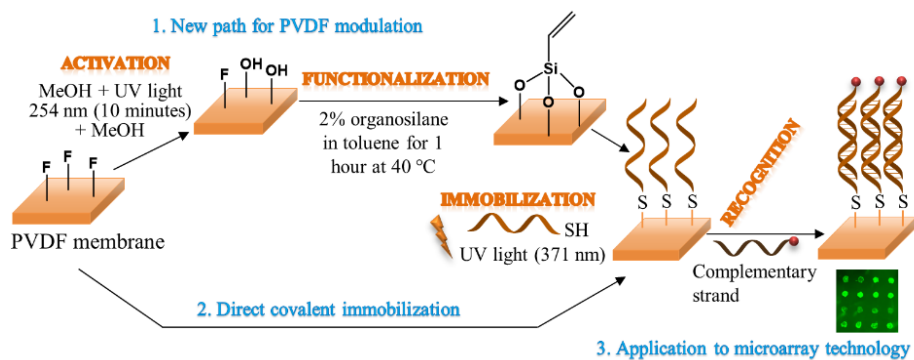
*Oligonucleotide immobilization.* See Experimental section from chapter 3.1 for anchoring of thiolated probes to surfaces containing C-F bonds through fluor-thiol photocoupling reaction.

*Hybridization Assays.* See the Experimental section from chapter 3.1 for recognition assays.

Methodology for immobilization and hybridization was performed as explained in section 3.1, excepting the irradiation resource employed. Instead, a UV-ozone surface cleaner, a portable mercury capillary lamp (6 mW/cm<sup>2</sup>, Jelight Irvine, USA) was employed for immobilization, by irradiating at 254 nm for 5 minutes. In addition, during the stay, 0.7 µL drops were deposited using a micropipette for spotting of the different probes, as an automatic dispensing system was not able at the host group.

## REFERENCES

- (1) Bañuls, M.-J.; Puchades, R.; Maquieira, Á. Chemical Surface Modifications for the Development of Silicon-Based Label-Free Integrated Optical (IO) Biosensors: A Review. *Anal. Chim. Acta* **2013**, *777*, 1–16.
- (2) Kim, D.-J.; Lee, J.-H.; Cho, S.-H.; Rizwan, M.; Venkatesh, R. P.; Chung, B. G.; Park, J.-G. Enhanced Fluorescence by Controlled Surface Roughness of Plastic Biochip. *Jpn. J. Appl. Phys.* **2011**, *50* (6), 06GL14.
- (3) Schyrr, B.; Pasche, S.; Voirin, G.; Weder, C.; Simon, Y. C.; Foster, E. J. Biosensors Based on Porous Cellulose Nanocrystal–Poly(Vinyl Alcohol) Scaffolds. *ACS Appl. Mater. Interfaces* **2014**, *6* (15), 12674–12683.
- (4) Guy, A. L.; Pemberton, J. E. Contributions of Atomic-Scale Roughness and Adsorbate Coverage to the Quenching of the SERS Response at Lead-Modified Silver Electrodes. *Langmuir* **1987**, *3* (1), 125–132.
- (5) Geddes, C. D.; Parfenov, A.; Roll, D.; Gryczynski, I.; Malicka, J.; Lakowicz, J. R. Roughened Silver Electrodes for Use in Metal-Enhanced Fluorescence. *Spectrochim. Acta. A. Mol. Biomol. Spectrosc.* **2004**, *60* (8–9), 1977–1983.



## 6. Thiol-click reactions for oligonucleotide microarrays onto polyvinylidene fluoride membranes



As established in the introduction, glass slides are the most employed material in microarray technology. Nevertheless, extrapolation to other materials is interesting to provide certain features in the substrate. In this chapter, microarrays using polymeric polyvinylidene fluoride (PVDF) membranes as solid substrate, are performed.

Because of its good resistivity and flexibility, PVDF membranes are widespread applied in numerous fields, such as separation process. Since the 1990s, PVDF substrates were broadly employed for the preparation of protein microarray by passive adsorption mainly, due to its efficient hydrophobic interactions. However, poor immobilization densities and high background were reached.

For that, a covalent anchoring is proposed in this work using two different routes, with the goal of improving the immobilization densities, and detection capacity.

The first one, performs a prior alkenyl functionalization of the PVDF substrate through organosilane chemistry. The activation of the membrane by UV light irradiation is widely studied, making use of a powerful lamp. This UV activation improves the previous activation methodologies, which entails an important milestone in this work, as well. Then, anchoring of thiolated oligonucleotides by the thiol-ene photocoupling reaction is carried out. These results demonstrate a novel activation (generation of hydroxyl groups) of PVDF membranes, and its application to microarray technology by thiol-ene photocoupling reaction.

The second strategy consists in the direct immobilization of thiolated oligonucleotides, by the fluor-thiol photoclick reaction. This result paves the way to apply this novel UV reaction to other substrates, in a fast and simple way. In addition, functionalization is not necessary, as PVDF membranes already provide the C-F bonds.

Both strategies are comparatively analyzed in terms of immobilization densities, hybridization capacity, and consumed bioassay time.

The applicability of thiol-click reactions to other systems is demonstrated in this work, therefore, further progresses could be done making use of these available methodologies.



## **6.1 Novel and rapid activation of polyvinylidene fluoride membranes by UV light**

"Reprinted with permission from *React. Funct. Polym.* **2019**, 140, 56–61. Copyright 2019 Elsevier





**ABSTRACT**

Polyvinylidene fluoride (PVDF) membranes have become essential because of their huge applicability to the industry; however, they still present some limitations. This study focuses on the modification of PVDF membrane properties such as hydrophobicity, wettability, and functionality. To obtain a stable grafting, the surface of the membrane is hydroxylated using UV light at 254 nm, followed by covalent immobilization of (3-aminopropyl)triethoxysilane (APTES) and vinyltriethoxysilane (VTES). The physicochemical and morphological properties of modified and raw PVDF membranes were analyzed by spectroscopy, microscopy, and goniometry. Finally, nucleic acid microarray technology results showed that PVDF and PVDF-VTES membranes had probe immobilization densities of 5 and 11 pmol/cm<sup>2</sup> and hybridization limits of detection of 1 and 5 nM, respectively.

**Keywords:** PVDF membranes; Hydroxylation; Silanization; Photoinduced immobilization; Nucleic acid microarrays

**1. Introduction**

PVDF membranes have been extensively applied to industrial processes and scientific research because of their mechanical, chemical, and thermal resistance properties, and their simple fabrication in mass scale [1,2]. PVDF is a semi-crystalline fluoropolymer that exists in four forms, and it is made of  $-\text{CH}_2\text{CF}_2-$  units. It has three types of bonds, namely, C-C, C-H, and C-F, whose energies are 88, 106, and 111 kcal/mol, respectively [1].

Because of the strong hydrophobic interactions exerted by the PVDF membrane, organic matter such as proteins accumulates into the pores, thereby lowering the filtration performance [3–5]; therefore, the antifouling properties of the membrane need to be improved. For that, if the membrane hydrophilicity is increased, protein adsorption and energy consumption can be reduced in separation processes [1,2,6]. In addition, enhancement of the membrane hydrophobicity increases the wetting resistance, which is an important property addressed in different ways [2,7–10].

Therefore, change in the PVDF membrane composition to improve its applicability and performance by addition of hydrophilic or hydrophobic compounds is still under

development. The main methodologies used thus far in the reformulation of PVDF membranes are surface modification by coating or grafting and blending modification by the addition of hydrophilic or amphiphilic polymers or inorganic nanoparticles in the fabrication process [1,2,11–13]. In this work, the membrane was modified by organosilane chemistry to achieve a covalent grafting. Hence, addition of hydroxyl groups onto the membrane surface by hydroxylation is necessary. Effective methodologies are necessary for hydroxylation, as most polymeric membranes such as PVDF do not present this functional group in their structure.

For a long time, hydroxylation by alkaline treatment using concentrated sodium hydroxide has been extensively performed to increase the resistivity of the membrane to harsh environments by generating hydroxyl groups over the surface [14,15]. However, membrane degradation by dehydrofluorination, as a secondary effect, has been broadly reported [1,10,14,16]. Alternative methods as piranha-based process [17] and plasma treatment [18,19] have been described, which show different limitations [10], and therefore, it is necessary to develop new methodologies to carry out PVDF membrane modification.

In this work, although direct activation of the PVDF membranes by UV light is difficult because of the good UV photo-irradiation resistance of the PVDF membrane [20], activation using methanol and a powerful UV lamp has been accomplished. This approach is easy and rapid for the generation of oxygen-based reactive motifs on the structure, and it is also cleaner, simpler, and milder than the previous reported methods [14,15,17–19]. Through this methodology, hydroxyl groups are formed onto the surface, without affecting the bulk properties of the membrane. Thus far, UV light has been extensively applied by our group as a powerful tool for the hydroxylation of silicon-based surfaces [21–23]. Hence, silanization was easily performed later, which allowed the docking of the membranes with different organosilanes. Functionalization of PVDF-based materials by organosilane chemistry is scarcely reported in the literature, and the available studies have always used the difficult activation processes mentioned above (alkaline, plasma, and piranha treatments); therefore, this field has to be explored [9,10,24].

Another interesting application of PVDF-based materials relies on the microarray technology. Since the advent of this technology in the 1990s, PVDF substrates have been widely used for the fabrication of protein microarrays. As mentioned before, PVDF

materials demonstrate efficient hydrophobic interactions; hence, passive binding of proteins and other biomolecules to the substrate occurs, thereby displaying limited immobilization densities and high background signals [25–30]. For that, as a proof of concept, raw PVDF membrane and those functionalized with vinyltriethoxysilane (PVDF-VTES) were used for the development of covalently anchored nucleic acid microarrays. The covalent immobilization of thiolated probes allows a rapid, stable, and orientated bonding, hence increasing the amount of active receptors over the surface. For the tethering of the thiolated probes to PVDF membranes, thiol-ene and fluor-thiol photocoupling reactions were applied. Thiol-ene reaction has been extensively applied in the preparation of high-density microarrays, taking the advantages of the click chemistry reactions [22,31–33]. For that, the surface functionalization of the PVDF membranes was carried out to generate active alkene groups on it. For raw PVDF membranes, fluor-thiol reaction was employed. This promising reaction has been recently proposed by our group and allows the direct covalent bonding of thiolated probes to C-F motifs over the surface [21]. Finally, detection capacity of both membrane types was compared to that obtained in a previous work by performing hybridization assays [21].

Hence, in this study, we demonstrate an easy, rapid, and effective method to graft PVDF membranes with different functional groups by using microarray technology applications.

## 2. Experimental section

*Chemicals, reagents, and buffers.* Immobilon-P PVDF membranes with 0.45  $\mu\text{m}$  nominal pore size were obtained from Merck Millipore (Spain). Ninhydrin, (3-aminopropyl)triethoxysilane (APTES), and vinyltriethoxysilane (VTES) were purchased from Sigma-Aldrich (Spain). Toluene and methanol were acquired from Scharlau (Spain). It is to be noted that all the chemicals were handled following the corresponding material safety data sheets. All chemicals were used without further purification.

Milli-Q water with a resistivity above 18  $\text{m}\Omega$  was used to prepare aqueous solutions. All the buffers employed, phosphate-buffered saline (PBS1x, 0.008 M sodium phosphate dibasic, 0.002 M sodium phosphate monobasic, 0.137 M sodium chloride, 0.003 M potassium chloride, pH 7.5), PBS-T (PBS1x containing 0.05% Tween 20), saline sodium citrate (SSC1x, 0.15 M sodium chloride, 0.02 M sodium citrate, pH 7), and SSC-T

(SSC1x comprising 0.5% Tween 20), were filtered through a 0.22  $\mu\text{m}$  pore size nitrocellulose membrane from Whatman GmbH (Germany), before use.

The oligonucleotides listed in Table 1 were acquired from Eurofins Genomics (Germany). The quality and concentration of DNA were determined by measuring optical density at 260/280 nm using a NanoDrop ND 1000 spectrophotometer from Thermo Fisher Scientific (USA).

*Instrumental methods.* Water contact angle (WCA) measurements were made with Attension Theta Lite from Biolin Scientific (Sweden), and images were processed with version 3.1 of One Attension software from Biolin Scientific (Sweden). The measurements were made in quintuplicate at room temperature with a volume drop of 2  $\mu\text{L}$  employing 18 m $\Omega$  water quality.

Microarray printing was carried out with a low-volume noncontact dispensing system (AD 1500 model, Biodot, USA). Irradiation at 254 nm was carried out using a UV-Ozone Surface Cleaner, UVOH 150 Lab, from FHR (Germany), while irradiation at 365 nm was performed with a mercury capillary lamp from Jelight Irvine (USA), 6 mW/cm<sup>2</sup>, placed at a fixed distance (0.5 cm).

The fluorescence signal of the spots was recorded with a homemade surface fluorescence reader (SFR) having a high sensitive charge-coupled device camera, Retiga EXi from QImaging Inc., (Canada), with light emitting diodes, Toshiba TLOH157P, as the light source [34]. For microarray image analysis and subsequent quantification, GenePix Pro 4.0 software from Molecular Devices, Inc. (USA), was employed.

X-ray photoelectron spectra were documented with a Sage 150 spectrophotometer from SPECS Surface Nano Analysis GmbH (Germany). Nonmonochromatic Al K $\alpha$  radiation (1486.6 eV) operating at 30 eV constant pass energy for elemental specific energy binding analysis was used as an X-ray source. Vacuum in the spectrometer chamber was 9 x 10<sup>-9</sup> hPa, and the sample area examined was 1 mm<sup>2</sup>. Attenuated total reflectance infrared spectra were recorded using a Bruker Tensor 27 FT-IR system coupled to a Platinum ATR accessory from Bruker (Germany). Atomic force microscopy (AFM) measurements were carried out with a Veeco model Dimension 3100 Nanoman from Veeco Metrology (USA) at a tapping mode of 300 kHz. Imaging was performed in AC mode in air using OMCL-AC240 silicon cantilevers from Olympus Corporation (Japan). The AFM images were taken at room temperature under ambient conditions, using tips from Nano World with a radius of 8 nm. All images were processed with NanoScope software.

*Derivatization of membranes.* Immobilon-P PVDF membranes were cut into 2 x 1 cm pieces, activated with methanol for 15 seconds, irradiated with a UV-Ozone surface cleaner for 10 minutes at 254 nm, and immersed again in methanol for 15 seconds. To modify the surface properties, the PVDF membranes were then immersed into a 2% v/v solution of the corresponding silane in toluene at 40 °C for 1 hour. Then, the samples were withdrawn from the silane solution, washed several times with toluene and isopropanol, and air-dried. Finally, substrates functionalized with (3-aminopropyl)triethoxysilane (PVDF-APTES) were baked for 1 hour at 60 °C, whereas those functionalized with vinyltriethoxysilane (PVDF-VTES) were baked for 1 hour at 80 °C. To corroborate the presence of primary amines in PVDF-APTES substrates, the ninhydrin test was performed. To carry out this selective test, a small piece of PVDF-APTES was immersed in 1.5 mL of ethanol. Then, 30 µL of fresh ninhydrin solution in ethanol at 1% was added to the membrane. Finally, the mixture was heated for 5 minutes at 100 °C. A piece of raw PVDF membrane underwent the same process to serve as a negative control.

*Microarray of nucleic acid probes by covalent anchoring.* Covalent anchoring of thiolated oligonucleotides onto raw PVDF and PVDF-VTES membranes by UV light at 365 nm was assessed. PVDF-VTES membranes were silanized as described above. Thus, 40 nL of Probe 1\*, bearing Cy5 fluorophore in the 3' position and SH motif in the 5' position (Table 1), prepared at 1 and 2 µM in PBS1x was spotted onto both surfaces to create the microarray (four spots per concentration). When the drops were dried, the PVDF membranes were exposed to UV light at 365 nm for 5 minutes to achieve immobilization. Afterwards, membranes were thoroughly rinsed with PBS-T for 10 minutes and air-dried, and fluorescence was measured using the SFR. Pictures of the membranes after irradiation as well as before and after washing were analyzed using GenePix software. Immobilization densities were calculated by comparing the fluorescence intensities before and after washing. For negative controls, two experiments were performed: first, adsorption of Probe 1\* was verified, and hence, the irradiation step was skipped; second, printing of a non-thiolated probe bearing a fluorophore in the 5' position (Target 1\*) was performed, followed by irradiation later.

Table 1. Oligonucleotide sequences used.

Name	Sequence (5' to 3')	5'	3'
Probe 1*	(T) <sub>15</sub> -CCCGATTGACCAGCTAGCATT	SH	Cy5
Probe 1	(T) <sub>15</sub> -CCCGATTGACCAGCTAGCATT	SH	-
Target 1*	AATGCTAGCTGGTCAATCGGG	Ax <sup>a</sup>	-

<sup>a</sup> Alexa Fluor® 647

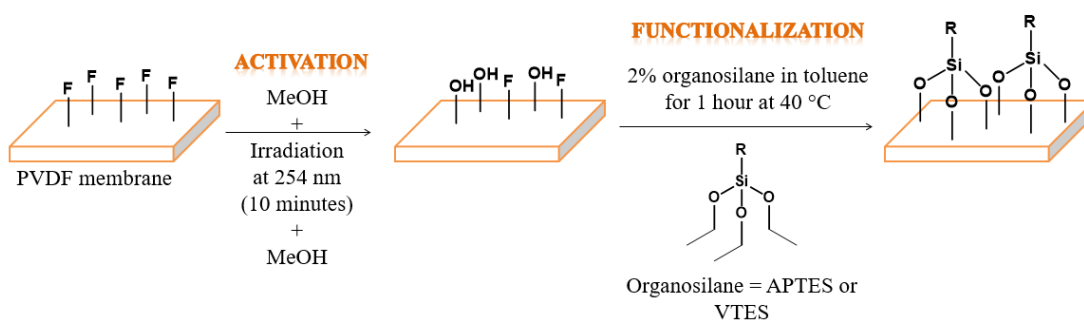
*Hybridization Assays.* To study the sensitivity of the modified and nonmodified surfaces, recognition assays were performed with raw PVDF and PVDF-VTES membranes. For that, PVDF-VTES membranes were functionalized as described above. Then, a thiolated oligonucleotide non-fluorescence labeled (Probe 1) prepared in 1 and 2  $\mu\text{M}$  PBS1x was spotted (40 nL/spot; 4 spots/row) onto both substrates. Once the drops dried, PVDF membranes were exposed to UV light at 365 nm for 5 minutes, washed with PBS-T, and air-dried. After washing, 25  $\mu\text{L}$  of Target 1\* (concentrations ranging from 0.0005 to 0.1  $\mu\text{M}$ , in SSC1x and SSC-T) was spread over the surface with a coverslip. After incubation in a humid chamber for 1 h at 37 °C, the coverslip was gently removed, and the chip was then washed with PBS-T. The fluorescence intensity of the spots was recorded using the SFR, as mentioned above.

### 3. Results and discussion

*Surface chemical derivatization.* Derivatization was performed as follows: first, PVDF membranes were immersed in methanol for 15 seconds to remove the air trapped inside the pores, following the instructions of the manufacturer. Then, the membrane was activated by irradiation with a UV lamp at 254 nm, as a promising procedure for the generation of hydroxyl groups onto the surface. Different irradiation times were assayed, and the contact angle was measured. As shown in Figure S1, the raw PVDF membranes showed a water contact angle of 130°, whereas contact angles of the activated surfaces lowered up to 83° after 10 minutes of UV irradiation because of the number of hydroxyl moieties generated on the surface by the oxidation and cleaning treatments. Membranes activated for a longer time did not show a stable contact angle and tended to filtrate quickly, which made us think that a change occurred in the physical structure. For that,

an activation time of 10 minutes, which displayed stable contact angles of  $83^\circ$ , was established for accomplishing this process (PVDF-OH). Then, the membranes were again soaked in methanol for 15 seconds to break the barrier between PVDF and the functionalization solution. Immediately, the membranes were functionalized by organosilane chemistry, considering different conditions such as solvents, reaction times, temperatures, and organosilanes. Finally, the membranes were immersed in a 2% organosilane solution in toluene for 1 hour at  $40^\circ\text{C}$  to create a thin layer over the surface. Compared to previous studies that used longer procedures [9,17,24], the present methodology required less time.

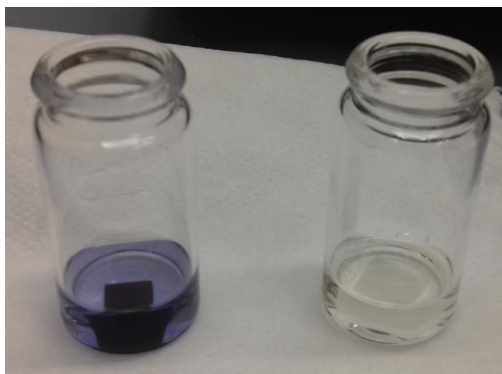
Two hydrophilic silanes were used for this work: APTES and VTES. APTES silane was chosen as the first functionalization reagent on the basis of the extended work performed by Arafat et al. [17], in which membrane activation by piranha treatment is performed, followed by silanization using the same silane later. In this way, comparison of our activation and functionalization methods can be done in an easy and rapid manner. In addition, primary amine groups allow a quick detection by the ninhydrin test and show characteristic peaks in FT-IR. VTES silane was selected to introduce alkene groups, which are necessary for the later thiol-ene photocoupling reaction. Moreover, hydrophobicity of the PVDF membranes is reduced, thereby allowing a better approximation of targets to the anchored probes. Figure 1 shows the layout of the general PVDF modification.



**Figure 1.** Layout of the simple activation and functionalization processes of PVDF membranes.

APTES and VTES functionalization slightly decreased the water contact angle of the raw PVDF membranes ( $119^\circ$  and  $118^\circ$ , respectively), thereby enhancing its hydrophilicity. To corroborate the presence of primary amines on the PVDF-APTES membrane, the

ninhydrin test was performed. The apparition of a deep blue color in the PVDF-APTES mixture verified the appropriate functionalization of the membrane. As a negative control, a piece of the raw PVDF membrane underwent the same test conditions to modify the membrane; however, no color change occurred [17,35] (Figure 2).



**Figure 2.** Ninhydrin test performed for a functionalized PVDF-APTES membrane (left) and a raw PVDF membrane (right). As can be seen, blue color indicating the presence of amines was developed only by the PVDF-APTES membrane.

Hence, the activation of PVDF membranes by UV light and the subsequent functionalization by organosilane chemistry constitute an advancement that allows a rapid, simple, mild, and effective procedure to modify PVDF properties.

Thus, to achieve a reproducible protocol to graft surfaces in a homogeneous, non-damaging, and stable way, a broad number of reaction conditions for hydroxylation and silanization processes were studied. A new protocol has been developed in this work, as hydroxyl groups over the membrane are necessary to silanize the substrates, and previously reported methods are aggressive and/or time consuming (alkaline, plasma, and piranha treatments) [14,15,17–19].

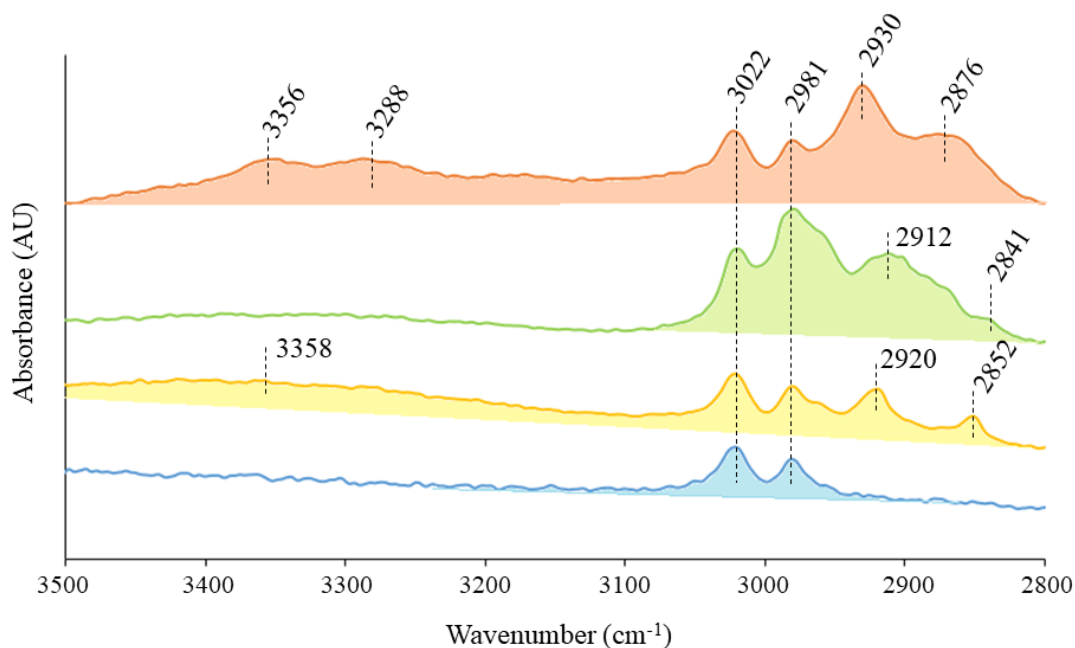
*Characterization of nonmodified and modified membranes.* To establish the chemical configuration of the raw and functionalized membranes, appropriate spectroscopic tools were applied.

#### ATR-FTIR

To detect the presence of new functional groups in the modified PVDF membranes, ATR-IR measurements of raw and modified membranes (PVDF-OH, PVDF-APTES, and PVDF-VTES) were made. The spectrum of the raw PVDF membrane displayed the characteristic bands corresponding to this material. With regard to the functional group



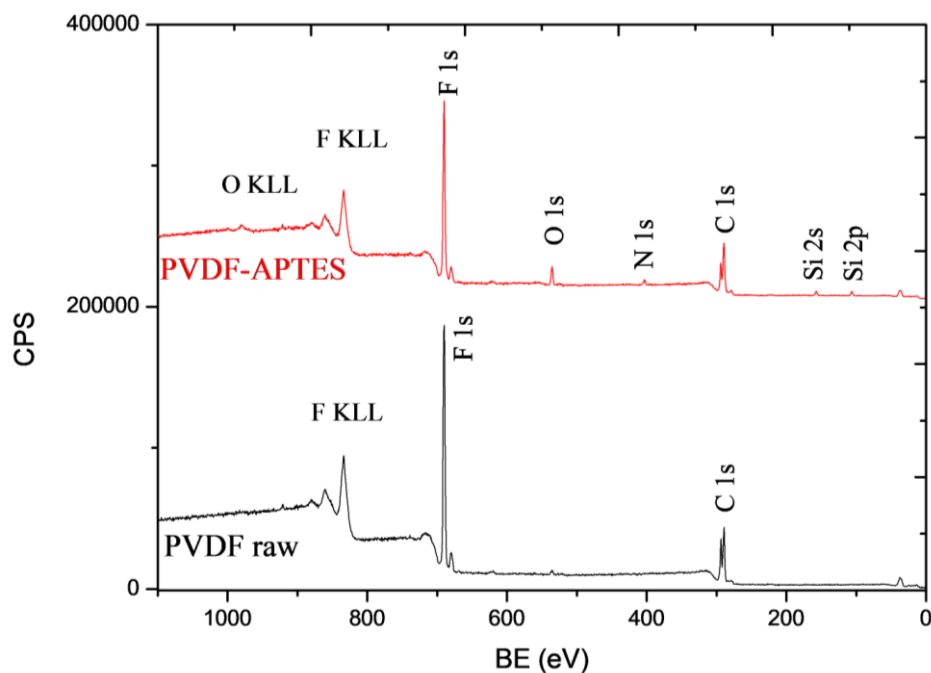
region, bands related to C–H stretching vibrations (symmetric and asymmetric modes) at 3022 and 2981  $\text{cm}^{-1}$  were identified [36]. These stretching bands appeared in all the modified membranes. Remarkably, in comparison to the spectrum of the raw PVDF membrane, the FT-IR spectrum of the PVDF-OH membrane showed the apparition of two additional C–H stretching bands located at 2920 and 2852  $\text{cm}^{-1}$ . This result, previously reported using piranha activation, [17] is due to the change in the environment of the  $\text{CH}_2$ , in which some neighbors have changed from  $\text{CF}_2$  to  $\text{CHOH}$  motifs as a result of UV light treatment; thus, a red shift is expected to occur. In addition, for functionalized membranes (PVDF-APTES and PVDF-VTES), new signals in the range of 3000 to 2800 were detected. In the case of PVDF-APTES, the new generated  $\text{CH}_2$  mode of vibration appeared at 2930 and 2876  $\text{cm}^{-1}$  with higher intensity and minor shift, which might be due to the contribution of the propyl group [17]. For PVDF-VTES, two new stretching vibrations situated at 2912 and 2841  $\text{cm}^{-1}$  were recognized. In addition, the spectrum of the PVDF-APTES membrane displayed two other new significant features related to primary amine groups. First, two characteristic peaks for the amine group can be clearly detected at 3349 and 3287  $\text{cm}^{-1}$ , which represent typical primary amine stretching vibrations (Figure 3). Second, two additional peaks related to bending vibrations of primary amines at 1574 and 1477  $\text{cm}^{-1}$  were observed (Figure S2). Figure S3 displays the fingerprint region (from 1500 to 400  $\text{cm}^{-1}$ ) of nonmodified and modified membranes. FT-IR spectra in this region followed a highly similar profile for all the membranes.



**Figure 3.** Comparison of ATR-IR spectra of nonmodified and modified PVDF membranes. Additional functional groups generated on the membranes displayed new peaks in the spectra. Blue: Raw PVDF membrane presents two C–H stretching vibrations, characteristic of this material ( $3022$  and  $2981\text{ cm}^{-1}$ ). Yellow: PVDF-OH membrane reveals two additional peaks at  $2920$  and  $2952\text{ cm}^{-1}$ , which corresponds to new C-H stretching bands and a broad band related to the hydroxyl groups. Green: PVDF-VTES membrane shows the emergence of  $\text{CH}_2$  vibrations at  $2912$  and  $2941\text{ cm}^{-1}$ . Orange: PVDF-APTES membrane displays two peaks related to primary amines ( $3356$  and  $3288\text{ cm}^{-1}$ ) and two additional peaks related to C–H stretching vibrations at  $2930$  and  $2876\text{ cm}^{-1}$ .

### XPS

XPS spectra of raw PVDF and PVDF-APTES membranes were also recorded. The spectrum of the PVDF-APTES membrane showed new peaks at  $398$ ,  $157$ , and  $102\text{ eV}$  related to the binding energies of  $\text{N}1s$ ,  $\text{Si}2s$ , and  $\text{Si}2p$ . These results corroborated the presence of silicon (Si) and nitrogen (N) motifs in the modified membrane, which demonstrated the successful functionalization. The intensity of the  $\text{O}1s$  band ( $531\text{ eV}$ ) was also increased because of the silanol groups generated onto the surface (Figure 4). In addition, quantification of peak  $\text{C}1s$  contributions revealed an increase in the signals due to the C–C band ( $284.8\text{ eV}$ ), which proved the presence of propyl groups of the organosilane, and a decrease in C–F bond contribution ( $289.4\text{ eV}$ ) due to the dehydrofluorination process [37]. (Figure S4, ESI).



**Figure 4.** XPS spectra comparison between the raw PVDF membrane and PVDF membrane functionalized with APTES. Apparition of new peaks in the functionalized membranes (PVDF-APTES) at 398, 157, and 102 eV, revealed the presence of N1s, Si2s, and Si2p motifs, respectively. Increase in the O1s intensity (531 eV) was appreciated.

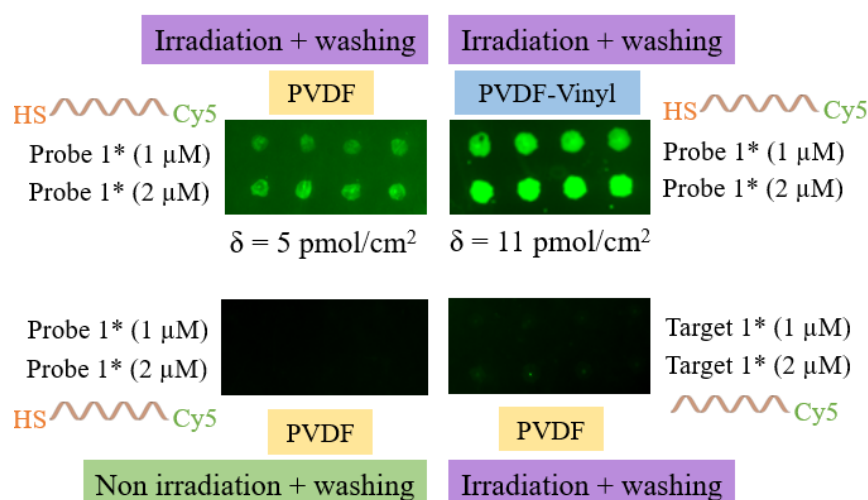
*Microarray bioassays.* The demonstration of the derivatization methodology of PVDF membranes by simple UV irradiation and silanization and its availability at a mass scale made us consider its use as a support for carrying out biological recognition assays to endow membranes for new applications. As a proof of concept, raw PVDF and PVDF-VTES membranes were applied for microarray technology. Hence, immobilization of nucleic acids and hybridization assays were performed with both membranes, and results were compared between the two assays and also with the results of a previous work [21].

#### Nucleic acid tethering

Here, we compare the immobilizations of thiolated probes onto the raw PVDF membrane and the PVDF-VTES membrane. The novel fluor-thiol photocoupling reaction allowed the covalent anchoring of thiolated probes onto the C–F bonds of the raw PVDF membrane [21], whereas the well-known thiol-ene photocoupling reaction allowed fixing of the probes to the alkene motifs generated on the membrane [10–12,15].

Thus, membranes were spotted with a thiolated probe that is fluorescent tag (Probe 1\*) in 1 and 2  $\mu$ M PBS1x. After the drops were dried, irradiated with UV light at 365 nm for

5 minutes, and washed with PBS-T, the fluorescence of the microarray was recorded using the SFR. Both membranes immobilized the thiolated nucleic acids successfully; however, the PVDF-VTES membrane showed a higher immobilization density (approximately twofold) than the raw PVDF membrane. As negative controls, two experiments were performed: First, the irradiation step was skipped to corroborate the use of UV light to immobilize the thiolated probe (Probe 1\*). Second, a nonthiolated probe (Target 1\*) was used to confirm the presence of the thiol group. Figure 5 displays both immobilization and negative control experiments.



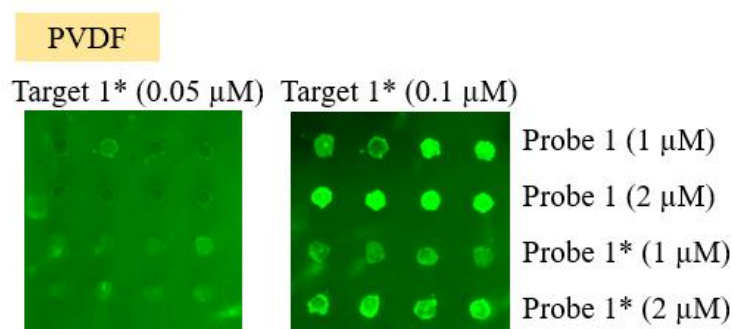
**Figure 5.** Top. Maximal immobilization densities of raw PVDF and PVDF-VTES membranes. Fluorescence intensities before and after washing were compared to calculate these values. Bottom. Negative controls corroborated the needed of irradiation and thiol group to undertake the fluor-thiol photocoupling reaction.

Immobilization studies were performed on both membrane sides. Although successful immobilizations were demonstrated on both sides, the bottom side displayed a better consistency and homogeneity of the spots (Figure S5). Therefore, further experiments were performed on the bottom side of the PVDF membranes.

#### Target detection

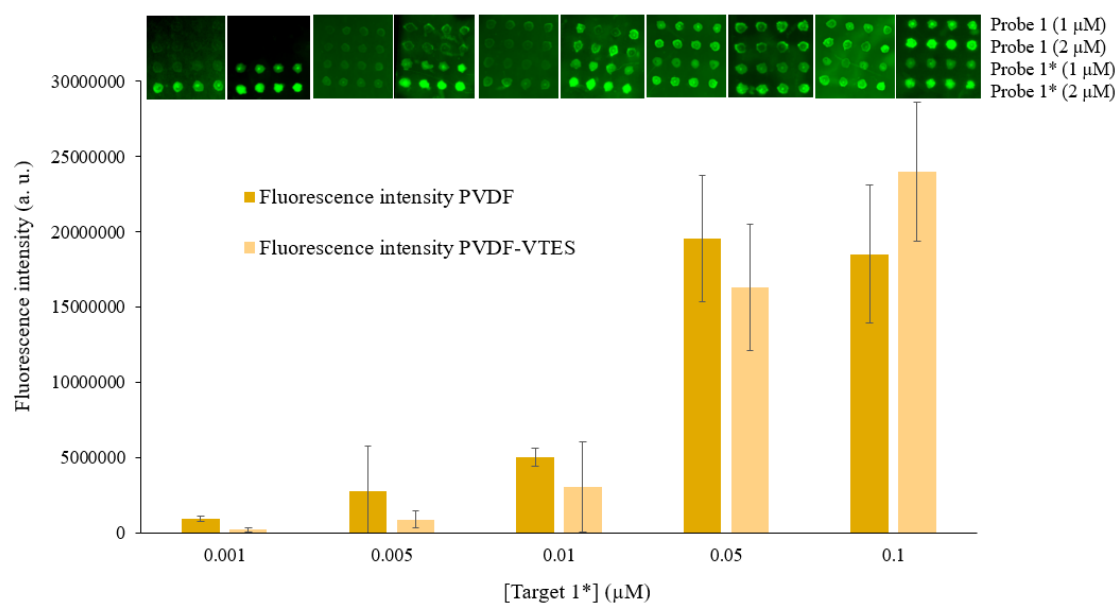
Hybridization with the complementary target was performed in raw PVDF and PVDF-VTES membranes. Thus, nonlabeled thiolated probe (Probe 1) in 1 and 2 μM PBS1x was spotted onto both surfaces, and immobilization was carried out in the same way as that before. After washing with PBS-T and drying, hybridization was carried out with a fully complementary AlexaFluor647-labeled probe (Target 1\*) at different concentrations

(from 0.0005 to 0.1  $\mu\text{M}$  in  $\text{SSC1x}$ ) in a humidity chamber. The microarrays were incubated for 1 h at 37  $^{\circ}\text{C}$  and then washed; the fluorescence intensity of the spots was recorded using the SFR. Owing to the high hydrophobicity of the raw PVDF membrane, the contact between the solution and the membrane surface was hindered; thus, a high amount of target (up to 0.1  $\mu\text{M}$ ) was necessary to achieve a detectable fluorescence signal (Figure 6).



**Figure 6.** Raw PVDF membranes showed a low sensitivity detection in the hybridization process using  $\text{SSC1x}$  as a hybridization buffer. Minimal concentration of target to detect worthy fluorescence signal was 0.1  $\mu\text{M}$ .

To solve this problem, SDS or Tween 20 surfactant was added to the target solution in the hybridization step to reduce the hydrophobic interactions and favor the approximation of the target to the anchored probe. Using a small amount of the detergent (0.5%) in the recognition process, up to 5 nM of Target 1\* was detected using the PVDF-VTES membrane as the substrate, whereas with the raw PVDF membrane, up to 1 nM was detected (Figure 7). The sensitivity of our microarray was limited by the sensitivity of the homemade fluorescence reader, SFR, which is within a detection limit of 1 and 5 nM, independent of the system and surface used. Considering the limitations of the reading device, both platforms revealed great suitability for the recognition of very low levels of nucleic acid sequences, and changing to other more sensitive detection devices or using colorimetric or enzymatic detection can lead to limits of detection in the range of pM, as we previously demonstrated [22, 23]. While the raw PVDF membrane showed slightly better limit of detection, the PVDF-VTES membranes could function without the need for surfactants and permit other methods of anchoring apart from thiol-ene coupling, i.e., alkene or acrylate polymerization.



**Figure 7.** Hybridization assays with decreasing concentrations of Target 1\*, using PVDF and PVDF-VTES membranes as substrates, were performed. Addition of SDS as a surfactant provided successful recognitions. The image shows the neat fluorescence intensity versus concentration of Target 1\* used in the hybridization process. Detection limits are 1 nM and 5 nM for PVDF and PVDF-VTES membranes, respectively.

Finally, if we compare the performance of the raw PVDF membranes with recently reported perfluorinated glass slides [21], in which 0.5 nM of the target was detected, a slightly lower detection capacity was presented by this novel material. However, the PVDF membrane did not require previous modification steps for the probe immobilization and hybridization processes, as in the case of functionalized glass slides, thus saving reagents and time. Hence, PVDF membranes allowed a quicker detection evaluation, which affords an encouraging substrate for microarray technologies. Furthermore, the flexibility of the membranes permits an easier integration and applicability to other fields.

#### 4. Conclusions

An alternative method for activating PVDF flat sheet membranes is shown in this study. The method is milder and easier than previous methods, as it uses only light for activation. The membranes activated in such way undergo silanization rapidly and as easily as membranes activated by other harsher methods.

As a proof of concept of its applicability, PVDF and PVDF-VTES membranes were used as substrates for microarray technology. For that, immobilization of thiolated nucleic acids and later hybridization with the complementary strand were carried out. The functionalized PVDF-VTES membrane displayed higher immobilization densities than the raw PVDF membranes; however, detection capacity was not improved. The raw PVDF membrane was had a detection of up to 1 nM of complementary strand by adding SDS surfactant to the target solution. This detection capacity is very close to the reported value using perfluorinated glass slides as supports and avoids the tedious previous functionalization process, thus saving reagents and time, without almost loss of sensitivity.

Finally, these advances pave the way to the biofunctionalization of raw PVDF membranes with other bioreceptors such as antibodies and the direct functionalization using thiolated organic compounds taking the advantage of UV irradiation. The second approximation would allow the modification of surface properties in a rapid, easy, and effective way without using organosilanes.

## **ACKNOWLEDGMENTS**

Financial support from BIHOLOG (Project CTQ2016-75749-R) and FEDER is acknowledged. P.J.-M. acknowledges the Spanish Ministry of Economy, Industry and Competitiveness for the public FPI grant (Project CTQ2013-45875-R) and cofinancing by the European Social Fund.

## REFERENCES

- [1] F. Liu, N.A. Hashim, Y. Liu, M.R.M. Abed, K. Li, Progress in the production and modification of PVDF membranes, *J. Membr. Sci.* 375 (2011) 1–27.
- [2] G. dong Kang, Y. ming Cao, Application and modification of poly(vinylidene fluoride) (PVDF) membranes - A review, *J. Membr. Sci.* 463 (2014) 145–165.
- [3] Y. Sui, Z. Wang, X. Gao, C. Gao, Antifouling PVDF ultrafiltration membranes incorporating PVDF-g-PHEMA additive via atom transfer radical graft polymerizations, *J. Membr. Sci.* 413–414 (2012) 38–47.
- [4] B. Onal-Ulusoy, Effects of Plasma-Modified Polyvinylidene fluoride and Polyethersulfone Ultrafiltration (UF) Membrane Treatments on Quality of Soybean Oil, *J. Food Qual.* 38 (2015) 285–296.
- [5] M.F. Rabuni, N.M. Nik Sulaiman, M.K. Aroua, N.A. Hashim, Effects of alkaline environments at mild conditions on the stability of PVDF membrane: An experimental study, *Ind. Eng. Chem. Res.* 52 (2013) 15874–15882.
- [6] X. Shen, X. Yin, Y. Zhao, L. Chen, Improved protein fouling resistance of PVDF membrane grafted with the polyampholyte layers, *Colloid Polym. Sci.* 293 (2015) 1205–1213.
- [7] S.-H. Lin, K.-L. Tung, H.-W. Chang, K.-R. Lee, Influence of fluorocarbon flat-membrane hydrophobicity on carbon dioxide recovery, *Chemosphere.* 75 (2009) 1410–1416.
- [8] X.X. Shen, W.F. Yang, Q.F. Zhang, Hydrophobic Modification of PVDF, in: *Funct. Electron. Mater. IUMRS-ICA2010*, Trans Tech Publications, 2011: pp. 658–661..
- [9] X. Yang, R. Wang, L. Shi, A.G. Fane, M. Debowski, Performance improvement of PVDF hollow fiber-based membrane distillation process, *J. Membr. Sci.* 369 (2011) 437–447.
- [10] S. Sairiam, C.H. Loh, R. Wang, R. Jiratananon, Surface modification of PVDF hollow fiber membrane to enhance hydrophobicity using organosilanes, *J. Appl. Polym. Sci.* 130 (2013) 610–621.
- [11] S. Hao, Y. Geng, Z. Jia, UV pre-activation/thermal initiated grafting of caffeic acid on PVDF for preparation of adsorptive membranes for cesium, *React. Funct. Polym.* 132 (2018) 120–126.
- [12] Y. He, X. Chen, F. Dai, R. Xu, N. Yang, X. Feng, Y. Zhao, L. Chen, Immobilization of poly(N-acryoyl morpholine) via hydrogen-bonded interactions for improved



- separation and antifouling properties of poly(vinylidene fluoride) membranes, *React. Funct. Polym.* 123 (2018) 80–90.
- [13] J. Zhao, H. Han, Q. Wang, C. Yan, D. Li, J. Yang, X. Feng, N. Yang, Y. Zhao, L. Chen, Hydrophilic and anti-fouling PVDF blend ultrafiltration membranes using polyacryloylmorpholine-based triblock copolymers as amphiphilic modifiers, *React. Funct. Polym.* (2019).
- [14] G.J. Ross, J. Watts, M. Hill, P. Morrissey, Surface modification of poly(vinylidene fluoride) by alkaline treatment Part 2. Process modification by the use of phase transfer catalysts, *Polymer*. 42 (2001) 403–413.
- [15] G.J. Ross, J.F. Watts, M.P. Hill, P. Morrissey, Surface modification of poly(vinylidene fluoride) by alkaline treatment1. The degradation mechanism, *Polymer*. 41 (2000) 1685–1696.
- [16] H. Dong, K. Xiao, X. Tang, Z. Zhang, J. Dai, R. Long, W. Liao, Preparation and characterization of polyurethane (PU)/polyvinylidene fluoride (PVDF) blending membrane, *Desalination Water Treat.* 57 (2016) 3405–3413.
- [17] S. Al-Gharabli, J. Kujawa, M.O. Mavukkandy, H.A. Arafat, Functional groups docking on PVDF membranes: Novel Piranha approach, *Eur. Polym. J.* 96 (2017) 414–428.
- [18] Y. Chen, H. Kim, Preparation of superhydrophobic membranes by electrospinning of fluorinated silane functionalized poly(vinylidene fluoride), *Appl. Surf. Sci.* 255 (2009) 7073–7077.
- [19] W.-T. Xu, Z.-P. Zhao, M. Liu, K.-C. Chen, Morphological and hydrophobic modifications of PVDF flat membrane with silane coupling agent grafting via plasma flow for VMD of ethanol–water mixture, *J. Membr. Sci.* 491 (2015) 110–120.
- [20] G. Botelho, M.M. Silva, A.M. Gonçalves, V. Sencadas, J. Serrado-Nunes, S. Lanceros-Mendez, Performance of electroactive poly(vinylidene fluoride) against UV radiation, *Polym. Test.* 27 (2008) 818–822.
- [21] P. Jiménez-Meneses, M.-J. Bañuls, R. Puchades, Á. Maquieira, Fluor-thiol Photocoupling Reaction for Developing High Performance Nucleic Acid (NA) Microarrays, *Anal. Chem.* 90 (2018) 11224–11231.
- [22] M.-J. Bañuls, P. Jiménez-Meneses, A. Meyer, J.-J. Vasseur, F. Morvan, J. Escorihuela, R. Puchades, A. Maquieira, Improved performance of DNA microarray

- multiplex hybridization using probes anchored at several points by Thiol-Ene or Thiol-Yne click chemistry, *Bioconjug. Chem.* 28 (2017) 496–506.
- [23] R. Alonso, P. Jiménez-Meneses, J. García-Rupérez, M.-J. Bañuls, Á. Maquieira, Thiol-ene click chemistry towards easy microarraying of half-antibodies, *Chem. Commun.* 54 (2018) 6144–6147.
- [24] Z. Zheng, Z. Gu, R. Huo, Z. Luo, Superhydrophobic poly(vinylidene fluoride) film fabricated by alkali treatment enhancing chemical bath deposition, *Appl. Surf. Sci.* 256 (2010) 2061–2065.
- [25] P. Angenendt, J. Glökler, D. Murphy, H. Lehrach, D.J. Cahill, Toward optimized antibody microarrays: a comparison of current microarray support materials, *Anal. Biochem.* 309 (2002) 253–260.
- [26] P. Angenendt, Progress in protein and antibody microarray technology, *Drug Discov. Today.* 10 (2005) 503–511.
- [27] S. Hu, Z. Xie, J. Qian, S. Blackshaw, H. Zhu, Functional protein microarray technology: Functional protein microarray technology, *Wiley Interdiscip. Rev. Syst. Biol. Med.* 3 (2011) 255–268.
- [28] F.X.R. Sutandy, J. Qian, C.-S. Chen, H. Zhu, Overview of Protein Microarrays, *Curr. Protoc. Protein Sci.* 72 (2013) 27.1.1-27.1.16.
- [29] K. Bussow, A method for global protein expression and antibody screening on high-density filters of an arrayed cDNA library, *Nucleic Acids Res.* 26 (1998) 5007–5008.
- [30] A. Lueking, M. Horn, H. Eickhoff, K. Büssow, H. Lehrach, G. Walter, Protein Microarrays for Gene Expression and Antibody Screening, *Anal. Biochem.* 270 (1999) 103–111.
- [31] J. Escorihuela, M.J. Bañuls, S. Grijalvo, R. Eritja, R. Puchades, Á. Maquieira, Direct covalent attachment of DNA microarrays by rapid thiol-ene “click” chemistry, *Bioconjug. Chem.* 25 (2014) 618–627.
- [32] J. Escorihuela, M.-J. Bañuls, R. Puchades, Á. Maquieira, Site-specific immobilization of DNA on silicon surfaces by using the thiol-yne reaction, *J Mater Chem B.* 2 (2014) 8510–8517.
- [33] J. Escorihuela, M.J. Bañuls, R. Puchades, Á. Maquieira, DNA microarrays on silicon surfaces through thiol-ene chemistry., *Chem. Commun.* 48 (2012) 2116–2118.

- [34] D. Mira, R. Llorente, S. Morais, R. Puchades, A. Maquieira, J. Marti, High throughput screening of surface-enhanced fluorescence on industrial standard digital recording media, *Proc SPIE*. 5617 (2004) 364–373.
- [35] E. Kaiser, R.L. Colescott, C.D. Bossinger, P.I. Cook, Color test for detection of free terminal amino groups in the solid-phase synthesis of peptides, *Anal. Biochem.* 34 (1970) 595–598.
- [36] H. Bai, X. Wang, Y. Zhou, L. Zhang, Preparation and characterization of poly(vinylidene fluoride) composite membranes blended with nano-crystalline cellulose, *Prog. Nat. Sci. Mater. Int.* 22 (2012) 250–257.
- [37] N. Akashi, S. Kuroda, Protein immobilization onto poly (vinylidene fluoride) microporous membranes activated by the atmospheric pressure low temperature plasma, *Polymer*. 55 (2014) 2780–2791.



## SUPPORTING INFORMATION

### **Novel and rapid activation of polyvinylidene fluoride membranes by UV light**

List of contents:

**Figure S1.** Water contact angles displayed for PVDF membranes after different activation times.

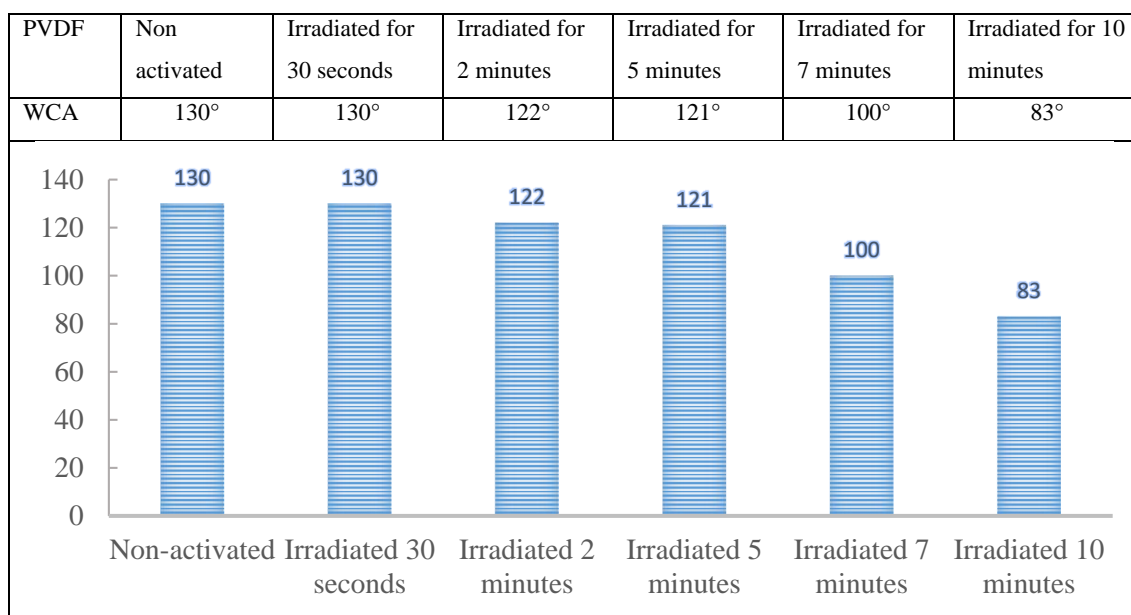
**Figure S2.** ATR-IR spectra (approximately 1700–1400  $\text{cm}^{-1}$ ) of the PVDF-APTES membranes.

**Figure S3.** ATR-IR spectra of the fingerprint region of the raw PVDF membrane, activated PVDF membrane, and functionalized PVDF-APTES and -VTES membranes.

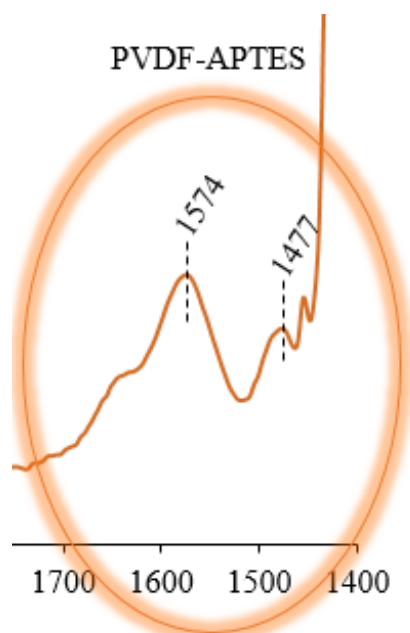
**Figure S4.** XPS experiments displayed the contributions of C–C and  $\text{CF}_2$  to the C1s binding energy for PVDF and PVDF-APTES membranes.

**Figure S5.** Comparison between the top and bottom sides of the PVDF membranes.

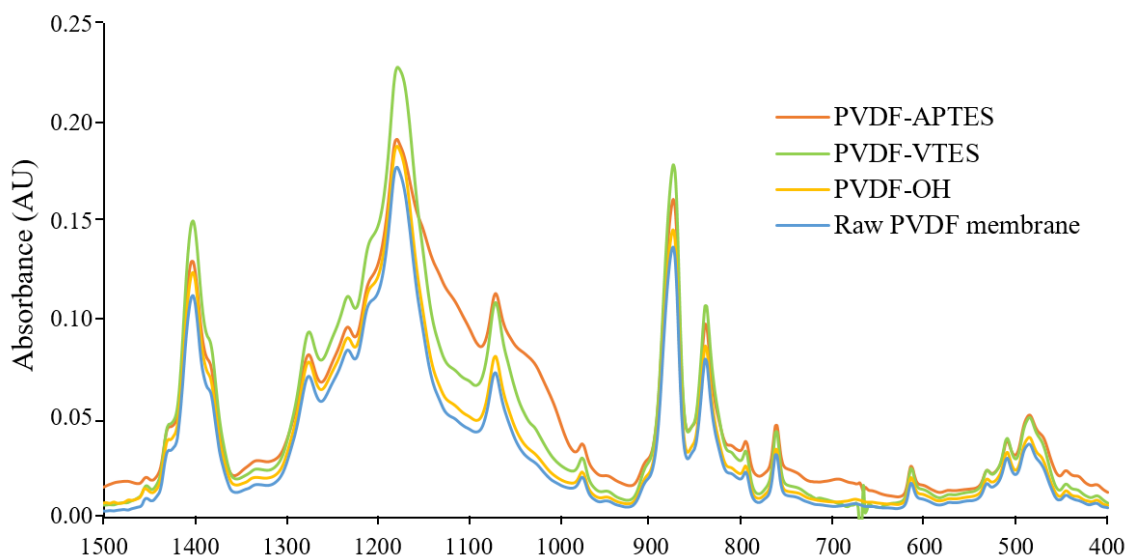
**Figure S1.** Water contact angles displayed for PVDF membranes after different activation times.



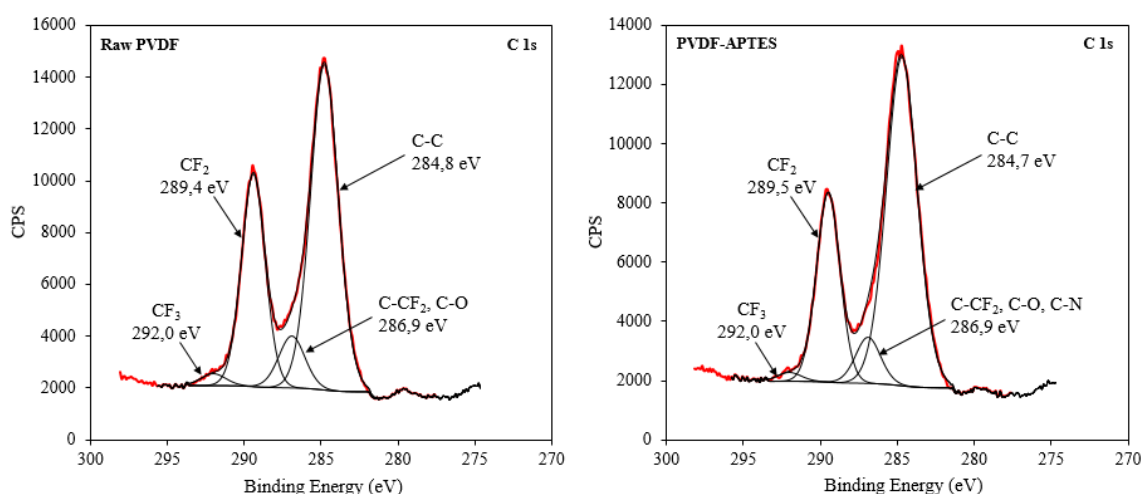
**Figure S2.** ATR-IR spectra (approximately 1700–1400  $\text{cm}^{-1}$ ) of the PVDF-APTES membranes. Bending vibrations corresponding to primary amines, at 1574 and 1477  $\text{cm}^{-1}$ , were recorded.



**Figure S3.** ATR-IR spectra (1500–400  $\text{cm}^{-1}$ ) of the fingerprint region of the raw PVDF membrane, activated PVDF membrane, and functionalized PVDF-APTES and –VTES membranes. A similar profile is observed.



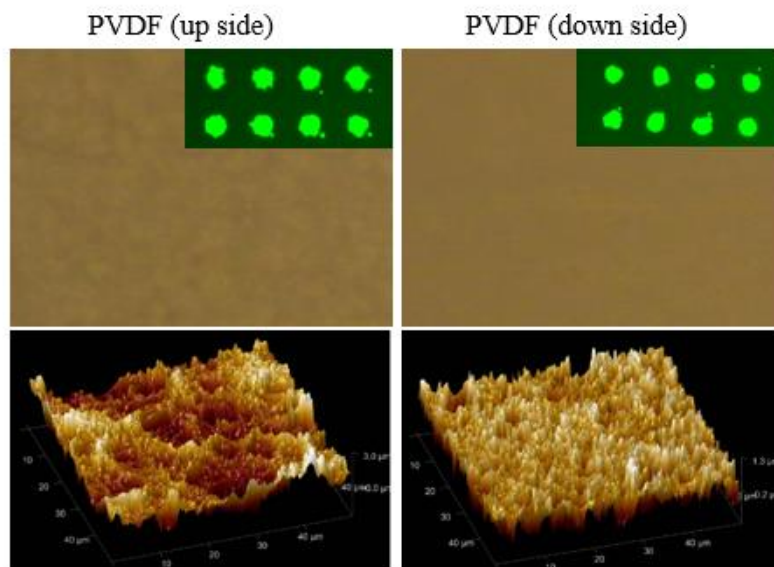
**Figure S4.** XPS experiments displayed the contributions of C–C and  $\text{CF}_2$  to the C1s binding energy for PVDF and PVDF-APTES membranes. For functionalized membranes, the amount of C–C groups (284.8 eV) increased, whereas the percentage of  $\text{CF}_2$  (289.4 eV) decreased, which corroborates the functionalization of the membrane.



Sample	Raw PVDF membrane			
Name	C–C	C–CF <sub>2</sub> , C–O	CF <sub>2</sub>	CF <sub>3</sub>
BE (eV)	284.8	286.9	289.4	292.0
% At	57.3	8.8	32.0	1.9

Sample	PVDF-APTES membrane			
Name	C–C	C–CF <sub>2</sub> , C–O, C–N	CF <sub>2</sub>	CF <sub>3</sub>
BE (eV)	284.7	286.9	289.5	292.0
% At	64.0	7.1	27.6	1.3

**Figure S5.** Comparison between the top and bottom sides of the PVDF membranes. Top. Microscope pictures and array image. Bottom. AFM measurements.





## **7. Conclusions and perspectives**



The present thesis, entitled “Study of substrate modulation and bioreceptor anchoring for the development of high performance microarrays”, was focused on the development of new designs able to improve microarray performance applied in biosensing. In the search of higher confinement of the probes that lead to the analytes approximating only where the probe is anchored while repulsion over the rest of the surface is increased, different solid substrates, surface modulation, and photoinduced anchoring strategies, for both oligonucleotide and antibodies, have been studied.

The most relevant conclusions are summarized below, classified according to the particular objectives initially proposed.

- ✓ Mono and polythiolated oligonucleotide probes have been immobilized onto alkenylated and alkynylated glass slides by thiol-ene and thiol-yne photocoupling reactions, respectively. Alkynylated surfaces displayed a higher immobilization and hybridization capacity. In addition, the higher the number of thiol groups was in the oligonucleotide, the higher the immobilization density and the hybridization capacity resulted. Nevertheless, this tendency was less pronounced in the case of alkynylated surfaces, as immobilization density of monothiolated probes is almost maximal for this surface.

Therefore, hydrophobicity modulation and multipoint attachment have demonstrated to be two ways to improve the performance of the microarray. Both approaches are related to the configuration adopted by the probe, as it will determine its bioavailability for hybridization.

- ✓ Thiol-ene photocoupling reaction has been applied for the first time to the covalent linking between the free thiol groups present in half-antibodies and alkenylated glass slides. This strategy is very interesting and innovative, improving the recognition capacity in comparison to whole antibodies, due to the orientation of immobilized half antibodies through their free thiol groups, which increased the bioavailability of the receptors. Moreover, this is an effective route for antibody immobilization under very mild, fast, easy and biocompatible conditions.

Finally, this methodology demonstrated successful multiplexing and it was applied to the level determination of interesting biomarkers, such as CRP and cTnI, very useful to assess the risk of cardiovascular diseases.

- ✓ The fluor-thiol photoclick reaction has been demonstrated for the first time, as a novel covalent anchoring methodology between free thiols and C-F motifs. This photoinduced reaction allows the modulation of highly hydrophobic surfaces, which is of outmost importance.

This radical initiated reaction has been applied to the preparation of oligonucleotide microarrays onto perfluorinated glass slides, being a fast, mild and biocompatible strategy. The high hydrophobicity of the surfaces allowed the confinement of the probes in very small spots, which favors the specific approximation of the analyte only where the probe is attached, reducing the nonspecific signals over the rest of the surface. This strategy has improved the immobilization capacity, in comparison to previous work (i.e. thiol-ene and thiol-yne approximations) and the assay sensitivity. Moreover, several irradiation setups have been employed to demonstrate the versatility of this reaction.

Finally, preliminary results have demonstrated that the physical structuration of these substrates previous functionalization, increases significantly the microarray performance, as well.

- ✓ Fluor-thiol and thiol-ene photoclick reactions have been applied for the first time to the development of oligonucleotide microarrays onto raw PVDF and alkenylated PVDF membranes, respectively.

Alkenylated membranes displayed higher immobilization densities than raw PVDF membranes, unlike hybridization capacity that was higher for raw PVDF membranes.

Modulation of the hydrophobicity of alkenylated membranes was done through a novel procedure that is milder and easier than previous methods, as it uses only light for activation. After the generation of the hydroxyl groups over the surface by UV irradiation, the membranes were successfully silanized by organosilane chemistry.

To sum up, click chemistry is an excellent via for the preparation of different microarray systems. Thiol-ene and thiol-yne reactions have demonstrated a successful anchoring capacity of thiolated nucleic acids, increasing the microarray performance. Besides, the thiol-ene reaction has proven to be a good manner to tether antibody fragments. Related

to the novel reaction developed in this work, the fluor-thiol photoclick reaction means a step forward in the modulation of highly hydrophobic surfaces. This reaction has allowed the anchoring of thiolated probes onto surfaces of different nature containing C-F motifs, improving the immobilization density, and reducing the spot size and nonspecific interactions, even more. Also, adjustment of the wettability through the hydrophobicity/hydrophilicity surface modulation to control immobilization and hybridization capacity has been another key during all the course of this thesis.

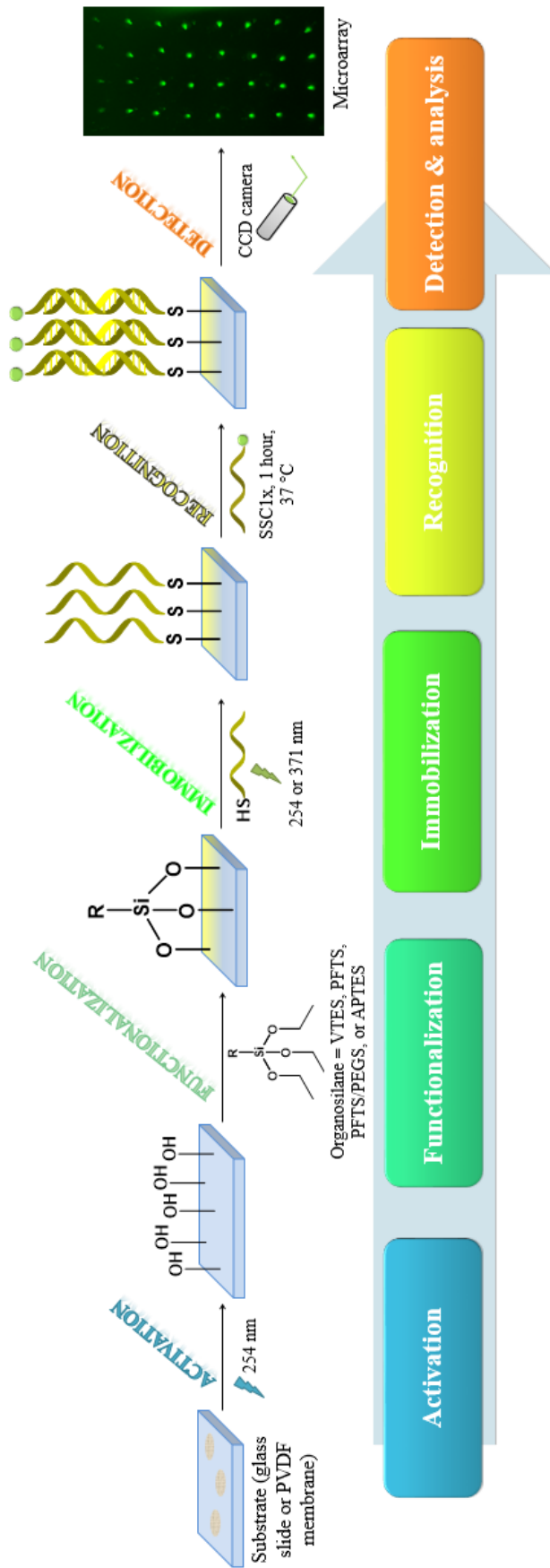
As we can observe, all the approaches presented in this thesis are especially focused on the surface properties, and interface interactions between the probes and the substrate. Thus, surface modulation, and exploration of novel anchoring methodologies, able to immobilize the probes in an easy, fast, and biocompatible way, was achieved. This rational design has contributed to the development of microarrays with improved performance in biosensing.



## **8. Annexes**







Annex 1. Work flow of the preparation and use of a microarray. Activation, functionalization, immobilization, recognition and detection are the five main steps in the fabrication and use of a microarray.

Annex 2. Schematic summary of the main features employed in each chapter. The solid substrate, functionalization, photoattachment and immobilized probe employed are displayed.

	<i>Solid substrate</i>	<i>Functionalization</i>	<i>Photoattachment</i>	<i>Immobilized probe</i>
<i>Chapter 3</i>	Glass slides	Alkenylated and alkynylated	Thiol-ene and thiol-yne photoinduced reactions	Mono-, di-, and tetra-oligonucleotides
<i>Chapter 4</i>	Glass slides	Alkenylated	Thiol-ene photoinduced reaction	Ab and hIgG
<i>Chapter 5</i>	Glass slides	Perfluorinated	Fluor-thiol photoinduced reactions	Mono-oligonucleotides (Ab and hIgG)
<i>Chapter 6</i>	PVDF membranes	Raw and alkenylated	Fluor-thiol and thiol-ene photoinduced reactions	Mono-oligonucleotides

